Investigating The Role of G protein βγ Specificity In Modulation of Synaptic Transmission

By

Katherine Michelle Betke

Dissertation

Submitted to the Faculty of the

Graduate School of Vanderbilt University

in partial fulfillment of the requirements

for the degree of

DOCTOR OF PHILOSOPHY

in

Pharmacology

August, 2014

Nashville, Tennessee

Approved:

Heidi E. Hamm, Ph.D.

P. Jeffrey Conn, Ph.D.

Kevin Currie, Ph.D.

Kevin Schey, Ph.D.

Danny Winder, Ph.D.

ACKNOWLEDGEMENTS

There are many people that I would like to thank for supporting me throughout my graduate studies and helping this work come to fruition. Dr. Heidi Hamm taught me to think critically and communicate my ideas. She kept me focused and motivated when things weren't going well while also encouraging me to pursue my ideas and supporting my future plans. I am forever grateful to her, as without this direction none of this work would have come together and I wouldn't be continuing on towards becoming a physician-scientist. I'm grateful to all of the members of my committee. They provided direction and a critical eye as projects progressed, challenging me but also encouraging me as I throughout the years. In addition, I want to acknowledge all of the members of the Hamm lab, particularly those in the $\beta\gamma$ group, who provided support and thoughtful questions. I'd like to thank Yun Young (Susan) Yim in particular, as without her assistance and support it wouldn't have been possible to complete many of the experiments.

In addition to Heidi, I was blessed to have other mentors who helped shape my development throughout my PhD and to whom I am immensely grateful. Dr. Anthony Baucum III spent countless hours discussing concepts, looking over data, and brainstorming experiments with me despite being in a different lab. He always made time to work through problems and answer my many, many questions. His guidance was invaluable in shaping my project and helping me to develop into a more confident scientist. Dr.'s Kevin Schey, Kristie Rose, Hayes MacDonald, and David Friedman allowed me to venture into the world of proteomics, despite having no background in it or training whatsoever. Each took time out of their very busy schedules to teach me concepts, review data, and discuss project directions. Without their help, I would not have been able to pursue the questions I was interested in, nor be able to speak about proteomics in a coherent manner. Dr. Lutz Hein made much of my work possible as he

graciously provided the use of his transgenic mice, as well as allowing me to visit his lab in Germany and perform experiments for weeks on end. Additionally, Dr. Ralf Gilsbach and the other members of the Hein lab were invaluable in providing assistance and making me feel welcome when I visited their lab. As well, I'd like to express my gratitude to Dr. Qin Wang at UAB for helping me to pilot all of my studies and providing the use of her transgenic animals in our ongoing collaboration.

Finally, I would like to thank my family for all of their support over the years. The path to this point was not always an easy one yet they always had words of encouragement and a firm belief in my abilities. I would not have been able to make it this far without them and cannot express how much I appreciate everything they have done for me.

TABLE OF CONTENTS

Page

LIST OF TABLES

Table

LIST OF FIGURES

Figure

ABBREVIATIONS

5-HT	serotonin
α_{2A}AR	α_{2A} adrenergic receptor
ADRA2A	α_{2A} adrenergic receptor gene
AID	α interaction domain
ATP	adenosine triphosphate
AUC	area under the curve
BLAST	basic alignment search tool
BME	β-mercaptoethanol
BONT/C	botulinum neurotoxin Type C
BSA	bovine serum albumin
CAPS	3-(cyclohexylamino)-1-propanonesulfonic acid
CHAPS	3-[(3-cholamidopropyl)dimethylammonio]-1-propanesulfonate
CID	collision induced dissociation
CNS	central nervous system
CRB	cerebellum
CSP	cysteine string protein
CTX	cortex
CV	coefficient of variation
DSP	3,3'-dithiobis[sulfosuccinimydlpropinate]
DTT	dithiothreitol
EDTA	ethylenediaminetetracetic acid
FACS	fluorescently-activated cell sorting
GABA	gamma-aminobutyric acid

GAPDH	glyceraldehyde-3-phosphate dehydrogenase
GGL	G protein γ-like
GDP	guanosine diphosphate
GIRK	G protein-coupled inward rectifier K+ channels
GPCR	G protein coupled receptors
GRK2	G protein-coupled receptor kinase 2
GTPγS	guanosine 5'-O-[gamma-thio]triphosphate
HEPES	4-(2-hydroxyethyl)-1-piperazineethanesulfonic acid
Hippo	hippocampus
HRP	horseradish peroxidase
Inp	input
IP	immunoprecipitation
K_{ir}	inwardly rectifying potassium channel
LC-MS/MS	liquid chromatography tandem mass spectrometry
LOD	limit of detection
LOQ	limit of quantitation
LTD	long-term depression
LTP	long-term potentiation
LRP	labeled reference peptide
mGluR	metabotropic glutamate receptor
MHD	Munc homology domain
MRM	multiple reaction monitoring
NMDAR1	*N*-methyl-d-aspartate receptor-1
PMSF	phenylmethanesulfonyl fluoride

RGS	regulator of G protein signaling
PLC	phospholipase C
PRE	presynaptic
PSD-95	postsynaptic density 95
PSD	postsynaptic density
R7BP	R7 family binding protein
RGS	regulators of G protein signaling
RIPA	radioimmunoprecipitation assay
RT	retention time
RWG	resonant waveguide
SD	standard deviation
SERT	serotonin transporter
SID	stable isotope dilution
SM	Sec-1/Munc-18
S/N	signal to noise
SNAP	synaptosome-associated protein
SNARE	soluble N-ethylmaleimide-sensitive factor attachment protein receptors
Str	striatum
Sup	depleted supernatant
TBS	tris buffered saline
TCA	tricholoroacetic acid
TX-100	triton X-100
QC	quality control
VAChT	vesicular acetylcholine transporter

VAMP	vesicle-associated membrane protein
VDCC	voltage-dependent calcium channels

CHAPTER I

INTRODUCTION

Portions of this chapter are published under the title "GPCR mediated regulation of synaptic transmission" in *Progress in Neurobiology*

Heterotrimeric G proteins play essential roles in cellular communication by transducing extracellular signals from G protein coupled receptors (GPCRs) to a wide range of downstream effectors. The fidelity of this process depends in part upon the G protein itself, as it requires guanine nucleotide-binding α subunits to exchange GDP for GTP and reversibly disassociate from $\beta\gamma$ dimers before each can interact with effectors[1]. Within the central nervous system, G$\beta\gamma$ subunits play an important role in ensuring efficient communication between neurons by regulating membrane voltage and neurotransmitter release at the synapse. Activated by inhibitory auto- and heteroreceptors, G$\beta\gamma$ subunits help guard against overstimulation by interacting with effectors such as voltage-dependent calcium channels, potassium channels, and the exocytotic machinery, to inhibit further transmitter release. While these effects are known, however, we have little understanding of which G$\beta\gamma$ isoforms exist *in vivo*, the factors controlling their distribution to specific synaptic terminals, whether specificity plays a role in regulating G protein interactions with the receptor and/or subsequent effector, what impact this may have in the context of the whole organism. Examining the distribution and specificity of G protein interactions following receptor activation will be of particular importance to understanding regulatory factors modulating synaptic transmission as it will help elucidate which of the many possible G$\beta\gamma$ combinations are likely to occur physiologically, what roles each

may play in regulating signaling cascades within the brain, and how these may be disrupted by injury and disease.

Synaptic Transmission

In its most elementary form, synaptic transmission is simply the communication between one presynaptic neuron and a single postsynaptic cell as well as the processing by the postsynaptic cell of the signal that it receives. At chemical synapses, signal transduction is achieved through the rapid conversion of an arriving electrical signal into a chemical one that diffuses between the cells[2,3]. Membrane depolarization caused by the arrival of presynaptic action potentials induces the opening of voltage-dependent calcium channels (VDCC), with the resulting calcium transients stimulating fusion of synaptic vesicles at the active zone of the presynaptic terminal[4]. Such regulated exocytosis releases neurotransmitter into the synaptic cleft whereupon it activates receptors or channels on the postsynaptic membrane to mediate voltage changes in the postsynaptic cell[4,5].

Organization of Synaptic Terminals

Structurally, chemical synapses are complex, asymmetrical cell-cell contact sites formed from the axon terminal membrane of the presynaptic neuron, juxtaposed with the postsynaptic density (PSD) on the postsynaptic cell[3,4]. Three morphological features of the presynaptic active zone are conserved across species, location in the CNS, or neuron type: an electron-dense, proteinaceous plasma membrane, precise alignment with the PSD, and a web-like cytomatrix responsible for organizing the area and facilitating neurotransmitter release[2]. Electron micrographs suggest the cytomatrix exists as a 'particle web' formed by a hexagonal array of electron-dense, pyramid-shaped particles extending into the cytoplasm that consist of a wide

variety of scaffolding proteins[2,3,6]. Particles are further interconnected by a meshwork of cytoskeletal fibrils, creating slots for synaptic vesicles to dock and fuse, as well as long, filamentous strands which align synaptic vesicles with active zone proteins[2,3,6,7]. Although the precise function of many of the scaffolding proteins is still unknown, it's believed they act together to maintain distinct pools of vesicles at the presynaptic terminal and facilitate fast exocytosis by regulating the maturation steps that render a vesicle fusion competent. Additionally, two distinct types of vesicles are observed at chemical synapses: small, clear synaptic vesicles which are filled with classical neurotransmitters such as acetylcholine, glutamate, and the monoamines, and large dense-core vesicles filled with neuropeptides and neurohormones. Although they differ in morphology, release kinetics, and distribution, both types of vesicles maintain conserved machinery for fusion events, and exhibit calcium-dependence for exocytosis[8.]

The Exocytotic Machinery

Regulatory Components Controlling Vesicle Docking, Priming, and Exocytosis at the Presynaptic Membrane

The short latency between calcium influx at a presynaptic terminal and the release of neurotransmitter suggests that a population of vesicles sits poised to fuse with the plasma membrane immediately following calcium entry[9,10]. To achieve such temporal precision, vesicles undergo a series of maturation steps at the presynaptic membrane known as docking and priming in order to become fusion competent (Figure 1). Docked vesicles were traditionally defined morphologically based on electron micrographs as those without measurable distance between vesicle and plasma membrane[11]. Based on this definition, docked vesicles were often reported to cluster around electron-dense pyramidal densities at the presynaptic terminal, and were suggested to make direct contact with the active zone[10,12]. Unfortunately, while

ultrastructure studies are unmatched in resolution, they cannot easily be used to study vesicle dynamics and preclude identification of different docked states, while potentially overestimating the number of docked vesicles through inclusion of those which are primed and/or being endocytosed[10,13]. Further, chemical fixation required for electron microscopy is known to introduce crosslinking artifacts, which can alter the distribution of synaptic vesicles at a presynaptic terminal[12]. More recent studies observing single synaptic vesicles using tools such as total internal reflection fluorescence microscopy show evidence for three distinct docking states by which vesicles approach the plasma membrane for variable lengths of time and contact it only during fusion events[10,12]. Such studies suggest that docking may be an easily reversible event prior to priming, where stable interactions with the plasma membrane would be established[10,12]. Despite increasing numbers of perturbation and biophysical studies, however, relatively few docking phenotypes have been associated with genetic mutations compared to secretion phenotypes[11]. Given the spatial fidelity by which synaptic vesicles cluster at an active zone, however, it is likely that specific molecular recognition mechanisms mediate attachment of the vesicles to the target membrane during the docking process.

Comparatively more is known about priming, a vesicle maturation process wherein vesicles transition from a docked but unprimed pool to a releasable pool which can fuse with the plasma membrane immediately upon calcium entry[10,14,15]. While the fidelity of vesicle priming and subsequent exocytosis has been shown to depend on the coordinated actions of a large number of proteins, the core machinery underlying this process revolves around members of the SNARE complex: syntaxin, SNAP-25, and synaptobrevin/VAMP. Further regulation is provided by a series of ancillary proteins such as the Sec-1/Munc-18 (SM) proteins Munc-18 and Munc-13, and the calcium sensor, synaptotagmin[16]. The SM proteins have been shown to have important interactions with syntaxin 1A that regulate the docking of vesicles to the synaptic

membrane by influencing the open and closed state of the SNARE protein[4,13,17-23]. In contrast, synaptotagmin 1 plays a role in both docking and priming through its ability to interact with and stabilize, t-SNARE, the complex of SNAP-25 and syntaxin 1A at the synaptic membrane, such that it can further interact with VAMP 2 on the synaptic vesicle[24].

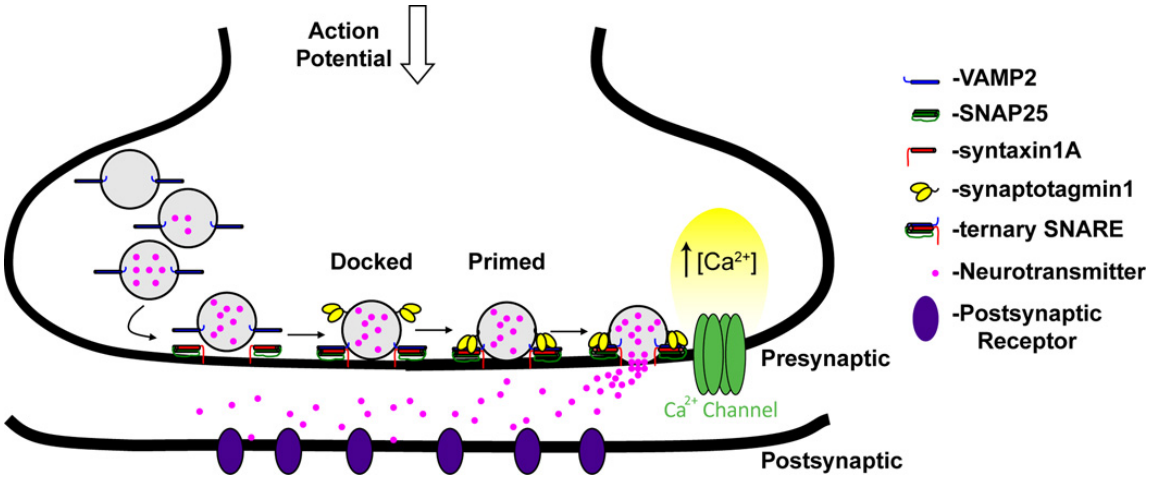

Figure 1. Overview of neurotransmission across a synapse. In the presynaptic neuron, synaptic vesicles expressing VAMP2, among other proteins embedded in their membrane, are loaded with neurotransmitters. Simplistically, docking of the vesicle occurs via interaction of VAMP2 with t-SNARE (SNAP-25/syntaxin 1A), a process that is guided and regulated by numerous proteins, while priming has been described as further zippering of the SNARE complex with interaction of other major components such as synaptotagmin, Munc-13, and Munc-18. Upon the arrival of an action potential, VDCCs facilitate a large increase in intracellular calcium concentration. This rise is sensed by proteins within the synaptic complex of the vesicle at the membrane such that fusion of the vesicle membrane with the presynaptic membrane occurs, resulting in release of neurotransmitter into the synaptic cleft to activate its respective receptor on the post-synaptic neuron ensuring propagation of action potentials from one neuron to another.

Soluble N-ethylmaleimide-sensitive factor attachment protein receptor (SNARE) proteins

The protein machinery that drives and regulates exocytosis is remarkably conserved, with SNARE proteins ubiquitously used for membrane fusion in organisms ranging from yeast to humans[16,25]. A mechanistic model has subsequently emerged termed the 'SNARE Hypothesis' whereby membrane fusion is thought to occur through formation of a four-helix bundle which draws opposing membranes into close proximity and releases enough free energy to drive fusion events[25-28]. Central to this hypothesis are the three proteins that make up the SNARE complex (Figure 2). The representative major isoforms in brain of t-SNAREs are syntaxin 1A and synaptosome-associated protein of 25 kDa (SNAP-25), and of the v-SNARE is synaptobrevin/VAMP (vesicle-associated membrane protein)-2. When the structure of syntaxin 1A is examined, three conserved domains are apparent: a carboxy-terminal transmembrane domain anchored to the presynaptic membrane, and two conserved α-helical structures - a SNARE domain single α–helix and an amino-terminal triple α–helix H_{abc} domain - which play a role in regulating synaptic transmission (Figure 2A). The SNARE domain mediates interaction of syntaxin with other members of the SNARE complex to form the exocytotic machinery. By folding back on itself to cover the SNARE domain, the H_{abc} domain places syntaxin in a 'closed' conformation and prevents the formation of the core fusion complex through further interaction with chaperone proteins such as Munc-18[4,29]. Similarly, synaptobrevin is also a transmembrane protein whose cytoplasmic domain forms an α-helical SNARE domain (Figure 2A). While *in vitro* studies have suggested synaptobrevin may interact with other synaptic proteins such as voltage-dependent calcium and sodium channels[30], the primary role for these proteins at this time appears to be mediating vesicle endo- and exocytosis[31,32]. The final member of the SNARE complex, SNAP-25, is unique in that while it is found localized to the presynaptic membrane, it lacks a transmembrane domain. Rather, it is anchored via post-translational

palmitoylation of four cysteine residues located near the central region of the molecule between two α-helical SNARE domains[33] (Figure 2A). Two other members of this family, SNAP-23 and SNAP-29, have also been shown to be important for regulating exocytotic events, but despite these isoforms co-localizing to regions such as the cerebellar cortex, SNAP-25 appears to be the major homolog mediating regulated exocytosis in the brain[33].

The predominant view of SNARE complex formation is that initial assembly of the intermediate binary complex between syntaxin and SNAP-25 (t-SNARE) is followed by formation of the ternary complex through interactions with synaptobrevin on the secretory vesicle as the vesicle is drawn to the presynaptic membrane during priming (Figure 2B). As vesicles approach the presynaptic membrane, the SNARE motifs interact in a process referred to as “zippering”, forming a stable, four-helical bundle that brings the vesicle progressively closer to the presynaptic membrane to allow fusion to occur (Figure 2B).

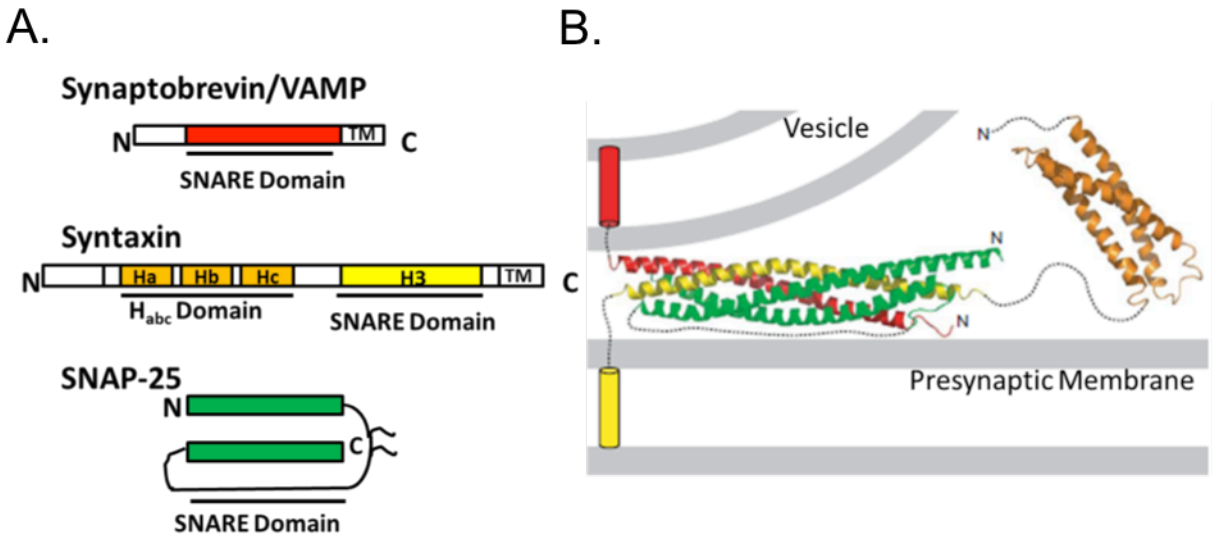

Figure 2. The SNARE complex. A) Domain structure of syntaxin, synaptobrevin, and SNAP 25. B) Cartoon showing the crystal structure of the SNARE complex with the NMR structure of the syntaxin H_{abc} domain. Adapted from Rizo, J., Chen, X., Arac, D., 2006. Unraveling the mechanisms of Synaptotagmin and SNARE function in neurotransmitter release. Trends Cell Biol. 16(7), 339-50.

Sec-1/Munc-18 (SM) Proteins

While formation of the SNARE complex has been shown to be sufficient to drive exocytosis, a number of studies examining fusion kinetics have suggested that additional proteins may be required. One group of such proteins includes the cytosolic SM proteins, Munc-18 and Munc-13[4]. All members of the SM family are composed of a conserved ≈600 amino acid sequence which folds into an arch-shaped structure important for protein-protein interactions[22]. Munc-18 is thought to serve multiple roles in exocytosis, the first being as an inhibitory protein which prevents assembly of the SNARE complex at inopportune times and which plays an important role in mediating vesicle docking[13,17,23,34,35]. Evidence for a second, post-docking role for this SM protein, however, comes from analysis of Munc-18-1 knockout mice which exhibit a total block of neurotransmitter release[11,37]. Recent evidence suggests that rather than dissociate completely, Munc-18 actually remains anchored to syntaxin by its N-terminal lobe, allowing it to take on an additional regulatory role. As ternary SNARE formation proceeds, Munc-18 is believed to fold back over the four helix SNARE bundle and in doing so, restrict the diffusion of the SNARE proteins in the membrane such that they are maintained in the correct orientation for fusion to occur, as well as allow energy transduction to the membranes[21,22].

A second SM protein, Munc-13, has also been shown to play a prominent role in vesicle exocytosis, although as opposed to Munc-18, Munc-13 primarily regulates the priming process to increase the number of primed vesicles. Munc-13 null mice demonstrate total abolishment of both evoked and spontaneous neurotransmitter release while docking remains unaffected[38], and this phenotype is also found in knockouts of homologs in both *C. elegans*[39] and *Drosophila*[40]. Its actions appear to be downstream of Munc-18 as overexpression of Munc-13 does not affect the number of docked vesicles, while open forms of syntaxin 1A are able to at least partially rescue the *unc-13* null phenotype in worms[41] but not that of *unc-18*[11,42]. It is thought that this

role in priming is mediated through both its C-terminal C2 domain as well as the Munc homology domains (MHD) located in the C-terminal third of the protein. These MHDs allow binding to syntaxin 1A after it forms a heterodimer with SNAP-25 or the fully formed SNARE complex[14,21,43]. In doing so, Munc-13 may help transform syntaxin to an open conformation to facilitate SNARE complex formation, or stabilize the exocytotic machinery to promote vesicle fusion once the complex is fully formed.

Synaptotagmins

In addition to SM proteins, synaptotagmin has also been shown to be essential for vesicle fusion to occur (Brose et al., 1992). Synaptotagmins are a family of calcium binding proteins[44-46]. Genetic ablation of synaptotagmin-1 results in abrogation of fast, synchronous neurotransmitter release without affecting asynchronous events, leading to the suggestion that this protein acts as a calcium sensor for calcium-dependent vesicle fusion[20,47-49]. This is supported by gene mutation in mice targeting the calcium-binding site of synaptotagmin. When calcium binding is disrupted but other structural features of the protein remain intact, calcium sensitivity of neurotransmitter release is reduced, but no effect is seen in regards to the size or spontaneous release of the ready releasable pool of synaptic vesicles[50]. Synaptotagmin-1 is localized to both synaptic and large dense core vesicle membranes and is characterized by two tandem, cytoplasmic, PKC-like C_2 domains: C_2A and C_2B respectively. Two of the most important binding partners for this protein are SNARE proteins and the lipid membrane, and it's believed that through cooperative interactions with each of these, the C_2 domains play an important role in exocytosis. Specifically, calcium influx has been shown to induce binding of synaptotagmin-1 to both syntaxin and the C-terminal of SNAP-25, as well as t-SNARE heterodimers and fully formed SNARE complexes[20,51-53]. This process may be mediated at least in part through

interactions between acidic residues on SNAP-25 and basic residues in the second loop of the C_2A domain[54], or perhaps with the polybasic region of the C_2B domain[21].

Anionic phospholipids are a second important effector for synaptotagmin-1[55-57] and mutations that reduce calcium-dependent synaptotagmin binding to the lipid membrane exhibit a decrease in synaptic release probability[53] suggesting that this function is essential for its role in exocytosis. While calcium-dependent binding of synaptotagmin to both SNARE proteins and lipid membranes is essential for fast exocytosis, debate still exists as to how exactly this occurs. One possibility is that synaptotagmin interacts with SNARE complexes prior to calcium influx, bringing the vesicle and plasma membranes into close apposition. This would be expected to promote vesicle fusion as it would enable tighter coiling of the SNARE complex, while subsequent interactions with the lipid bilayer upon calcium entry may accelerate membrane fusion through electrostatic interactions acting to perturb the lipid bilayer and overcome the energy barrier to fusion[21]. Another unanswered question is how synaptotagmin interacts on a molecular level with the SNARE complex. Fluorescence resonance energy transfer–based studies detected an interaction of the SNARE complex on the opposing surfaces of the C_2 domains of synaptotagmin[58]. Further, NMR data demonstrated a primary interaction interface with SNARE may be through a polybasic region on the C_2B domain[51]. Most recently, electron paramagnetic resonance spectroscopy data reveal a structurally heterogeneous interaction maintaining the polybasic and C_2B domain interactions, but also a site near loop 2 of the calcium binding site in C_2A; an interaction not seen in the other two studies mentioned[59]. These authors suggest that this new binding mode allows for simultaneous interaction with the SNARE complex as well as two membrane surfaces in apposition such as the cell membrane and the docked synaptic vesicle. Regardless of how exactly this process functions, however, synaptotagmin clearly plays a major role in regulating synchronous release with both SNARE interactions and phospholipid

binding playing a crucial part. Further, synaptotagmins or other calcium sensors may play an important role in regulating asynchronous release events, which are unrelated to action potentials. Studies examining synaptotagmin 1 and 2 knockout mice both demonstrate increases in the frequency of spontaneous release, suggesting an important role for these proteins in regulating this process[60,61], doc2, a protein that is related to synaptotagmin in that it also has two homologous calcium-binding domains, has been shown to act as the calcium sensor for asynchronous release in cerebellar slices[62] and cultured hippocampal neurons[62,63], highlighting the importance of these sensors in many aspects of vesicle exocytosis.

Complexin, tomosyn, and heterotrimeric G proteins

Taken together, the SNARE proteins, as well as ancillary players such as SM proteins and synaptotagmin, function as the classical exocytotic machinery required for fusion events to occur. Studies in which individual components have been removed or inhibited, display severe disruption of synaptic transmission. Further exploration of processes that modulate their function has provided useful information about how exocytosis is regulated. Several additional proteins such as complexin, tomosyn, and heterotrimeric G proteins have also been shown to interact with either the SNARE proteins individually, the t-SNARE dimer, or the full ternary SNARE. Complexin is a regulatory protein thought to play a role in calcium-sensitive fusion[49,64] as well as vesicle priming[49,65,66]. X-ray crystallography studies demonstrate that it interacts with the ternary SNARE complex by binding as a fifth α-helix to the SNARE bundle of ternary SNARE[67,68]. More recent x-ray crystallography and FRET data suggest that complexins can simultaneously bind to two neighboring incompletely "zippered" SNARE complexes stabilizing a structural state that is incompatible with fusion. After full incorporation of VAMP2 into the ternary SNARE bundle, complexin remains bound to the SNARE complex, but loses its interaction with the neighboring SNARE complex[69]. Tomosyn is a protein that binds to the t-SNARE

complex[70] and prevents the association of VAMP2[71]. Tomosyn has two domains, an N-terminal domain of two sets of 7 WD 40 repeats that form two tandem 7-bladed β-propellers, and a C-terminal domain with a SNARE binding motif. Both domains are needed to regulate exocytosis *in vivo*[72]. The C-terminal SNARE motif binds to t-SNARE in a way similar to that of VAMP2 binding to t-SNARE[73]. Finally, the G-protein dimer, Gβγ, interacts with ternary SNARE as well as the individual SNARE proteins to mediate inhibition of exocytosis by GPCRs[74-81]. This novel interaction and its role in the context of GPCR regulation of synaptic transmission is the subject of the remainder of this introduction.

GPCR Mediated Regulation of Synaptic Transmission

G protein Coupled Receptors

GPCRs are a large superfamily of proteins that convey the majority of signal transduction across cell membranes and mediate a vast array of cellular responses necessary for the normal physiology of the body[1,82,83]. Encoded by nearly 800 different genes in humans, these proteins are activated by a wide variety of ligands ranging from single photons, odorants, and amino acids to hormones, neurotransmitters, and proteolytic enzymes as well as many others[1,84]. All GPCRs share a common architecture consisting of seven transmembrane-spanning α-helices, an extracellular N-terminus, an intracellular C-terminus, and three interhelical loops on each side of the membrane (Figure 3A)[1], but exhibit unique combinations of signal transduction pathways as well as complex regulatory processes controlling their activity and expression[85]. At present, these receptors are phylogenetically divided into five main families: Glutamate, Rhodopsin, Adhesion, Frizzled-Taste-2, and Secretin, based on sequence and structural similarities[86], with each family exhibiting unique ligand binding properties. Schiöth *et al.* give an in-depth description of their GRAFS classification system in their publication, but the

families will be briefly described here based on their review[86]. The Glutamate family includes mostly the glutamate receptors, but also GABA receptors and the taste 1 receptor. A common feature is a large bilobed N-terminus, which is the binding site for their respective ligands. The largest and most diverse, the Rhodopsin family are activated by a variety of ligands including peptides, glycoproteins, prostaglandins as well as photons of light. This group can be divided into 4 subgroups: α, β, γ, and δ, although common amongst them is a relatively short N-terminus. Comparatively, the Adhesion family is mostly comprised of orphan receptors without known ligands. Receptors in this family generally have many N-terminal serine and threonine residues that are sites of glycosylation, and most have proteolytic recognition sites that result in cleavage of the extracellular N-terminus. The Frizzled-Taste-2 family is a phylogenetic combination of two groups of GPCRs, the frizzled receptors, most notably F2DR being the receptor for the Wnt glycoprotein involved in controlling cell fate, proliferation and polarity, and the taste-2 receptors, which largely have unknown functions except their expression in tongue and palate suggests a probable role in bitter taste. The last group is the Secretin family, which in some classification systems was grouped with the Adhesion receptor family. Schioth *et al.* make their reasoning clear that despite structural similarities, evolutionarily the secretin receptors are a separate family[87]. These receptors typically have long N-terminal domains with frequent conserved cysteine bridges, and it is through these large N-termini that they bind typically peptide ligands[86].

GPCRs are known to mediate their effects through coupling to heterotrimeric G proteins in order to modulate downstream effectors, but it is only recently that combinations of biochemical, crystallographic, and biophysical studies have begun to elucidate the structural basis by which this is accomplished[85]. These studies demonstrate a complex picture by which specific ligands stabilize unique active state receptor conformations for interaction with

particular effector molecules[85]. The results of these conformational changes is an increase the receptor's affinity for the G protein heterotrimer, resulting in the formation of a transient ligand-GPCR-G protein ternary complex necessary for G protein activation[88].

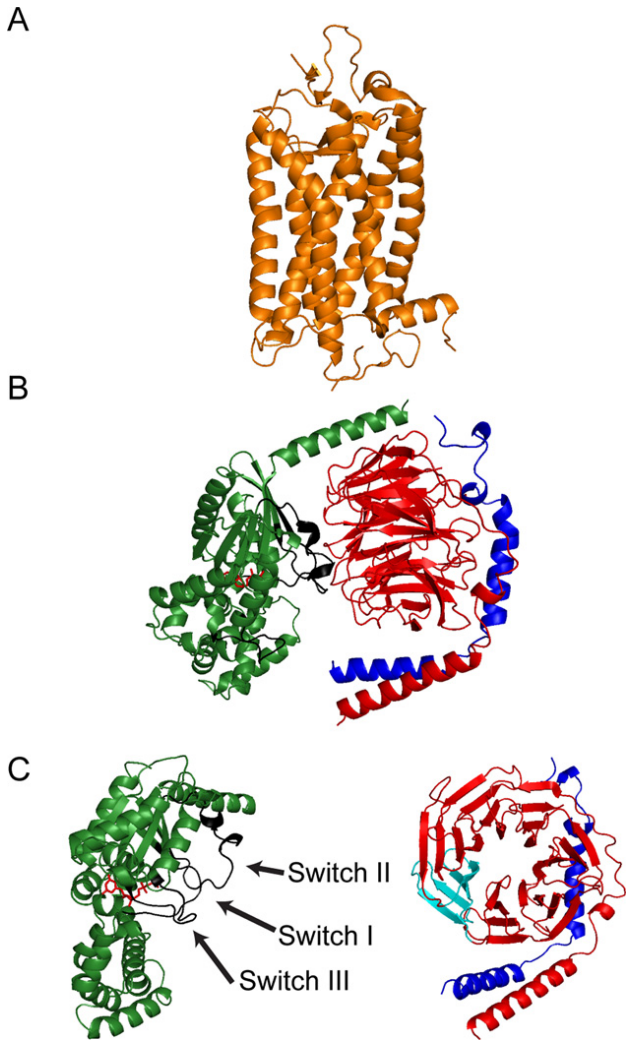

Figure 3. Structure of G protein Coupled Receptors and Heterotrimeric G proteins. Shown in ribbon diagrams are representative examples of GPCRs and heterotrimeric G proteins. A) The structure of rhodopsin (PDB ID: 1F88) (Palczewski et al., 2000) is shown in orange, and it depicts the seven transmembrane α-helices and the respective extracellular and intracellular surfaces that interact with agonists and heterotrimeric G proteins, respectively. B) The structure of the heterotrimer transducin (PDB ID: 1GOT) (Lambright et al., 1996) is shown. The Gα subunit (green) has two domains, a GTPase domain and an α-helical domain. Within the GTPase domain, there are three regions termed Switch I, II, and III, (C), that have different orientations depending on which guanine nucleotide is present. In the GDP-bound form, Switches I–III form the major interface that interacts with the Gβγ dimer. The structure of the Gβ subunit (red) is an N-terminal α-helix followed by a series of β sheets that make a seven-bladed propeller or toroid. A single blade (light blue) is based on the amino acid motif termed WD-40 repeat. The structure of the Gγ subunit (dark blue) is two tandem α-helices that form interactions with the N-terminal α-helix of Gβ and a surface of the Gβ toroid on the opposite face from where Gα interacts with Gβ.

Heterotrimeric G proteins

Despite the diversity of the GPCR superfamily, interestingly enough, they mediate their effects through relatively few heterotrimeric G proteins. G proteins consist of α, β and γ subunits, and in humans, 16 genes and 11 splice variants account for 27 Gα isoforms[89,90], while 5 and 12 genes encode 5β and 12γ protein subunits, respectively[91,92]. Heterotrimers are generally classified into four families, G_s, $G_{i/o}$, G_q, and $G_{12/13}$, based on the functional similarity of the Gα subunit[93], but all Gα subunits share a similar tertiary structure composed of two domains: a GTPase domain and a helical domain[1]. Crystal structures demonstrate that the GTPase domain is conserved among all members of the G protein superfamily, including small G proteins and elongation factors[1]. This domain contains the site of GTP hydrolysis as well as the sites for binding to the G$\beta\gamma$ dimer, receptors, and a wide variety of effectors. In contrast, the helical domain is unique to the heterotrimeric Gα subunit and functions as a lid to cover the nucleotide-binding pocket such that it is retained deep within the core of the protein (see Figure 3B). Further, post-translational modifications at the N-terminus of all Gα subunits help regulate membrane localization and protein-protein interactions[1].

G protein β subunits are made up of two structurally distinct regions, an amino terminal segment which is an α helix of approximately 20 amino acids, and a propeller-like structure comprising seven blades of four anti-parallel β strands known as a WD repeat[94-96] (see Figure 3C). In contrast, the Gγ subunit is much smaller, composed of only two α-helices, a carboxy-terminal helix which extends across the surface of blade 5 on Gβ as well as a small section of the N-terminal region, and an amino terminus helix which forms a coiled-coil with the amino terminal non-WD repeat region of the β subunit[94] (see Figure 3C). All Gγ subunits are post-translationally modified at the C-terminus with a methylation group as well as either a farnesyl or geranylgeranyl moiety, which aids in membrane localization and may play a role in receptor

interactions[96,97]. Together, Gβ and Gγ form a functional dimer as subunits cannot be dissociated except with denaturants[96] and neither subunit can signal on its own.

Specificity of Gβγ Interactions

Sequence comparisons show that $G\beta_{1-4}$ share up to 90% sequence identity compared to 50% identity for $G\beta_5$ while Gγ subunits are much more divergent, with isoforms sharing only 30-70% sequence identity[96,98]. Given the high sequence identity shared among the isoforms, it might be expected that functional dimerization of all isoforms would be possible. While most Gβ and Gγ subunits have been shown to form dimer pairs *in vitro*, studies have shown that subtypes do not randomly associate, but rather show distinct affinities for one another, and even, that certain combinations are unable to pair. As with Gβγ dimerization, it is increasingly becoming evident that unique Gβγ combinations play specific roles in mediating interactions with receptors and effectors[99-101]. Indeed, while early biochemical studies found few clear functional differences in the ability of isoform combinations to regulate effectors *in vitro*, subsequent studies using anti-sense oligonucleotides, site directed ribozymes, and genetic deletion have suggested very specific roles for Gβ and Gγ isoforms in signaling in intact cells[95]. For example, $G\gamma_7$ knockout mice exhibit reduced expression of $G\alpha_{olf}$ and reduced adenylyl cyclase activity[102], while $G\gamma_3$ knockout mice show increase susceptibility to seizures, reduced body weight, and decreased adiposity. It is possible even, that isoforms may show tissue-dependent specificity for an individual effector[103]. Given that most cell types express multiple Gα, Gβ, and Gγ subtypes, a greater understanding of Gβγ-effector regulation is necessary to fully elucidate how specificity is achieved.

Gβγ Interaction with Effectors

Initially, Gβγ was thought to play a passive, inhibitory role by facilitating the completion of intracellular information transfer by merely returning Gα to a heterotrimeric state while also preventing Gα-mediated signaling in the absence of receptor activation[104]. One of the earliest independent roles in cellular signaling, however, was shown in 1987 when Logothetis *et al.* showed that Gβγ subunits could activate potassium-selective ion channels in cardiac atrial cells[105]. Today, Gβγ subunits are known to regulate a wide variety of effectors including phospholipase C-β, adenylyl cyclase, calmodulin, PI 3-kinase, and components of the mitogen-activated protein kinase cascade (among others). Additional effectors such as voltage-gated calcium and potassium channels, as well as members of the exocytotic machinery regulate membrane voltage and neurotransmitter release[75,77,81,96,104] (Figure 4).

Although Gβγ-effector interaction sites were initially hypothesized to be localized to the Gα interface, this is not the only site important for effector regulation. Mutagenesis studies have since identified binding regions within the blades of the Gβ propeller and along its N-terminal coiled-coil, as well as areas outside of the Gα subunit interface, and regions on Gγ subunits[94,96,106-108]. An example of this is the interaction between Gβγ and the GIRK channels. Zhao *et al.* (2003) demonstrated that mutation of residues Thr-86, Thr-87, and Gly-131 on $G\beta_1$, which are outside of the Gα binding site, resulted in decreased GIRK activity[109]. As such, while the Gα interface likely represents a core site for effector binding being that it is primarily exposed when a GPCR has activated the Gα subunit, other regions may also play important roles in facilitating downstream signaling for Gβγ subunits.

Mechanisms of Presynaptic Regulation By Heterotrimeric G proteins

GPCRs have been shown to play an important role in controlling synaptic transmission, as activation of presynaptic $G_{i/o}$-coupled auto- and heteroreceptors such as $5HT_1$ serotonin receptors, D_2 dopamine receptors, M_4 muscarinic receptors, α_{2A} adrenergic receptors, opioid receptors, as well as many others, is known to inhibit evoked transmitter release[110,111]. Such regulation is attributed to the actions of both the α and $G\beta\gamma$ subunits of heterotrimeric G proteins. Activation of $G\alpha$ subunits leads to diffusible second messengers that can have effects at a distance from the site of activation. The $G\alpha$ subunits of G_s and G_q have facilitatory roles on exocytosis through activation of adenylyl cyclase and phospholipase C, leading to second messengers that activate downstream kinases (protein kinase A, by increasing cyclic adenosine monophosphate levels by $G\alpha_s$ activation of adenylyl cyclase, and protein kinase C, by $G\alpha_q$ activation of phospholipase $C\beta$). The phosphorylation of proteins involved in vesicle recruitment, docking, and fusion can cause either inhibition, or facilitation of synaptic transmission[112]. Activation of presynaptic $G\alpha_q$ has been described to play a role in slow voltage-independent inhibition[113,114] through activation of phospholipase C and reduction of the second messenger phosphatidylinositol-4, 5-bisphosphate (PIP_2)[115]. Other regulatory pathways downstream of GPCRs include arrestin signaling, which can also affect second messenger systems[116]. Arrestin signaling processes can affect, for example, scaffolding of phosphodiesterase close to G_s-coupled receptors[117].

The activation of presynaptic GPCRs also leads to dissociation of $G\beta\gamma$ subunits whose actions remain local as they are membrane-associated via $G\gamma$ C-terminal prenylation. Autoreceptors sensing neurotransmitter released from the activated synapse, or heteroreceptors, sensing neurotransmitters from neighboring nerve terminals, activate $G_{i/o}$ receptors, and release $G\beta\gamma$. Obviously, the effects of neurotransmitters depend not only on the

pharmacology of the receptors, but also on the spatial arrangement in relation to the sites of transmitter release. Some presynaptic GPCRs are found distant from the active zone[118], and thus are not likely to affect active zone processes, but most probably work by traditional mechanisms of second messenger generation. Those presynaptic $G_{i/o}$-coupled GPCRs that are localized to the active zone or peri-active zone region[119] are likely to generate G$\beta\gamma$ subunits that can diffuse to the exocytotic machinery and mediate fast regulation of exocytosis[75-77]. The detailed localization of GPCRs must be done by electron microscopic immunocytochemistry, and though there are perhaps hundreds of presynaptic receptors, fine localization is limited to a very few subtypes (see Table 1). Further work will be needed to determine subcellular localization of other $G_{i/o}$-coupled presynaptic receptors. On the other hand, there is much more information on the ability of presynaptic GPCRs to influence postsynaptic responses in paired recordings. Whether they work by modifying voltage-gated Ca^{2+} channels, or downstream of Ca^{2+} entry directly on the exocytotic machinery is known in some cases via studies of the effects of blocking various voltage-dependent calcium channels or inhibition of "minis" (see Table 1). Presynaptic G$\beta\gamma$ modulation of synaptic transmission occurs mainly through three mechanisms: inhibition of voltage-dependent calcium channels at presynaptic nerve terminals, regulation downstream of calcium entry via direct interaction with of one or more of the components of the exocytotic machinery[120], or regulation of GIRK channels that affect the shape of the invading action potential[121] (Figure 5). Such diversity highlights the physiological importance of G proteins in regulating synaptic transmission but also raises numerous questions about which mechanism functions at particular synapses, the relevance of each mechanism *in vivo,* and the contribution of each mechanism to modulation. While we attempt to highlight some of the key findings for each mechanism below, further work is needed to clarify these questions and assess the importance of each at a systems level.

	Synapse		Soma
	VDCC	**Fusion Apparatus**	**VDCC**
M2/M4 Ach receptor	(Higley et al., 2009)	(Bellingham and Berger, 1996, Scanziani et al., 1995)	(Allen and Brown, 1993, Delmas et al., 1998)
Group II mGlu receptor		(Capogna, 2004, Glitsch, 2006, Scanziani et al., 1995)	
Group III mGlu receptor	(Giustizieri et al., 2005)	(Gereau and Conn, 1995)	
$GABA_B$ receptor	(Dittman and Regehr, 1996, Isaacson, 1998, Wu and Saggau, 1995)	(Dittman and Regehr, 1996, Harvey and Stephens, 2004, Wu and Saggau, 1995)	
μ opioid receptor	(Heinke et al., 2011)	(Heinke et al., 2011)	(Wilding et al., 1995)
CB1 cannabinoid receptor	(Brown et al., 2004)		
A1 adenosine receptor	(Dittman and Regehr, 1996, Scholz and Miller, 1992, Umemiya and Berger, 1994)	(Scholz and Miller, 1992)	(Umemiya and Berger, 1994)
D2 dopamine receptor	(Hamilton and Smith, 1991, Higley and Sabatini, 2010)	(Nicola and Malenka, 1997)	(Cabrera-Vera et al., 2004)
α_2 adrenergic receptor	(Boehm, 1999)	(Delaney et al., 2007)	(Boehm, 1999)

Table 1. Inhibitory GPCR function at synapses and cell bodies in the central nervous system. Listed are examples of $G_{i/o}$-coupled GPCRs known to inhibit synaptic transmission via actions on voltage-dependent calcium channels or exocytotic machinery downstream of calcium entry. Receptors are separated depending on localization to the synapse or soma of neurons in the central nervous system.

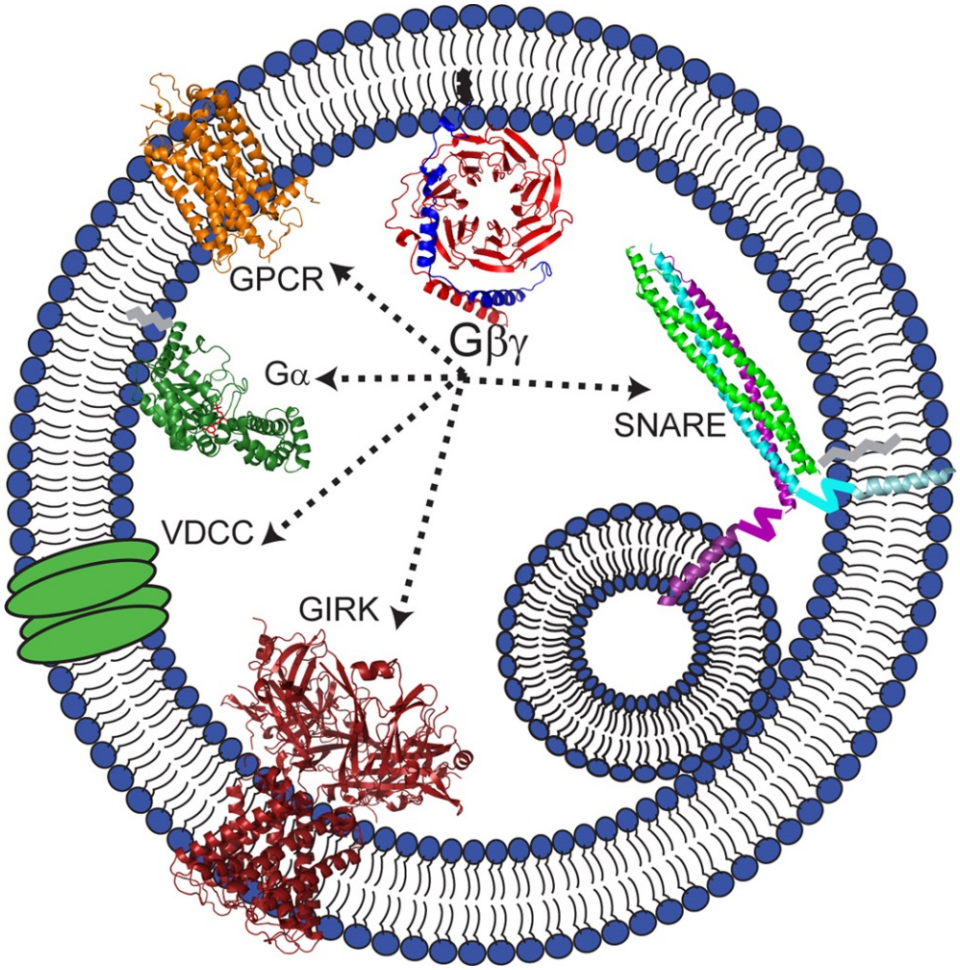

Figure 4. The interactions with Gβγ during exocytosis. Gβγ subunits are known to have a variety of interactions during exocytosis - GPCRs and Gα subunits during its activation, as well as a number of effectors. Shown are the structures, if known, of those proteins that interact with Gβγ and play a role in exocytosis. THE GPCRs and Gα are discussed in Figure 3. The SNARE proteins (SNAP-25/Syntaxin 1A/VAMP2) form a trimeric complex through interaction of their α-helical SNARE motifs, SNAP-25 having 2 two of them (PDB ID: 1SFC) (Sutton et al., 1998). VAMP2 (purple) and syntaxin 1A (cyan) have transmembrane domains through which they interact with membranes. SNAP-25 (green) has a palmitoylation site near the C-terminal portion of its first SNARE motif by which it is tethered to the membrane. Not shown is the N-terminal helical domain of syntaxin 1A, H_{abc}. The crystal structure of syntaxin 1A without the transmembrane domain confirms the triple helix H_{abc} domain at its N-terminus. The GIRK channel is represented by the crystal structure for the structurally similar ATP-sensitive K_{ir} channel 10, which is a tetramer with both transmembrane and intracellular domains (PDB ID: 2X6A) (Clarke et al., 2010). There is no structure determined yet for VDCC; it is shown as a simple transmembrane cartoon.

Gβγ Regulation of Presynaptic Voltage-Dependent Calcium Channels

As mentioned, GPCR mediated regulation of synaptic transmission has been shown to occur through multiple mechanisms, the best characterized of which is through direct inhibition of VDCC (Figure 5). These channels play an essential role in regulating vesicle exocytosis as they control calcium influx into the cell. As the presynaptic membrane is depolarized, VDCC become activated resulting in an influx of calcium into the cell, which can then bind to synaptotagmin to trigger exocytotic events. At present, five classes of VDCC have been identified in mammals based on their pharmacological and electrophysiological properties, with further delineation of subtypes into low-voltage (T-type) and high-voltage (N-, P/Q-, and R-type) activated channels based on the strength of depolarization necessary to trigger them[122]. The core of the calcium channel complex that forms the channel is the α_1 subunit. This subunit has 4 transmembrane subdomains and is believed to organize and form the pore. Other subunits that have been determined to associate with and modulate the calcium channel are an intracellular β subunit and an $\alpha_2\delta$ subunit complex. Lastly, there is a γ subunit with variable tissue expression that also is part of some calcium channels[122]. G$\beta\gamma$ can directly bind to N-and P/Q-type calcium channels[122-127]. Examination of the structural determinants which underlie this modulation have identified regions within the N-terminal loop[128], the I–II loop[124,129], and the C-terminal loop[130-132] of the pore-forming α_1-subunit of the calcium channels which are important for G$\beta\gamma$ modulation. Within the I–II loop, there are two regions that have been implicated in binding to the G$\beta\gamma$ dimer. The first overlaps with the α-interaction domain (AID) and contains the consensus sequence QXXER[124,129,133]. A second domain within the I–II loop is located C-terminal to the AID, and is termed the G protein interaction domain[129]. Although still subject to a great deal of study, it's believed that G$\beta\gamma$ binding actually stabilizes the channel in a conformational state which permits only reluctant opening, thus preventing vesicle exocytosis[134-139].

G protein inhibition of inward calcium currents was initially demonstrated by Dunlap and Fischbach (1978) when they were able to show that the contribution of calcium channels to action potentials in chick dorsal root ganglion neurons was reduced following activation of gamma-aminobutyric acid $(GABA)_B$, serotonin, or adrenergic receptors[140]. Subsequent studies over the next 20 years have implicated primarily $G_{i/o}$-coupled GPCRs in this regulation as muscarinic, opioid, dopamine, and many other $G_{i/o}$-coupled receptors all have the propensity to exert negative control over calcium currents and exhibit sensitivity to pertussis toxin[134, 136,137,139]. However, it should be noted that modulation of VDCC may not occur solely through the actions of $G_{i/o}$-coupled GPCRs as activation of G_s and G_z-coupled G proteins has also been shown to mediate voltage-dependent inhibition of N-type calcium[141]. Whether this reflects a ubiquitous mechanism of regulation remains unclear; however, it is apparent that inhibition of calcium channels by GPCRs is widespread and an important regulatory factor mediating control of neurotransmitter release.

In addition to $G\beta\gamma$ regulation of VDCC, there is evidence of syntaxin 1A regulation of the channels themselves, as well as an intersection between VDCC, syntaxin, and $G\beta\gamma$. Syntaxin 1A was initially found to be associated with N-type calcium channels in a pre-fusion complex[142-144]; however, later studies confirmed the molecular and functional interactions between these proteins[145,146]. Further, in addition to the previously mentioned studies of $G\beta\gamma$ regulation of VDCC above, there is evidence of syntaxin 1A promoting inhibition of VDCC by $G\beta\gamma$[138,145] and that this may occur through $G\beta\gamma$ and VDCC binding to separate domains of syntaxin 1A[138].

$G\beta\gamma$ Regulation of G protein-Activated Inward Rectifying (GIRK) Potassium Channels

GIRK channels are largely believed to be expressed somatodendritically[121,147,148] where they act to hyperpolarize the cell membrane, making it harder to reach the threshold for initiation of an action potential[148,149]. They are members of the inwardly rectifying potassium

channel (K_{ir}) superfamily of proteins and are abundantly distributed in atrial cells and neurons where they function to regulate heart rate and neuronal excitability[94,151]. Upon activation, they facilitate efflux of potassium ions out of the cell, hyperpolarizing the cell membrane and dampening electrical activity by making it more difficult to elicit an action potential[153]. To date, four mammalian GIRK subunits (GIRK 1–4) have been identified which assemble to form functional channels although studies have shown that generally only heterotetramers composed of GIRK 1/2 and to a lesser extent GIRK 2/3 as well as GIRK 2 homotetramers are expressed in the brain[108,152-154].

Unique to the K_{ir} family, however, the activity of postsynaptic GIRK channels is regulated through activation of $G_{i/o}$-coupled GPCRs such as opioid, M_2 muscarinic, α_2 adrenergic, 5-HT_{1a} serotonin, and $GABA_B$ receptors[150,155,156], with activation occurring as a result of direct interactions of $G\beta\gamma$ subunits with the N and C-termini[105,154,157] (Figure 5). As with many $G\beta\gamma$ effectors, regulation of GIRK channels was initially proposed to occur at sites along the $G\alpha$-$G\beta\gamma$ interface. Studies by Ford *et al.*[158] and Albsoul-Younes *et al.*[159] demonstrated that eight residues falling within this region (Leu55, Lys78, Ile80, Lys89, Trp99, Asp228, Asp246 and Trp332) were important for channel activation. Subsequent work went on to identify additional sites of interaction with Absoul-Younes *et al.* first showing that mutation of residues along or near the loops connecting blades 1 and 2 of the $G\beta$ torus was sufficient to disrupt GIRK channel activation. Subsequent work by Mirshahi *et al*.[160] and Zhao *et al.*[161] narrowed this to five specific residues within these loops (Ser67, Thr86, Thr87, Thr128, and Gly131) as playing a crucial role in GIRK activation, while Li *et al.*[162] recently reported the ability of the C-terminal region of $G\beta_2$ (residues 271–305) to induce GIRK channel activation. It should be noted, however, that in addition to $G\beta$, $G\gamma$ has been shown to be essential for G protein activation of GIRK channels. A recent study by Peng *et al.* demonstrated that residues 35–71 of $G\gamma_2$ are required for full

stimulation of GIRK4 currents by $G\beta_1\gamma_2$[108]. Further, within this region, ten residues form an intricate network of interactions with Gβ to determine the stimulatory effects on the channel while Asp36 and Asp48 maintain the conformation of the $G\beta_1\gamma_2$ subunits to allow full stimulation of GIRK4. Together, these results highlight the fact that Gβγ regulation of GIRK channels may be much more complicated than originally believed and illustrate the need for further research in this area.

Studies examining specificity of GIRK channel regulation have further shown that only Gβγ dimers containing $G\beta_{1-4}$ could enhance GIRK channel activity while those containing $G\beta_5$ subunits actually suppress it[163-168]. While the exact reason for this discrepancy is still being elucidated, a plausible explanation presented by Lei *et al.*is that $G\beta_5$ containing dimers actually displace activating Gβγ pairs by competitively binding to the same regions on the cytoplasmic domains of the GIRK channels[169]. Although no hypothesis was put forth to explain how this would prevent channel opening, given that $G\beta\gamma_5$ is the most divergent of the Gβ subunits, it is possible that while sufficient sequence identity exists between the isoforms to permit binding to cytoplasmic domains, critical residues necessary for channel activation may be missing. As such, by competitively displacing activating Gβγ dimers, $G\beta_5$ pairs could occupy binding sites and prevent channel activation. Conversely, however, Xie et al. recently showed that $G\beta_5$ subunits in complex with members of the Regulator of G protein Signaling (RGS) 7 family bound to the C-terminal cytoplasmic domains of GIRK channels in order to facilitate their coupling to $GABA_B$ receptors[170]. In doing so, they found that the $G\beta_5$/RGS complex acted to influence the sensitivity of the inhibitory signaling pathway in hippocampus and that further, the absence of the $G\beta_5$ subunits disrupted the temporal fidelity of the GIRK response. Such discrepancies highlight that the role of $G\beta_5$ subunits in regulating potassium currents merits further investigation.

While a postsynaptic role for GIRK channels has been recognized in many studies, consistent presynaptic labeling of these channels via immunostaining and electron microscopy in the proximity of the active zone also hints for a role in modulating exocytotic release[121,155,171-173]. At least in the case of GABA signaling, there is evidence to support this assumption as recent reports from Ladera et al.[171] as well as Michaeli and Yaka[173] suggest new mechanisms in which presynaptic GIRK channels play a significant role. For example, Ladera et al. demonstrated via electron microscopy, that GIRK channels and $GABA_B$ receptors were co-expressed in a restricted subset of cerebrocortical nerve terminals and that further, these GIRK channels mediated the inhibition of glutamate release[171]. Similarly, Michaeli and Yaka recently proposed a new mechanism for dopamine-induced inhibition of $GABA_A$ neurotransmission whereby activation of D_2-like receptors is thought to lead to activation of presynaptic GIRK channels in ventral tegmental neurons[173]. As opposed to postsynaptic GIRK regulation, however, such effects may not be mediated through $G\beta\gamma$ subunits. In the case of the $GABA_B$ receptor-GIRK pathway in cerebrocortical nerve terminals, responses exhibited resistance to pertussis toxin, whereas in the case of $GABA_A$ currents in the ventral tegmental area, the authors propose regulation through protein kinase A substrates given attenuation of effects with protein kinase A inhibitors. It remains to be elucidated whether this represents regulation unique to presynaptic GIRK channels in addition to the well-characterized regulation by $G\beta\gamma$ subunits.

Although a great deal of work has been done to decipher the mechanism by which $G\beta\gamma$ subunits regulate activation of GIRK channels and thus synaptic transmission, many questions remain unanswered. Given the diversity of binding sites on both the channel and the G protein, it is possible that multiple dimers bind to the channel at the same time to elicit the rotation and expansion of the N- and C-termini required for GIRK channel activation[154]. How this

may occur and how it would affect synaptic regulation remains to be seen but such a possibility certainly highlights that a great deal of work still remains.

Modulation of Synaptic Transmission Downstream of Ion Channels: Gβγ Modulation of SNARE Proteins

While G protein modulation of calcium and potassium entry is well established, more recently, modulation of synaptic transmission distal to calcium entry has been demonstrated. G protein modulation of vesicle release in a manner independent of calcium entry via calcium channels was first noted by Silinsky in 1984, who observed that evoked acetylcholine release at the frog neuromuscular junction could be reduced following activation of presynaptic adenosine A1 receptors[174]. He suggested that this inhibition was exerted at an intracellular site associated with the exocytotic process, such as the synaptic vesicles or the active zone, as miniature end plate potentials could still be reduced when the normal route of calcium entry was bypassed[174,175]. These observations have been corroborated over the years as studies investigating receptor function in the hippocampus and other brain regions have indicated that activation of $G_{i/o}$-coupled presynaptic receptors such as such as $GABA_B$, muscarinic, metabotropic glutamate (mGluR), serotonergic, and opioid receptors all result in a reduction in the frequency of miniature excitatory post-synaptic currents[175]. Similarly, the use of agents such as ionomycin and α-latrotoxin which enhanced secretion while bypassing calcium channels lent further support to this conclusion as GPCR-mediated inhibition was maintained in permeabilised cells[75,176]. Taken together, these results suggested the presence of a novel mechanism controlling vesicle release which needed to be characterized.

Given that receptor-mediated inhibition can be mimicked by treatment with non-hydrolyzable GTP analogues[177-179], a great deal of work went into identifying the G protein responsible for mediating the effect. This was initially challenging due to an inability of

exogenous peptides to access presynaptic terminals but was overcome by direct injection of Gβγ subunits into the Calyx of Held[180] and lamprey reticulospinal-motor neuron synapses[74]. In the latter case, Gβγ subunits not only were able to inhibit evoked transmitter release, but did so without an effect on presynaptic calcium entry[74] suggesting that these subunits were responsible for the observed inhibition. Subsequent injection of a Gβγ scavenger, G protein-coupled receptor kinase 2 (GRK2)[74] or phosducin[75] supported this, as the inhibitory actions of Gβγ were completely alleviated. Investigations into the mechanism by which Gβγ inhibited vesicle exocytosis initially focused on known effectors in Gβγ signaling cascades. However, as blockade of classical effectors did little to attenuate Gβγ-mediated inhibition[74] and the onset of inhibition due to laser uncaging of 5HT was too rapid to affect docking and priming mechanisms[76], it was proposed that Gβγ may act directly upon the already-primed exocytotic machinery. In fact, inhibition was already initiated by 20 ms after uncaging 5HT, suggesting that both the GPCR and the Gβγ were close to the active zone. Interestingly, the ability of Gβγ to modulate the inhibitory effect on exocytosis was abolished by treatment with botulinum toxin A, which cleaves 9 amino acids from the C-terminus of SNAP-25[76,77,81,181,182]. The relevance of this C-terminal region of SNAP-25 was additionally demonstrated as the C-terminal 14 amino acid peptide from SNAP-25 itself eliminated the Gβγ-mediated inhibition[75,76]. In addition, removal of the C-terminal residues from SNAP-25 decreased binding to Gβγ *in vitro*[79,81,185]. These findings provided a "fingerprint" for studies of the mechanism of inhibition of exocytosis downstream from modulation of voltage-dependent Ca^{2+} channels directly on the exocytotic fusion apparatus that later studies have taken advantage of[77,183,184,185]

In vitro binding studies also demonstrated direct interaction between Gβγ subunits and syntaxin 1A, SNAP-25B and VAMP/synaptobrevin that make up the SNARE complex[74,75,79,81] while subsequent electrophysiological studies, fluorescence-based assays, and PC12 "cracked cell"-

based amperometry studies provided evidence of Gβγ binding to the H_3 SNARE domain of syntaxin and confirmed the importance of the carboxy-terminal residues of SNAP-25[79,185]. Additional sites of interaction may be important including the H_{abc} domain[79] or even the C-terminal transmembrane domain of syntaxin, which has been suggested to potentially form a binding pocket for anesthetic molecules[186]. Similarly, mutagenesis studies suggest SNARE binding sites on Gβγ subunits may reside outside the Gα binding face, the site of interaction with many Gβγ effectors[75,186] demonstrated that mutation of residues that contact Gα subunits, as well as numerous other effectors such as adenylyl cyclase, GRK2, and phospholipase C β2, did not induce a loss of function in the ability of the Gβγ subunit to inhibit calcium-triggered exocytosis. Rather, several mutations demonstrated increased potency for inhibiting secretion; suggesting further studies are necessary to characterize the binding surface required for Gβγ-SNARE interactions.

Regardless of the site at which Gβγ binds to SNARE proteins, in doing so, it is thought to prevent the tight zippering of the SNARE complex necessary to drive membrane fusion, and thus can inhibit vesicle exocytosis. However, the H_3 domain and the C-terminus of SNAP-25 are also known to constitute functionally important calcium-dependent synaptotagmin binding sites, and detailed examination has revealed that Gβγ subunits and synaptotagmin actually compete with one another for binding to the SNARE proteins as calcium levels increase; at low intracellular calcium, Gβγ binding predominates, while after increasing intracellular calcium, synaptotagmin binding actually competes with Gβγ[9]. Although the significance of such competition is as yet unknown, the current working hypothesis is that Gβγ inhibits exocytosis by competing with synaptotagmin for binding to the SNARE proteins. Increasing intracellular calcium due to repetitive stimulation of neurons may serve to attenuate this by increasing synaptotagmin's affinity for the SNARE proteins and allowing it to displace Gβγ subunits from the exocytotic

machinery. Thus, depending on presynaptic $G_{i/o}$-coupled GPCR activation and calcium influx in response to synaptic activity, it is possible that G$\beta\gamma$-mediated regulation of synaptic transmission could occur independently through more than one mechanism, or potentially even be additive or synergistic at a particular synapse (see Figure 5). These has recently been corroborated, as Hamid et al., demonstrated that $5HT_{1b}$ and $GABA_B$ receptors colocalized to the same terminal inhibited evoked release through different mechanisms[77].It should be noted, however, that regardless of whether G protein modulation occurs via calcium currents or not, intact SNARE proteins have been shown in each instance to be required for the effect to be seen[188,189,190]. Furthermore, synaptotagmin or another calcium sensor in addition to intact SNARE was important for G protein modulation of calcium dependent miniature endplate potentials, but not calcium independent miniature endplate potentials[188].

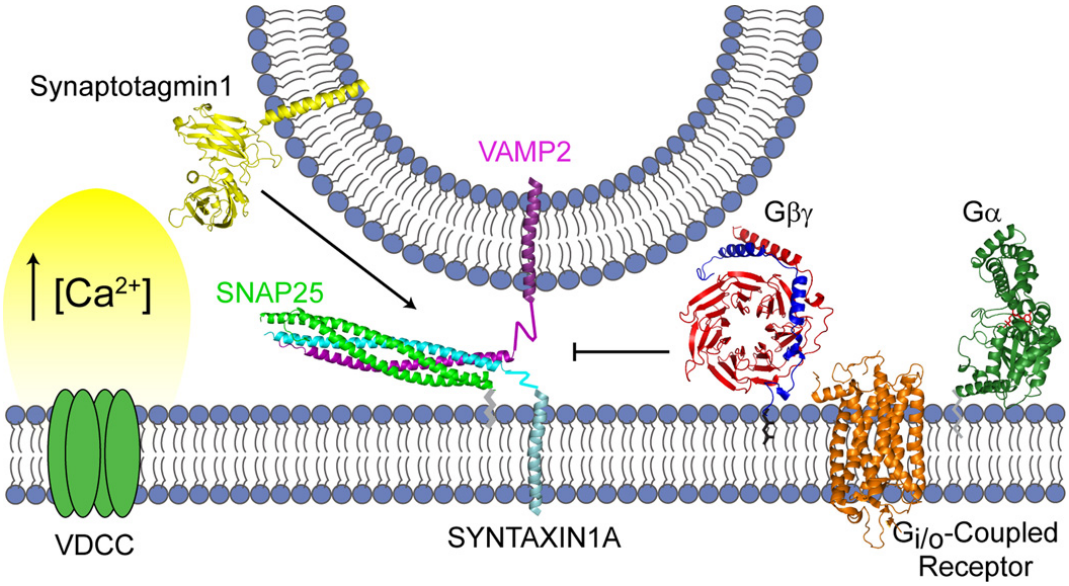

Figure 5. Hypothesis of Gβγ regulation of presynaptic vesicle release. Synaptic vesicles are primed by a tethering interaction between VAMP2 on the vesicle and the SNAP-25/syntaxin 1A dimer at the plasma membrane. At low intracellular concentrations of calcium, activation of $G_{i/o}$-coupled receptors results in release of Gβγ that will bind to the SNARE proteins and prevent binding of synaptotagmin. However, high enough intracellular calcium concentrations, such as with repetitive neuronal stimulation, synaptotagmin is able to compete with Gβγ for binding to SNARE, and thereby promote fusion of the vesicles with the plasma membrane. Figure adapted from Wells et al. (Wells et al., 2011).

While the implications for such a graded physiological mechanism are profound, currently little is known about the occurrence or relevance of this mechanism *in vivo*. Studies examining rhythmic motor activities in vertebrate species, have suggested a role for Gβγ interactions in modulating fictive locomotion, which drives the coordinated contraction of muscles necessary for behaviors such as swimming. In their 2005 paper, Schwartz *et al*., demonstrated that inhibition of glutamate release via activation of $5HT_{1D}$ receptors prolonged the frequency of ventral root bursting in lamprey reticulospinal neurons by presynaptically inhibiting synaptic transmission[191]. In doing so, 5-HT was shown to slow the rhythm of fictive locomotion[76,78,191,192]. As extensive evidence previously demonstrated a role for Gβγ/SNARE interactions in the lamprey during serotonergic modulation, the authors suggest that 5-HT mediates its effects through activation of presynaptic receptors to inhibit transmitter release and decrease glutamatergic synaptic drive[191]. This mechanism was elucidated further in 2009, when Gerachshenko *et al.* demonstrated that 5-HT_{1D} receptor-mediated reductions in glutamate release acted to modulate locomotor rhythms[76]. During physiologically relevant trains of activity similar to those that evoke locomotion, the authors were able to show that 5-HT/Gβγ-mediated inhibition is relieved over time, consistent with the idea that rising presynaptic calcium concentrations permit synaptotagmin competition with Gβγ[76]. As a result, frequency-dependent increases in synaptic concentrations of glutamate are observed which serve to reestablish synaptic vesicle release[76]. Modulation of locomotor patterns and motor outputs by presynaptic GPCRs has further been explored in other vertebrate species including Xenopus[193], neonatal rats[194], and zebrafish [192]. For example, Gabriel et al. show that 5-HT is endogenously released during fictive locomotion in juvenile and adult zebrafish and acts to potentiate inhibitory synaptic transmission resulting in a decrease in the locomotor frequency, similar to that seen in lamprey[192]. While the exact mechanism is not elucidated in their papers, it is conceivable that

much like what is seen in lamprey, release of Gβγ subunits modulate SNARE function to limit frequency and duration of synaptic vesicle release and thus alter locomotor behaviors.

While such effects in lower vertebrate species is interesting, extrapolating these results to mammals is difficult, particularly as very few of the mechanisms by which $G_{i/o}$-coupled GPCRs modulate synaptic transmission in humans have been fully explored; further, those that have primarily point to activated Gβγ modifying channel properties. Some recent studies have begun to counteract this, giving evidence for the relevance of the Gβγ/SNARE mechanism in a variety of systems. For example, insulin secretion from pancreatic β cells has been shown to be reduced following activation of GPCRs in a number of ways, the most powerful of which is a distal inhibitory effect occurring downstream of increased intracellular calcium[195]. Zhao *et al.,* demonstrated in 2010 that the ability of noradrenaline to mediate this inhibition was due to a reduction in the number of exocytotic events without changes in vesicle size or fusion pore properties[185]. Further efforts attributed these effects to Gβγ subunits as the βγ-activating peptide, mSIRK, inhibited exocytosis to a similar extent as noradrenaline, while anti-Gβγ antibodies were able to eliminate it[185]. Further, the authors went on to suggest that such modulation occurs via Gβγ binding directly to SNARE proteins, as pretreatment with botulinum toxin A, which cleaves the C-terminal 9 amino acids of SNAP 25, a functionally important Gβγ binding site[79], was able to prevent noradrenaline from inhibiting exocytosis. Finally when the duration of calcium influx was extended via longer depolarizing pulses, the authors were able to show that both noradrenaline-induced and mSIRK-mediated inhibition was abolished, consistent with the idea that with higher calcium synaptotagmin is able to successfully compete with Gβγ for binding to SNAP-25[75,76,185]. While the relative importance of this mechanism *in vivo* has yet to be fully elucidated, it is conceivable that it may play an important modulatory role,

which is disrupted, in diabetic patients. As such, further efforts into understanding its role may provide insight into disease progression and highlight new avenues of treatment.

Such actions also appear to exist in the central nervous system as Delaney et al. recently provided evidence to support the idea that the nociceptive actions of noradrenaline may be mediated through Gβγ/SNARE interactions in the central nucleus of the amygdala[183]. This region receives dense ascending noradrenergic projections and exhibits high levels of α_{2A} adrenergic receptors, stimulation of which modulates nociceptive information into the amygdala via a presynaptic mechanism[183]. Using whole-cell recording techniques, the authors were able to show that both noradrenaline and clonidine dose-dependently inhibited parabranchial excitatory input into the central amygdala, an effect that was reversed through application of the selective α_2-adrenoceptor antagonist, yohimbine[183]. Using strontium, they went on to demonstrate that the effect occurred via a presynaptic mechanism while application of pertussis toxin or the sulphydryl alkylating agent N-ethylmaleimide both abolished inhibition, confirming a $G_{i/o}$-mediated effect[183]. Such actions were further attributed to Gβγ subunits as application of a Gβγ binding peptide blocked the effect of noradrenaline, while examination of changes in the action potential-driven rise in terminal free calcium levels confirmed the effect was downstream of calcium entry[183]. Finally, direct interactions with SNARE proteins were confirmed through incubation with botulinum toxin A, yielding similar results to previously published reports[75,76,79] whereby noradrenergic inhibition was reduced with increasing incubation times[183] . Similarly Iremonger and Bains demonstrated that dynorphin released from dendritic vesicles in response to postsynaptic activity acted in a retrograde manner to inhibit excitatory neurotransmission through a presynaptic mechanism downstream of calcium entry in the hypothalamus[196]. Using whole-cell patch recordings from magnocellular neurosecretory cells in the paraventricular nuclei of the hypothalamus, the authors showed that dynorphin produced a robust inhibition of

glutamate release onto vasopressin-expressing magnocellular neurosecretory cells via activation of presynaptic κ-opioid receptors. Further, they showed that this effect did not require inhibition of the adenylyl cyclase/protein kinase A pathway, and that it persisted despite inhibition of N- or P/Q-type calcium channels. Rather, the authors suggest that activation of presynaptic κ-opioid receptors directly modulates glutamate release through direct interaction of the Gβγ subunits with the exocytotic machinery, given that such inhibition could be alleviated through rising intracellular calcium, consistent with competition for binding to SNARE proteins by synaptotagmin[196].

While these examples support the idea that Gβγ/SNARE interactions play important roles in transient presynaptic inhibition, questions remain as to whether they play a role in long-term alterations of presynaptic signals associated with long-term potentiation (LTP) or long-term depression (LTD). Activity dependent, long-term changes in synaptic strength associated with LTP and LTD play important roles in CNS functions such as learning and memory, development of neural networks, and fine-tuning of synaptic connections[184]. GPCRs have been shown to be central to induction of LTD, but until recently it was believed that this process was primarily mediated by $G\alpha_i$ subunits. This was recently questioned as Zhang *et al.* sought to investigate whether Gβγ released along with $G\alpha_i$ may also be necessary for the transition from transient inhibition to presynaptic LTD in the hippocampus[184]. Using botulinum toxin-A, the authors showed that the C-terminus of SNAP 25 is critical for LTD but not LTP at Schaffer collateral-CA1 synapses. Cleavage of residues 198–206 on SNAP 25 completely prevented the induction of stimulus-evoked LTD, but alterations in extracellular calcium concentrations demonstrated that this reduction by botulinum toxin-A was not simply due to a reduction in vesicle release probabilities[184]. To examine the possibility that binding of Gβγ to SNAP 25 was a necessary step in mediating the presynaptic component of LTD, the authors then went on to electroporate a 14

amino acid peptide of the C-terminus of SNAP 25 into presynaptic CA3 pyramidal neurons as this peptide had previously been shown to scavenge free Gβγ. Compared to a scrambled peptide, infusion of the SNAP-25 peptide significantly reduced mGluR-mediated presynaptic depression and stimulus-evoked LTD. Further, infusion of a Gβγ binding peptide, mSIRK, which similarly blocked induction of LTD, suggested that scavenging of Gβγ at Schaffer collateral release sites could reverse GPCR mediated reductions in transmitter release[184]. Finally, imaging of calcium concentrations showed that presynaptic calcium influx was not significantly altered following cleavage of SNAP 25, suggesting that presynaptic LTD is not a result of long-term reductions in calcium concentrations[184]. Taken together, such data led the authors to conclude that Gβγ released along with $G\alpha_i$ may play an important role in mediating long term changes at presynaptic release sites and postulate that a greater understanding of such molecular mechanisms will be critical to evaluating the role that presynaptic long-term plasticity plays in persistent changes associated with learning and memory[184].

Additionally, recent studies examined the role of microarchitecture in mediating inhibition of evoked exocytosis through different $G_{i/o}$-coupled GPCRs at the same terminal. Hamid et al. (2014) showed $5HT_{1B}$ and $GABA_B$ receptors localized to the same presynaptic terminal in CA1 pyramidal neurons in the hippocampus each inhibited evoked release through the actions of Gβγ subunits, but did so through different mechanisms; i.e. inhibition of calcium channels ($GABA_B$ receptors) or direct interaction with the SNARE complex ($5HT_{1B}$ receptors)[77]. The authors propose selectivity of effectors is regulated through microarchitecture whereby Gβγ prefers the nearest effector. By removing SNARE complexes using botulinum neurotoxin Type C (BoNT/C), the authors showed the $5HT_{1B}$ receptors were now able to inhibit calcium channels, suggesting that effectors of $5HT_{1B}$ and $GABA_B$ receptors are at opposite ends of primed SNARE complexes, and this separation is sufficient to confer Gβγ specificity[77].

Implications of G protein Modulation of Synaptic Transmission for Disease

As many $G_{i/o}$-coupled GPCRs act as feedback regulators for transmitter release from presynaptic terminals, a greater understanding of the mechanisms by which they operate will be important for understanding normal neural processing, but also because dysregulation of this process can have serious health consequences. For example, mutations in the promoter of the $5HT_{1a}$ serotonin receptor results in abnormally high autoreceptor expression, decreased serotonin release, and increased susceptibility to depression[197]. Patients known to carry a risk-associated α_{2a}-adrenergic receptor *(ADRA2A)* polymorphism have been shown to express increased levels of presynaptic α_{2A}-adrenergic receptors and reduced glucose-stimulated insulin release, resulting in higher incidences of diabetes[198]. This effect was also seen in mice with restricted overexpression of *ADRA2A* in pancreatic islet cells[199]. In Alzheimer's patients, activation of M_2 autoreceptors during anticholinesterase treatment has been suggested to actually contribute to disease progression by reducing acetylcholine release[200] while continuous D_2 autoreceptor–mediated attenuation of dopamine release during dopamine agonist treatment is thought to contribute to the deterioration of cognitive function in Parkinson's patients[201,202]. As such, these receptors represent major targets in drug development, with agonists such as risperidone[203-205] targeting the D_2 dopamine, $5HT_{1a}$ serotonin, and α_{2A} adrenergic receptors for the treatment of schizophrenia, anxiety disorders, and attention deficit hyperactivity disorder, respectively. In addition, a number of drugs at various stages in the development pipeline target this class of receptors, such as M_4 muscarinic receptors for schizophrenia, Parkinson's disease, psychosis and dystonia, H_3 histamine receptors for cognitive deficits, sleep-wake disorders, and attention-deficit disorder, mGluR2 and 3 metabotropic glutamate receptors for schizophrenia and anxiety, and mGluR4 receptors for Parkinson's disease and dystonia. Unfortunately, many current therapies exhibit significant side effects that limit their efficacy. For instance,

risperidone is often associated with severe weight gain while guanfacine can induce orthostatic hypotension in patients. In some cases, these side effects may be due to off-target effects such as seen with risperidone where weight gain is thought to be mainly associated with an affinity of the molecule for serotonin $5HT_{2A}$ receptors; in others, the effects may be because these receptors modulate differing functions in various brain regions. Regardless, these examples highlight the fact that targeting the GPCRs directly may mediate both the therapeutically desirable effect but also untoward side effects. As such, a better understanding of the downstream mechanisms by which presynaptic inhibitory GPCRs modulate exocytosis, such as through Gβγ/SNARE interactions, may reveal more disease-selective targets for therapeutic intervention.

Conclusion

GPCR mediated regulation of synaptic transmission is complex and transcends many different pathways. While a great deal has been learned to date, numerous questions still remain as to the mechanisms underlying this process in the brain as well as other systems. While interactions between Gβγ subunits and classical effectors are well established, newer mechanisms such as Gβγ-SNARE interactions highlight levels of intricacy as yet unknown. Further research into this novel protein-protein interaction will be essential for elucidating its role in regulating synaptic transmission, as well as its integration with other effectors. Only in doing so will it be possible to accurately describe normal synaptic functioning as well as develop strategies to correct situations where it has gone awry.

CHAPTER II

PROJECT RATIONALE AND SPECIFIC AIMS

Synaptic transmission is characterized by exocytotic events, which mediate the release of chemical transmitters to facilitate neuronal communication. Inhibitory presynaptic GPCRs act as feedback regulators in this process, limiting transmitter release from presynaptic terminals via the actions of their G protein $\beta\gamma$ subunits. Although G$\beta\gamma$ subunits have been shown to regulate exocytosis through direct interaction with the exocytotic machinery (the SNARE proteins) to limit both the number and duration of fusion events, relatively little is known about the specificity of this interaction or its physiological consequences. Given the diversity of β and γ isoforms, and the number of effectors they've been shown to act upon, it is conceivable that regulatory mechanisms exist which define the signaling pathways specific G$\beta\gamma$ isoforms participate in. In the case of G$\beta\gamma$ modulation of SNARE function, *in vitro* data supports this idea, as G protein isoforms exhibit differential abilities to bind and inhibit SNARE function[74]. This led us to **hypothesize that endogenous G protein $\beta\gamma$ subunits exhibit specificity when interacting with SNARE proteins to modulate synaptic transmission**. To address this, we proposed the following two aims:

Specific Aim 1: Evaluate the subcellular distribution of Gβγ subunits in the central nervous system and examine localization of unique isoforms to presynaptic terminals expressing α_{2A} adrenergic receptors

1a: Evaluate the distribution of Gβγ isoforms at pre- and postsynaptic terminals in the hippocampus, striatum, cerebellum, and cortex

1b: Evaluate the localization of Gβγ isoforms at presynaptic terminals expressing α_{2A} adrenergic receptors

Specific Aim 2: Determine if Gβγ subunits known to interact with α_{2A} adrenergic receptors may act to modulate noradrenaline release via interactions with SNARE proteins

2a: Determine which Gβγ isoforms couple to the α_{2A} adrenergic receptor upon receptor activation

2b: Characterize which Gβγ isoforms activated by α_{2A} adrenergic receptors go on to interact with SNARE proteins

CHAPTER III

DIFFERENTIAL LOCALIZATION OF G PROTEIN βγ SUBUNITS

Portions of this chapter have been published under the same title in *Biochemistry*

Introduction

Heterotrimeric G proteins play essential roles in cellular communication by transducing extracellular signals from G protein coupled receptors (GPCRs) to a wide range of downstream effectors. The fidelity of this process depends in part upon the G protein itself, as it requires guanine nucleotide-binding α subunits to exchange GDP for GTP and reversibly disassociate from βγ dimers before each can interact with effectors[1]. Originally, signaling was thought to be mediated solely through Gα subunits[206]; however, Gβγ complexes are now widely recognized as independent signaling molecules, with effectors such as adenylyl cyclase, phospholipase C-β, PI 3-kinase and components of the mitogen-activated protein kinase cascade[94,104,207-210]. Additional effectors such as voltage-gated calcium and potassium channels, as well as members of the exocytotic machinery, regulate membrane voltage and neurotransmitter release[74-76,79,81,123,124,154,157]. With such diversity, it is hardly surprising that Gβγ subunits are a highly expressed, structurally diverse family, with 5 and 12 genes encoding 5 β and 12 γ protein subunits, respectively[91,92]. Historically, specificity has largely been attributed to the α subunits as only modest functional differences were observed in the ability of βγ isoform combinations to regulate effectors *in vitro*[211,212]. More recent evidence indicates this may not be the case in intact cells, however, as studies have suggested very specific roles for Gβ and Gγ isoforms[102,184,213-216]. However, while specific receptors and effectors may utilize unique

complements of G protein α β and γ subunits, we have little understanding of which G protein heterotrimers exist *in vivo*, the factors controlling their distribution in tissues, their subcellular expression, or their functional relevance in the context of the whole organism. To this end, a greater understanding of the tissue localization and subcellular distribution of Gβγ isoforms throughout the CNS, as well as at specific synaptic terminals, will be of particular importance in determining which of the many possible combinations are likely to occur physiologically, what roles each may play in regulating signaling cascades, and their impact in disease.

The majority of G protein β and γ subunits have been detected in the central nervous system (CNS)[91,217-222]. Our understanding of their distributions largely stems from *in situ* hybridization studies; specifically, RNA from some β and γ isoforms exhibit wide distributions, while others show more restricted expression to specific brain regions and cell types, possibly reflecting unique functions[98,223-227]. Although a few studies have examined protein expression[223,226-229], efforts at this level have been less reliable as high sequence identity between isoforms has limited the development of reliable subunit-specific reagents[230]. Proteomic analysis offers a powerful way to deepen our understanding of the regional and subcellular localization patterns of Gβγ isoforms as they can be undertaken using endogenous tissue without the need for isoform specific antibodies. Studies examining synaptic proteomes to date have largely focused on analyzing the global expression of proteins involved in synaptic functions[231-240] and as yet no study has sought to specifically examine G protein localization patterns. As a result, while a few β and γ isoforms have been identified or even localized to subcellular fractions in discovery-based experiments[241-245], the majority have yet to be described. Such studies demonstrate that even at isolated nerve endings, cells express large numbers of proteins, making identification of all of the proteins in a sample problematic. Further, highly abundant proteins may mask those expressed at lower levels. To overcome these

problems, we applied a targeted proteomics approach known as multiple reaction monitoring (MRM)[246,247], which enabled us to accurately identify unique G protein isoforms in complex mixtures. Using this approach we analyzed regional and subcellular localization patterns of Gβ and Gγ isoforms in different brain regions before specifically looking at localization patterns at synaptic terminals. Interestingly, we found that these subunits exhibit distinct regional and subcellular localization patterns throughout the CNS, suggesting roles for individual subunits in regulating specific signaling pathways.

Experimental Procedures

Part A: Examining regional and subcellular localization of G protein βγ subunits within the CNS

Protein Standards. $G\beta_1\gamma_1$ was purified from bovine retina as described previously[248]. Recombinant $G\beta_1\gamma_2$ and $G\beta_5\gamma_2$ were expressed in Sf9 cells and purified via a His6-tagged $G\gamma_2$ using nickel-nitrilotriacetic acid affinity chromatography (Sigma-Aldrich, St. Louis, MO). Human Gγ subunit cDNAs for $G\gamma_{4,5,7,11,13}$ were subcloned by PCR from pcDNA3.1+ clones (Missouri S&T cDNA Resource Center) into pGEX-6p-1 (GE Healthcare). The resultant vectors, hGgamma($_x$).pGEX-6p-1, were sequence verified and GST-fusion proteins were expressed in Rosetta™ Competent Cells (EMD Millipore). After induction with 1mM IPTG followed by a four hour incubation at 37°C, the resultant Gγ proteins were batch purified using Glutathione Sepahrose 4 Fast Flow (GE Healthcare) and eluted with 10 mM reduced free acid glutathione (Calbiochem).

Animals. Adult, male C57Bl6/J mice were decapitated and cortex, cerebellum, neostriatum (referred to as striatum), and hippocampus dissected, frozen on dry ice, and stored at -80°C until processed. To minimize post-mortem differences, all brain regions were dissected at the same time and processed in parallel. All animal protocols were carried out in accordance with the recommendations in the Guide for the Care and Use of Laboratory Animals of the NIH, and were approved by the Vanderbilt Institutional Animal Care and Use Committee.

Antibodies. The following primary antibodies were used for immunoblotting (dilutions indicated): rabbit anti- Gβ, (Santa Cruz, catalog #sc-378, 1:15,000); mouse anti-N-Methyl-D-Aspartate Receptor-1 (NMDAR1) (BD Pharmingen, catalog #556308, 1:2000); mouse anti-postsynaptic density-95 (PSD-95) (Neuromab, catalog #75-028, 1:20,000); mouse anti-

Glyceraldehyde-3-Phosphate Dehydrogenase (GAPDH) (Millipore, catalog #MAB374, 1:20,000), and mouse anti-syntaxin-1 (Santa Cruz, catalog #sc-12736, 1:2000). Horseradish peroxidase-conjugated secondary antibodies were obtained from Perkin-Elmer and used at the following dilutions: goat anti-rabbit (1:20,000) and goat anti-mouse (1:10,000 for NMDAR1 and syntaxin; 1:20,000 for PDS-95 and GAPDH).

Synaptosome preparation and subcellular fractionation. Subcellular fractions were prepared using a modified protocol based on Phillips et al (2001)[249]. Briefly, four whole mouse cortex (CTX), cerebellum (CRB), striata (Str), or hippocampi (Hippo) were pooled and homogenized in 10ml of a 0.32M sucrose solution [0.32M sucrose, 4.2mM potassium 4-(2-hydroxyethyl)-1-piperazineethanesulfonate (HEPES) pH 7.4, 0.1mM $CaCl_2$, 1mM $MgCl_2$, 1.54μM aprotinin, 10.7μM leupeptin, 0.95μM pepstatin, and 200mM phenylmethylsulfonyl fluoride (PMSF)]. Homogenates were centrifuged at 1,000 x g at 4°C for 10 minutes to pellet nuclei and membrane debris before supernatants were transferred to clean conical tubes. Pellets were resuspended in 10ml 0.32M sucrose, the centrifugation step repeated, and supernatants combined. Following mixing, supernatants were centrifuged at 10,000 x g at 4°C for 20 minutes to produce crude synaptosome preps. Supernatants were discarded and pellets gently resuspended in 4ml hypotonic lysis buffer (20mM Tris pH 6.0, 0.1mM $CaCl_2$, 1mM $MgCl_2$, 1% Triton X-100, 1.54μM aprotinin, 10.7μM leupeptin, 0.95μM pepstatin, and 200μM PMSF) before being incubated on ice for 20 minutes to lyse membranes. Lysates were cleared via ultracentrifugation at 100,000 x g, 4°C for 2 hours in a SW-55 Ti rotor (Beckman Coulter) and supernatants (consisting of the 'perisynaptic/cytosolic' fraction) transferred to clean conical tubes. Pellets were resuspended in 1ml Tris buffer (20mM Tris pH 8.0, 1% Triton X-100 1.54μM aprotinin, 10.7μM leupeptin, 0.95μM pepstatin, and 200μM PMSF) and incubated on ice for 20 minutes. Lysates were centrifuged at 10,000 x g at 4°C for 30 minutes and supernatants

containing enriched presynaptic fractions collected. Finally, pellets were resuspended in 200ml 1x phosphate buffered saline/1% SDS and centrifuged at 10,000 x g at 4°C for 30 minutes. Supernatants containing enriched postsynaptic fractions were collected. Protein concentrations were determined with a BCA assay kit (Pierce).

Immunoblot analysis. To examine enrichment of pre- and postsynaptic fractions, Western blot analysis was performed. 7μg of each fraction was diluted in 4X SDS-PAGE sample buffer containing 100mM dithiothreitol, heated for 5 minutes at 70°C, and resolved on 10 or 15% SDS-PAGE gels. Proteins were transferred electrophoretically to a nitrocellulose membrane in cold transfer buffer consisting of 200ml 3-[cyclohexylamino] 1-propanone-sulphonic acid (CAPS), 200ml methanol, and 1600ml water. Following transfer, membranes were ponceau stained and cut between appropriate molecular weight markers. Membranes were blocked with slight agitation for 1 hour in a buffer of tris-buffered saline (TBS) with 5% milk and 0.1% Tween-20 (Sigma-Aldrich). Membranes were then washed 5 times for 5 minutes in TBS with 0.1% Tween-20 on a shaker before being incubated with appropriate primary antibodies in TBS with 5% milk and 0.2% Tween-20 on a shaker table at 4°C overnight. The next day, membranes underwent five 5-minute washes on a shaker table in TBS with 0.1% Tween-20 before appropriate secondary antibodies were diluted into TBS with 5% milk and 0.2% Tween-20 followed by gentle agitation on a shaker with the membranes for 1 hour at room temperature. Finally, membranes were washed three times for 10-minute washes in TBS with 0.1% Tween-20 followed by two 15-minute washes in TBS. Immunoblots were developed using Western Lightning™ Chemiluminescence Reagent Plus (NEL104) from Perkin-Elmer as per their published protocols. Imaging was collected using a Bio-rad Imager.

Development and Validation of Targeted Mass Spectrometry Methods. Purified Gβγ isoforms or enriched protein pre- and postsynaptic fractions were separated by SDS-PAGE (15% acrylamide) and stained with colloidal Coomassie Blue (Invitrogen). Gel bands corresponding to the molecular weights of Gβ and Gγ subunits were excised, chopped into $1mm^3$ pieces, reduced with 100mM dithiothreitol, alkylated with 200mM iodoacetamide, and digested with trypsin. Individual G protein subunit digests from purified proteins were analyzed via nanoflow reverse-phase liquid-chromatography-tandem mass spectrometry (LC-MS/MS) on an LTQ-Orbitrap XL mass spectrometer (Thermo Scientific) while those from enriched protein synaptic fractions were analyzed on an LTQ-Orbitrap Velos mass spectrometer (Thermo Scientific). Peptides were loaded onto a capillary reverse phase analytical column (360mm O.D. x 100mm I.D.) using an Eksigent NanoLC HPLC and autosampler. The analytical column was packed with 20cm of C18 reverse phase material (Jupiter, 3mm beads, 300Å, Phenomenex), equipped with a laser-pulled emitter tip. Peptides were gradient-eluted at a flow rate of 500nL/min, and the mobile phase solvents consisted of 0.1% formic acid, 99.9% water (solvent A) and 0.1% formic acid, 99.9% acetonitrile (solvent B). A 45-minute gradient was performed for purified G protein samples, consisting of the following: 0-10 min, 2% B (during sample loading); 10-28 min, 2-40% B; 28-34 min, 40-90% B; 34-35 min, 90% B, 35-37 min, 90-2% B, 37-45 min, 2% B (column equilibration). In comparison, a 90 minute gradient was performed for G protein samples isolated from enriched protein presynaptic fractions consisting of the following: 0-10 min, 2% B; 10-50 min, 2-35% B; 50-60 min, 35-90% B; 60-65 min, 90% B, 65-70 min, 90-2% B, 70-90 min, 2% B. Upon gradient-elution, peptides were mass analyzed on a LTQ Orbitrap XL or LTQ Orbitrap Velos mass spectrometer (Thermo Scientific). The instruments were operated using a data-dependent method with dynamic exclusion enabled. Full scan (m/z 300-2000) spectra were acquired with the Orbitrap as the mass analyzer (resolution 60,000), and the five most abundant (LTQ Orbitrap

XL) or sixteen most abundant ions (LTQ Orbitrap Velos) in each MS scan were selected for fragmentation via collision-induced dissociation (CID) in the LTQ. For selected LC-MS/MS analyses, the LTQ Orbitrap Velos was operated using a combination method of data-dependent and targeted scan events. Targets were of specific m/z values corresponding to unique Gβ or Gγ peptides selected from theoretical *in silico* digestions of the G protein subunits. *In silico* digests were generated by importing FASTA sequences for the G protein isoforms from the UniprotKB protein database (www.uniprot.org) into MS Digest (http://prospector.ucsf.edu/prospector/mshome.htm) and performing theoretical tryptic digests. Theoretical digests accounted for variable modifications of carbamidomethylation of cysteine and oxidation of methionine. Digest results were then imported into spreadsheets and sorted to identify and remove precursor peptides that shared identical m/z values as well as any precursors that contained missed cleavages. The remaining peptides further screened for uniqueness by performing a protein basic alignment search tool (BLAST) search. Unique peptides identified from data-dependant and targeted Velos scans were identified via database searching with Sequest[250] (Thermo Scientific). Tandem mass spectra were searched against *Bos taurus, Mus musculus, or Homo sapiens* subsets of the UniprotKB protein database, and search results were assembled using Scaffold 3.0 (Proteome Software). Although isoforms were purified from bovine retina, as well as cloned using human sequences, peptides unique to each Gβγ isoform being monitored were shown to be identical across all three species enabling use of these proteins for assay development. All searches were configured to use variable modifications of carbamidomethylation on cysteine and oxidation of methionine. The selected peptides from each G protein β and γ subunit were validated via manual interrogation of the raw tandem mass spectra using QualBrowser software (Xcalibur 2.1.0, Thermo Scientific) against theoretical fractionation patterns generated in MS Product

(http://prospector.ucsf.edu/prospector/mshome.htm). As an additional validation criterion, the observed monoisotopic m/z value was required to be within 5ppm of the theoretical m/z value for a given peptide. PPM was calculated using the formula:

$$ppm = \frac{(oberved\ monoisotopic\ mass - \ theoretical\ monoisotopic\ mass)}{observed\ monoisotopic\ mass}\ x\ 1\ million$$

where monoisotopic mass refers to the monoisotopic mass of the precursor peptide. Identified peptides unique to G protein isoforms were selected, and their MS/MS spectra examined to select precursor/product ion transitions for targeted MRM experiments. MRM methods were generated in Skyline[251] before being exported and employed for G protein targeted experiments on a TSQ Vantage triple quadrupole mass spectrometer (Thermo Scientific). Unscheduled MRM runs were performed on purified Gβγ isoforms when available, as well as enriched pre- and postsynaptic fractions from mouse cortex, to evaluate intensities of precursor and product ions identified in early discovery proteomic runs. The resulting MRM data were imported and analyzed in Skyline. Extracted ion chromatographic peaks were manually interrogated and correct peaks chosen based on retention times, how well the relative distribution of transition ions matched those from discovery experiments, and dot product values. Dot product values were calculated by comparison of transition ion intensities in MRM data relative to product ion intensities observed in tandem mass spectra acquired in LTQ-Orbitrap discovery experiments. Following validation, precursor and product ion lists were refined to only include the optimal precursor and transitions necessary to accurately identify each G protein isoform. Refined methods were required to include at least two distinct peptides for each G protein isoform, as well as three transitions for each peptide being monitored. These data and criteria were then used to generate scheduled MRM methods that could be applied to pre- and postsynaptic fractions from different brain regions.

Application of targeted proteomics methods to enriched synaptic fractions. Once refined, scheduled MRM methods were applied to in-gel digested proteins from mouse brain enriched pre- and postsynaptic fractions isolated from cortex, cerebellum, hippocampus, and striatum. 50μg of total protein from each fraction was separated by SDS-PAGE for each brain region and digested as described. Gβ peptides were analyzed by a single 60 minute scheduled MRM analysis while Gγ peptides were split into two 60 minute scheduled MRM runs. Biological samples were randomized to ensure any drift in assay performance would not affect subsets disproportionally. Briefly, utilizing a trap column setup, peptides were first loaded onto a 100 μm x 4 cm C18 reverse phase column, which was connected in line to a 20cm by 100mm (Jupiter 3mm, 300Å), analytical column. Peptides were gradient-eluted into a TSQ-Vantage (Thermo Scientific) using a nanoelectrospray source. Peptides were resolved using an aqueous to organic gradient with a 60 minute total cycle time. Scheduled instrument methods encompassing a 10 minute window around the measured retention time along with calculated collision energies were created using Skyline. Q1 peak width resolution was set to 0.7, collision gas pressure was 1 mTorr, and a cycle time of 5 seconds was utilized. The resulting RAW instrument files were imported into Skyline for peak-picking and quantitation. Data analysis using Skyline was performed to assess enrichment of individual G protein subunits in pre- or postsynaptic fractions. Transition ion intensities were summed for each precursor and these data were used to generate extracted ion chromatographic peaks of co-eluting transitions. As described previously, chromatographic peaks were manually interrogated and correct peaks chosen based on retention times, dot product values, and relative distributions of transition ions. For peptides where a correct peak could confidently be chosen, a signal to noise (S/N) ratio of at least 30 was required to be included in analyses; those that did not meet this criterion were removed from further analyses. Four internal reference peptides, SSAAPPPPPR, TASEFDSAIAQDK,

ELGQSGVDTYLQTK, and LTILEELR (Table 2) were used to evaluate drift in assay performance as well as enable data to be normalized. Each reference peptide (5fmol) was spiked in to all samples and monitored throughout all MRM experiments. BSA controls were monitored at regular intervals between samples to evaluate instrument performance. The integrated area under the curve was calculated for all transitions. Coefficients of variation (CV) were calculated for BSA controls and spiked in reference peptides using $CV = \frac{(average\ total\ AUC)}{(SD\ of\ total\ AUC)}$, where AUC represents the integrated area under the curve for all transitions, and SD represents the standard deviation of the total AUC. To allow comparison between experiments done on different days, the integrated area under the curve for each peptide was normalized relative to the internal reference peptide that was closest in retention time to it. This generated a normalized total area for each peptide.

Peptide Sequence	Precursor m/z	Charge	Collison Energy	Product Ion m/z
SSAAPPPPPR	493.7683	2+	18	287.1728, 379.2327, 476.2855, 670.3910
TASEFDSAIAQDK	695.8324	2+	24	740.4028, 855.4298, 1002.4982, 1218.5728
ELGQSGVDTYLQTK	773.8956	2+	26	761.4286, 876.4553, 1032.5452, 1119.5772
LTILEELR	498.8018	2+	18	214.1306, 427.2539, 669.3805, 782.4646

Table 2. Internal reference peptides and MRM transitions added to all G protein samples.

A modified labeled reference peptide (LRP) method[252] was applied using the internal reference peptides described above to compare brain regions and subcellular fractions for each G protein isoform. To evaluate expression of each G protein isoform using this method, a ratio between the normalized total area for each peptide being monitored and the total area for one internal reference peptide, ELGQSGVSTYLQTK, was calculated. The ratios for all peptides monitored for a given isoform were then averaged and the averages plotted for each protein. Fold differences were calculated to compare expression of each G protein isoform in pre- *and* postsynaptic fractions within a brain region, as well as pre- *or* postsynaptic fractions between brain regions. To compare expression within a brain region, the average normalized total area calculated from the postsynaptic fraction was divided by the average normalized total area calculated from the presynaptic fraction of that same region (e.g. CTX post normalized total area /CTX pre normalized total area). To compare expression in presynaptic fractions of different brain regions, the average normalized total area from a presynaptic fraction in one brain area was divided by the average normalized total area from a presynaptic fraction from another brain region (e.g. CTX pre normalized total area/CRB pre normalized total area). This was also done for comparisons of postsynaptic fractions between brain regions.

Statistical Analysis. To evaluate data for comparison of brain regions and subcellular fractions, a two way ANOVA was used to account for differences in isoform expression that could be due to location in the CNS (i.e. CTX, CRB; referred to as brain region effect), subcellular location (i.e. pre- or postsynaptic; referred to as fraction effect) or the combination of the two (referred to as interaction effect). To determine where specific differences in expression occurred, a Tukey *post hoc* test was used. In the case of $G\beta_5$, data was evaluated using an unpaired t-test.

Part B. Pilot studies examining localization of G protein $\beta\gamma$ subunits at specific synaptic terminals

Note: all flow cytometry and cell sorting experiments were done in collaboration with Dr. Ran Ye from Dr. Randy Blakely's laboratory at Vanderbilt University.

Animals. Adult, male C57Bl/6 mice or adult male HA-tagged α_{2A} adrenergic receptor (α_{2A}AR) KI mice (C57Bl/6 background; provided by Qin Wang at University of Alabama) were decapitated and brains dissected, frozen in liquid nitrogen, and stored at -80°C until processed. To minimize post-mortem differences, all brains were dissected at the same time and processed in parallel. Similarly, adult, male TPH2-ChR2(H13R)-EYFP mice and ChAT-ChR2(123R)-EYFP mice (provided by Randy Blakely at Vanderbilt University) were decapitated and midbrains dissected immediately prior to use in flow cytometry or cell sorting experiments. All animal protocols were carried out in accordance with the recommendations in the Guide for the Care and Use of Laboratory Animals of the NIH, and were approved by the Vanderbilt Institutional Animal Care and Use Committee.

Antibodies. The following primary antibody was used for flow cytometry experiments (dilution indicated): mouse anti-HA Alexa Fluor 647 (Cell Signaling, 1:50). The following primary antibodies were used for immunoblotting (dilutions indicated): rabbit anti-SERT (Frontier Science Institute, catalog #HTT-GP-Af1400, 1:2500), rabbit anti-vesicular acetylcholine transpoter (VAChT) (Synaptic Systems, catalog #139 103, 1:500), mouse anti-Syntaxin 1A (Sigma, catalog #S0664, 1:10,000). Horseradish peroxidase-conjugated secondary antibodies were obtained from Jackson ImmunoResearch and used at 1:10,000.

Synaptosome preparation and enrichment. Synaptosomes were prepared as described in Part A. Initial experiments with HA-tagged α_{2A}AR (HA-α_{2A}AR) mice and later experiments using TPH2-ChR2(H13R)-EYFP and ChAT-ChR2(123R)-EYFP mice, made use of a discontinuous sucrose

gradient in an attempt to enrich synaptosomes and remove any cellular components that may interfere with flow cytometry. For gradient experiments, crude synaptosome pellets were resuspended in 3ml of 0.32M sucrose solution following centrifugation. To create sucrose gradients, 3ml of 0.8, 1.0, and 1.2M sucrose solutions were layered in 14ml ultracentrifuge tubes (Beckman Coulter) at room temperature. Layers were added to the bottom of the tube slowly by increasing density (i.e. 0.8M first, followed by 1.0M and finally 1.2M). Once gradients were created, 3ml of crude synaptosomes were added to the top of the gradient and samples centrifuged at 100,000 x g, 4°C for 2 hours in a SW-40 Ti rotor (Beckman Coulter). Enriched synaptosomes were collected from the 1.0/1.2M sucrose interface and transferred to clean 15ml conical tubes. Fractions were washed with 3ml of 0.32M sucrose and centrifuged at 100,000 x g, 4°C for 30 minutes in a SW-40 Ti rotor (Beckman Coulter). Supernatants were discarded and pellets resuspended in 500ul of stimulation buffer [1 part 10x DPBS pH 6.8-7.0 (26.7mM KCl, 14.7mM KH2PO4, 1379mM NaCl, 80mM Na_2HPO_4 x 7H20), 10mM Hepes pH 7.4, 1.54μM aprotinin, 10.7μM leupeptin, 0.95μM pepstatin, and 200μM phenylmethylsulfonyl fluoride (PMSF)].

Flow cytometry and cell sorting. To fluorescently detect synaptosomes expressing the HA-α_{2A}AR, enriched synaptosome preps were generated from the whole brain of WT or KI mice as described above. Synaptosomes were resuspended in 200μl of stimulation buffer and incubated with anti-HA antibody for two hours on ice. Samples were centrifuged at 10,000 x g at 4°C for 20 minutes and the supernatants discarded. Pellets were resuspended in 3ml of stimulation buffer and the centrifugation step repeated. Supernatants were discarded and pellets resuspended in 500μl stimulation buffer. These samples were further diluted 1:25 in stimulation buffer before being analyzed on a FACS Canto II (Becton Dickson). Fluorescence intensity was determined for 100,000 events within the synaptosome gate. Data were analyzed via FACS DiVA acquisition

software (Becton Dickson). To fluorescently detect synaptosomes expressing EYFP, enriched synaptosome preps were generated from the midbrains of four TPH2-ChR2(H13R)-EYFP or ChAT-ChR2(123R)-EYFP mice and enriched using a discontinuous sucrose gradient. Synaptosomes were resuspended and analyzed as above. Preliminary experiments aimed at isolating serotonergic terminals used fluorescently-activated cell sorting (FACS). Enriched synaptosomes from TPH2-ChR2(H13R)-EYFP mice were prepared as described above using the midbrains from four pooled animals, and samples sorted on a BD FACS Aria II flow cytometer based on EYFP intentisy and forward scatter, using a wildtype control and 1μm beads for reference. The fluorescence excitation wavelength was 488nm and the emission was measured with a filter of 530 nm (with a 30nm band pass). Non-fluorescent, low fluorescence (containing fluorescent and non-fluorescent particles), and high fluorescence fractions were collected for analysis. Following collection, fractions were centrifuged at 10,000 x g at 4°C for 20 minutes to pellet synaptosomes before being frozen at -80°C for later use in western blot analysis or targeted proteomics experiments.

Immunoblot analysis of synaptosome fractions collected via cell sorting. To examine the expression of SERT, VAChT, and synaptic markers in sorted synaptosome fractions collected during FACS experiments, Western blot analysis was performed by Dr. Ran Ye. 10μg of each fraction was diluted in 2X SDS-PAGE sample buffer, equilibrated at RT for 10 minutes, and resolved on 10% SDS-PAGE gels. Proteins were transferred electrophoretically to a PDVF membrane in cold Tris Glycine transfer buffer consisting of 25mM Tris and 192mM glycine. Following transfer, membranes were blocked with slight agitation for 1 hour in a buffer of TBS with 5% milk and 0.1% Tween-20 (Sigma-Aldrich) before being incubated with appropriate primary antibodies in TBS with 5% milk and 0.2% Tween-20 on a shaker table at 4°C overnight. The next day, membranes underwent three 10-minute washes on a shaker before appropriate

secondary antibodies were diluted into TBS with 5% milk and 0.2% Tween-20 followed by gentle agitation on a shaker with the membranes for 1 hour at room temperature. Finally, membranes were washed three times for 10-minute washes in TBS with 0.1% Tween-20. Immunoblots were developed using ECL Chemiluminescence Reagent from Perkin-Elmer and Amersham X-ray films.

Targeted proteomic analysis of fluorescent synaptosome fractions collected via cell sorting. To examine expression of Gβγ isoforms at serotonergic terminals, scheduled MRM methods were applied to in-gel digested proteins from a single fluorescent fraction collected during FACS experiments using TPH2-ChR2(H13R)-EYFP mice. The sample was resuspended in 20μl of 2X SDS-PAGE sample buffer containing 100mM dithiothreitol, heated for 5 minutes at 70°C, and resolved on a 15% SDS-PAGE gel before being stained with colloidal Coomassie Blue (Invitrogen). Gel bands corresponding to the molecular weights of Gβ and Gγ subunits were excised and proteins digested with trypsin as described in Part A. Scheduled MRM methods were applied to in-gel digested proteins as described. Data analysis using Skyline was performed as described in Part A to assess expression of individual G protein subunits at serotonergic terminals. Transition ion intensities were summed for each precursor and these data were used to generate extracted ion chromatographic peaks of co-eluting transitions. As described previously, chromatographic peaks were manually interrogated and correct peaks chosen based on retention times, dot product values, and relative distributions of transition ions. Four internal reference peptides, SSAAPPPPPR, TASEFDSAIAQDK, ELGQSGVDTYLQTK, and LTILEELR (Table 2) were used to evaluate drift in assay performance. Each reference peptide (5fmol) was spiked in to all samples and monitored throughout all MRM experiments. BSA controls were monitored at regular intervals between samples to evaluate instrument performance. As only a single sample was analyzed from FACS experiments involving TPH2-ChR2(H13R)-EYFP mice, the integrated area under the curve was summed for all peptides that met S/N criteria and net AUC plotted for each

isoform. Statistical analysis was not possible as the results are from a single sample and isoforms cannot be directly compared.

Results

Part A: Examining regional and subcellular localization of G protein βγ subunits within the CNS

Synaptosome Subcellular Fractionation Efficiency

In order to assess the localization patterns of different G protein isoforms, we made use of a brain synaptosomal preparation and subcellular fractionation protocol that would allow us to reduce sample complexity (Figure 6A). Synaptosomes are a widely used preparation for studying synaptic biochemistry as they contain the complete presynaptic terminal, including mitochondria and synaptic vesicles, as well as the postsynaptic membrane and postsynaptic density (PSD)[44,53]. To verify the efficiency of our fractionation protocol, we examined the enrichment of well-established synaptic markers in our pre- and postsynaptic fractions. Protein (7mg of total protein) from each isolated fraction was separated on SDS-PAGE gels, electroblotted onto nitrocellulose membranes and immunostained with antibodies against NMDAR1, PSD-95, GAPDH, syntaxin-1 and Gβ, respectively. Figure 6B reveals the high enrichment of NMDAR1 and PSD-95 in the postsynaptic fraction whereas syntaxin-1 is enriched in the presynaptic fraction. Although syntaxin-1 is thought to be primarily concentrated at the site of neurotransmitter release in neurons, it has also been shown to be expressed postsynaptically[253], accounting for its presence in the postsynaptic fraction following enrichment in the present study. Conversely, GAPDH, a cytosolic protein, shows equal expression in both fractions, although expression in pre- and postsynaptic fractions was lower than that seen in cytosolic fractions (data not shown). Similarly, Gβ was expressed equally in both pre- and postsynaptic factions using a pan-Gβ antibody (Figure 6B).

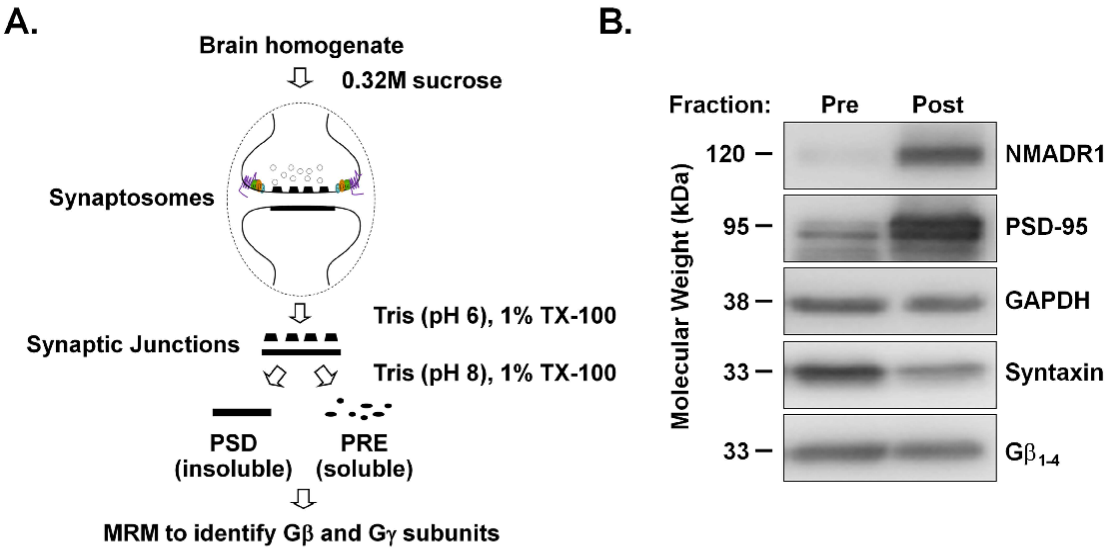

Figure 6. Distribution of marker proteins in pre- and postsynaptic fractions. A) Experimental protocol for the isolation of synaptosomes from mouse brain tissue and the enrichment of pre- and postsynaptic fractions. B) Representative immunoblots for NMDAR1, PSD-95, GAPDH, syntaxin-1, and Gβγ isolated from enriched pre- and postsynaptic fractions of adult mice.

Development and Validation of Targeted Mass Spectrometry Methods

Target peptides and transitions for MRM studies were obtained by analyzing purified, recombinant Gβγ proteins ($G\beta_1$, $G\beta_5$, and $G\gamma_{2,4,5,7,11,13}$ respectively) when available, as well as enriched pre- and postsynaptic fractions from mouse cortex. Figure 7A illustrates a schematic of the workflow for targeted MRM development. *In silico* tryptic digests were initially performed and peptides pre-selected that were unique to a single G protein isoform. Peptides were then further screened for uniqueness by performing a protein BLAST search. Only precursor peptides unique to a single G protein isoform and not found in protein sequences belonging to related or unrelated proteins were chosen. Following tryptic digestion, extracted peptides from purified G protein samples were initially analyzed on an LTQ-Orbitrap XL mass spectrometer while those from enriched pre- and postsynaptic fractions were analyzed on an LTQ-Orbitrap Velos mass spectrometer. Data-dependent LC-MS/MS runs identified >200 proteins in synaptic fractions from gel regions corresponding to the expected molecular weight of Gβ and Gγ subunits (data not shown). From these initial experiments, peptides corresponding to four of the five Gβ isoforms ($G\beta_{1,2,4}$, and $_5$) were identified and validated, as well as 8 of the Gγisoforms ($G\gamma_{2,3,4,5,7,11,12}$, and $_{13}$ respectively). Unique peptides corresponding to $G\beta_3$, $G\gamma_8$, and $G\gamma_{10}$ were not identified in subcellular fractions during discovery experiments. Polymorphisms in the $G\beta_3$ gene have been shown to dramatically alter its amino acid sequence[254] while $G\gamma_8$ is expressed only in olfactory and vomeronasal neuroepithelia[255] and $G\gamma_{10}$ is only a minor isoform in the CNS[228]. Such factors may account for why we were unable to identify unique peptides using published sequences. These isoforms were excluded from the targeted LC-MS/MS analysis. Further, $G\gamma_1$ was not investigated, as its expression is limited to the retina[256]. Figure 7B shows a representative spectrum for the LC-MS/MS identification of a $G\beta_1$ peptide,

ACADATLSQITNNIDPVGR. Gβγ precursor peptides with appropriate m/z values (< 5ppm relative to theoretical values) were fragmented to generate MS/MS spectra. Unique precursor peptides identified in data-dependent runs were verified by manual interrogation of the MS/MS spectra and product ions ranked based on intensity. Discovery experiments were leveraged such that isoform specific peptides showing both strong signal and fragmentation were chosen as precursors and transitions to monitor via MRM. Chromatographic peaks were selected using criteria previously described. If purified samples were available, peptides identified in complex mixtures had to match the RTs for those of the purified sample (Figure 7C). Similarly, relative intensities of transitions were required to mirror those of purified samples and correlate closely with that seen in discovery experiments (Figure 7C). Dot product values were used as an aid to assess how well MRM results matched MS/MS data obtained with the Orbitrap. MRM methods were refined to pare down the number of peptides and transition ions being evaluated. Table 3 shows the list of finalized precursor peptides and product ions being monitored in MRM experiments for each G protein isoform in experimental samples.

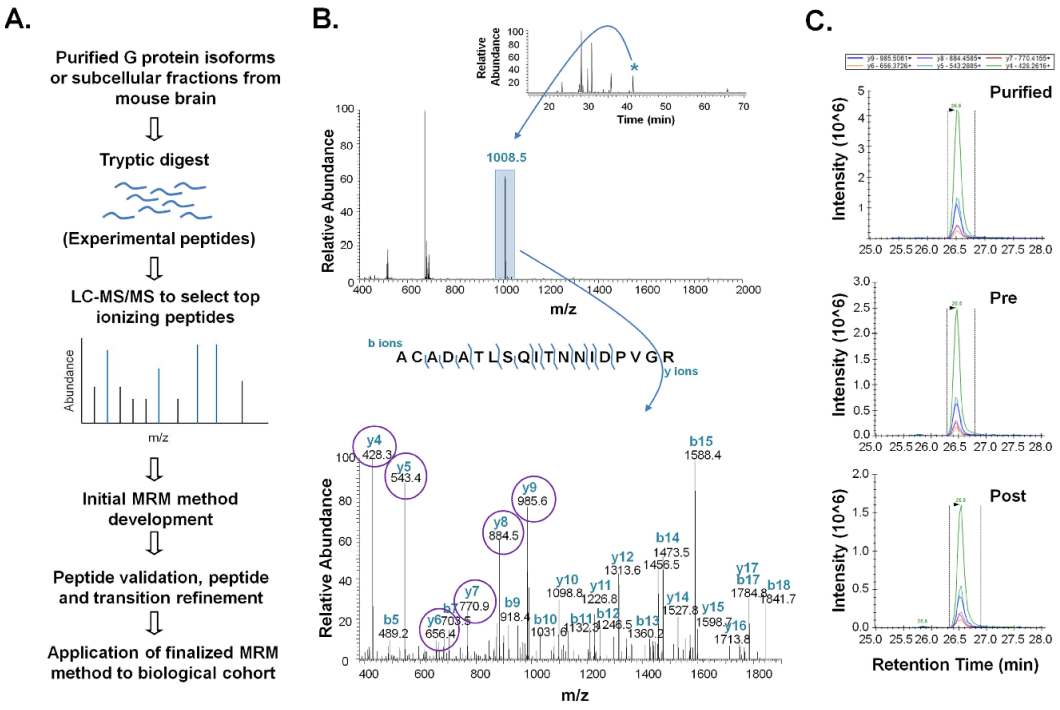

Figure 7. Development and validation of targeted mass spectrometry methods. A) Workflow for the development and validation of multiple-reaction monitoring (MRM) methods. B) LC–MS/MS identification of the Gβ_1 peptide, ACADATLSQITNNIDPVGR. The top panel shows the mass spectrum of peptides eluting at 42 min. The peak at *m/z* 1008.5 (blue) corresponds to the [M + 2H]2+ precursor ion of the Gβ_1 peptide. The inset shows the base peak chromatogram; the asterisk denotes the peak of the peptide at 42 min. The bottom panel shows the MS/MS spectrum of the ion at *m/z* 1008.5. Observed b- and y-type product ions are labeled, and sites of amide bond cleavage are denoted with brackets. Circles indicate product ions imported into initial MRM methods for evaluation. C) Chromatographic traces for each transition generated from fragmentation of the [M + 2H]2+ precursor (*m/z* 1008.5) to its corresponding y product ions (y4–y9; different colours) during MRM. Transition peaks were readily observed following analysis of purified Gβ_1 (top), and equivalent transitions were evident upon analysis of pre- and postsynaptic fractions isolated from mouse brain cortical tissue (middle and bottom, respectively).

G protein isoform	Sequence Position	Peptide Sequence	Precursor m/z	Charge	Collison Energy	Product Ion m/z
$G\beta_1$	2-24	(K)A**C**ADATLSQITNNIDPVGR(I)	1008.4944	2+	33	428.2616, 543.2885, 884.4585, 985.5061
	138-150	R)ELAGHTGYLS**CC**R(F)	762.3401	2+	26	641.2768, 858.3597, 915.3811, 1016.4288
	198-209	(R)LFVSGA**C**DASAK(L)	613.2977	2+	21	483.2215, 779.3352, 866.3673, 965.4357
	284-301	(R)LLLAGYDDFN**C**NVWDALK(A)	1064.0144	2+	35	632.3402, 894.3883, 950.9304, 1119.5252
$G\beta_2$	24-42	(K)A**C**GDSTLTQITAGLDPVGR(I)	966.4782	2+	32	428.2616, 543.2885, 713.3941, 885.4789
		(K)A**C**GDSTLTQITAGLDPVGR(I)	644.6546	3+	27	428.2616, 543.2885, 713.3941, 885.4789
	198-209	(R)TFVSGA**C**DASIK(L)	628.3030	2+	22	504.2449, 821.3822, 908.4142, 1007.4826
	257-280	(R)ADQELLMYSHDNII**C**GITSVAFSR(S)	914.1072	3+	37	409.2194, 480.2565, 666.3570, 767.4046
		(R)ADQELL**M**YSHDNII**C**GITSVAFSR(S)	919.4388	3+	37	409.2194, 480.2565, 666.3570, 937.5102
$G\beta_4$	198-209	(R)TFVSGA**C**DASSK(L)	615.2770	2+	21	491.2189, 667.2716, 795.3301, 882.3622, 981.4306
	305-314	(R)SGVLAGHDNR(V)	513.2598	2+	18	391.6988, 598.2692, 669.3063, 782.3904
		(R)SGVLAGHDNR(V)	342.5089	3+	15	335.1568, 391.6988, 441.2330, 469.7438
$G\beta_5$	45-54	(R)VEALGQFVMK(T)	561.3048	2+	20	709.3702, 822.4542, 893.4913, 1022.5339
		(R)VEALGQFV**M**K(T)	569.3023	2+	20	540.2850, 725.3651, 838.4491, 909.4863
	87-97	(K)VIVWDSFTTNK(E)	655.3430	2+	23	679.3515, 812.3785, 998.4578, 1097.5262
	280-296	(K)ESIIFGASSVDFSLSGR(L)	886.4467	2+	30	666.3570, 781.3839, 967.4843, 1054.5164
	318-327	(R)VSILFGHENR(V)	586.3146	2+	21	493.2643, 612.2848, 759.3533, 872.4373
$G\gamma_2$	21-27	(K)MEANIDR(I)	424.7002	2+	16	517.2729, 588.3100, 717.3526
	33-46	(K)**M**EANIDR(I)	432.6976	2+	16	517.2729, 588.3100, 717.3526
		(K)AAADLMAY**C**EAHAK(E)	761.3449	2+	26	715.3192, 878.3825, 1080.4601, 1193.5442
	47-62	(K)AAADL**M**AY**C**EAHAK(E)	769.3423	2+	26	698.3052, 878.3825, 949.4196, 1096.4550
		(K)EDPLLTPVPASENPFR(E)	891.4571	2+	30	769.4223, 917.4476, 1113.5687, 1214.6164
$G\gamma_3$	3 to 17	(K)GETPVNSTMSIGQAR(K)	774.3778	2+	26	431.2361, 544.3202, 630.8219, 681.3457, 950.4724, 1064.5153
		(K)GETPVNST**M**SIGQAR(K)	782.3752	2+	26	431.2361, 638.8193, 689.3432, 1080.5102
	25-31	(K)IEASLCR(I)	424.7184	2+	16	448.2337, 535.2657, 606.3028, 735.3454
$G\gamma_4$	3 to 17	(K)EGMSNNSTTSISQAR(K)	791.8599	2+	27	431.2467, 661.3628, 863.4581, 950.4901
	34-50	K)EG**M**SNNSTTSISQAR(K)	799.8574	2+	27	461.2467, 574.3307, 661.3628, 863.4581
	51-66	(K)VSQAASDLLAY**C**EAHVR(E)	630.6440	3+	26	717.3457, 752.8643, 788.3828, 895.9281
		(R)EDPLIIPVPASENPFR(E)	897.4753	2+	30	917.4476, 1113.5687, 1226.6528
$G\gamma_5$	28-36	(K)VSQAAADLK(Q)	451.7507	2+	17	260.1969, 358.7005, 588.3352, 803.4258
	64-68	(K)V**C**SFL(-)	625.3014	2+	22	279.1703, 366.2023, 526.2330
$G\gamma_7$	19-25	(R)IEAGIER(I)	394.2191	2+	15	474.2671, 545.3042, 674.3468
	45-60	(R)NDPLLVGVPASENPFK(D)	848.9489	2+	28	734.4139, 889.4414, 1045.5313, 1144.5997
$G\gamma_{11}$	17-23	(K)MEVEQLR(K)	425.7315	2+	17	416.2616, 545.3042, 644.3726, 773.4152
		(K)**M**EVEQLR(K)	460.7289	2+	17	416.2616, 545.3042, 644.3726, 773.4152
	42-47	(K)NYIEER(S)	823.3945	2+	28	278.1135, 304.1615,391.1976, 520.2402,
$G\gamma_{12}$	5-15	(K)TASTNSIAQAR(R)	560.2913	2+	20	445.2515, 645.3678, 759.4108, 947.4905
	23-29	(R)LEASIER(I)	409.2243	2+	15	504.2776, 575.3148, 704.3573
	49-64	(R)SDPLLMGIPTSENPFK(D)	873.4426	2+	29	772.4131, 919.4520, 1089.5575, 1220.5980
		(R)SDPLL**M**GIPTSENPFK(D)	881.4400	2+	29	780.4105, 919.4520, 1089.5575, 1236.5929
$G\gamma_{13}$	18-23	(K)YQLAFK(R)	385.2158	2+	15	365.2183, 478.3024, 606.3610
	37-44	(K)WIEDGIPK(D)	479.2556	2+	17	244.1656, 414.2711, 529.2980, 658.3406
	55-61	(K)NNPWVEK(A)	443.7245	2+	16	276.1554, 386.7030, 658.3559

Table 3. Precursor peptides and MRM transitions used for the identification of Gβ and Gγ isoforms in enriched pre- and postsynaptic fractions. Letters C and M in bold represent carbamidomethylation and oxidation of cysteine and methionine, respectively.

Evaluating regional and subcellular G protein localization patterns

We next applied our refined MRM method to subcellular fractions isolated from mouse cortex, cerebellum, hippocampus, and striatum. All four of the beta isoforms ($G\beta_{1,2,4}$, and $_5$) being targeted were detected in pre- and postsynaptic fractions in all four brain regions, as well as 6 of the 8 gamma isoforms ($G\gamma_2$, $_3$, $_4$, $_7$, $_{12}$, and $_{13}$ respectively). Chromatographic peaks of monitored transition ions could not be confidently identified for $G\gamma_5$ and $G\gamma_{11}$ despite target peptides having been validated using recombinant proteins in the development phase. $G\gamma_{11}$ is thought to be a minor isoform in the brain with expression highest in lung and platelets[41]. In addition, both $G\gamma_5$ and $G\gamma_{11}$ exhibit unique attributes that were not accounted for in method development and could explain why peptides could not be confidently identified in CNS fractions. For example, the amino terminus of $G\gamma_{11}$ contains an unmodified proline, whereas most Gγ isoforms are thought to be acetylated in this region[228]. Further, similar to $G\gamma_1$, this isoform is believed to exist in both a methylated and unmethylated form[228]. If peptides being monitored carried such a modification, they would not be detected with the current MRM method. Comparatively, $G\gamma_5$ is unique in that the major variant of this isoform contains a C terminus that is not proteolytically processed[257]. If the processed form of this isoform was in lower abundance, this could explain why the C terminal peptide being monitored in our MRM experiments was not readily observed. Neither isoform was included in analyses. No significant variance in system performance was observed across quality control (QC) runs as measured by examining BSA peptide peak areas across the experiment, or peak area CVs for replicate QC analyses (Figure 8). Similarly, no significant drift in assay performance was observed as measured by monitoring peak areas as well peak area CVs for internal reference peptides (Figure 9 and 10). Although stable isotope dilution (SID) is the gold standard for quantifying

protein expression[252,258], the cost prohibitive nature prevented its use when trying to evaluate a large number of G protein isoforms. Instead, application of an LRP method[252] allowed relative abundance of G protein isoforms to be examined. With this method, direct comparisons between isoforms cannot be made; rather, comparisons are only possible across brain regions and subcellular fractions for each individual isoform, as described below. As a result, average normalized areas for each isoform were each plotted on different axes in Figures 11 and 12.

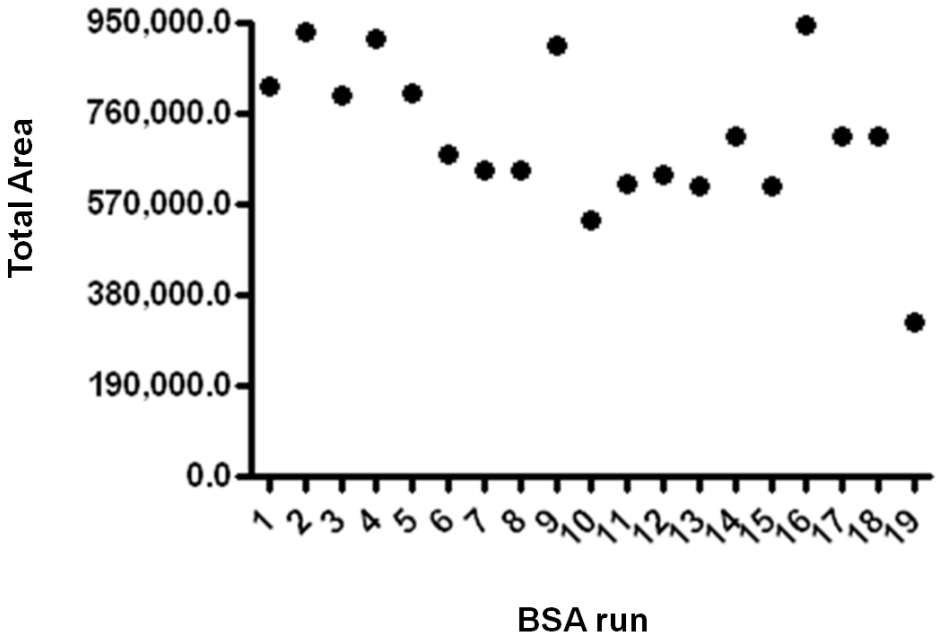

Figure 8. Total area under the curve for BSA controls run between experimental samples during MRM experiments. Dots represent total summed area for all peptides being monitored in BSA control samples. BSA runs are arranged in chronological order in which they were analysed via MRM. CV: 0.22.

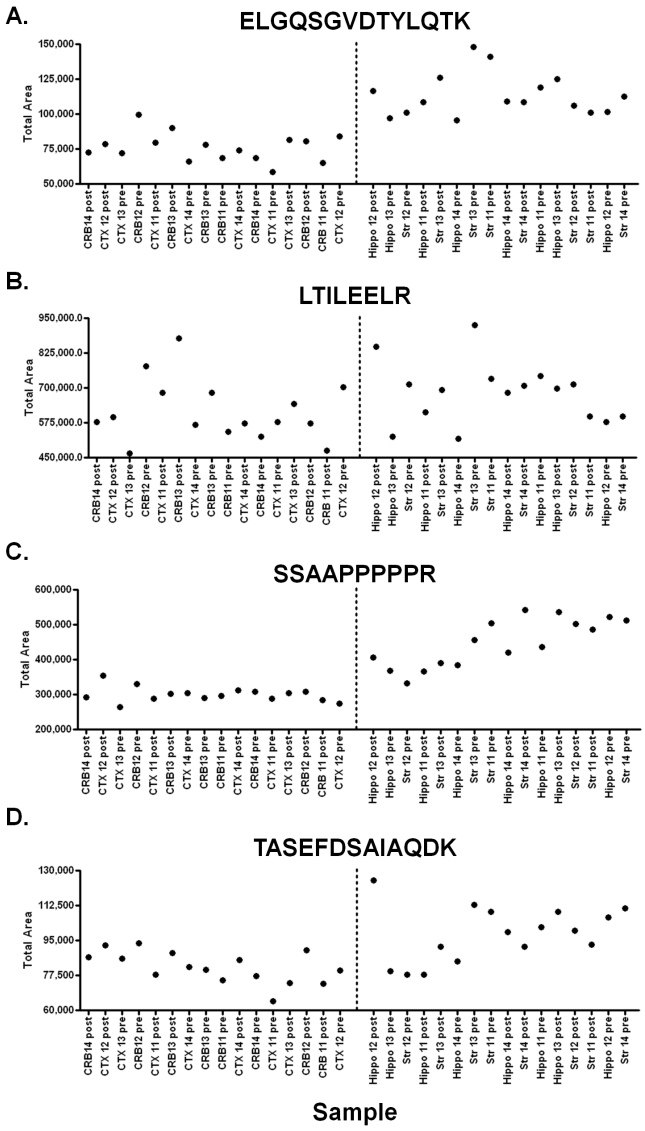

Figure 9.Total area under the curve for internal reference peptides A) ELGQSGVDTYLQTL, B) LTILEELR, C) SSAAPPPPPR, and D) TASEFDSAIAQDK added to Gβ experimental samples. Dots represent total area for each experimental sample. Samples are arranged in chronological order in which they were analysed on MRM. CTX,CRB and Hippo,Str samples were evaluated separately as they were run on separate days (depicted by dashed line). ELGQSGVDTYLQTL CTX,CRB VS: 0.05; Hippo,Str CV 0.08; LTILEELR CTX,CRB CV: 0.04; Hippo,Str CV: 0.10; SSAAPPPPPR CTX,CRB VS: 0.05; Hippo,Str CV 0.05; TASEFDSAIAQDK CTX,CRB CV: 0.03; Hippo,Str CV: 0.05. CTX: cortex; CRB: cerebellum; Hippo: hippocampus; Str: striatum; pre: presynaptic fraction; post: postsynaptic fraction

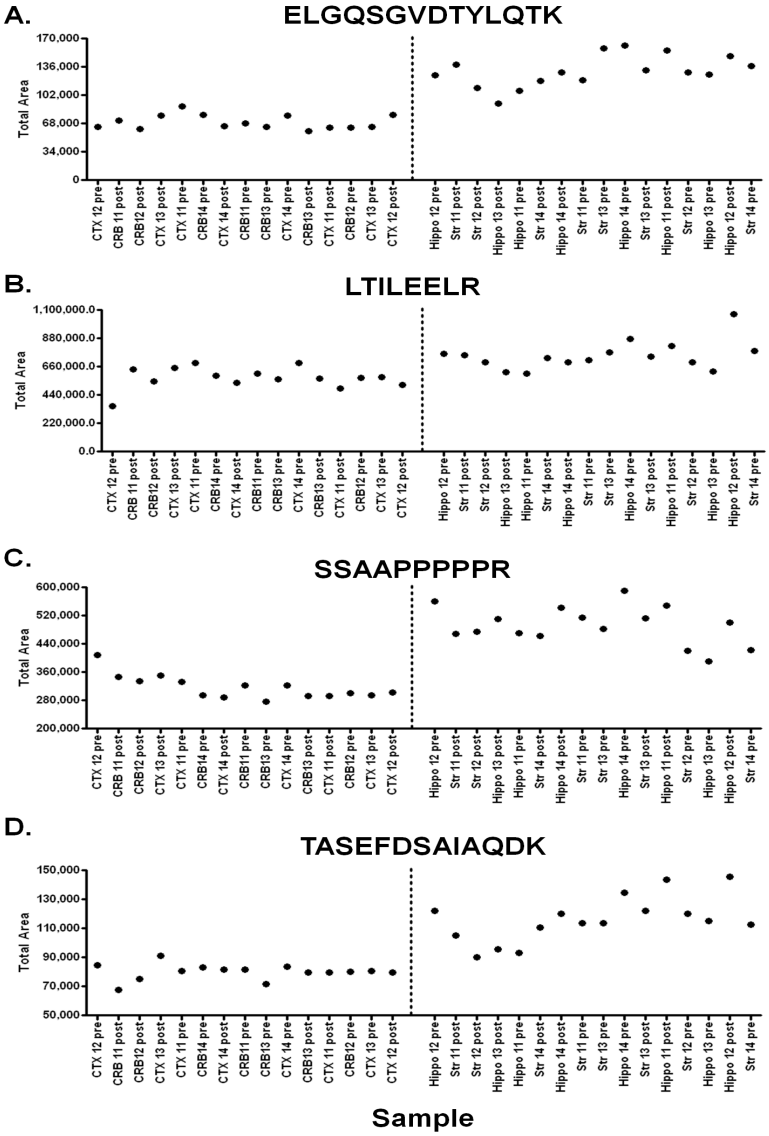

Figure 10.Total area under the curve for internal reference peptides A) ELGQSGVDTYLQTL, B) LTILEELR, C) SSAAPPPPPR, and D) TASEFDSAIAQDK added to Gγ experimental samples. Dots represent total area for each experimental sample. Samples are arranged in chronological order in which they were analysed on MRM. CTX,CRB and Hippo,Str samples were evaluated separately as they were run on separate days (depicted by dashed line). ELGQSGVDTYLQTL CTX,CRB VS: 0.06; Hippo,Str CV 0.03; LTILEELR CTX,CRB CV: 0.03; Hippo,Str CV: 0.05; SSAAPPPPPR CTX,CRB VS: 0.06; Hippo,Str CV 0.06; TASEFDSAIAQDK CTX,CRB CV: 0.05; Hippo,Str CV: 0.07. CTX: cortex; CRB: cerebellum; Hippo: hippocampus; Str: striatum; pre: presynaptic fraction; post: postsynaptic fraction

Gβ isoforms

Subcellular localization patterns were evaluated for each of the four Gβ isoforms being monitored by MRM. Although there was a trend toward higher expression of $G\beta_1$ and $G\beta_4$ in the cortex and cerebellum, expression levels were not significantly different within or across most brain regions for three of the four isoforms (Figure 11A,B,C). Within the striatum, however, $G\beta_1$, $G\beta_2$, and $G\beta_4$ were all expressed at significantly greater levels in the postsynaptic fraction compared to the presynaptic fraction (Figure 11A,B,C). An interaction effect was seen for $G\beta_1$ (ANOVA p-value = 0.0321); specifically: $G\beta_1$ Str post/Str pre fold difference: 2.63, p-value <0.05 (Table 4), whereas there was a brain region, fraction, and interaction effect for $G\beta_2$ (ANOVA p-value = 0.0362, 0.0039, and 0.0023, respectively; $G\beta_2$ Str post/Str pre fold difference: 3.78, p-value <0.001; Table 5) and a fraction effect for $G\beta_4$ (ANOVA p-value = 0.0066; Str post/Str pre fold difference: 4.06, p-value <0.05; Table 6). In addition, postsynaptic expression of $G\beta_2$ was significantly greater in the striatum compared to postsynaptic fractions from the cortex, cerebellum, or hippocampus (Figure 11B; Str post/CTX post fold difference: 1.55, p-value <0.05; Str post/CRB post fold difference: 1.08, p-value <0.01; Str post/Hippo post fold difference: 2.08, p-value <0.05; Table 5). In comparison, $G\beta_5$ was only detected in the striatum based on our peak criteria and S/N requirements (Figure 11D). As was seen for the other Gβ isoforms, expression of $G\beta_5$ was significantly higher in the postsynaptic fraction compared to the presynaptic fraction (Figure 12D; Str post/Str pre fold difference: 4.07, p-value <0.05; Table 7).

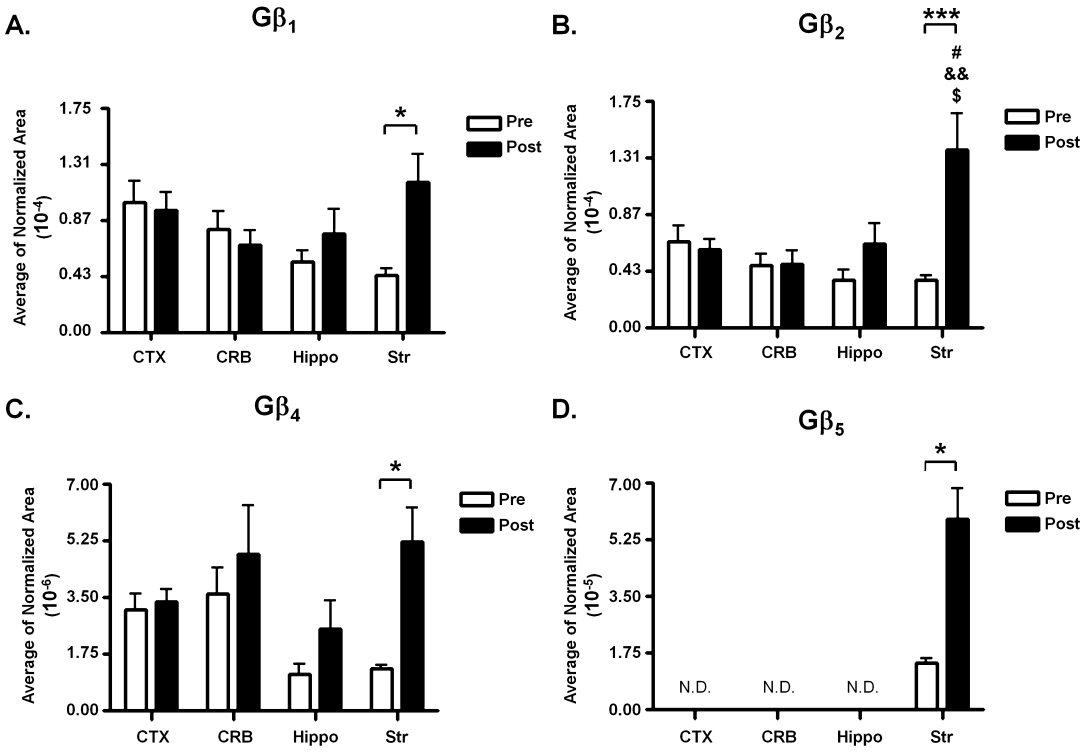

Figure 11. Gβ isoforms exhibit differential regional and subcellular localization patterns within the mouse brain. Expression of specific Gβ isoforms A) $G\beta_1$, B) $G\beta_2$, C) $G\beta_4$, and D) $G\beta_5$ in cortex, cerebellum, hippocampus, and striatum. Data for panels A–C were compared by a two-way ANOVA. The two-way ANOVA results were as follows: A) $G\beta_1$ interaction effect $p = 0.0321$; (B) $G\beta_2$, brain region affect $p = 0.0362$, fraction effect $p = 0.0039$, and interaction effect $p = 0.0023$; C) $G\beta_4$, fraction effect $p = 0.0066$. Post hoc analysis was achieved by Tukey's multiple-comparison test. *$p < 0.05$. **$p < 0.01$. ***$p < 0.001$. ****$p < 0.0001$. Data for panel D were evaluated by an unpaired *t* test ($p = 0.01$). Comparison to cortex represented by #, to cerebellum by &, and to hippocampus by $. Significance for each symbol as indicated for asterisks. N.D., not detected. $N = 4$ for all brain regions.

$G\beta_1$		**Fold Difference Numerator** (Fold Difference Numerator Raw Value)							
Fold Difference Denominator (Fold Difference Denominator Raw Value)		**CTX pre** (1.02E-4)	**CRB Pre** (8.03E-05)	**Hippo pre** (5.50E-05)	**Str pre** (4.48E-05)	**CTX post** (9.58E-05)	**CRB post** (6.86E-05)	**Hippo post** (7.74E-05)	**Str post** (1.18E-4)
	CTX pre (1.02E-4)	--	0.79	0.54	0.44	0.94			
	CRB pre (8.03E-05)	1.26	--	0.68	0.56		0.85		
	Hippo pre (5.50E-05)	1.85	1.46	--	0.81			1.41	
	Str pre (4.48E-05)	2.27	1.79	1.23	--				**2.63**
	CTX post (9.58E-05)	1.06				--	0.72	0.81	1.23
	CRB post (6.86E-05)		1.17			1.40	--	1.13	1.72
	Hippo post (7.74E-05)			0.71		1.24	0.89	--	1.52
	Str post (1.18E-4)				0.38	0.81	0.58	0.66	--

Table 4. Fold differences comparing expression of G protein β_1 in pre or postsynaptic fractions between brain regions and pre- and postsynaptic fractions within a brain region. Fold differences comparing expression of $G\beta_1$ in postsynaptic fractions to $G\beta_1$ expression in presynaptic fractions within a brain region were calculated by dividing the total normalized area for $G\beta_1$ peptides within the postsynaptic fraction by the total normalized area for $G\beta_1$ peptides within the presynaptic fraction (e.g. CTX post/CTX pre). Fold differences comparing expression of $G\beta_1$ in presynaptic fractions within one brain region to presynaptic expression within another brain region were calculated by dividing the total normalized area for $G\beta_1$ in the presynaptic fraction of one brain region by expression in the presynaptic fraction within a second brain region (e.g. CTX pre/ CRB pre). This was also done to compare expression of $G\beta_1$ in postsynaptic fractions between brain regions. Comparisons were not made between pre and postsynaptic fractions of different brain regions. Brain regions and raw total area values for the numerator in these calculations are shown along the top of the table, highlighted in bold and parentheses respectively. Brain regions and raw total area values for the denominator in these calculations are shown along the left of the table, highlighted in bold and parentheses respectively. Raw values and fold differences were rounded to two decimal places. Fold differences that are significant are shown in bold. CTX:cortex; CRB: cerebellum; Hippo: hippocampus; Str: striatum; pre: presynaptic fraction; post: postsynaptic fraction.

$G\beta_2$		**Fold Difference Numerator** (Fold Difference Numerator Raw Value)							
Fold Difference Denominator (Fold Difference Denominator Raw Value)		**CTX pre** (6.67E-5)	**CRB Pre** (4.81E-5)	**Hippo pre** (3.73E-5)	**Str pre** (3.65E-5)	**CTX post** (6.03E-5)	**CRB post** (4.93E-5)	**Hippo post** (6.46E-5)	**Str post** (1.38E-4)
	CTX pre (6.67E-5)	--	0.72	0.56	0.55	0.90			
	CRB pre (4.81E-5)	1.39	--	0.78	0.76		1.03		
	Hippo pre (3.73E-5)	1.79	1.29	--	0.98			1.73	
	Str pre (3.65E-5)	1.83	1.32	1.02	--				**3.78**
	CTX post (6.03E-5)	1.11				--	0.82	1.07	**2.28**
	CRB post (4.93E-5)		0.98			1.22	--	1.31	**2.80**
	Hippo post (6.46E-5)			0.58		0.93	0.76	--	**2.13**
	Str post (1.38E-4)				0.26	0.44	0.36	0.47	--

Table 5. Fold differences comparing expression of G protein β_2 in pre or postsynaptic fractions between brain regions and pre- and postsynaptic fractions within a brain region. Fold differences comparing expression of $G\beta_2$ in postsynaptic fractions to $G\beta_2$ expression in presynaptic fractions within a brain region were calculated by dividing the total normalized area for $G\beta_2$ peptides within the postsynaptic fraction by the total normalized area for $G\beta_2$ peptides within the presynaptic fraction (e.g. CTX post/CTX pre). Fold differences comparing expression of $G\beta_2$ in presynaptic fractions within one brain region to presynaptic expression within another brain region were calculated by dividing the total normalized area for $G\beta_2$ in the presynaptic fraction of one brain region by expression in the presynaptic fraction within a second brain region (e.g. CTX pre/CRB pre). This was also done to compare expression of $G\beta_2$ in postsynaptic fractions between brain regions. Comparisons were not made between pre and postsynaptic fractions of different brain regions. Brain regions and raw total area values for the numerator in these calculations are shown along the top of the table, highlighted in bold and parentheses respectively. Brain regions and raw total area values for the denominator in these calculations are shown along the left of the table, highlighted in bold and parentheses respectively. Raw values and fold differences were rounded to two decimal places. Fold differences that are significant are shown in bold. CTX:cortex; CRB: cerebellum; Hippo: hippocampus; Str: striatum; pre: presynaptic fraction; post: postsynaptic fraction.

$G\beta_4$		**Fold Difference Numerator** (Fold Difference Numerator Raw Value)							
Fold Difference Denominator (Fold Difference Denominator Raw Value)		**CTX pre** (3.12E-6)	**CRB pre** (3.61E-6)	**Hippo pre** (1.13E-6)	**Str pre** (1.29E-6)	**CTX post** (3.35E-6)	**CRB post** (4.84E-6)	**Hippo post** (2.51E-6)	**Str post** (5.23E-6)
	CTX pre (3.12E-6)	--	1.16	0.36	0.41	1.08			
	CRB pre (3.61E-6)	0.86	--	0.31	0.36		1.34		
	Hippo pre (1.13E-6)	2.75	3.19	--	1.14			2.22	
	Str pre (1.29E-6)	2.42	2.80	0.88	--				**4.06**
	CTX post (3.35E-6)	0.93				--	1.44	0.75	1.56
	CRB post (4.84E-6)		0.75			0.69	--	0.52	1.08
	Hippo post (2.51E-6)			0.45		1.34	1.93	--	2.08
	Str post (5.23E-6)				0.25	0.64	0.92	0.48	--

Table 6. Fold differences comparing expression of G protein β_4 in pre or postsynaptic fractions between brain regions and pre- and postsynaptic fractions within a brain region. Fold differences comparing expression of $G\beta_4$ in postsynaptic fractions to $G\beta_4$ expression in presynaptic fractions within a brain region were calculated by dividing the total normalized area for $G\beta_4$ peptides within the postsynaptic fraction by the total normalized area for $G\beta_4$ peptides within the presynaptic fraction (e.g. CTX post/CTX pre). Fold differences comparing expression of $G\beta_4$ in presynaptic fractions within one brain region to presynaptic expression within another brain region were calculated by dividing the total normalized area for $G\beta_4$ in the presynaptic fraction of one brain region by expression in the presynaptic fraction within a second brain region (e.g. CTX pre/ CRB pre). This was also done to compare expression of $G\beta_4$ in postsynaptic fractions between brain regions. Comparisons were not made between pre and postsynaptic fractions of different brain regions. Brain regions and raw total area values for the numerator in these calculations are shown along the top of the table, highlighted in bold and parentheses respectively. Brain regions and raw total area values for the denominator in these calculations are shown along the left of the table, highlighted in bold and parentheses respectively. Raw values and fold differences were rounded to two decimal places. Fold differences that are significant are shown in bold. CTX:cortex; CRB: cerebellum; Hippo: hippocampus; Str: striatum; pre: presynaptic fraction; post: postsynaptic fraction.

$G\beta_5$		**Fold Difference Numerator** (Fold Difference Numerator Raw Value)							
Fold Difference Denominator (Fold Difference Denominator Raw Value)		**CTX pre** (N.D.)	**CRB pre** (N.D.)	**Hippo pre** (N.D.)	**Str pre** (2.48E-6)	**CTX post** (N.D.)	**CRB post** (N.D.)	**Hippo post** (N.D.)	**Str post** (1.01E-5)
	CTX pre (N.D.)								
	CRB pre (N.D.)								
	Hippo pre (N.D.)								
	Str pre (2.48E-6)				--				**4.07**
	CTX post (N.D.)								
	CRB post (N.D.)								
	Hippo post (N.D.)								
	Str post (1.01E-5)				0.25				--

Table 7. Fold differences comparing expression of G protein β_5 in pre or postsynaptic fractions between brain regions and pre- and postsynaptic fractions within a brain region. Fold differences comparing expression of $G\beta_5$ in postsynaptic fractions to $G\beta_5$ expression in presynaptic fractions within a brain region were calculated by dividing the total normalized area for $G\beta_5$ peptides within the postsynaptic fraction by the total normalized area for $G\beta_5$ peptides within the presynaptic fraction (e.g. CTX post/CTX pre). Fold differences comparing expression of $G\beta_5$ in presynaptic fractions within one brain region to presynaptic expression within another brain region were calculated by dividing the total normalized area for $G\beta_5$ in the presynaptic fraction of one brain region by expression in the presynaptic fraction within a second brain region (e.g. CTX pre/ CRB pre). This was also done to compare expression of $G\beta_5$ in postsynaptic fractions between brain regions. Comparisons were not made between pre and postsynaptic fractions of different brain regions. Brain regions and raw total area values for the numerator in these calculations are shown along the top of the table, highlighted in bold and parentheses respectively. Brain regions and raw total area values for the denominator in these calculations are shown along the left of the table, highlighted in bold and parentheses respectively. Raw values and fold differences were rounded to two decimal places. Fold differences that are significant are shown in bold. CTX:cortex; CRB: cerebellum; Hippo: hippocampus; Str: striatum; pre: presynaptic fraction; post: postsynaptic fraction.

Gγ isoforms

In contrast to the Gβ isoforms, the Gγ isoforms showed greater diversity in their subcellular and regional localization patterns. $G\gamma_{2,3,4,7,12}$, and $_{13}$ were clearly detected in each of the four brain regions being studied. In the case of $G\gamma_2$, no significant differences in regional or subcellular fractions were observed, except within the hippocampus. Expression of this isoform was found to be significantly greater in the postsynaptic fraction of the hippocampus compared to the cerebellum (Figure 12A). There was a brain region and fraction effect for $G\gamma_2$ (ANOVA p-value = 0.002 and 0.0035, respectively); specifically, $G\gamma_2$ Hippo post/CRB post fold difference: 3.61, p-value <0.05 (Table 8). Additionally, there was a trend toward greater expression in the postsynaptic fraction of the hippocampus and striatum compared to presynaptic fractions within these same regions (Figure 12A). Similar patterns of expression were observed for $G\gamma_3$. No significant differences were observed across the four brain regions. When comparisons were made between subcellular fractions, however, there was a trend towards higher expression in postsynaptic fractions, although this was only significant within the striatum (Figure 12B). In this case, there was also a brain region and fraction effect (ANOVA p-value = 0.0125 and 0.0003, respectively); specifically, $G\gamma_3$ Str post/Str pre fold difference: 2.60, p-value <0.05 (Table 9). $G\gamma_4$ and $G\gamma_7$ were somewhat different in that significant differences were observed in both regional and subcellular expression. There was a brain region, fraction, and interaction effect for both isoforms ($G\gamma_4$ ANOVA p-value = 0.0093, 0.001, and 0.04 respectively; $G\gamma_7$ ANOVA p-value = <0.0001 for all three affects). In the case of $G\gamma_4$, postsynaptic expression in the hippocampus and striatum was found to be significantly greater than that in the cerebellum (Figure 12C; Hippo post/CRB post fold difference: 4.00, p-value <0.05; Str post/CRB post fold change: 3.83, p-value <0.05; Table 10). Further, while there was a trend toward higher expression in the

postsynaptic fraction compared to the presynaptic fraction within both the hippocampus and striatum, it was only significant within the striatum (Figure 12C; Str post/Str pre fold difference: 3.71, p-value <0.05; Table 10). Expression of $G\gamma_7$ was not significantly different between pre- and postsynaptic fractions in the cortex, cerebellum, and hippocampus. Within the striatum, however, expression was significantly higher in the postsynaptic fraction compared to the presynaptic fraction (Figure 12D; Str post/Str pre fold difference: 5.55, p-value <0.0001; Table 11). Further, postsynaptic expression of this isoform was significantly higher in the striatum compared to the postsynaptic expression in each of the other three brain regions (Figure 12D; Str post/CTX post fold difference: 5.47, p-value <0.0001; Str post/CRB post fold difference: 8.41, p-value <0.0001; Str post/Hippo post fold difference: 3.13, p-value <0.0001; Table 11). $G\gamma_{12}$ was unique among the isoforms in that although no regional differences were observed, subcellular expression was significantly higher in postsynaptic fractions across all brain regions compared to presynaptic fractions (Figure 12E). There was a brain region and fraction effect for $G\gamma_{12}$. Specifically, CTX post/CTX pre fold difference: 2.81, p-value <0.01; CRB post/CRB pre fold difference: 3.16, p-value <0.001; Hippo post/Hippo pre fold change: 5.36, p-value <0.05; and Str post/Str pre fold difference 10.46, p-value <0.001; Table 12). Finally, $G\gamma_{13}$ exhibited both regional and subcellular differences in localization and there was both a brain region and fraction effect for this isoform (ANOVA p-value <0.0001 in both cases). Expression of this isoform in the cortex was found to be significantly higher in both the pre- and postsynaptic fractions as compared to the hippocampus and striatum (Figure 12F; CTX pre/Hippo pre fold difference: 4.03, p-value <0.05; CTX pre/Str pre fold difference: 8.76, p-value <0.01; CTX post/Str post fold difference: 2.86, p-value <0.05; Table 13). Similarly, expression of $G\gamma_{13}$ was found to be significantly higher in the postsynaptic fraction of the cerebellum when compared to the postsynaptic fractions of the hippocampus and striatum (Figure 12F; CRB post/Hippo post fold

difference: 2.38, p-value <0.01; CRB post/Str post fold difference: 3.06, p-value <0.01; Table 13). No significant differences in subcellular localization were observed in the cortex, hippocampus, or striatum but expression was significantly higher in the postsynaptic fraction within the cerebellum compared to the presynaptic fraction (Figure 12F; CRB post/CRB pre fold difference: 2.22, p-value <0.01; Table 13).

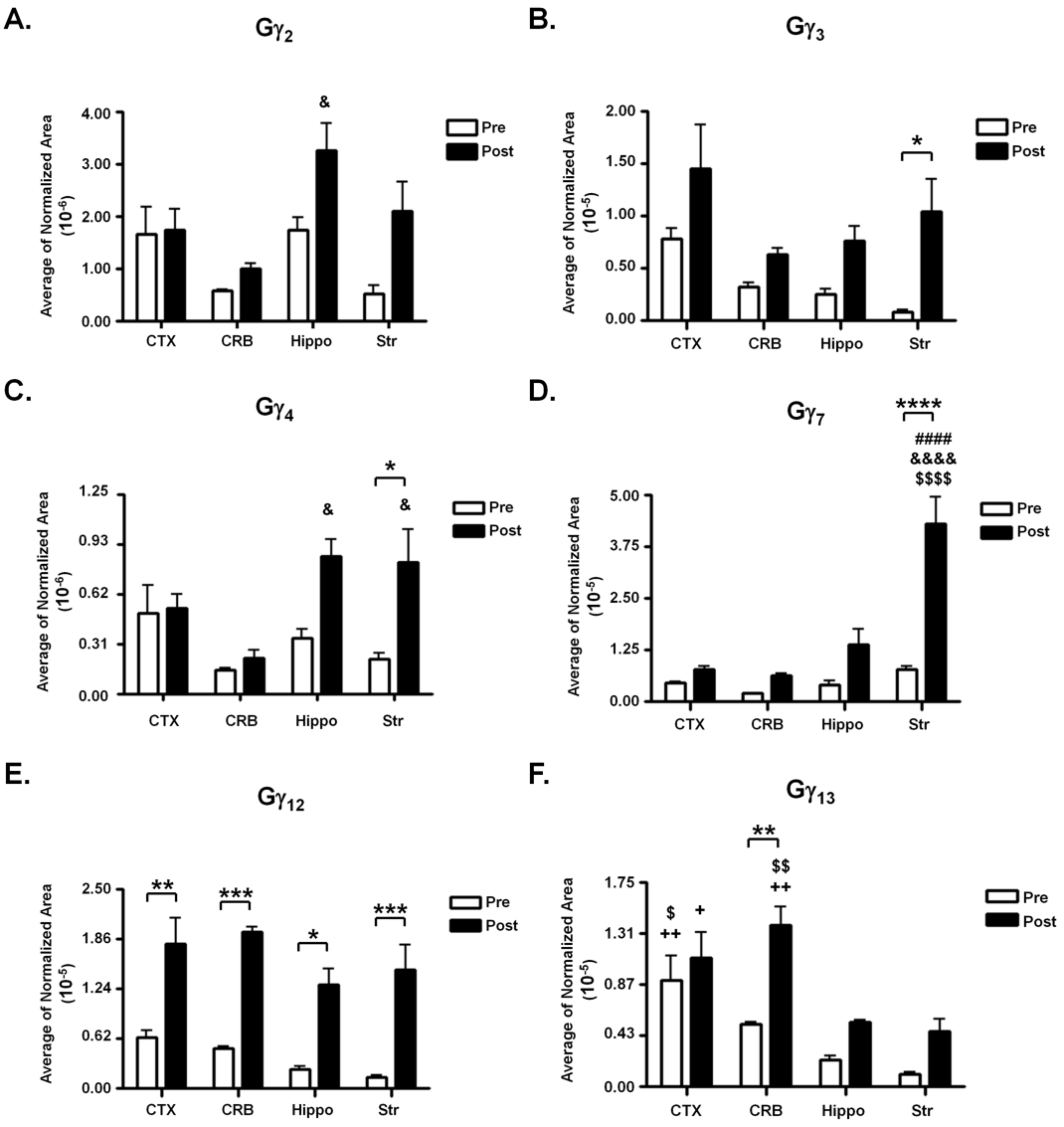

Figure 12. Gγ isoforms exhibit differential regional and subcellular localization patterns within the mouse brain. Expression of specific Gγ isoforms A) $G\gamma_2$, B) $G\gamma_3$, C) $G\gamma_4$, D) $G\gamma_7$, E) $G\gamma_{12}$, and F) $G\gamma_{13}$ in cortex, cerebellum, hippocampus, and striatum. Data were compared by a two-way ANOVA. The two-way ANOVA results were as follows: A) $G\gamma_2$, brain region effect $p = 0.002$ and fraction effect $p = 0.0035$; B) $G\gamma_3$, brain region effect $p = 0.0125$ and fraction effect $p = 0.0003$; C) $G\gamma_4$, brain region effect $p = 0.0093$, fraction effect $p = 0.001$, and interaction effect $p = 0.04$; D) $G\gamma_7$, brain region effect $p < 0.0001$, fraction effect $p < 0.0001$, and interaction effect $p < 0.0001$; E) $G\gamma_{12}$, brain region effect $p = 0.0304$ and fraction effect $p < 0.0001$; F) G $G\gamma_{13}$, brain region effect $p < 0.0001$ and fraction effect $p < 0.0001$. Post hoc analysis was achieved by Tukey's multiple-comparison test. *$p < 0.05$. **$p < 0.01$. ***$p < 0.001$. ****$p < 0.0001$. Comparison to cortex represented by #, to cerebellum by &, to hippocampus by $, and to striatum by +. Significance for each symbol as indicated for asterisks. $N = 4$ for all brain regions.

$G\gamma_2$		**Fold Difference Numerator** (Fold Difference Numerator Raw Value)							
Fold Difference Denominator (Fold Difference Denominator Raw Value)		**CTX pre** (1.66E-6)	**CRB pre** (5.74E-7)	**Hippo pre** (1.74E-6)	**Str pre** (5.25E-7)	**CTX post** (1.74E-6)	**CRB post** (9.03E-7)	**Hippo post** (3.26E-6)	**Str post** (2.10E-6)
	CTX pre (1.66E-6)	--	0.34	1.05	0.32	1.05			
	CRB pre (5.74E-7)	2.90	--	3.04	0.92		1.57		
	Hippo pre (1.74E-6)	0.96	0.33	--	0.30			1.87	
	Str pre (5.25E-7)	3.17	1.09	3.32	--				3.99
	CTX post (1.74E-6)	0.96				--	0.52	1.87	1.20
	CRB post (9.03E-7)		0.64			1.93	--	**3.61**	2.32
	Hippo post (3.26E-6)			0.53		0.53	0.28	--	0.64
	Str post (2.10E-6)				0.25	0.83	0.43	1.56	--

Table 8. Fold differences comparing expression of G protein γ_2 in pre or postsynaptic fractions between brain regions and pre- and postsynaptic fractions within a brain region. Fold differences comparing expression of $G\gamma_2$ in postsynaptic fractions to $G\gamma_2$ expression in presynaptic fractions within a brain region were calculated by dividing the total normalized area for $G\gamma_2$ peptides within the postsynaptic fraction by the total normalized area for $G\gamma_2$ peptides within the presynaptic fraction (e.g. CTX post/CTX pre). Fold differences comparing expression of $G\gamma_2$ in presynaptic fractions within one brain region to presynaptic expression within another brain region were calculated by dividing the total normalized area for $G\gamma_2$ in the presynaptic fraction of one brain region by expression in the presynaptic fraction within a second brain region (e.g. CTX pre/CRB pre). This was also done to compare expression of $G\gamma_2$ in postsynaptic fractions between brain regions. Comparisons were not made between pre and postsynaptic fractions of different brain regions. Brain regions and raw total area values for the numerator in these calculations are shown along the top of the table, highlighted in bold and parentheses respectively. Brain regions and raw total area values for the denominator in these calculations are shown along the left of the table, highlighted in bold and parentheses respectively. Raw values and fold differences were rounded to two decimal places. Fold differences that are significant are shown in bold. CTX:cortex; CRB: cerebellum; Hippo: hippocampus; Str: striatum; pre: presynaptic fraction; post: postsynaptic fraction.

$G\gamma_3$		**Fold Difference Numerator** (Fold Difference Numerator Raw Value)							
Fold Difference Denominator (Fold Difference Denominator Raw Value)		**CTX pre** (7.84E-6)	**CRB pre** 7.84E-6)	**Hippo pre** (2.51E-6)	**Str pre** (8.06E-7)	**CTX post** (1.45E-5)	**CRB post** (5.25E-6)	**Hippo post** (7.62E-6)	**Str post** (1.04E-5)
	CTX pre (7.84E-6)	--	0.40	0.32	0.10	1.85			
	CRB pre (7.84E-6)	2.47	--	0.79	0.25		1.66		
	Hippo pre (2.51E-6)	3.13	1.26	--	0.32			3.04	
	Str pre (8.06E-7)	9.73	3.93	3.11	--				**12.90**
	CTX post (1.45E-5)	0.54				--	0.36	0.52	0.72
	CRB post (5.25E-6)		0.60			2.76	--	1.45	1.98
	Hippo post (7.62E-6)			0.33		1.91	0.69	--	1.36
	Str post (1.04E-5)				0.08	1.40	0.51	0.73	--

Table 9. Fold differences comparing expression of G protein γ_3 in pre or postsynaptic fractions between brain regions and pre- and postsynaptic fractions within a brain region. Fold differences comparing expression of $G\gamma_3$ in postsynaptic fractions to $G\gamma_3$ expression in presynaptic fractions within a brain region were calculated by dividing the total normalized area for $G\gamma_3$ peptides within the postsynaptic fraction by the total normalized area for $G\gamma_3$ peptides within the presynaptic fraction (e.g. CTX post/CTX pre). Fold differences comparing expression of $G\gamma_3$ in presynaptic fractions within one brain region to presynaptic expression within another brain region were calculated by dividing the total normalized area for $G\gamma_3$ in the presynaptic fraction of one brain region by expression in the presynaptic fraction within a second brain region (e.g. CTX pre/CRB pre). This was also done to compare expression of $G\gamma_3$ in postsynaptic fractions between brain regions. Comparisons were not made between pre and postsynaptic fractions of different brain regions. Brain regions and raw total area values for the numerator in these calculations are shown along the top of the table, highlighted in bold and parentheses respectively. Brain regions and raw total area values for the denominator in these calculations are shown along the left of the table, highlighted in bold and parentheses respectively. Raw values and fold differences were rounded to two decimal places. Fold differences that are significant are shown in bold. CTX:cortex; CRB: cerebellum; Hippo: hippocampus; Str: striatum; pre: presynaptic fraction; post: postsynaptic fraction.

$G\gamma_4$		**Fold Difference Numerator** (Fold Difference Numerator Raw Value)							
Fold Difference Denominator (Fold Difference Denominator Raw Value)		**CTX pre** (5.09E-7)	**CRB pre** (1.49E-7)	**Hippo pre** (3.51E-7)	**Str pre** (2.22E-7)	**CTX post** (5.42E-7)	**CRB post** (2.15E-7)	**Hippo post** (8.61E-7)	**Str post** (8.26E-7)
	CTX pre (5.09E-7)	--	0.29	0.69	0.44	1.06			
	CRB pre (1.49E-7)	3.42	--	2.36	1.49		1.45		
	Hippo pre (3.51E-7)	1.45	0.42	--	0.63			2.45	
	Str pre (2.22E-7)	2.29	0.67	1.58	--				**3.71**
	CTX post (5.42E-7)	0.94				--	0.40	1.59	1.52
	CRB post (2.15E-7)		0.69			2.52	--	**4.00**	**3.83**
	Hippo post (8.61E-7)			0.41		0.63	0.25	--	0.96
	Str post (8.26E-7)				0.27	0.66	0.26	1.04	--

Table 10. Fold differences comparing expression of G protein γ_4 in pre or postsynaptic fractions between brain regions and pre- and postsynaptic fractions within a brain region. Fold differences comparing expression of $G\gamma_4$ in postsynaptic fractions to $G\gamma_4$ expression in presynaptic fractions within a brain region were calculated by dividing the total normalized area for $G\gamma_4$ peptides within the postsynaptic fraction by the total normalized area for $G\gamma_4$ peptides within the presynaptic fraction (e.g. CTX post/CTX pre). Fold differences comparing expression of $G\gamma_4$ in presynaptic fractions within one brain region to presynaptic expression within another brain region were calculated by dividing the total normalized area for $G\gamma_4$ in the presynaptic fraction of one brain region by expression in the presynaptic fraction within a second brain region (e.g. CTX pre/CRB pre). This was also done to compare expression of $G\gamma_4$ in postsynaptic fractions between brain regions. Comparisons were not made between pre and postsynaptic fractions of different brain regions. Brain regions and raw total area values for the numerator in these calculations are shown along the top of the table, highlighted in bold and parentheses respectively. Brain regions and raw total area values for the denominator in these calculations are shown along the left of the table, highlighted in bold and parentheses respectively. Raw values and fold differences were rounded to two decimal places. Fold differences that are significant are shown in bold. CTX:cortex; CRB: cerebellum; Hippo: hippocampus; Str: striatum; pre: presynaptic fraction; post: postsynaptic fraction.

$G\gamma_7$		**Fold Difference Numerator** (Fold Difference Numerator Raw Value)							
Fold Difference Denominator (Fold Difference Denominator Raw Value)		**CTX pre** (4.51E-6)	**CRB pre** (1.97E-6)	**Hippo pre** (3.97E-6)	**Str pre** (7.74E-6)	**CTX post** (7.85E-6)	**CRB post** (5.11E-6)	**Hippo post** (1.37E-5)	**Str post** (4.29E-5)
	CTX pre (4.51E-6)	--	0.44	0.88	1.72	1.74			
	CRB pre (1.97E-6)	2.29	--	2.01	3.93		2.59		
	Hippo pre (3.97E-6)	1.14	0.50	--	1.95			3.46	
	Str pre (7.74E-6)	0.58	0.25	0.51	--				**5.55**
	CTX post (7.85E-6)	0.57				--	0.65	1.75	**5.47**
	CRB post (5.11E-6)		0.39			1.54	--	2.69	**8.41**
	Hippo post (1.37E-5)			0.29		0.57	0.37	--	**3.13**
	Str post (4.29E-5)				0.18	0.18	0.12	0.32	--

Table 11. Fold differences comparing expression of G protein γ_7 in pre or postsynaptic fractions between brain regions and pre- and postsynaptic fractions within a brain region. Fold differences comparing expression of $G\gamma_7$ in postsynaptic fractions to $G\gamma_7$ expression in presynaptic fractions within a brain region were calculated by dividing the total normalized area for $G\gamma_7$ peptides within the postsynaptic fraction by the total normalized area for $G\gamma_7$ peptides within the presynaptic fraction (e.g. CTX post/CTX pre). Fold differences comparing expression of $G\gamma_7$ in presynaptic fractions within one brain region to presynaptic expression within another brain region were calculated by dividing the total normalized area for $G\gamma_7$ in the presynaptic fraction of one brain region by expression in the presynaptic fraction within a second brain region (e.g. CTX pre/CRB pre). This was also done to compare expression of $G\gamma_7$ in postsynaptic fractions between brain regions. Comparisons were not made between pre and postsynaptic fractions of different brain regions. Brain regions and raw total area values for the numerator in these calculations are shown along the top of the table, highlighted in bold and parentheses respectively. Brain regions and raw total area values for the denominator in these calculations are shown along the left of the table, highlighted in bold and parentheses respectively. Raw values and fold differences were rounded to two decimal places. Fold differences that are significant are shown in bold. CTX:cortex; CRB: cerebellum; Hippo: hippocampus; Str: striatum; pre: presynaptic fraction; post: postsynaptic fraction.

$G\gamma_{12}$		**Fold Difference Numerator** (Fold Difference Numerator Raw Value)							
Fold Difference Denominator (Fold Difference Denominator Raw Value)		**CTX pre** (6.44E-6)	**CRB pre** (5.08E-6)	**Hippo pre** (2.43E-6)	**Str pre** (1.42E-6)	**CTX post** (1.81E-5)	**CRB post** (1.60E-5)	**Hippo post** (1.30E-5)	**Str post** (1.49E-5)
	CTX pre (6.44E-6)	--	0.79	0.38	0.22	**2.81**			
	CRB pre (5.08E-6)	1.27	--	0.48	0.28		**3.16**		
	Hippo pre (2.43E-6)	2.65	2.09	--	0.58			**5.36**	
	Str pre (1.42E-6)	4.53	3.57	1.71	--				**10.46**
	CTX post (1.81E-5)	0.36				--	0.89	0.72	0.82
	CRB post (1.60E-5)		0.32			1.13	--	0.81	0.93
	Hippo post (1.30E-5)			0.19		1.39	1.23	--	1.14
	Str post (1.49E-5)				0.10	1.22	1.08	0.88	--

Table 12. Fold differences comparing expression of G protein γ_{12} in pre or postsynaptic fractions between brain regions and pre- and postsynaptic fractions within a brain region. Fold differences comparing expression of $G\gamma_{12}$ in postsynaptic fractions to $G\gamma_{12}$ expression in presynaptic fractions within a brain region were calculated by dividing the total normalized area for $G\gamma_{12}$ peptides within the postsynaptic fraction by the total normalized area for $G\gamma_{12}$ peptides within the presynaptic fraction (e.g. CTX post/CTX pre). Fold differences comparing expression of $G\gamma_{12}$ in presynaptic fractions within one brain region to presynaptic expression within another brain region were calculated by dividing the total normalized area for $G\gamma_{12}$ in the presynaptic fraction of one brain region by expression in the presynaptic fraction within a second brain region (e.g. CTX pre/CRB pre). This was also done to compare expression of $G\gamma_{12}$ in postsynaptic fractions between brain regions. Comparisons were not made between pre and postsynaptic fractions of different brain regions. Brain regions and raw total area values for the numerator in these calculations are shown along the top of the table, highlighted in bold and parentheses respectively. Brain regions and raw total area values for the denominator in these calculations are shown along the left of the table, highlighted in bold and parentheses respectively. Raw values and fold differences were rounded to two decimal places. Fold differences that are significant are shown in bold. CTX:cortex; CRB: cerebellum; Hippo: hippocampus; Str: striatum; pre: presynaptic fraction; post: postsynaptic fraction.

$G\gamma_{13}$		**Fold Difference Numerator** (Fold Difference Numerator Raw Value)							
Fold Difference Denominator (Fold Difference Denominator Raw Value)		**CTX pre** (9.11E-6)	**CRB pre** (5.32E-6)	**Hippo pre** (2.26E-6)	**Str pre** (1.04E-6)	**CTX post** (1.10E-5)	**CRB post** (1.18E-5)	**Hippo post** (4.96E-6)	**Str post** (3.86E-6)
	CTX pre (9.11E-6)	--	0.58	0.25	0.11	1.21			
	CRB pre (5.32E-6)	1.71	--	0.43	0.20		**2.22**		
	Hippo pre (2.26E-6)	**4.03**	2.35	--	0.46			2.19	
	Str pre (1.04E-6)	**8.76**	5.12	2.18	--				3.71
	CTX post (1.10E-5)	0.83				--	1.07	0.45	0.35
	CRB post (1.18E-5)		0.45			0.93	--	0.42	0.33
	Hippo post (4.96E-6)			0.46		2.22	**2.38**	--	0.79
	Str post (3.86E-6)				0.27	**2.86**	**3.06**	1.29	--

Table 13. Fold differences comparing expression of G protein γ_{13} in pre or postsynaptic fractions between brain regions and pre- and postsynaptic fractions within a brain region. Fold differences comparing expression of $G\gamma_{13}$ in postsynaptic fractions to $G\gamma_{13}$ expression in presynaptic fractions within a brain region were calculated by dividing the total normalized area for $G\gamma_{13}$ peptides within the postsynaptic fraction by the total normalized area for $G\gamma_{13}$ peptides within the presynaptic fraction (e.g. CTX post/CTX pre). Fold differences comparing expression of $G\gamma_{13}$ in presynaptic fractions within one brain region to presynaptic expression within another brain region were calculated by dividing the total normalized area for $G\gamma_{13}$ in the presynaptic fraction of one brain region by expression in the presynaptic fraction within a second brain region (e.g. CTX pre/CRB pre). This was also done to compare expression of $G\gamma_{13}$ in postsynaptic fractions between brain regions. Comparisons were not made between pre and postsynaptic fractions of different brain regions. Brain regions and raw total area values for the numerator in these calculations are shown along the top of the table, highlighted in bold and parentheses respectively. Brain regions and raw total area values for the denominator in these calculations are shown along the left of the table, highlighted in bold and parentheses respectively. Raw values and fold differences were rounded to two decimal places. Fold differences that are significant are shown in bold. CTX:cortex; CRB: cerebellum; Hippo: hippocampus; Str: striatum; pre: presynaptic fraction; post: postsynaptic fraction.

Part B: Pilot studies examining localization of G protein $\beta\gamma$ subunits at specific synaptic terminals

To evaluate G protein distribution at specific synaptic terminals, in collaboration with the Blakely lab, we performed pilot studies using a synaptosomal preparation as it would allow us to detect fluorescently tagged HA-α_{2A}AR or EYFP expressing terminals using flow cytometry (Figure 13A). Initial studies were carried out using transgenic mice expressing HA-α_{2A}AR (Figure 13B) to evaluate the feasibility of this approach. Synaptosomes enriched from the whole brain of wildtype or transgenic mice were incubated with an anti-HA primary antibody conjugated to Alexa Fluor 647 before being analyzed by flow cytometry. Figure 13C shows forward scatter and fluorescence plots of events detected by the flow cytometer from wildtype and transgenic samples. While fluorescent populations (purple particles) from transgenic synaptosomes spanned a range of sizes (as denoted by forward scatter), they represent only a minor subset of particles detected (7%) which is appropriate given the low abundance of HA-expressing synaptosomes in samples compared to total synaptosome populations. Significantly more fluorescent particles were detected in transgenic samples (7%; lower panel) compared to wildtype (0.9%; upper panel) suggesting specific labeling of HA-α_{2A}AR. Experiments carried out with synaptosomes isolated from midbrains of TPH2-ChR2(H13R)-EYFP and ChAT-ChR2(123R)-EYFP mice showed similar increases in fluorescence when compared to wildtype samples (data not shown). Subsequent experiments used FACS to collect serotonergic synaptosomes from TPH2-ChR2(H13R)-EYFP mice for use in western blot and proteomic studies. Synaptosomes were generated from the pooled midbrains of four TPH2-ChR2(H13R)-EYFP mice and enriched on a sucrose gradient. Samples were sorted and non-fluorescent, low, and high fluorescence fractions collected for analysis (Figure 14A). Immunoblots revealed enrichment of synaptophysin, and syntaxin in the low fluorescence and high fluorescence fractions compared

to the non-fluorescent fraction (Figure 14B) suggesting that the collected fractions contained intact synaptosomes. Enrichment of SERT in these two fractions confirmed that serotonergic synaptosomes had been collected (Figure 14B). To evaluate G protein expression, we next applied our refined MRM method (described in Part A) to a high fluorescence fraction collected from a FACS experiment using TPH2-ChR2(H13R)-EYFP mice. Midbrains from four transgenic mice were pooled, and non-fluorescent, low, and high fluorescence fractions collected. Only the high fluorescence fraction was used for MRM experiments as this showed the greatest enrichment of SERT in WB analysis (Figure 14B). Chromatographic peaks of monitored transition ions could only be confidently identified for $G\beta_1$ and $G\beta_2$ (Figure 14C). As these results are from a single biological sample, data was not normalized. Rather, transition ion intensities were summed for each precursor to generate the total AUC seen in Figure 14C.

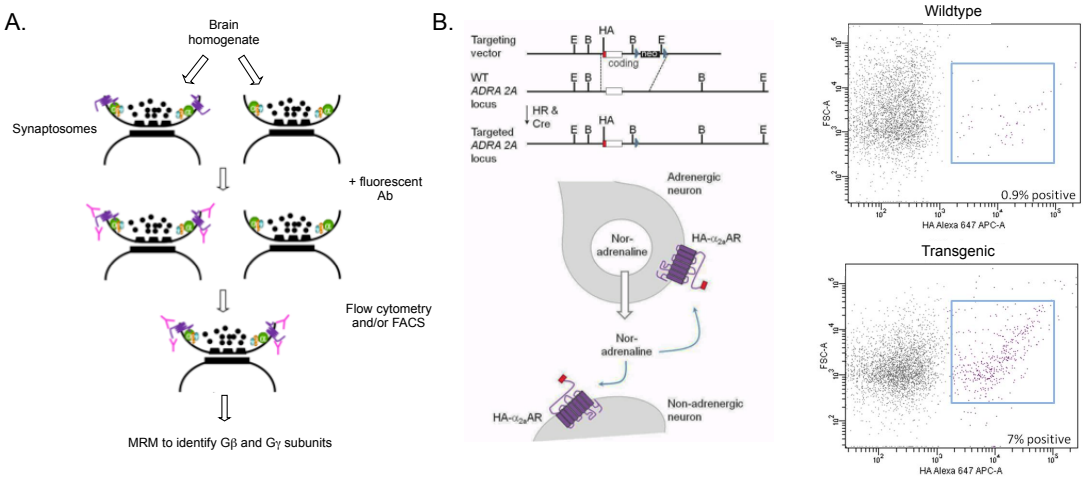

Figure 13. Fluorescent detection of synaptosomes expressing HA-tagged α_{2A} receptors (HA-α_{2A}AR). A) General experimental protocol for the isolation of synaptosomes from mouse brain tissue and the fluorescent labeling of tagged receptors for use in flow cytometry and FACS experiments. B) Targeting strategy for the generation of HA-α_{2A}AR mice (Lu et al., 2009). Boxes show flow cytometry of HA-α_{2A}AR on the surface of synaptosomes from wildtype (top) and transgenic (bottom) mice. % positive indicates the positive fraction for representative plots of fluorescent anti-HA antibody.

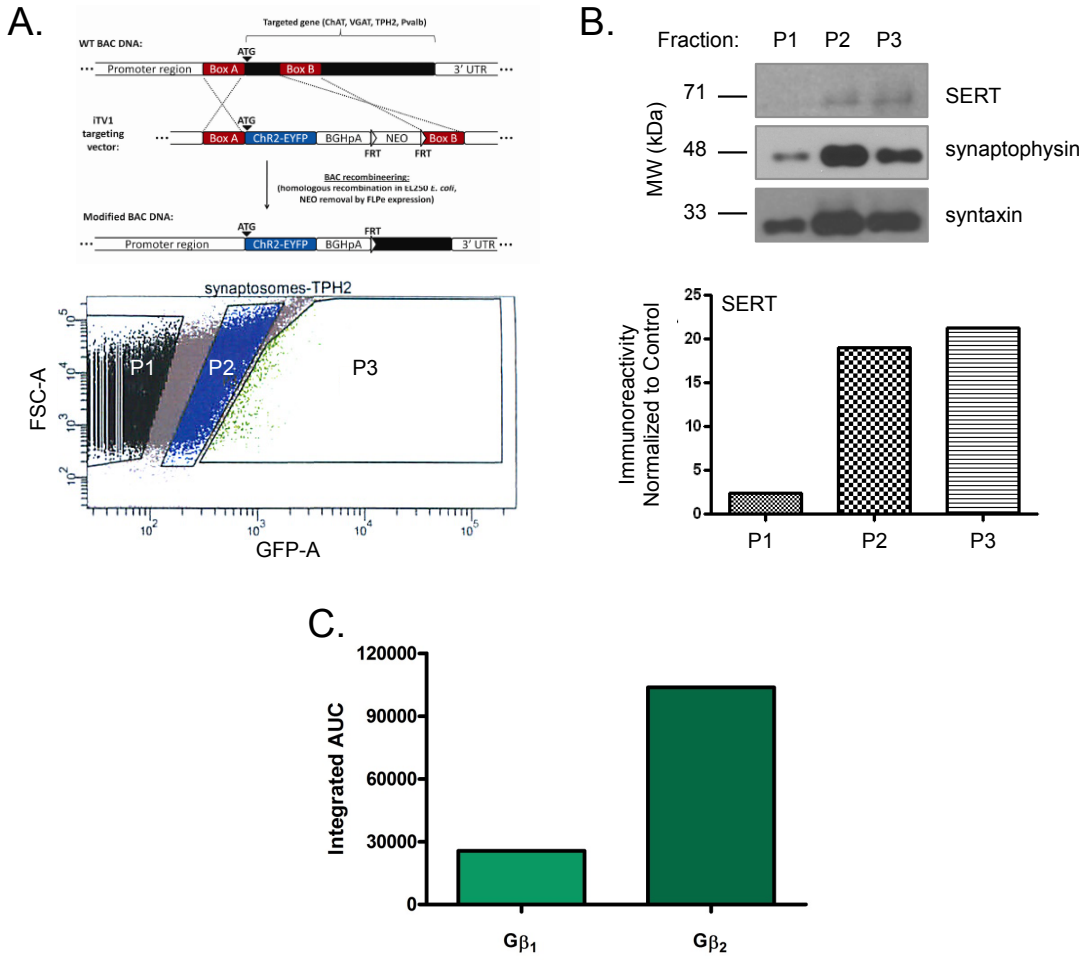

Figure 14. Identification of G protein βγ isoforms localized to serotonergic neurons. A) Top panel: targeting strategy for the generation of TPH2-ChR2-EYFP (Zhao *et al.*, 2011). Bottom panel: Flow cytometric detection of fluorescent populations of synaptosomes isolated from midbrain of TPH2 transgenic mice. Gating was based on size and fluorescence to collect 3 fractions using FACS – nonfluorescent (P1), low fluorescence (P2), and high fluorescence (P3). B**)** Representative immunoblots of sorted fractions blotted for SERT, synaptophysin, and syntaxin. SERT expression is quantified in lower panel. Immunoblots performed by Dr. Ran Ye. C) Total integrated area under the curve for all peptides unique to a G protein isoform that were detected in MRM experiments from high fluorescence fraction (P3).

Discussion

G protein βγ subunits are known to play essential roles in cellular communication via complex regulatory mechanisms. Increasingly, studies are demonstrating that receptors and effectors preferentially interact with unique complements of Gβγ isoforms[213,214,230,259-261], suggesting that precise regulation of expression and localization is important[77] for maintaining the fidelity of signaling pathways. Transcript expression suggests these isoforms are distributed across many brain regions but less is known about protein localization as high sequence identity makes development of subunit specific antibodies difficult. The novel application of MRM techniques to this question allows accurate identification and quantification of endogenous Gβγ subunits from complex mixtures of brain tissue. With this approach, we demonstrate brain region specific differences in the protein expression patterns of individual G protein Gβ and Gγ isoforms in pre and postsynaptic fractions. Further, we present pilot study data suggesting synaptic terminals expressing different neurotransmitters may express only a subset of G protein isoforms. To look at subcellular expression patterns, we employed an LRP method to evaluate the relative expression of each isoform, as SID methods that include labeled internal protein standards for each peptide being monitored are cost-prohibitive given the number of peptides to be analyzed. Zhang et al. recently showed that an LRP method is a reasonable alternative to SID as it is well suited for comparing relative protein levels, and is capable of detecting the same significant differences in biological samples[252]. Application of this technique to the current study is a first required step toward a more complete understanding of specificity in Gβγ signaling. The observed differences suggest neuronal cells would be able to channel information differentially through signaling complexes and second messenger pathways in different brain regions.

Differential expression and distribution of Gβγ isoforms between brain regions

Several studies have demonstrated that Gβ and Gγ isoforms show differential patterns of expression throughout the CNS. Although the data obtained in those studies are in general agreement with those presented here, ours is the first to provide a comprehensive map of their protein distribution to distinct subcellular fractions; previously, only $G\beta_1$ has been reported at both the presynaptic active zone[243] and PSD[244]. $G\beta_1$ is expressed ubiquitously throughout the brain[98,226], correlating well with our findings that this isoform was detectable at comparable levels within pre- and postsynaptic fractions across most of the brain regions examined (Figure 11A) but also at serotonergic terminals (Fig14C). A similar range of expression was observed for $G\beta_2$ (Figure 11A; Figure 14C) and $G\beta_4$ (Figure 11A). *In vitro* data show that $G\beta_1$, $G\beta_2$, and $G\beta_4$ can all pair with numerous Gγ isoforms, as well as couple to a variety of receptors and effectors[262]. While this implies involvement in a wide range of signaling pathways and supports the broad distribution we observed, their function *in vivo* is poorly understood. What is known is that $G\beta_1$ plays an important role in neural development; its removal is perinatally lethal and pups exhibit reduced cortical thickness, brain volume, and impaired neural progenitor cell proliferation[263]. Comparatively, $G\beta_2$ may play a role in neuronal excitability as mice in which Gγ3 is lost exhibit a severe seizure phenotype and a reduction of $G\beta_2$ within the cortex, cerebellum, and striatum[102,264]. Further, knockdown studies demonstrate $G\beta_1$, $G\beta_2$, and $G\beta_4$ each signal downstream of specific GPCRs found throughout the CNS[265,266]. The extensive expression patterns we observed for each isoform may thus be expected, as a broad distribution would be required to support such diverse signaling pathways.

In contrast to the other Gβ isoforms, expression of $G\beta_5$ was seen exclusively within the striatum, as levels within the cortex, cerebellum, and hippocampus were below the limit of

detection (Figure 11D). Similarly, levels were below the limit of detection looking at serotonergic terminals from the midbrain (Fig. 14C). This result differs from previously published reports that suggested a wide distribution similar to that of the other Gβ isoforms[98,226,227]. While we cannot rule out that such disparity reflects physiological differences in the expression of the protein product or differential post-translational processing between brain regions, such a limited distribution may also correspond to the interaction of $G\beta_5$ with regulators of G protein signaling (RGS) proteins. $G\beta_5$ forms a stable obligate dimer with members of the RGS R7 subfamily to modulate G_i-mediated signal transduction pathways[267-271]. One member, RGS9-2, is enriched in the striatum and the complex of RGS9-2/ $G\beta_5$ is localized to the membrane through its interaction the R7 family binding protein (R7BP)[269,272-274]. Conversely, RGS7/ $G\beta_5$ complexes are found intracellularly throughout the CNS[269,274]. This may explain why, in the present study, $G\beta_5$ was only detectable in the striatum. Our fractionation protocol aimed to enrich the presynaptic active zone membrane fraction as well as the PSD membrane fraction, while cytosolic fractions were not analyzed. The $G\beta_5$/RGS9-2 association with the plasma membrane in the striatum is consistent with our detection of $G\beta_5$ in this region. Further, as R7BP and RGS9-2 co-localize predominantly to postsynaptic membranes[273,275], enrichment of $G\beta_5$ in postsynaptic fractions within this region would be expected (Figure 12D). If, in other brain regions, $G\beta_5$ is primarily complexed with RGS7 and found intracellularly, it would not have been detected in our current study as these fractions were not analyzed. Conversely, intracellular $G\beta_5$ could have been detected in serotonergic synaptosomes collected from pilot studies using FACS , as these samples were not fractionated into pre- and postsynaptic fractions. As a result, both membrane-bound and cytosolic $G\beta_5$ would have been present and detectable. The lack of $G\beta_5$ in these samples is consistent with the idea that this isoform is only highly expressed in the striatum, however, it must be noted that these results are preliminary and reflect only one biological

sample. Further efforts will be needed to determine whether $G\beta_5$ is detectable in cytosolic fractions to address this hypothesis.

In comparison, the $G\gamma$ subunits show more varied expression patterns; however, with the exception of $G\gamma_5$ and $G\gamma_{11}$, each isoform was clearly identifiable within each of the four brain regions examined (Figure 12). Conversely, $G\gamma$ isoforms could not be confidently identified in samples collected using FACs from the midbrains of TPH2-ChR2(H13R)-EYFP mice. Since G proteins are found as a functional dimer, it is assumed that serotonergic synapses express both $G\beta$ and $G\gamma$ isoforms. The lack of $G\gamma$ isoforms identified in the collected midbrain samples likely reflects a lack of material and as such future studies will need to pool more animals to ensure detection of the various G proteins.

Although immunohistochemical studies have localized particular isoforms to the CNS in general, a detailed examination of their expression to brain regions and cell types has been limited to transcript levels[226,276]. For some $G\gamma$ isoforms, transcript expression reported previously correlates well with the localization patterns observed in the present study, whereas in others it differs notably. For example, using *in situ* hybridization, Betty et al.[98] showed strong expression of $G\gamma_7$ within the striatum, followed closely by the hippocampus, cortex, and cerebellum, similar to what is seen in the present study (Figure 12D). Conversely, the authors reported $G\gamma_4$ to be highly expressed in the hippocampus and cerebellum but lower in the striatum, whereas our analyses show the opposite: strong expression in the striatum but significantly lower levels in the cerebellum (Figure 12C). It is difficult to say whether these differences reflect physiological effects relating to the expression of the protein product or possible protein modifications that were not accounted for in the present study. One factor that may contribute to the disparities, however, is that the present study examined expression patterns at subcellular levels. In comparison, previous *in situ* studies were only able to evaluate

Gγ expression at the cellular level, which would have included both the soma as well as the nerve terminals. Thus, direct comparison between such studies is not possible.

Little is known about the subcellular distribution of Gγ isoforms within the CNS. Moricano et al. localized $G\gamma_3$ to the presynaptic active zone, but subcellular localization patterns for the remaining Gγ isoforms have not been previously evaluated[243]. The wide discrepancy in expression patterns within subcellular fractions and across the four brain regions could reflect unique contributions by each isoform to unique signaling pathways. This is supported by the distinct phenotypes observed when Gγ isoforms are genetically knocked out. In the case of $G\gamma_3$, genetic deletion results in mice with increased susceptibility to seizures, as well as resistance to diet induced obesity; implying a role in neuronal excitability and regulation of appetite or metabolism[215,264]. Loss of $G\gamma_3$ suppresses expression of $G\beta_1$ and $G\beta_2$ within the cortex, cerebellum, and striatum, implicating a $G\beta_{1/2}\gamma_3$ dimer within these regions and in agreement with our expression results (Figure 12B). Of note, significant enrichment of $G\gamma_3$ was observed in the postsynaptic fraction of the striatum. Although further efforts are needed to understand the physiological consequences of this finding, one possibility may be related to the activity of μ-opioid receptors within this region. Loss of $G\gamma_3$ results in defective signaling through the μ-opioid receptor[264]. Within the striatum, these receptors have been implicated in the hedonic response to food[277,278], and act via a postsynaptic mechanism[279]. As a result, the enrichment seen in the postsynaptic fraction of the striatum could represent an important signaling cascade activated by μ-opioid receptors and involving the $G\gamma_3$ subunit; further efforts will be needed to explore this possibility. In comparison, animals in which $G\gamma_7$ has been knocked out exhibit an increased startle response, which may result from defective D_1 dopamine and A_{2A} adenosine receptor activation within the striatum[102,280,281]. This correlates well with our findings, and previously published reports[98,282], that $G\gamma_7$ is most highly expressed in the striatum (Figure 12D).

While further efforts will be needed to confirm the exact mechanism, given that both D_1 and A_{2A} receptors are localized primarily to dendritic spines[283,284], and that we observed significant enrichment of $G\gamma_7$ within the postsynaptic fraction (Figure 12D), suggests a predominately postsynaptic role for $G\gamma_7$ within this region.

Although no genetically modified animals are available for $G\gamma_2$ and $G\gamma_4$, knockdown of these isoforms offers insight into the expression patterns we observed. Early work by Kalkbrenner et al.[285] demonstrated that silencing of endogenous $G\gamma_2$ and $G\gamma_4$ in cultured cells reduced galanin-induced calcium inhibition. More recently, a role in nociception was suggested for $G\gamma_2$, as injection of antisense oligonucleotides into the CNS of mice attenuated the analgesic effects of opioid, cannabinoid, and adrenergic agonists[286,287] . Such a range of effector interactions would be expected to contribute to the observed localization patterns. Galanin, cannabinoid, and adrenergic receptors all exhibit a broad distribution in the CNS[288], while opioid receptor subtypes are highly expressed within the striatum and cortex[289-291]. As a result, if $G\gamma_2$ and $G\gamma_4$ acted via these receptors *in vivo*, the wide distribution we observed (Figure 12A) could be because their expression parallels that of their target GPCRs.

Finding $G\gamma_{13}$ within each of the brain regions we examined was exciting as this G protein has largely been reported in sensory tissues, where it is required for olfactory and gustatory transduction[292]. While transcript expression within the brain closely mirrors our results[293,294] (Figure 12F), little is known about the function of this isoform in the CNS. $G\gamma_{13}$ has been shown to interact with the third PDZ domain of PSD-95 via a PDZ binding C-terminal sequence, and the two proteins can be efficiently pulled down together from brain lysates[295]. It is possible that this association aids in targeting the G protein to particular subcellular locations and/or facilitates interactions with appropriate effectors such as GIRK channels and $PLC\beta_2$[293], accounting for the greater expression of $G\gamma_{13}$ in postsynaptic fractions (Figure 12F).

Additional factors that may contribute to differential expression patterns

In addition to signaling requirements, other factors are likely to influence the observed localization patterns. A striking feature from our data was that while most G protein isoforms were found in all four brain regions, prominent differences were observed between regions. Such disparity may reflect G protein expression within individual cells types as well as patterns of innervation to specific brain regions. This is supported by our preliminary data examining G protein localization at serotonergic synapses within the midbrain. When specific synapses were isolated using FACS, only a subset of G protein isoforms were found to be expressed. While this result is preliminary, and we can't rule out that the discrepancy is due to lack of sample material and/or only having a single biological replicate, it does suggest that cell type and innervation could play important roles in controlling which G proteins are expressed. For example, the striatum is composed largely of γ-aminobutyric acid (GABA)-containing medium spiny neurons yet receives excitatory inputs from the cortex and dopaminergic innervations from the midbrain[296,297]. Glutamatergic pyramidal neurons predominate in the hippocampus, but this region also receives monoamine and cholinergic inputs from the median raphe[298,299], locus coeruleus[300], and basal forebrain[301]. In contrast, the cerebellum could be considered more homogeneous as Purkinje cells represent the sole output of the cerebellar cortex, but even these integrate excitatory afferent pathways as well as strong inhibitory GABAergic inputs[302]. Such diversity in cell type and innervation patterns may provide clues as to why differences in G protein expression patterns were observed between brain regions as well as subcellular fractions. This is supported by early work by Betty et al.[98] and Liang et al.[226], as well as more recent efforts from Schwindinger et al.[102]. Thus, G protein expression within particular cell types, as well as the innervation within a brain region, would influence the results seen in the current study. Synaptosomal preparations and subcellular fractionation techniques such as those

described do not allow for Gβγ expression patterns to be evaluated endogenously within specific cell types. However, with recent advances in optogenetics, transgenic mice such as the ones used in the present study are becoming available that express fluorescent proteins under the control of cell-type specific promoters. By taking advantage of these mice in future studies, it will be possible to evaluate localization patterns within specific neuron populations and subcellular fractions in order to determine if these factors contribute to the expression of specific isoforms.

Summary

In summary, we report that G protein β and γ isoforms exhibit distinct patterns of localization across brain regions as well as to subcellular fractions. This is particularly interesting as it implies specific functions for individual isoforms in modulating cellular responses and signaling cascades. Further efforts will be necessary to determine the relevance of these patterns of distribution, evaluate which Gβγ dimers exist endogenously, and the contribution each makes to cellular communication.

CHAPTER IV

EXAMINING THE ROLE OF G PROTEIN βγ SPECIFICITY IN MODULATING SYNAPTIC TRANSMISSION

Introduction

Efficient communication between neurons is crucial to the normal functioning of the central and peripheral nervous systems as it ensures efficient integration of both external and internal sensory input and permits the generation of appropriate behaviours. As a result, understanding the factors controlling synaptic transmission is essential to understanding how normal processes are coordinated, but also how they may be disrupted by injury and disease. At chemical synapses, signal transduction is regulated by a series of complex mechanisms that ensure precise control of release. Inhibitory GPCRs play an important role in this process as they guard against overstimulation by inhibiting evoked transmitter release through the actions of released G protein βγ subunits[303,304]. While these receptors act through numerous mechanisms, regulation of fast, membrane-delimited inhibition has largely been attributed to the action of βγ subunits on VDCC[112,124], although activation of presynaptic potassium channels has also been reported[305]. In addition, GPCR-mediated inhibition of transmitter release has been reported at sites distal to calcium entry[74,75, 138,174,306-308] with Gβγ subunits binding directly to members of the exocytotic machinery[74,75,79,309]. In doing so, Gβγ subunits compete with the calcium sensor, synaptotagmin, to limit the number and duration of fusion events[74,75,79,309]. Despite an understanding of the mechanisms by which feedback inhibition occurs, however, the factors controlling the specificity of G protein interactions are poorly understood.

Traditionally, G protein specificity has been attributed to Gα subunits as *in vitro* studies examining Gβγ combinations revealed only modest discrimination during receptor and effector interactions[212,213]. More recently, however, cell-based and *in vivo* studies have suggested that the composition of Gβγ subunits plays an important role in defining the specificity of GPCR mediated signaling cascades. Membrane reconstitution studies demonstrated a preference of Adenosine A_1 and $5HT_{1A}$ receptors for G proteins containing $G\gamma_{11}$, while α_{2A}AR and μ-opioid receptors were shown to bind more potently to subunits containing $G\gamma_7$[310]. Similarly, antisense studies from Kleuss et al. revealed a requirement for $G\beta_3$ and $G\gamma_4$ in the M1 muscarinic receptor signaling pathway in rat pituitary cells[213,214], while those from Varga et al. demonstrated a role for $G\gamma_2$ in nociception through the attenuation of opioid, cannabinoid, and adrenergic agonists[286,287]. Perhaps most convincingly, however, genetic deletion of particular G protein isoforms results in mice with distinct phenotypes including seizures[102,264], increased startle responses[102,280,281], severe heart defects[311], widespread neural malformation, as well as impaired development and motor learning[312]. While none of these studies specifically looked at G protein/SNARE interactions, *in vitro* data suggest that different G protein isoforms could have differential effects on SNARE function. Blackmer et al.[74] demonstrated a 40 fold difference in the ability of $G\beta_1\gamma_2$ to bind SNARE proteins compared to $G\beta_1\gamma_1$. Similarly $G\beta_1\gamma_2$ isoforms were 20 fold more potent at inhibiting calcium-trigged exocytosis than $G\beta_1\gamma_1$. Taken together, this suggests that isoforms may exhibit differences in their ability to modulate SNARE function endogenously.

α_{2A}ARs are of interest in understanding the functional consequence of Gβγ/SNARE interactions as they operate as the main feedback regulator of noradrenaline release from presynaptic terminals[304,313,314]. Polymorphisms in the *ADRA2A* gene results in expression of increased levels of presynaptic α_{2A}ARs and predispose patients to alcohol dependence, reduced glucose-stimulated insulin release[315], changes in memory and behaviour[316], as well as reduced

response to antidepressants[317]. Additionally, dysregulation of these receptors has been associated with enhanced fear memory[318] and deficits in spatial working memory[319], making them important targets for therapeutic intervention. While these receptors operate through numerous effectors, α_{2A}AR-mediated inhibition of neurotransmitter release has been shown to occur downstream of calcium entry in both the amygdala[183] and pancreatic β cells[185], with G$\beta\gamma$ subunits inhibiting vesicle fusion in both instances through direct interactions with the SNARE proteins.

When considering how G$\beta\gamma$-selective targeting to SNARE proteins could occur, two potential sites of interaction may play a role. The first is at the level of the receptor/G protein interaction, where activated α_{2A}ARs may preferentially release particular G$\beta\gamma$ subunits in order to modulate SNARE function. Alternatively, the GPCR could be promiscuous and not discriminate between which heterotrimers it interacts with; instead targeting could be defined at the level of the effector, with only a subset of released G$\beta\gamma$ subunits able to bind to SNARE proteins and inhibit vesicle fusion. To distinguish between these possibilities, we utilized a transgenic mouse line in which tagged α_{2A} receptors are only expressed presynaptically at noradrenergic terminals. Using immunoprecipitation and targeted proteomics, we were able to assess which G$\beta\gamma$ isoforms interacted with the receptor or SNARE proteins following stimulation of the receptor. Interestingly, we found that α_{2A} receptors preferentially interact with a subset of G$\beta\gamma$ isoforms when activated, suggesting receptor/G protein specificity could be important for directing SNARE modulation.

Experimental Procedures

Animals. Adult, FLAG-tagged α_{2A} adrenergic receptor transgenic or α_{2A} knockout [303, 304] mice were decapitated and tissue immediately homogenized to produce synaptosomes as described below. All animal protocols were carried out in accordance with the recommendations in the Guide for the Care and Use of Laboratory Animals of the NIH, and were approved by the Vanderbilt Institutional Animal Care and Use Committee.

Antibodies. The following primary antibodies were used for immunoprecipitation: mouse anti-FLAG (Sigma, catalog #F3165) rabbit anti-SNAP 25 (Sigma, catalog #S9684), rabbit ChromePure IgG (Jackson Immuno Research, catalog # 011-030-003). The following primary antibodies were used for immunoblotting (dilutions indicated): rabbit anti-FLAG (Sigma, catalog #F7425, 1:100), rabbit anti-Gβ, (Santa Cruz, catalog #sc-378, 1:10,000); mouse anti-SNAP 25 (Santa Cruz, catalog #sc-378, 1:500). Horseradish peroxidase (HRP)-conjugated secondary antibodies were obtained from Perkin-Elmer and used at the following dilutions: goat anti-rabbit (1:10,000), goat anti-mouse (1:10,000). Additionally, an HRP-conjugated mouse anti-rabbit light chain specific secondary was used for Gβ blots (Jackson Immuno research, 1:7500).

Synaptosome preparation and stimulation protocol. Synaptosomes were prepared as described in Chapter III. Briefly, mouse brains from KO and Tg animals were homogenized in 20ml of a 0.32M sucrose solution [0.32M sucrose, 4.2mM Hepes pH 7.4, 0.1mM $CaCl_2$, 1mM $MgCl_2$, 1.54mM aprotinin, 10.7mM leupeptin, 0.95mM pepstatin, and 200mM PMSF] and homogenate divided into two equal aliquots. Homogenates were centrifuged at 1,000 x g at 4°C for 10 minutes to pellet nuclei and membrane debris before supernatants were transferred to clean conical tubes. Pellets were resuspended in 20ml 0.32M sucrose, the centrifugation step repeated, and supernatants combined. Following mixing, supernatants were centrifuged at

10,000 x g at 4°C for 20 minutes to produce crude synaptosome preps. Supernatants were discarded and pellets gently resuspended in 2ml stimulation buffer that did not contain epinephrine (10X DPBS (26.7mM KCl, 14.7mM KH2PO4, 1379 mM NaCl, 80mM Na2HPO4 x 7H2O, pH 6.8-7), 1uM prazosin (Sigma, catalog #P7791), 1uM propranolol (Sigma, catalog #P0884), and 1uM JP 1302 (Tocris, catalog #2666)) before being transferred to 6ml culture vials and placed on ice. For experiments examining receptor/G protein specificity, FLAG-tagged α_{2A}ARs were stimulated by adding 2ml of stimulation buffer containing epinephrine (10X DPBS (26.7mM KCl, 14.7mM KH2PO4, 1379 mM NaCl, 80mM Na2HPO4 x 7H2O, pH 6.8-7), 1uM prazosin (Sigma, catalog #P7791), 1uM propranolol (Sigma, catalog #P0884), 1uM JP 1302 (Tocris, catalog #2666)and 200uM epinephrine (Sigma, catalog #E4642) to each vial and gently mixing. For experiments examining G protein/SNARE specificity, FLAG-tagged α_{2A}ARs were stimulated by adding 2ml of stimulation buffer containing epinephrine (10X DPBS (26.7mM KCl, 14.7mM KH2PO4, 1379 mM NaCl, 80mM Na2HPO4 x 7H2O, pH 6.8-7), 1uM propranolol (Sigma, catalog #P0884), 1uM JP 1302 (Tocris, catalog #2666), 10mM ethylenediaminetetraacetic acid (EDTA), and 200uM epinephrine (Sigma, catalog #E4642) to each vial and gently mixing. Final concentrations of epinephrine were 100uM. In both cases, following mixing, vials were placed in a 37°C water bath for 2 minutes before being transferred back to ice and incubated with the lipid soluble crosslinker, 3,3'-dithiobis[sulfosuccinimydlypropinate] (DSP) (Pierce, catalog #22585) for 30 minutes. The requirement of a crosslinker for immunoprecipitatation (IP) experiments, as well as the concentration needed, was determined empirically. At the end of 30 minutes, crosslinking reactions were quenched with 20mM Tris, pH 7.4 For 15 minutes on ice. Samples were then were centrifuged at 10,000 x g at 4°C for 20 minutes to pellet the synaptosome, washed in 4ml stimulation without epinephrine (10X DPBS (26.7mM KCl, 14.7mM KH2PO4, 1379 mM NaCl, 80mM Na2HPO4 x 7H2O, pH 6.8-7), 1uM prazosin (Sigma, catalog

#P7791), 1uM propranolol (Sigma, catalog #P0884), and 1uM JP 1302 (Tocris, catalog #2666), and the centrifugation step repeated. After centrifugation, supernatants were discarded and pellets frozen in liquid nitrogen until used in immunprecipitation experiments.

Immunoprecipitation. Frozen synaptosome pellets were thawed and resuspened in 2ml of radioimmunoprecipitation assay (RIPA) buffer (50mM Tris, pH 7.4, 150mM NaCl, 0.1% SDS, 1% sodium deoxycholate, 1% Triton X-100, 1mM EDTA, 1.54uM aprotinin, 10.7uM leupeptin, 0.948 uM pepstatin, 200uM PMSF) before being passed through a 25-gauge needle 6-8 times to lyse membranes. A BCA protein assay was performed and samples diluted to 1mg/ml in RIPA buffer before being placed on a rotator in the cold room for 1 hour. 300ul of homogenate was transferred to a 1.5ml eppendorf tube and combined with 100ul of 4x sample buffer containing DTT as well as 5% β-mercaptoethanol (BME) before being heated at 70°C for 5min and frozen at -80°C for later use. The remaining homogenate was transferred to 2ml eppendorff tubes and centrifuged at 14,000rpm for 10 minutes at 4°C to separate the triton soluble and insoluble fractions. After centrifugation supernatants were transferred to clean 2ml eppendorff tubes and precleared for 1 hour in the cold room with 50ul of Protein G agarose beads (Pierce, catalog #20398. Triton insoluble fractions were resuspended in 1ml of 2x containing DTT as well as 5% BME, heated at 70°C for 5min, and frozen at -80°C. After preclearing, samples were centrifuged at 14,000rpm for 1 minute to pellet beads. 300ul of lysate was transferred to 1.5ml eppendorff tubes and combined with 100ul 4x sample buffer containing DTT as well as 5% BME before being heated at 70°C for 5 minutes and frozen at -80°C for later use as input samples during western blot analysis. The remaining lysate was transferred to clean 1.5ml eppendorf tubes in 400ul aliquots and incubated for 1 hour at 4°C with either an anti-FLAG primary antibody for receptor/G protein specificity experiments or an anti-SNAP25 antibody for G protein/SNARE specificity experiments. IgG controls were used in SNAP experiments as no true KO animal was

available. After 1 hour, 50ul of agarose beads was added to each tube, and tubes placed on rotators at 4°C overnight. The following day, samples were centrifuged at 14,000 rpm for 1 minute to pellet beads and 300ul of supernatant transferred to clean, labeled 1.5ml eppendorf tubes. Supernatants were combined with 100ul of 4x sample buffer containing DTT as well as 5% BME before being heated at 70°C for 5min and frozen at -80°C for later use in western blot analysis. The remaining supernatant was aspirated from the beads, and beads washed twice for 5 minutes in 500ul IP buffer (50mM Tris, pH 7.4, 150mM NaCl, 0.5% Triton X-100, 1.54uM aprotinin, 10.7uM leupeptin, 0.948 uM pepstatin, 200uM PMSF). Following the second wash, beads were resuspended in 500ul IP buffer and transferred to clean 1.5ml eppendorf tubes.

Elution and TCA precipitation of IP samples. For receptor/G protein specificity experiments, following final washes, the receptor/G protein complex was eluted from the anti-FLAG antibody using a FLAG peptide (Sigma, catalog #F3290) product number). Stock aliquots of 5mg/ml FLAG peptide were diluted with 122.2ul of 1x TBS and 40ul added to IP beads for a final amount of 28ng FLAG peptide. Samples were placed on a vortex shaker at medium speed at 4°C for 30min, centrifuged at 14,000rpm for 1 minute to pellet beads, and supernatants transferred to clean 1.5ml eppendorf tubes. The elution was repeated a second time and the supernatants pooled. Supernatants for all IP samples from an animal were pooled together following elution. For MRM experiments, IP samples from two mice were pooled together to yield enough protein for proteomic detection. For G protein/SNARE specificity experiments, complexes were eluted using 100mM glycine (pH 2.5). IP beads were resuspended in 40ul of glycine and placed on a vortex shaker at medium speed for 5 minutes at room temperature. Samples were then centrifuged at 14,000rpm for 1 minute to pellet beads and supernatants transferred to clean 1.5ml eppendorf tubes before repeating the elution for a second time. Supernatants for all IP samples from an animal were pooled together following elution. For MRM experiments, IP samples from two

mice were pooled together to yield enough protein for proteomic detection. For both receptor/G protein experiments and G protein/SNARE experiments, following elution, IP samples were TCA precipitated to concentrate the G proteins for MRM analysis. Samples were incubated with 25% trichloroacetic acid (TCA) (Sigma, catalog #T6399) on ice for 30 minutes before being centrifuged at 14,000rpm at 4°C for 30 minutes. Following centrifugation, supernatants were aspirated off. Pellets were washed with 500ul of cold actetone and centrifuged at 14,000 rpm, 4°C for 15 minutes before carefully aspirating off supernatants. The wash step was repeated but following centrifugation, supernatants were carefully removed using a pipettor before being dried down in the speed vac for 5 minutes. Following TCA precipitation, samples were resuspended in 1x sample buffer.

Immunoblot analysis. To examine the results of immunoprecipitation, Western blot analysis was performed. Equal volumes of Input, IP, and Depleted Supernatant samples were resolved on 10% or 15% SDS-PAGE gels (10% to confirm FLAG/G protein immunoprecipitation and 12.5% to confirm G protein/SNAP 25 immunoprecipitation). Input and depleted supernatant samples were diluted 1:1 with blanks due to the amount of G protein present in each sample. Proteins were transferred electrophoretically to a nitrocellulose membrane in cold transfer buffer consisting of 200ml 10X CAPS, 200ml methanol, and 1600ml water. Following transfer, membranes were ponceau stained and cut between appropriate molecular weight markers. Membranes were blocked with slight agitation for 1 hour in a buffer of TBS with 5% milk and 0.1% Tween-20 (Sigma-Aldrich). Membranes were then washed 5 times for 5 minutes in TBS with 0.1% Tween-20 on a shaker before being incubated with appropriate primary antibodies in TBS with 5% milk and 0.2% Tween-20 on a shaker table at 4°C overnight. The next day, membranes underwent five 5-minute washes on a shaker table in TBS with 0.1% Tween-20 before appropriate secondary antibodies were diluted into TBS with 5% milk and 0.2% Tween-20

followed by gentle agitation on a shaker with the membranes for 1 hour at room temperature. Finally, membranes were washed three times for 10-minute washes in TBS with 0.1% Tween-20 followed by two 15-minute washes in TBS. Immunoblots were developed using Western Lightning™ Chemiluminescence Reagent Plus (NEL104) from Perkin-Elmer as per their published protocols. Imaging was collected using a Bio-rad Imager.

Limit of detection. To estimate the number of IPs that would be necessary for MRM experiments, a limit of detection experiment was performed. A dilution series of purified $G\beta_1\gamma_1$ from 1pg to 10ng was resolved on a 15% SDS-PAGE gel and the $G\beta_1$ bands tryptically digested as described in Chapter III. Targeted MRM methods were applied to the dilution series to estimate the limit of detection (LOD) and limit of quantification (LOQ) for our studies. With the LOD estimate, quantitative western blots were done using IP samples to estimate the amount of G protein that was co-immunoprecipitated following IP of the FLAG-tagged α_{2A}AR or SNAP 25. This could then be used to estimate the number of IPs (and subsequent number of animals) that would need to be pooled MRM experiments. Quantitative western blots were done using IP sample following coimmunoprecipitation of both FLAG/G$\beta\gamma$ and SNAP 25 G$\beta\gamma$. 40ul of IP sample was resolved on 10% or 15% SDS-PAGE gels along with a dilution series of purified $G\beta_1\gamma_1$ from 1pg to 4ng. Gels were transferred and immunoblotted as described. G protein estimates were done by analyzing images for densitometry using ImageJ (available from http://rsbweb.nih.gov.proxy.library.vanderbilt.edu/ij/index.html).

Application of targeted proteomics methods to immunoprecipitated samples.
Immunoprecipitated G$\beta\gamma$ isoforms were separated by SDS-PAGE (15% acrylamide) and stained with colloidal Coomassie Blue (Invitrogen). Gel bands corresponding to the molecular weights of Gβ and Gγ subunits were excised, chopped into $1mm^3$ pieces, reduced with dithiothreitol,

alkylated with iodoacetamide, and digested with trypsin. Gβ and Gγ peptides were each analyzed by a single 90 minute scheduled MRM analysis. Scouting runs were performed initially using postsynaptic samples isolated from striatum (described in Chapter III) to confirm isoforms could be detected with the 90 minute gradient, as well as narrow the scheduled window. Biological samples were randomized to ensure any drift in assay performance would not affect subsets disproportionally. Briefly, utilizing a trap column setup, peptides were first loaded onto a 100 μm x 4 cm C18 reverse phase column, which was connected in line to a 20cm by 100mm (Jupiter 3μm, 300Å), analytical column. Peptides were gradient-eluted into a TSQ-Vantage (Thermo Scientific) using a nanoelectrospray source. Peptides were resolved using an aqueous to organic gradient with a 90 minute total cycle time. Scheduled instrument methods encompassing a 6 minute window around the measured retention time along with calculated collision energies were created using Skyline. Q1 peak width resolution was set to 0.7, collision gas pressure was 1.5 mTorr, and a cycle time of 3 seconds was utilized. The resulting RAW instrument files were imported into Skyline for peak-picking and quantitation. Data analysis using Skyline was performed to assess enrichment of individual G protein subunits in KO or Tg samples. Transition ion intensities were summed for each precursor and these data were used to generate extracted ion chromatographic peaks of co-eluting transitions. As described previously, chromatographic peaks were manually interrogated and correct peaks chosen based on retention times, dot product values, and relative distributions of transition ions. Three internal reference peptides, SSAAPPPPPR, TASEFDSAIAQDK, and LTILEELR (Table 2) were used to evaluate drift in assay performance. Each reference peptide (5fmol) was spiked in to all samples and monitored throughout all MRM experiments. BSA controls were monitored at regular intervals between samples to evaluate instrument performance as previously described. To allow comparison between G proteins immunoprecipitated from Tg or KO animals, fold

differences were calculated by dividing the integrated area under the curve for all KO or Tg animals by the average of the integrated AUC for the KO animals. An *N* of 2 Tg and 2 KO animals was quantified for FLAG-tagged α_{2A} coimmunoprecipitation experiments.

Results

Crosslinker Efficiency

In order to assess the specificity of G protein interactions with the α_{2A} adrerengic receptor or SNARE proteins following receptor activation, we made use of a synaptosomal preparation that would allow us to IP tagged α_{2A}ARs or SNAP 25 in complex with G$\beta\gamma$ (Figure 15A). To ensure the receptor/G protein or G protein/SNARE complexes remained intact during IP experiments, a lipid soluble crosslinker, DSP, was added to samples following stimulation. To determine the optimal concentration of crosslinker for these experiments, synaptosomes isolated from HA-tagged α_{2A}AR transgenic mice were incubated with increasing concentrations of DSP. The amount of G$\beta\gamma$ coimmunoprecipitating with the HA-tagged α_{2A}AR was determined by western blot analysis. Figure 15B reveals a concentration dependent increase in the amount of G$\beta\gamma$ pulled down with the HA-tagged α_{2A}AR in the presence of DSP. Maximal recovery occurred in the presence of 2mM DSP. As a result, all future experiments used this concentration of crosslinker.

CoImmunoprecipitation of FLAG-tagged α_{2A}ARs with G protein $\beta\gamma$ subunits

Transgenic mice expressing a FLAG-tagged α_{2A}AR under the control of dopamine beta hydroxylase promoter were used for MRM studies. These animals only express the α_{2A}AR presynaptically on noradrenergic neurons (Figure 16A), making them useful for investigating both receptor/G protein interactions as well as G protein/SNARE interactions. KO mice lacking both the α_{2A} and α_{2C} adrenergic receptors were used as controls. Brain homogenates from Tg and KO were split in half when generating synaptosomes such that each animal could act as its own internal control during stimulation experiments. To evaluate the interaction between the FLAG-tagged α_{2A}AR with G$\beta\gamma$ subunits, synaptosomes were generated from Tg and KO mice and

stimulated with 100μM of epinephrine or an equal volume of buffer and incubated with DSP. Complexes were immunoprecipitated and interactions confirmed by western blot analysis. Figure 17B shows that stimulation with epinephrine significantly increases the amount of Gβγ that is coimmunoprecipitated with the FLAG-tagged receptor. This interaction is specific as it is absent in the KO animals. Using a dilution series of purified $G\beta_1$, a limit of detection experiment was performed (Figure 17). Peaks for the four $G\beta_1$ peptides being monitored by MRM ACADATLSQITNNIDPVGR, ELAGHTGYLSCCR, LLLAGYDDFNCNVWDALK and LFVSGACDASAK) could confidently be identified well above the noise in samples containing 10pg of purified $G\beta_1$. The limit of quantitation were of quantitation was estimated to be around 250pg as this was the bottom of the linear range within the dilution series (Figure 17). Quantitative western blot experiments estimated between 400-700ng of G protein was pulled down with the FLAG-tagged α_{2A} receptor per IP sample (data not shown).

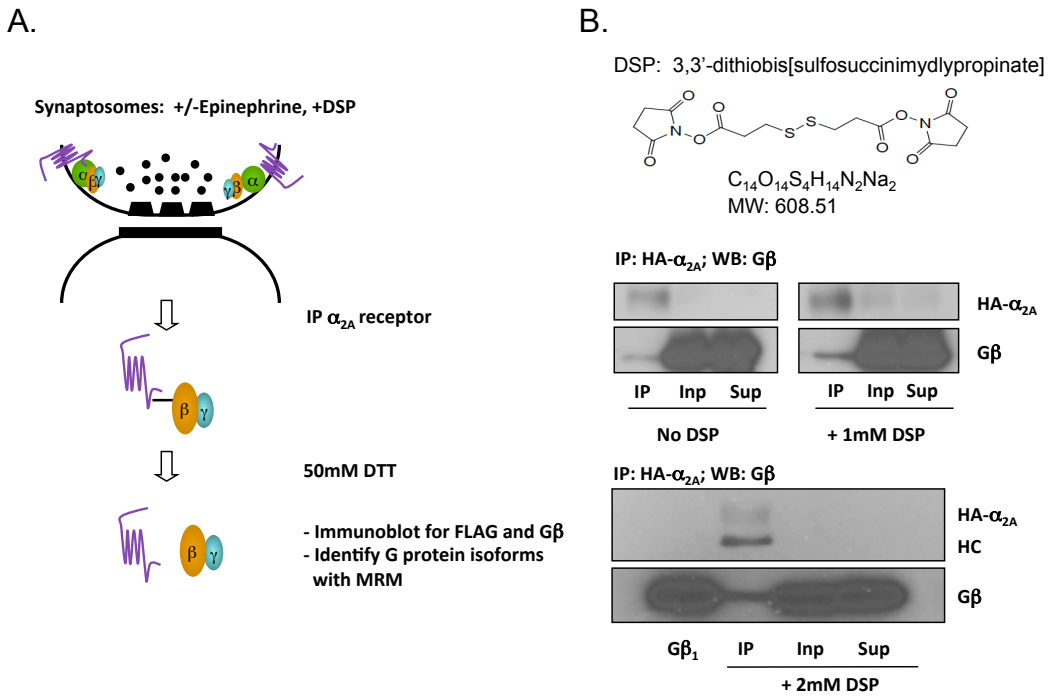

Figure 15. Coimmunoprecipitation of Gβγ with the HA-tagged α_{2A} adrenergic receptor (HA-α_{2A}AR) in the presence of a lipid soluble crosslinker. A) Schematic showing coimmunoprecipitation of the HA-α_{2A}AR with Gβγ subunits from stimulated synaptosomes. B) Top: chemical structure of the lipid soluble crosslinker, DSP. Bottom: representative immunoblots of the coimmunoprecipitation of the HA-α_{2A}AR and Gβ following stimulation of synaptosomes with epinephrine in the presence of increasing concentrations of crosslinker. IP: immunoprecipitated fraction; Inp: Input; Sup: depleted supernatant

A.

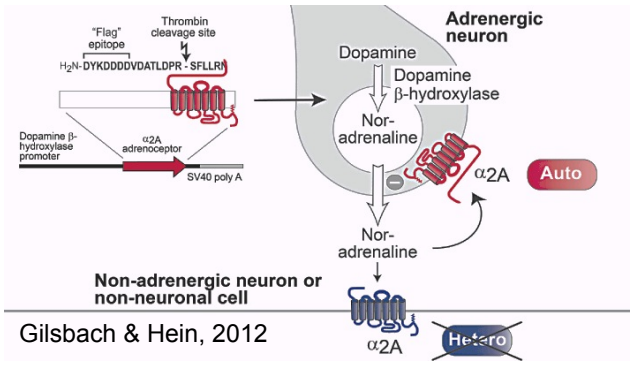

B.

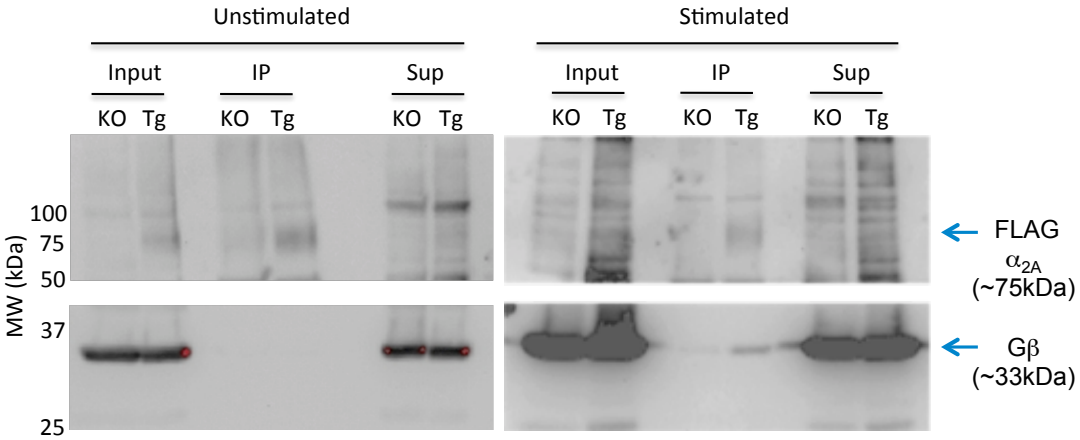

Figure 16. Coimmunoprecipitation of Gβγ with the FLAG-tagged α_{2A} adrenergic receptor (FLAG-α_{2A}AR). A) Schematic showing generation of FLAG-α_{2A}AR transgenic mice (Gilsbach and Hein, 2012) B**)** Representative immunoblots of the coimmunoprecipitation of the FLAG-α_{2A}AR and Gβ following stimulation of synaptosomes with buffer (unstimulated) or 100μM epinephrine (stimulated). IP: immunoprecipitated fraction; Sup: depleted supernatant

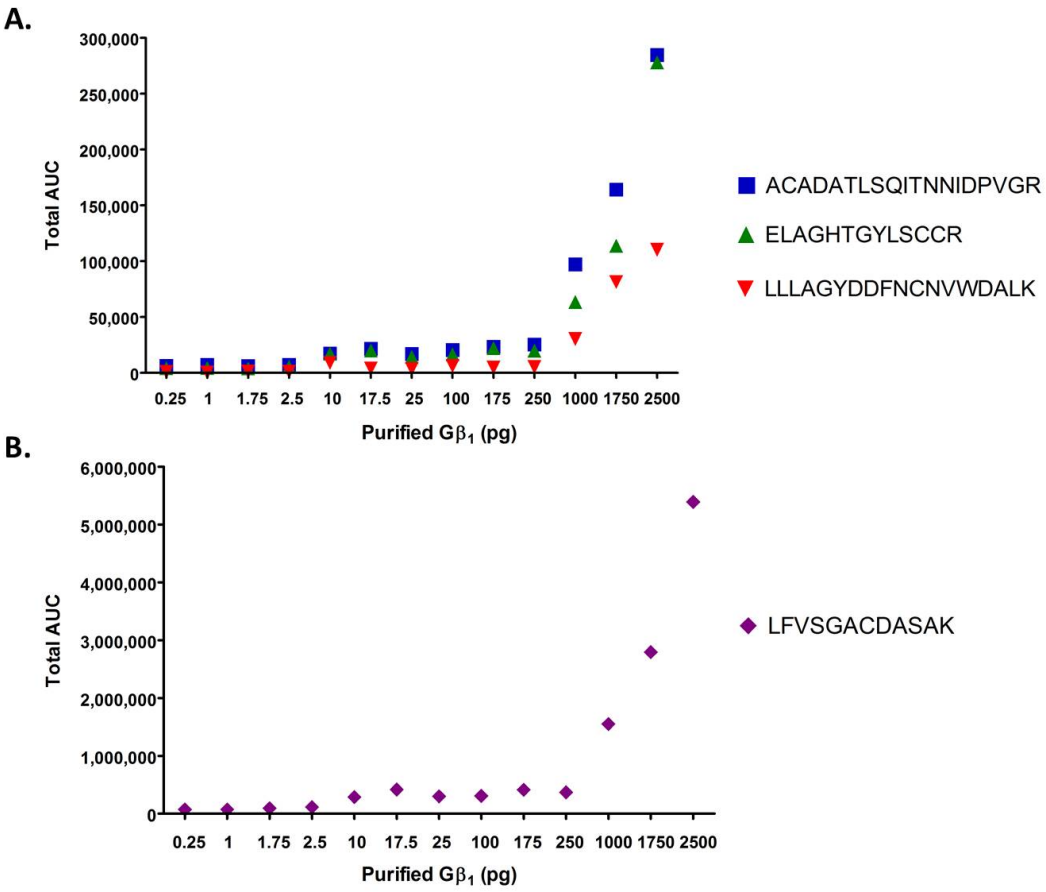

Figure 17. Estimation of the limit of detection and limit of quantitation for MRM experiments. Total area under the curve for $G\beta_1$ peptides A) ACADATLSQITNNIDPVGR, ELAGHTGYLSCCR, and LLLAGYDDFNCNVWDALK and B) LFVSGACDASAK, monitored by MRM across a dilution series of purified $G\beta_1$.

Evaluating specificity of interactions between the FLAG-tagged α_{2A} adrenergic receptor and G protein $\beta\gamma$ subunits

To examine the specificity of interactions between the FLAG-α_{2A}AR and G protein $\beta\gamma$ isoforms at presynaptic terminals, we applied our refined MRM method (described in Chapter III) to IP samples that had been TCA precipitated and digested. Synaptosomes were generated from whole brains of four Tg and KO mice and stimulated with 100 μM of epinephrine or an equal volume of buffer in the presence of DSP as described. Synaptosomes were processed by immunoprecipitation to isolate receptor/G protein complexes from noradrenergic terminals. To maximize the amount of G proteins recovered from IPs, the entire volume of precleared, 1mg/ml homogenate from each animal was aliquoted and incubated with anti-FLAG antibody (~15 IPs per animal). Following immunoprecipitation, IP samples were eluted with FLAG peptide and TCA precipitated to concentrate the G proteins. Initial experiments with Tg and KO samples stimulated with epinephrine (+epi) utilized sequential precipitations to pool IPs from two animals (≈ 30 IPs were pooled for each genotype). Subsequent experiments with Tg and KO samples that were not stimulated with epinephrine (no epi) only pooled IPs from a single animal (i.e. ~15 IPs total for each sample). As a result at the time of writing this dissertation, we had an N=2 for +epi samples and N=4 for no epi samples Following tryptic digest, the refined MRM method was applied to IP samples. Fold differences were calculated against KO no epi samples to allow comparison between G proteins identified in KO and Tg samples with and without stimulation with epinephrine. All four of the beta isoforms (G$\beta_{1,2,4}$, and $_5$) being targeted were detected in KO and Tg samples, as well as 6 of the 8 gamma isoforms (G$\gamma_{2,3,4,7,12}$, and $_{13}$ respectively). Chromatographic peaks of monitored transition ions could not be confidently identified for Gγ_5 and Gγ_{11}. Neither isoform was included in analyses. Gγ_4 was ultimately left out of analysis as chromatographic peaks for only one peptide in the KO no epi samples could

confidently be identified. As a result, this isoform could not be assessed and as such fold differences could not be evaluated in Tg no epi or KO and Tg + epi samples. No significant drift in assay performance was observed as measured by monitoring peak areas as well peak area CVs for internal reference peptides (data not shown). Fold differences showed clear enrichment of $G\beta_1$ in Tg samples that were stimulated with epinephrine compared to compared to both KO and Tg unstimulated samples (Figure 18A). Comparatively $G\beta_2$ was enriched in Tg unstimulated samples as well as KO stimulated samples compared to KO unstimulated samples, yet fold differences did not differ between these conditions. Similar to $G\beta_1$, however, the greatest fold differences were observed in Tg samples stimulated with epinephrine as $G\beta_2$ was greatly enriched as compared to all other conditions (Figure 18A). In contrast, $G\beta_4$ and $G\beta_5$ were not enriched in any condition (Figure 18A). Comparatively, 4 of the 5 detected gamma isoforms ($G\gamma_2$, $_7$, $_{12}$ and $_{13}$ respectively) showed clear fold increases in Tg samples following stimulation with epinephrine (Figure 18B). In contrast, $G\gamma_2$ was not enriched in any of the samples compared to KO unstimulated samples (Figure 18B). These results indicate a preference of α_{2A} receptors for heterotrimers containing $G\beta_1$, $G\beta_2$, $G\gamma_2$, $_7$, $_{12}$ and $_{13}$ (Figure 18). Fold differences for $G\beta_4$, $G\beta_5$ and $G\gamma_3$ were found to be equal to unstimulated KO samples and thus assumed to be nonspecific.

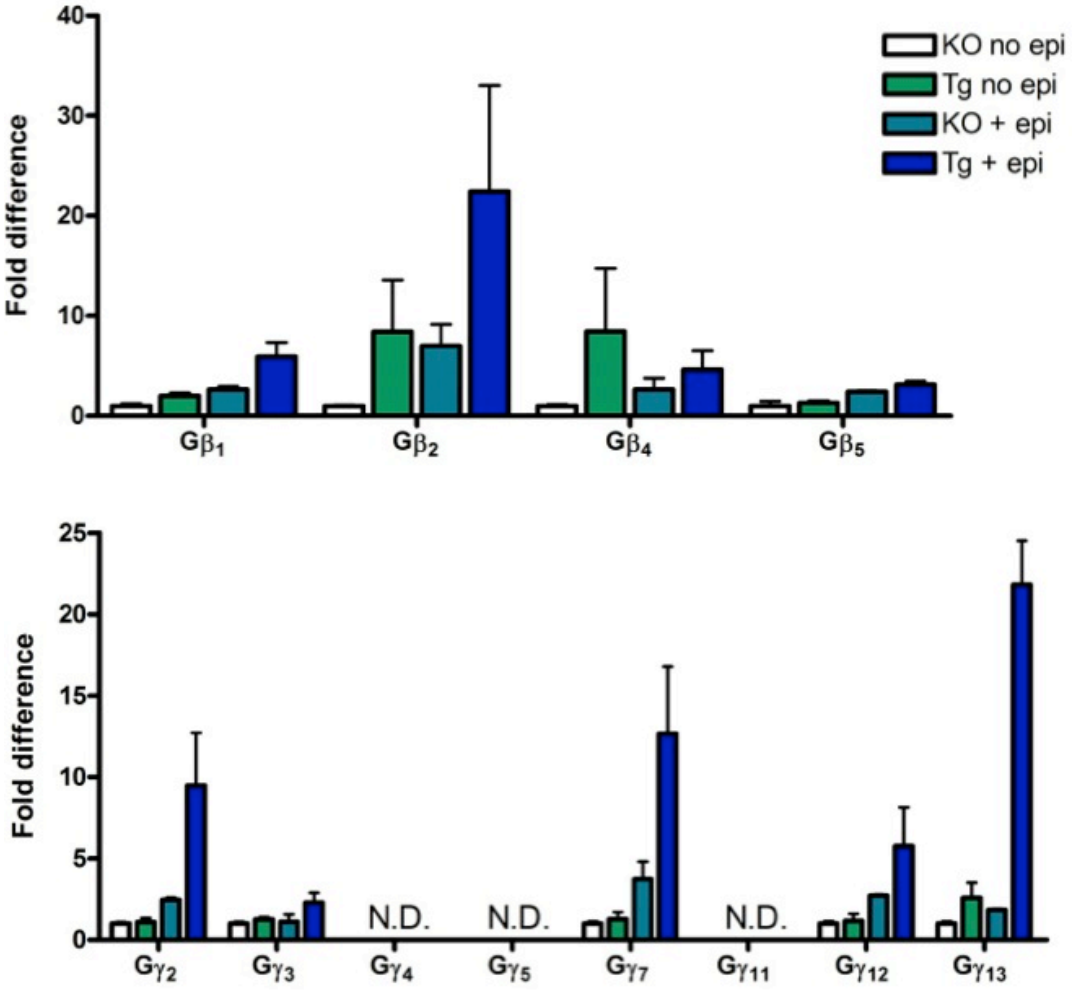

Figure 18. α_{2A} receptors exhibit specificity when interacting with G protein βγ subunits. G protein βγ subunits were co-immunoprecipitated with the α_{2A} receptor following stimulation of the receptor with epinephrine in FLAG-tagged α_{2A} adrenergic receptor transgenic (Tg) and α_{2A} / α_{2C} double KO (KO) mice. Fold differences were calculated for the expression of A) Gβ isoforms and B) Gγ isoforms in Tg IP samples compared to KO IP samples. N.D., not detected. *N* = 4 for no epi samples and N = 2 for + epi samples.

CoImmunoprecipitation of SNAP 25 with G protein βγ subunits

To evaluate the interaction between the Gβγ subunits and SNAP 25, synaptosomes were generated from Tg and KO mice, stimulated with 100μM of epinephrine or an equal volume of buffer, and incubated with DSP. Complexes were immunoprecipitated and interactions confirmed by western blot analysis. G proteins were detected in stimulated and unstimulated IP samples in both Tg and KO animals (Figure 19A). Association of Gβγ and SNAP25 in stimulated in KO samples cannot be attributed to activation α_1 or β–adrenergic receptors, as these were blocked using specific antagonists. Rather, we expect that the association is caused through non-adrenergic GPCRs such as dopamine D2 receptors, as epinephrine has previously been shown to activate them. Coimmunoprecipitation of G proteins with SNAP 25 in the absence of epinephrine activation was surprising in both KO and Tg animals. To ensure this result wasn't due to an effect of the crosslinker, coimmunoprecipitation studies were done in the presence and absence of both crosslinker and epinephrine. Western blots reveal that while coimmunoprecipitation of the G protein/SNARE complex requires the addition of a crosslinker, the interaction is specific, as little non-specific binding was observed in IgG controls (Figure 19B). Given that the G protein/SNARE association is low affinity, the requirement for a crosslinker was not surprising[79]. Consequently, crosslinker was used in all future MRM experiments. Quantitative western blot experiments estimated ≈1000ng of G protein was pulled down with SNAP 25 per IP sample (data not shown).

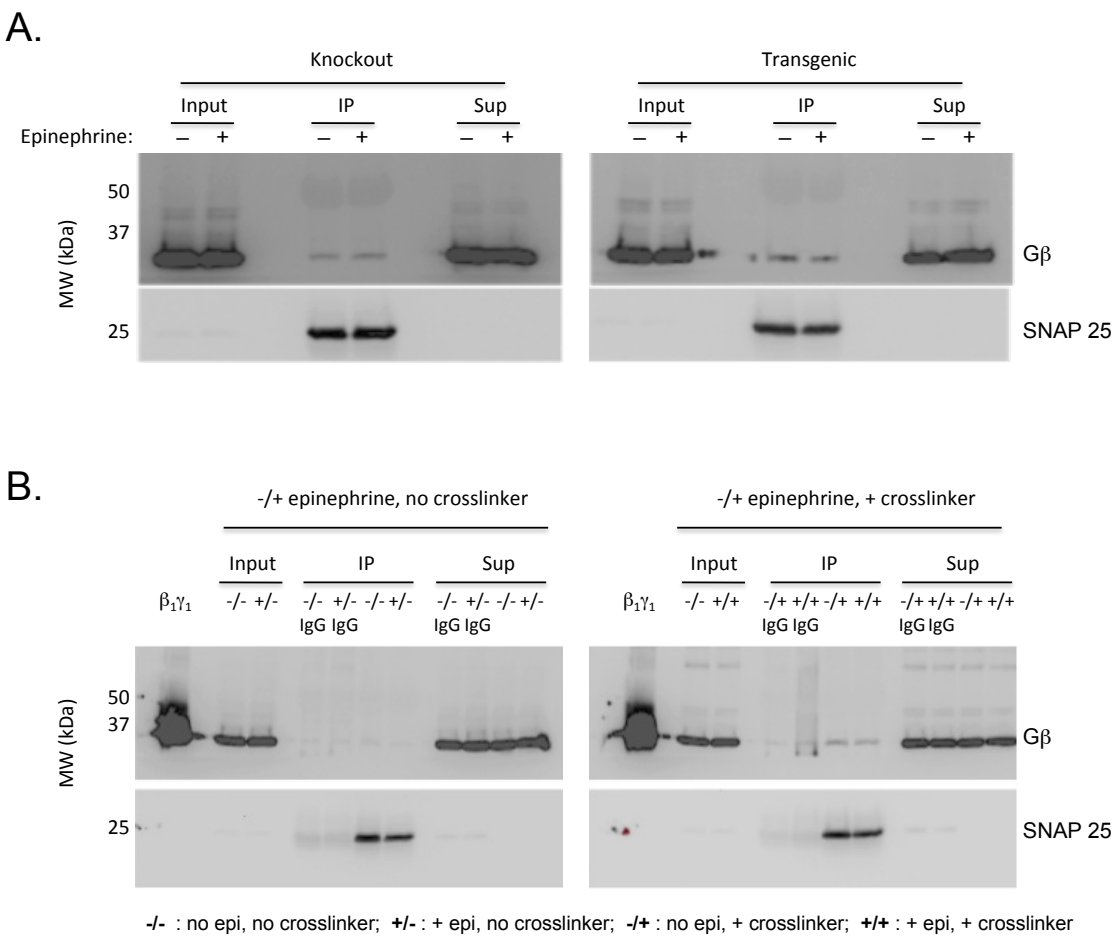

Figure 19. Coimmunoprecipitation of Gβγ with SNAP 25. A) Representative immunoblots of the coimmunoprecipitation of SNAP 25 and Gβ following stimulation of FLAG-tagged α_{2A} adrenergic receptor transgenic mouse or α_{2A} / α_{2C} double KO mouse synaptosomes with buffer (-) or 100μM epinephrine (+). B) Representative immunoblots of the coimmunoprecipitation of SNAP 25 and Gβ or IgG controls following stimulation of WT synaptosomes with buffer (-) or 100μM epinephrine (+) in the presence or absence of DSP. IP: immunoprecipitated fraction; Sup: depleted supernatant

Evaluating specificity of interactions between the G protein βγ subunits and SNARE proteins

To examine the specificity of interactions between the G protein βγ isoforms and SNARE proteins at presynaptic terminals, we applied our refined MRM method to IP samples that had been stimulated with epinephrine or buffer alone. Data collection was hampered by an inconsistent contaminant within the samples, which caused degradation of column performance for certain samples. This was likely to be excess coomassie stain based on observations of the tubes. Degradation was manifested by wider or tailing peaks and chromatographic shifts which were sometimes great enough as to shift the peak outside of the time window in which it was being monitored (data not shown). Significant experimental and instrument drift was observed when internal reference peptides and BSA controls were examined but degradation appeared to be sample dependent as a single blank or QC injection was sufficient to recover performance. Although preliminary data was collected, no consistent criteria could be resolved to allow it to be confidently analyzed and thus it was excluded from this dissertation until samples could be redone. At the time of writing this dissertation, experimental conditions had been revised resolve contamination issues and allow samples to be analyzed by MRM. Synaptosomes were generated from whole brains of Tg and KO mice and stimulated as described above. Synaptosomes were processed by immunoprecipitation to isolate G protein/SNAP 25 complexes from noradrenergic terminals. To maximize the amount of G proteins recovered from IPs, the entire volume of precleared, 1mg/ml homogenate from each animal was aliquoted and incubated with anti-SNAP antibody (~15 IPs per animal). Following immunoprecipitation, IP samples were eluted with glycine and TCA precipitated to concentrate the G proteins. To avoid contamination issues, only half of the IPs were pooled (~7-8) and precipitated together. Both halves were then run out on gels and digested yielding more digestions but less IgG contamination of gels. Digested samples were then sequentially resolubilized in formic acid prior

to being analyzed on the Vantage to ensure coomassie contamination was as reduced as possible. At the time of writing this dissertation, an N=2 for +epi samples and N=4 for no epi samples have been digested and are waiting to be analyzed by MRM.

Discussion

$G_{i/o}$-coupled GPCRs such as the α_{2A}AR play an important role in the CNS as they act as feedback regulators to mediate inhibition of presynaptic release. Upon stimulation, these GPCRs release G protein $\beta\gamma$ subunits which act to prevent neurotransmitter realease through actions on VDCC, potassium channels, and members of the exocytotic machinery[74,75,79,81,124,112,305,309]. While the actions of $\beta\gamma$ subunits are known, an understanding of how they are directed toward specific effectors is lacking. With the majority of the 5β and 12γ isoforms able to form dimers, and *in vitro* studies showing significant redundancy in the ability of different dimers to interact with receptors and effectors[213,262,320], questions persist about whether G$\beta\gamma$ subunits paly a role in defining the specificity of signaling pathways. Countering this, are cell based assays and genetic models which suggest specific G protein β and γ isoforms play distinct roles within an organism[102,215,263,280]. In this study we have demonstrated that α_{2A}AR preferentially interact with a subset of G protein $\beta\gamma$ isoforms at presynaptic terminals suggesting that the receptor/ G$\beta\gamma$ interaction may be important in determining effector interactions.

The central noradrenergic system modulates diverse biological functions including attention, arousal, learning and memory, stress responses, and sensory information processing[321-323]. Innervation is extensive, as noradrenergic fiber bundles originate from clusters of cell bodies within the pons and medulla oblongata, extending to the midbrain, thalamus, amygdala, hippocampus, cortex, and cerebellum, among others[321,324,325]. Of the nine adrenergic GPCR subtypes, the α_{2A}AR plays an important role in regulating synaptic transmission, acting presynaptically as auto-[303, 304] and heteroreceptors[326] in feedback mechanisms, but also postsynaptically and soma-dendritically to mediate hyperpolarization and reduce firing[327,328]. Direct measurements of GPCR-G protein interactions in reconstituted systems has not revealed

a high degree of discrimination at the level of the receptor as many GPCRs are able to couple to heterotrimers containing multiple Gα or Gβγ subunits[213,262,320]. This paucity for GPCR specificity has been seen for the α_{2A} receptor as overexpression studies revealed that α_{2A}AR could couple to both $G\alpha_i$ and $G\alpha_o$, but also activate phospholipase C via a $G_{q/11}$ pathway and stimulate adenylyl cyclase through G_s[329-331]. A greater fidelity of α_{2A}AR-G protein interactions appears physiologically, however, as virtually all α_{2A}AR-mediated effects are mediated through pertussis-sensitive $G_{i/o}$ pathways[332-335].

Gα and Gβγ subunits may both define selectivity of G protein activation by α_{2A}ARs. Using FRET, Gibson and Gilman[333] demonstrated that endogenous α_{2A}ARs preferentially stimulated $Gi\alpha_1$ heterotrimers that were paired with $G\beta_1$ or $G\beta_4$ subunits. In contrast, $G\beta_2$ permitted 2-fold higher activation by α_{2A}ARs when bound to $Gi\alpha_3$ yet this was lost when $G\beta_2$ was replaced by $G\beta_1$. Similarly, Richardson and Robishaw[335] showed higher levels of coupling of $G\alpha_i$ containing heterotrimers to the α_{2A}AR in the presence of $G\beta_1\gamma_3$ and $G\beta_1\gamma_7$ compared to $G\beta_1\gamma_1$ or $G\beta_1\gamma_{10}$. Further, α or βγ-mediated selectivity may be specific to a physiological function as Albarrán-Juárez et al.[334] demonstrated individual $G\alpha_i$ isoforms mediated sedative anesthetic-sparing effects but not inhibition of evoked release. Although Gα subunits were not investigated in the current study, this raises the possibility that specificity of evoked released through the α_{2A}AR could be mediated by Gβγ subunits. This is consistent with our finding that only a subset of Gβ and Gγ isoforms interact with the receptor following stimulation with epinephrine. $G\beta_1$ and $G\beta_2$ were previously shown to support strong G protein activation through the α_{2A}AR, as were $G\gamma_{2,3,4,}$ and $_7$[333,335], similar to what was observed the present study (Figure 18A,B). Conversely, $G\beta_4$ was previously shown to be very effective at facilitating activation of G protein heterotrimers whereas in our study, fold differences examining the expression of $G\beta_4$ subunits in IP samples were almost the same between Tg and KO animals. Whether these discrepancies

represent experimental differences in cell-based vs tissue systems remains to be determined. Given the low number of biological samples in the current study, additional experiments will be needed to elucidate this. Similar to $G\beta_4$, $G\beta_5$ showed no specific interaction with the α_{2A}AR following stimulation of the receptor (Figure 18A). Although in vitro $G\beta_5$ has been shown to pair with $G\gamma$ isoforms, *in vivo*, $G\beta_5$ forms a stable obligate dimer with members of the RGS R7 subfamily to modulate G_i-mediated signal transduction pathways[267-271]. This may explain why, in the present study, no specific interaction with the α_{2A} receptor was observed.

Although MRM data could not yet be completed for $G\beta\gamma$ associations with SNARE proteins following activation of the α_{2A}AR, *in vitro* data suggests specificity at this site of interaction could occur. Binding studies and calcium-trigged exocytosis experiments demonstrated functional differences in the ability of $G\beta\gamma$ isoforms to modulate SNARE proteins (Blackmer et al 2005). Similarly, Hamid et al.[77] recently demonstrated that SNARE complexes govern the mechanisms by which $5HT_{1b}$ and $GABA_B$ receptors inhibit exocytotic release at the same synaptic terminal. Although it wasn't examined, the authors note that $G\beta\gamma$ identity could add a further layer to effector targeting. Our western blot analysis raises some interesting questions about the microarchitecture surrounding $G\beta\gamma$/SNARE associations. $G\beta\gamma$ subunits were found associated with SNAP 25 regardless of receptor stimulation (Figure 19A); an effect which was not the result of a crosslinker artifact (Figure 19B). While we can't rule out the possibility that G proteins and SNARE complexes are in such close apposition at the membrane that we can't distinguish movements from the receptor to the effector with stimulation, the possibility that G proteins may be precoupled to SNARE complexes also exists. The fast rate of SNARE mediated inhibition suggests that the components must only diffuse small distances upon receptor activation, if at all. It is possible therefore, that G proteins and SNARE proteins may be scaffolded together prior to receptor activation, which in turn would allow for fast, receptor-

mediated activation. The existence of precoupled complexes between GPCRs and G proteins has been shown previously for the α_{2A}AR and Adenosine 1 receptors using FRET, and were proposed to increase effector activation and possibly play a role in ensuring signaling fidelity[336]. If a similar mechanism existed for G protein/SNARE associations, it could contribute to the specificity of the signaling pathway. If precoupled complexes exist, questions remain as to the composition of the G protein subunits. Stimulation could theoretically alter the G proteins that can bind to SNARE proteins as an added measure of selectivity, or alternatively, different binding sites on the SNARE proteins may be important following receptor activation. Multiple G$\beta\gamma$ binding sites have been demonstrated on the amino- and carboxy-terminus of SNAP 25[74,79,81] yet the physiological relevance of this is unknown. Potentially activation of the α_{2A}AR could result in a conformational shift such that G$\beta\gamma$ could more effectively compete with synaptotagmin to inhibit exocytosis. Detailed proteomic analysis will help answer some of these questions but additional efforts will be needed to elucidate these and other questions.

Summary

In summary, we report that α_{2A}AR exhibits specificity in their interactions with G protein $\beta\gamma$ subunits. This is interesting as it implies that specificity of signaling pathways could be in part, mediated through the receptor. Further efforts will need to be made to determine if further selectivity is applied at the SNARE complex, and the physiological consequences of this to the organism.

CHAPTER V

DEVELOPMENT OF SMALL MOLECULE MODULATORS OF THE Gβγ/SNARE INTERACTION

This chapter has been published under the title "Label-free detection of G protein-SNARE interactions and screening for small molecule modulators" in *ACS Chemical Neuroscience*.

Introduction

Release of chemical transmitters by regulated exocytosis underlies many forms of intercellular communication. In the brain, neurotransmitter release is controlled by a series of intricate regulatory mechanisms, the best characterized of which includes formation of the SNARE complex. Formation of this complex occurs as the SNARE domains of three proteins: syntaxin, SNAP25, and synaptobrevin, interact to form a stable, four-helical bundle which brings the vesicle and presynaptic membranes into close proximity[16,25]. As intracellular calcium rises due to membrane depolarization, it induces a tight association between the SNARE proteins and the calcium sensor, synaptotagmin, bringing the vesicle into close apposition with the membrane[47]. In doing so, the energy barrier for fusion is reduced, and neurotransmitter is released into the synaptic cleft[4]. This simplistic view of fusion events is complicated by intricate interactions with a number of proteins that define stages in the process including priming, docking, and modes of fusion such as full fusion or kiss-and-run[4]. Such a complicated mechanism requires new techniques and probes to identify and define the importance of the spectrum of protein-protein and protein-lipid interactions that transpire.

GPCRs are seven transmembrane-spanning proteins that transduce extracellular signals such as hormones or light into intracellular pathways through heterotrimeric G proteins which

consist of three subunits: Gα which has a nucleotide-binding domain specifically for guanosine nucleotides, and Gβγ, a functional dimer that dissociates from Gα upon activation of the heterotrimer by a stimulated GPCR. Activation is initiated via exchange of GDP for GTP in the Gα subunit, yet terminates through the actions of an inherent GTPase activity within Gα, which hydrolyzes the terminal phosphate of GTP to result in a Gα-GDP with renewed affinity for binding to Gβγand reforming the heterotrimer. $G_{i/o}$-coupled GPCRs play an intricate role in controlling neurotransmitter release, as G protein βγ, subunits are known to interact directly with voltage-dependent calcium channels to inhibit calcium influx at the presynaptic terminal[123-127]. Examples of such GPCRs include adenosine, $GABA_B$, CB1, and mGluR III receptors as demonstrated by Straiker *et al*. in their studies on cultured rat hippocampal cells[337]. In addition, $G_{i/o}$-coupled GPCRs are known to inhibit sites distal to calcium entry, with G protein Gβγ subunits modulating synaptic transmission by binding directly to the SNARE proteins themselves, thereby limiting the number and duration of fusion events (Figure 20A)[75,79,185].

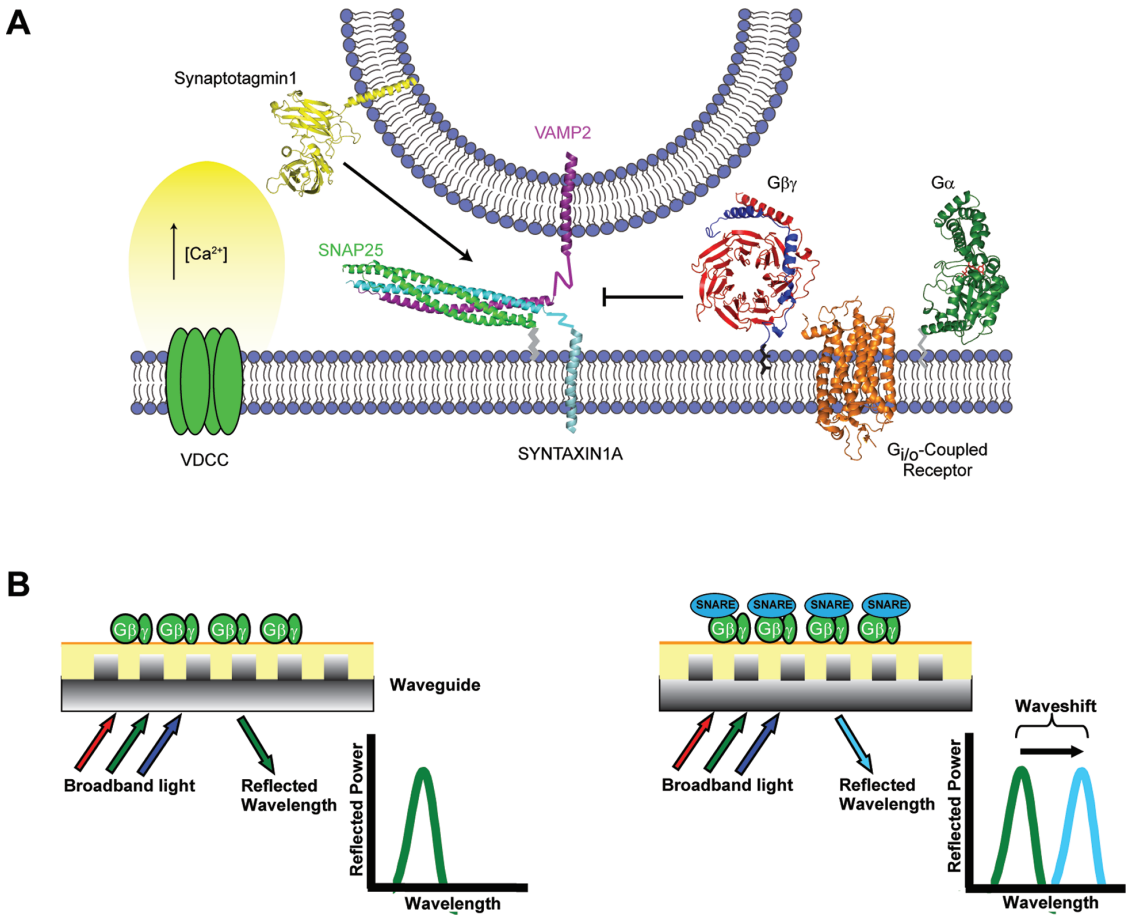

Figure 20. Role of Gβγ interaction with SNARE proteins and the scheme to detect that interaction with EPIC. A) Upon activation of a presynaptic $G_{i/o}$ coupled receptor, Gβγ will interact with the ternary SNARE complex of VAMP2/SNAP 25/Syntaxin 1A. Upon sufficient elevation of intracellular calcium, synaptotagmin with be able to compete for interaction with the SNARE complex, displacing Gβγ, and thereby promoting fusion of the synaptic vesicle. B) Gβγ that is immobilized to the surface on the waveguide of the microplate will result in a specific reflected wavelength when exposed to broadband light. Binding of t-SNARE complex to immobilised Gbg results in increased size and mass on the surface of the microplate, resulting in a reflected wavelength that will be shifted to a higher wavelength (waveshift, reported in picometers) when exposed again to broadband light.

We have shown that this direct effect on the exocytotic apparatus downstream of calcium entry works both on small clear synaptic vesicles as well as large dense core granules[79]. Additionally, such regulation of vesicle fusion by Gβγ has been reported by others in several areas of the brain[183,184], as well as non-neuronal tissues such as the pancreas[185]. Further, this binding occurs in the same molecular region on the SNARE proteins as that seen for the calcium sensor, synaptotagmin, and a competitive interaction between Gβγ and synaptotagmin for binding SNARE has been demonstrated[79]. Thus, the effects of Gβγ on calcium channels and on the exocytotic fusion machinery may be additive or synergistic, and depend on synaptic activity[79].

New methods are needed to study the novel association of Gβγ with SNARE and how it relates to SNARE binding with synaptotagmin or other binding partners in the regulated cascade of exocytosis. High-throughput screening systems would allow examination of binding partners, as well as permit testing of small molecule libraries which could later be taken forward into *in vitro* or *in vivo* assays of exocytosis. At present, the majority of screens require modification of one or more of the reaction components via enzymatic-, radio-, or fluorescent-labelling to report binding interactions. While such assays are robust in their responses, the addition of labels may interfere with molecular interactions by occluding binding sites or introduce significant background which limits signal to noise ratios[338-340]. Label-free technology is an emerging field that overcomes the need for labeling of one or more of the binding partners of interest[328]. Such technology is advantageous as it enables non-invasive and sensitive measurements of many cellular responses and protein-protein interactions, yet requires minimal manipulation of the reactants and does not suffer from potential assay artifacts seen in more traditional methods, such as autofluorescence[339,341]. Innovations in this field include impedance-based, optical biosensor-based, automated patch clamp, and mass spectrometry

technologies, to name a few; however, for the sake of this article we will focus solely on optical biosensors (for detailed review of these and other label-free technologies, please see references 338-341).

Optical biosensor-based technologies include surface plasmon resonance (SPR) and resonant waveguide grating (RGW), both of which use evanescent waves to characterize changes in refractive index at the surface of a sensor. In the case of SPR, light energy is transferred to electrons on a metallic surface, resulting in the propagation of charged density waves, surface plasmons, along the surface of the metal[338,339]. When the surface of the metal is exposed to polarized light, a reduction in the amount of reflected light is observed due to the resonant transfer of energy from the incoming light to the surface plasmons generated at the metal interface[338,339]. As a result, by monitoring the shift in the observed resonant angle, it is possible to detect molecular binding events in real time. Similarly, RWG also employs an evanescent wave for detection. In this case, however, RWG uses a nanograting structure to couple light into a waveguide composed of plastic and a thin dielectic coating via diffraction, in order to generate the wave[339,341]. By then exposing the sensors to wide spectrum light and measuring changes in the wavelength of the light that is reflected, it is possible to analyze biomolecular interactions.

Such technology was recently developed by Corning to detect protein-protein interactions. Immobilization of a target protein to a 384-well plate can be screened for its ability to interact with various binding partners by measuring waveshifts at the surface of the plate, with changes proportional to changes in mass and indicative of binding interactions. When incorporated with liquid handling, this technology permits high-throughput screening both of potential binding partners, as well as small molecules that may inhibit or enhance that interaction.

Experimental Procedures

Plasmids. The open reading frames for the SNARE component proteins were subcloned into the glutathione-s-transferase (GST) fusion vector, pGEX6p1, (GE Healthcare, Chalfont St. Giles, Buckinghamshire, UK) for expression in bacteria.

Preparation and purification of SNARE proteins. Recombinant bacterially expressed GST fusion proteins were expressed in *Escherichia coli* strain BL21(DE3). Protein expression was induced with 0.1 mM isopropyl β-D-thiogalactoside for 16 h at room temperature. Bacterial cultures were pelleted, washed with 1x phosphate-buffered saline, and then re-suspended in lysis buffer [50 mM NaCl, 50 mM Tris, pH 8.0, 5 mM EDTA, 0.1% Triton X-100, 2 mM PMSF, and 1 mM DTT]. Cells were lysed with a sonic dismembrator at 4°C. GST-SNAP25 was purified from cleared lysates by affinity chromatography on glutathione-agarose (GE Healthcare), following the manufacturer's instructions. While the proteins were bound to the column, the buffer was exchanged to 20mM HEPES, pH 7.4, 100mM NaCl, 0.05% *n*-octyl β-D-glucopyranoside (OG), and 5 mM DTT. The proteins were eluted by cleaving from GST with PreScission protease (GE Healthcare) for 4 h at 4°C. GST-H3 domain of syntaxin1A was purified from the sonicated bacterial supernatant by affinity chromatography on glutathione-agarose (GE Healthcare) in 10 mM HEPES, pH 7.4, 0.05% OG, and 2 mM DTT. Protein concentrations were determined with a Bradford assay kit (Pierce, Rockford, IL), and purity was verified by SDS/PAGE analysis.

t-SNARE Complex Reassembly. A slight excess of SNAP25 (4 μM) to GST-H3 (3 μM) on glutathione-agarose beads was incubated overnight at 4°C in 20 mM HEPES, pH 7.4, 100 mM NaCl, 0.1% OG, and 2.0 mM DTT. The binary t-SNARE complex (SNAP25 with the H3 domain of syntaxin 1A) was washed three times with phosphate-buffered saline and eluted from the

column by removing GST with PreScission protease (GE Healthcare) for 4 h at 4°C. Equimolar protein – protein interaction was confirmed by SDS-PAGE/Coomassie staining analysis.

Gβγ Purification. $G\beta_1\gamma_1$ was purified from bovine retina as described previously. Recombinant $G\beta_1\gamma_2$ was expressed in Sf9 cells and purified via a His6 tag on $G\gamma_2$ using nickel-nitrilotriacetic acid affinity chromatography (Sigma-Aldrich, St. Louis, MO).

Resonant waveguide grating biosensor detection. A beta version of the Corning EPIC™ was used for all experiments. Briefly, binding interactions between Gβγ subunits and SNARE proteins were evaluated using a novel, label-free system from Corning, called the EPIC™, which allows detection of protein-protein interactions without the need for fluorescent- or radio-labeling. The system comprises two components: an optical reader and a 384 well microplate containing an optical sensor within each well, known as a resonant waveguide (RWG). When plates are illuminated with broadband light, one dominant wavelength of light resonates within the waveguide, and is strongly reflected. The addition of proteins to the surface of the plate, however, changes the local index of refraction, changing the resonant wavelength that is reflected (known as a waveshift). These waveshifts (measured in picometers (pm)) can therefore be used to evaluate protein-protein interactions. Further, each well is partitioned to allow for self-referencing. This is accomplished by only applying binding chemistry to one half of each well, thereby allowing for simultaneous measurement of target protein interactions with immobilized partners as well as interactions with the well surface itself.

Detection of t-SNARE (SNAP25-syntaxin1A H3) on the EPIC™. The initial step of the assay is the immobilization of either $G\beta_1\gamma_1$ or $G\beta_1\gamma_2$ to the plate. A variety of conditions were explored as described in the Results section. The resulting common immobilization protocol from this work was the addition of 25ug/ml of either $G\beta_1\gamma_1$ or $G\beta_1\gamma_2$ in 20 mM sodium acetate, pH 5.0 and 5%

glycerol to the respective wells overnight at 4°C. This timeframe ensured quenching the plate chemistry that did not react with Gβγ. The following day, wells were then washed twice with 20 mM sodium acetate, pH 5.0, with 5% glycerol followed by two washes with a common HEPES binding buffer (20 mM HEPES, pH 7.5, 5% glycerol, 2 mM magnesium chloride, 10 uM guanosine diphosphate (GDP), and 5% DMSO). This HEPES binding buffer was determined by a series of experiments to determine the tolerances of the microplate and of the detection of interaction between immobilized Gβγ and t-SNARE. The plates were allowed to thermally equilibrate in the EPIC™ before an initial immobilization read was done. Purified t-SNARE or other binding partners were then added to wells, and the plate was allowed to re-equilibrate for one hour before a binding reading was done. Figure error bars represent within-experiment errors based on each plate tested.

Chemical Synthesis and Purification. All ^{1}H & ^{13}C NMR spectra were recorded on Bruker AV-400 (400 MHz) or Bruker AV-NMR (600 MHz) instrument. Chemical shifts are reported in ppm relative to residual solvent peaks as an internal standard set to δH 7.26 or δC 77.0 ($CDCl_3$) and δH 3.31 or δC 49.0 (CD_3OD). Data are reported as follows: chemical shift, multiplicity (s =singlet, d = doublet, t = triplet, q = quartet, br = broad, m = multiplet), integration, coupling constant (Hz). IR spectra were recorded as thin films and are reported in wavenumbers (cm-1). Low resolution mass spectra were obtained on an Agilent 1200 LCMS with electrospray ionization. High resolution mass spectra were recorded on a Waters Qtof-API-US plus Acquity system. The value Δ is the error in the measurement (in ppm) given by the equation $\Delta = [(ME - MT)/ MT] \times 10^6$, where *M*E is the experimental mass and *M*T is the theoretical mass. The HRMS results were obtained with ES as the ion source and leucine enkephalin as the reference. Optical rotations were measured on a Perkin Elmer-341 polarimeter. Analytical thin layer chromatography was performed on 250 μM silica gel 60 F254 plates. Visualization was accomplished with UV light,

and/or the use of ninhydrin, anisaldehyde and ceric ammonium molybdate solutions followed by charring on a hot-plate. Chromatography on silica gel was performed using Silica Gel 60 (230-400 mesh) from Sorbent Technologies. Analytical HPLC was performed on an Agilent 1200 analytical LCMS with UV detection at 214 nm and 254 nm along with ELSD detection. Solvents for extraction, washing and chromatography were HPLC grade. All reagents were purchased from Aldrich Chemical Co. and were used without purification. All polymer-supported reagents were purchased from Biotage, Inc. Flame-dried (under vacuum) glassware was used for all reactions. All reagents and solvents were commercial grade and purified prior to use when necessary. Mass spectra were obtained on a Micromass Q-Tof API-US mass spectrometer was used to acquire high-resolution mass spectrometry (HRMS) data.

General Procedure:

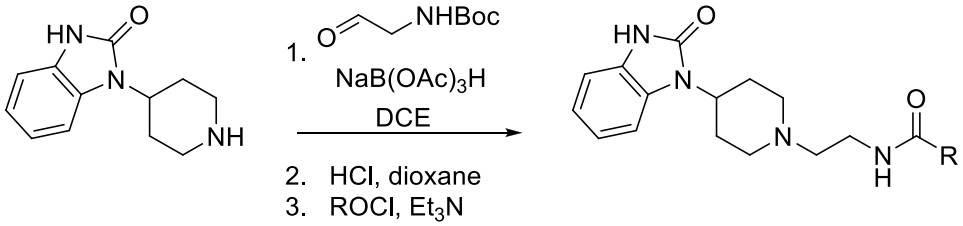

To a 10 mL vial was placed 1-(piperidin-4-yl)-1*H*-benzo[*d*]imidazol-2(3*H*)-one (0.1 mmol) and diluted with 2 mL of DCE, followed by *tert*-butyl 2-oxoethylcarbamate (0.12 mmol). $NaB(OAc)_3H$ (0.25 mmol) was added and the vial placed on a rotator for 6 hours, followed by an aqueous wash and extraction with DCM (2 x 5 mL). The crude extract was then treated with 4.0 M HCL in dioxane for 1 hour, which provided full deprotection of the Boc group, and uniformly affording the crude primary amine in >95% purity as judged by liquid chromatography mass spectrometry (LCMS) and nuclear magnetic resonance (NMR). Finally, the crude amine was dissolved in DCM,

Et_3N added (1.5 equiv.) and one of 48 ROCls (1.2 equiv.) added and allowed to rotate for 24 hours. Concentration and mass-directed high performance liquid chromatography (HPLC) afforded the final compounds in excellent yields (70-99%) and purity (>98%).

Screening of the ligand library. Microtiter plates with immobilized Gβγ were prepared as above. Compounds were then added at a concentration of 250 μM individually to groups of at least four wells in the presence of t-SNARE. To assess non-specific waveshift changes induced by interaction of the compounds with either Gβγ or the plate itself, at least four wells were exposed to compound alone. The difference between the waveshift of compound alone with Gβγ and in the presence of t-SNARE was defined as the effect of the compound on the interaction between Gβγ and t-SNARE. For select "hits" that produced a significant change from waveshifts seen for t-SNARE binding to Gβγ alone, a concentration response curve was determined with at least four wells for each concentration of compound.

Results

The ability of Gβγ to directly bind to SNARE proteins has been previously determined[74,76,185]. Small molecules that can alter this interaction are needed to evaluate and manipulate it at a cellular level to further investigate exocytosis and the role that Gβγ plays in its regulation. High-throughput screening of this bimolecular interaction would be advantageous not only for characterizing the protein-protein interactions but also for development of small molecule modulators that would allow further definition of the role of this interaction in cells and tissues. In this study we sought to develop a method to examine Gβγ/SNARE interactions *in vitro* using this label-free technology. After establishing conditions necessary to reproducibly immobilize Gβγ and bind SNARE proteins, a library of biased protein-protein modulator ligands was screened to examine the ability of individual compounds to alter this interaction. This library has compounds containing a piperidine benzimidazolone moiety, a well-known GPCR privileged structure that has been shown to enhance protein-protein interactions between the pleckstrin homology (PH) domains and the catalytic domains of both Akt, a kinase, and phospholipase D, a lipid signaling enzyme[339-344]. Use of the Corning EPIC™ in this manner resulted in the discovery of 3 compounds with 50-100 μM activity that represent lead compounds in iterative development of small molecular probes that affect the ability of Gβγ to bind to SNARE proteins.

Protein Immobilization

Binding interactions between Gβγ subunits and SNARE proteins were evaluated using the EPIC™ system. The experimental scheme began with covalently immobilizing purified $G\beta_1\gamma_1$ or $G\beta_1\gamma_2$ to the surface of a microplate as depicted in Figure 20B through primary amine coupling

chemistry in a 384-well microplate. Changes in waveshift were used to evaluate the effects of compound addition on t-SNARE binding to Gβγ.

To optimize immobilization of the Gβγ dimer to the plate, we tested the pH, salt, and glycerol-dependence. The pH dependence of $G\beta_1\gamma_1$ attachment to the plate was investigated by varying pH from 4.0 to 7.2. As can be seen in Figure 21A, the largest waveshift detected occurred at a pH of 5.0. This waveshift was comparable to that obtained for a positive control, streptavidin. Selecting the optimal sodium acetate buffer of pH 5.0, the buffer was then further tested for the effect of other reagents on the ability to immobilize Gβγ to the plate. The addition of 100 mM sodium chloride, 5% glycerol, or a combination of both, to the 20mM sodium acetate immobilization buffer yielded no changes in waveshift as seen in Figure 21B. To test for saturation of immobilization of Gβγ, serial dilutions of Gβγ were exposed to a microplate overnight and analyzed the next day. As can be seen in Figure 21C, there was a steep decline in immobilized protein as detected by the EPIC plate-reader below a Gβγ concentration of 10 μg/ml. Based on the above data, the optimal immobilization buffer used for all subsequent assays was 20mM sodium acetate, pH 5.0, and 5% glycerol.

We then turned to optimization of binding of partner proteins to Gβγ to establish conditions that would allow optimal detection of interaction with SNARE proteins. We altered the concentration of Gβγ immobilized over the range of 25-100 μg/ml. The partner protein of Gβγ, $G\alpha_t$, was successfully detected at all Gβγ protein immobilization concentrations, although not to saturation. Similarly, we could detect the binding of t-SNARE to the plate. Over this range of concentrations of immobilized Gβγ, there was no effect on the ability of t-SNARE to bind as seen by similar waveshifts in all cases (Figure 21D). We also included a negative control, bovine serum albumin (BSA), a protein with no expected binding affinity for Gβγ. It had no measurable interaction with Gβγ bound to the microplate.

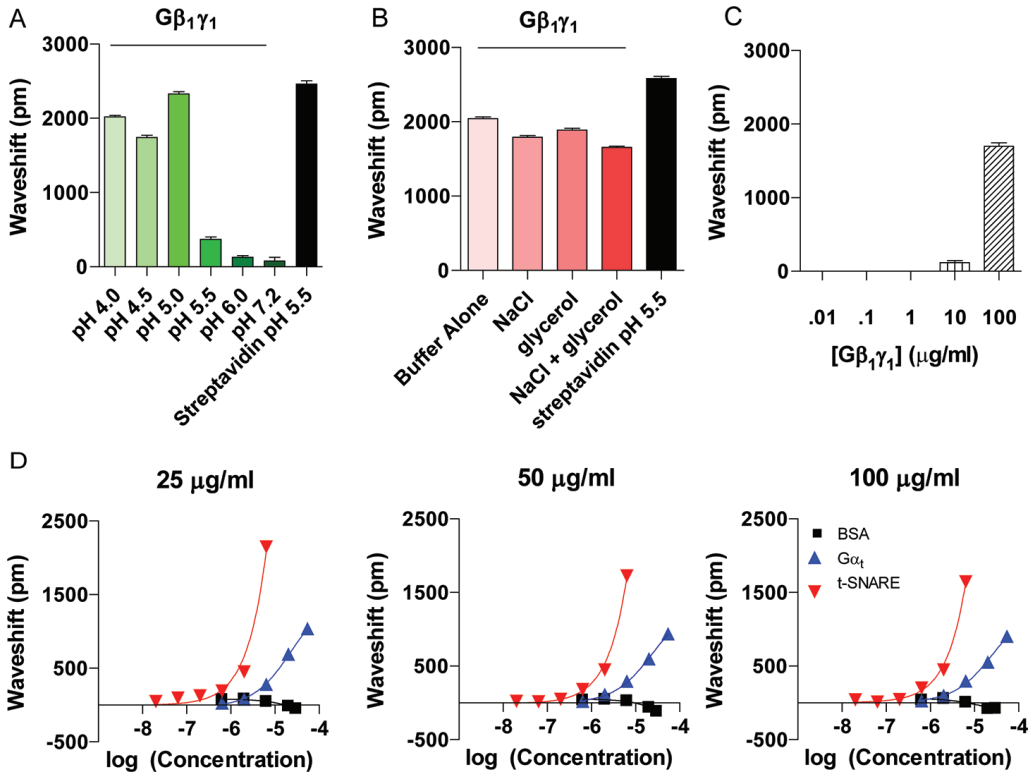

Figure 21. Optimization of immobilization of Gβγ. A) $G\beta_1\gamma_1$ was diluted in 20mM sodium acetate of varying pH from 4.0 to 7.2 to a final concentration of 25μg/ml. Streptavidin was mixed in 20mM sodium acetate, pH 5.5 as a control. After allowing to immobilized overnight and quenching the remaining aminereactive coupling on the plate, plates were washed, thermally equilibrated within the EPIC plate-reader, and then an immobilization read was measured. Shown are the averages and SEM over 64 wells for pH 4.0-6.0 and 16 wells for pH 7.2 and for streptavidin. B) $G\beta_1\gamma_1$ was diluted into 20mM sodium acetate, pH 5.0 either alone, with 100mM sodium chloride, 5% glycerol, or a combination of both. Again, streptavidin was added as control as in A). After overnight immobilization, washes, and thermal equilibration, an immobilization measurement was taken. Shown are the averages and SEM over 64 wells for buffer alone, NaCl, and glycerol; 128 wells for NaCl + glycerol; and 16 wells for streptavidin. C) $G\beta_1\gamma_1$ was diluted to varying concentrations as shown in 20mM sodium acetate, pH 5.5. As above, the plate was washed and thermally equilibrated prior to an immobilization read being taken. Shown are the averages and SEM over 48 wells.

Figure 21 continued. Optimization of immobilization of Gβγ. D) $G\beta_1\gamma_1$ was immobilized on plates at three concentrations that were detectable during immobilization reads, 25, 50, and 100ugml. Immobilization reads were taken the next day as above. After the initial read, increasing amounts of t-SNARE, Gat, or BSA were exposed to the plate for one hour. A second read was performed with resulting waveshifts in the presence of those additional proteins shown. t-SNARE complex (red triangles) and Gat (blue triangles) resulted in an increase in waveshift, whereas BSA (black squares), a protein not expected to bind $G\beta_1\gamma_1$, had no increase in waveshift at all concentrations tested. Binding curves were similar across the three immobilization concentrations performed. Shown are the averages and SEM over 5 wells for each point on each of the curves.

Optimization of Ligand Interaction

After optimizing Gβγ immobilization, the binding of t-SNARE was then optimized. As noted above, immobilization of differing amounts of Gβγ had little or no effect on t-SNARE binding as measured by the waveshift. However, selection of a buffer to perform the binding did have an effect. Initially, the presence or absence of sodium chloride or glycerol was tested compared to buffer alone, 20 mM HEPES, pH 7.5. The presence of 100 mM sodium chloride appeared to attenuate the signal of t-SNARE binding to Gβγ as seen in Figure 22A. Conversely, the addition of glycerol to the binding buffer improved the signal detected as compared to buffer alone. In fact, across almost all immobilization and binding conditions, a binding buffer of 20 mM HEPES, pH 7.5 that included 5% glycerol yielded significantly higher waveshifts ($p<0.001$ – $p<0.05$). Based on this result, binding buffers contained 5% glycerol.

Two other binding buffer variables explored included the effect on waveshifts in the presence of dimethyl sulfoxide (DMSO) or detergent. DMSO concentrations were examined as the small molecules to be screened were dissolved in 100% DMSO. The EPIC™ system was reported to be able to tolerate up to 5% DMSO without an effect on the signal or deterioration of the plate. A wide variety of DMSO concentrations were examined for their effect on the

waveshift detected during the interaction between t-SNARE protein and immobilized Gβγ. As seen in Figure 22B, no degradation of signal was apparent in the presence of DMSO up to 5%, the maximum concentration allowable for screening. Similarly, to evaluate if a detergent affected the detection of t-SNARE–Gβγ interactions, the effect of the addition of various concentrations of CHAPS was tested. Figure 22C shows that the addition of up to 0.1% CHAPS did not deteriorate the signal detected when t-SNARE was exposed to immobilized Gβγ, although it did statistically increase the waveshift detected in the presence of t-SNARE. CHAPS was not included in the final buffer to simplify the constituents of that buffer. Additionally, 10 μM GDP and 2 mM magnesium chloride were added to all buffers, as they are necessary for stability of the Gα subunit. In each case, no deleterious effect on signal was observed.

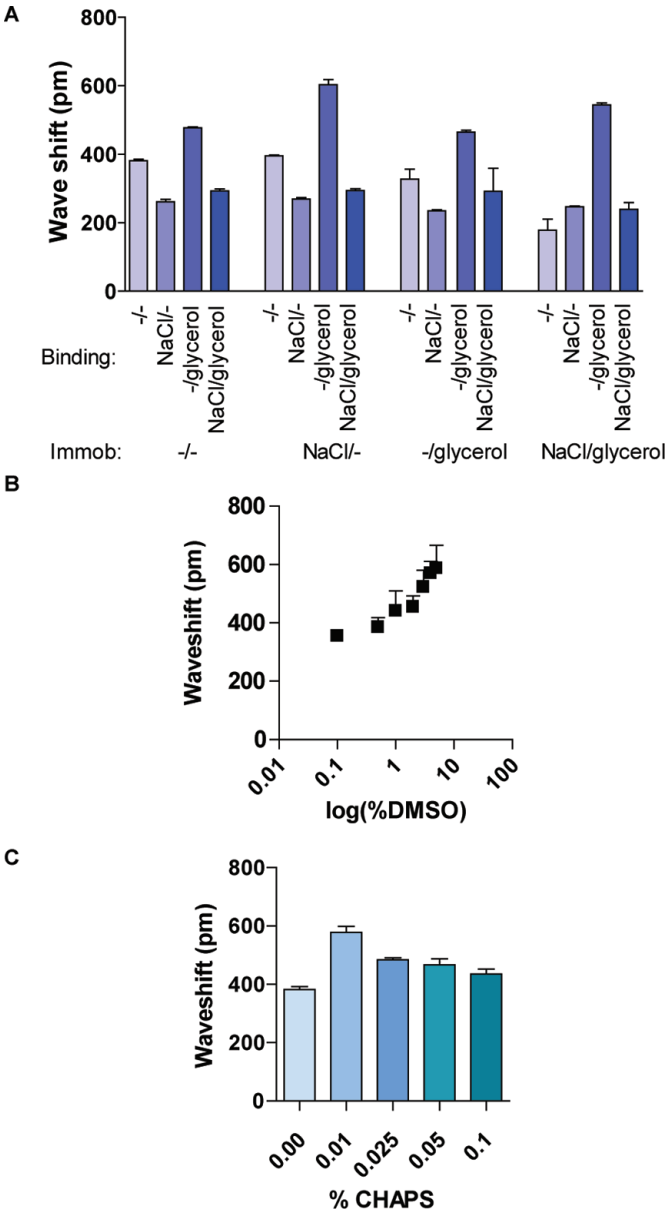

Figure 22. Optimization of the detection of t-SNARE binding to immobilized $G\beta_1\gamma_1$. A) $G\beta_1\gamma_1$ was immobilized to the microplate in 20mM sodium acetate, pH 5.0 alone, or in the presence of 100mM NaCl, 5% glycerol, or both. After washing, t-SNARE was then diluted to 2uM in either binding buffer alone, or with the addition of 100mM NaCl, 5% glycerol, or both. Shown are the averages and SEM over four wells. B) Varying amounts of DMSO ranging from 0.1 to 5% was added to the bindng buffer when a fixed concentration of t-SNARE was exposed to immobilized $G\beta_1\gamma_1$. The waveshifts detected are similar to that without any addition of DMSO. Shown are the averages and SEM over 5 wells. C) Varying amounts of a detergent, CHAPS, from 0.01 to 0.1% were added to the binding buffer to assess effect of presence of detergent on detection of t-SNARE binding to $G\beta_1\gamma_1$. The waveshifts detected in the presence of CHAPS are similar to that obtained without the presence of the detergent. Shown are the averages and SEM over five wells.

As seen in Figure 23A, $G\alpha_t$ and t-SNARE had significantly increased waveshifts when compared to $G\beta\gamma$ exposed to buffer alone or BSA. To examine whether the binding between $G\beta\gamma$ and $G\alpha$ was physiologically relevant, we tested the ability of $G\alpha$-GTPγS to bind to $G\beta\gamma$. This non-hydrolysable guanine nucleotide decreases the affinity of $G\alpha$ for $G\beta\gamma$ subunits, and as such would be expected to reduce binding of $G\alpha$ to immobilized $G\beta\gamma$. As expected, the addition of GTPγS reduced the detected waveshift of $G\alpha_t$ significantly ($p<0.0001$) compared to GDP-$G\alpha_t$ (Figure 23A). Concentration response curves were generated examining the ability of increasing concentrations of t-SNARE, $G\alpha_t$, or BSA to bind to immobilized $G\beta\gamma$. As was seen with t-SNARE, waveshifts detected for $G\alpha_t$ increased in a concentration dependent manner (Figure 21D). Similarly, the ability of immobilized $G\beta\gamma$ to recognize and interact with another binding partner, $G\alpha_i$, was also explored (Figure 23B). As seen for $G\alpha_t$, $G\alpha_i$ was also able to bind to immobilized $G\beta_1\gamma_1$ in a concentration dependent manner. Again, similar concentrations of BSA demonstrated very little change in waveshift when compared with those found with t-SNARE or $G\alpha_i$. When compared to $G\alpha_t$, $G\alpha_i$ produced a greater waveshift when exposed to the same concentration of t-SNARE. However, when compared to t-SNARE, $G\alpha_i$ had very similar waveshifts across multiple concentrations (Figure 23B). The difference between $G\alpha_i$ and $G\alpha_t$ is either due to plate-to-plate differences, or the specific activity of our source of $G\alpha_t$ was reduced compared to $G\alpha_i$ and therefore bound less.

Finally, the interaction of t-SNARE with another $G\beta\gamma$ dimer, $G\beta_1\gamma_2$, was determined to explore both if a different dimer could be immobilized and participate in binding as has been demonstrated with $G\beta_1\gamma_1$, as well as to determine if differences in waveshift would be detected depending on the $G\beta\gamma$ isoform immobilized. Immobilization of $G\beta_1\gamma_2$ was comparable to that of

$G\beta_1\gamma_1$ (Figure 24A). Concentration response experiments were carried out with results shown in Figure 24B. $G\beta_1\gamma_1$ and $G\beta_1\gamma_2$ both had similar concentration response curves as seen with the increase in waveshift with increasing concentrations of t-SNARE bound to the respective $G\beta\gamma$ dimer.

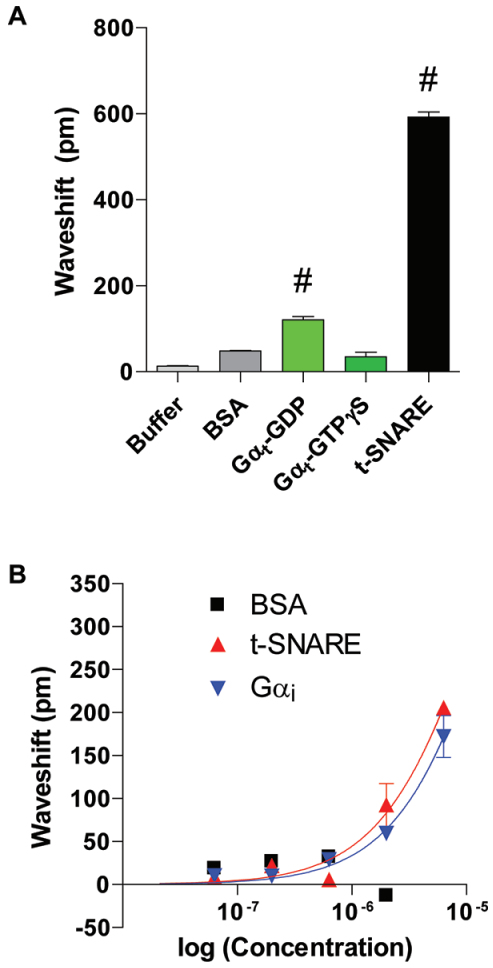

Figure 23. Evaluation of binding of immobilized Gβγ by $G\alpha_t$ and $G\alpha_i$. A) $G\beta_1\gamma_1$ was immobilized as described previously. Equal concentrations of $G\alpha_t$-GDP, $G\alpha_t$-GTPγS, BSA, and t-SNARE were allowed to bind to the immobilized Gβγ for 1 hour before a read was taken. The waveshift for $G\alpha_t$-GDP was significantly different from buffer alone, BSA, or $G\alpha_t$-GTPγS, suggesting that $G\alpha_t$-GDP was binding to immobilized Gβγ. The t-SNARE had a significantly greater waveshift than $G\alpha_t$-GDP, as well as the waveshifts for buffer, BSA, and $G\alpha_t$-GTPγS. Shown are the averages and SEM for at least 12 wells on the plate. B) $G\beta_1\gamma_1$ was immobilized as described previously. Increasing amounts of t-SNARE, $G\alpha_i$, and BSA were exposed to the plate for 1 hour. A second read was performed with resulting waveshifts in the presence of those additional proteins shown. t-SNARE complex (red triangles) and $G\alpha_i$ (blue triangles) resulted in an increase in waveshift whereas BSA (black squares), a protein not expected to bind $G\beta_1\gamma_1$, had no increase in waveshift at all concentrations tested. Shown are averages and SEM over five wells on the plate for each point on the concentration response curves.

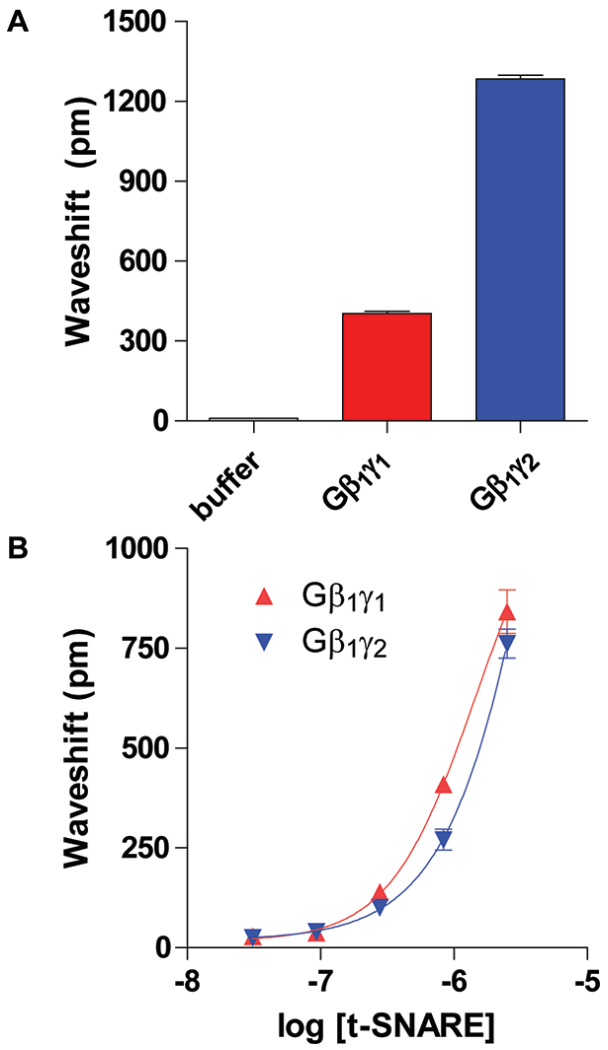

Figure 24. Similarity between immobilized Gβγ dimers binding to t-SNARE. A) $G\beta_1\gamma_2$ (blue) was immobilized onto the microplate in previously described buffer alongside $G\beta_1\gamma_1$ (red). $G\beta_1\gamma_2$ appeared to have an increased immobilization efficiency with the plate as seen by the greater increase in initial waveshift detected after the immobilization step. Data shown are averages with SEM over 126 wells for $G\beta_1\gamma_1$, 126 wells for $G\beta_1\gamma_2$, and 16 wells for buffer alone. B) This difference did not result in a difference of binding of t-SNARE. Increasing amounts of t-SNARE were exposed to the immobilized Gβγ dimers with a corresponding increase in waveshift. There was very little difference between fitted curves for binding to the two isoforms. Each point on the curves are the averages with SEM over at least four wells on the plate.

Use of EPIC™ in high-throughput screening of a chemical library

As the detection method for protein-protein interactions seemed reproducible and robust, we chose to use it in a search for small molecule modulators of the Gβγ/SNARE interaction. The initial library was designed based on known chemotypes which modulate protein-protein interactions (α-helical mimetics, β-turn mimetics (types I-VI), flat surface interaction ligands)[345,346] as well as GPCR-biased ligands known to enhance protein-protein interactions[339-344] with compounds added simultaneously with t-SNARE to react with the immobilized $G\beta_1\gamma_1$. Compounds were added at final concentration of 250 μM using a volume equal to that in the well, with stock concentrations of 500 mM in DMSO. Final well volume was 40μL in each well. Waveshifts were assessed in at least four replicates for each compound in the presence or absence of t-SNARE.

Screening of this library of biased protein-protein modulator ligands[339-344] identified four lead compounds from two structural series (Figure 25A), three of which greatly diminished the waveshift produced upon Gβγ binding to SNARE (63V, 85M and 85B), and one (6EQ) which significantly enhanced it. An example of a screen of thirty of the initial 69 compounds is shown in Figure 25B. Non-specific binding (as measured by SNARE binding to streptavidin coated wells) was subtracted from the Gβγ–SNARE binding signal, resulting in the black line for the basal level of binding. By comparison to the waveshift achieved by interaction with t-SNARE alone (yellow column), most compounds had minimal to no effect. Based on the activities of the first four hits, further iterative synthesis and screening of related small molecules resulted in the discovery of additional compounds with modulatory effects on the interaction of Gβγ with t-SNARE.

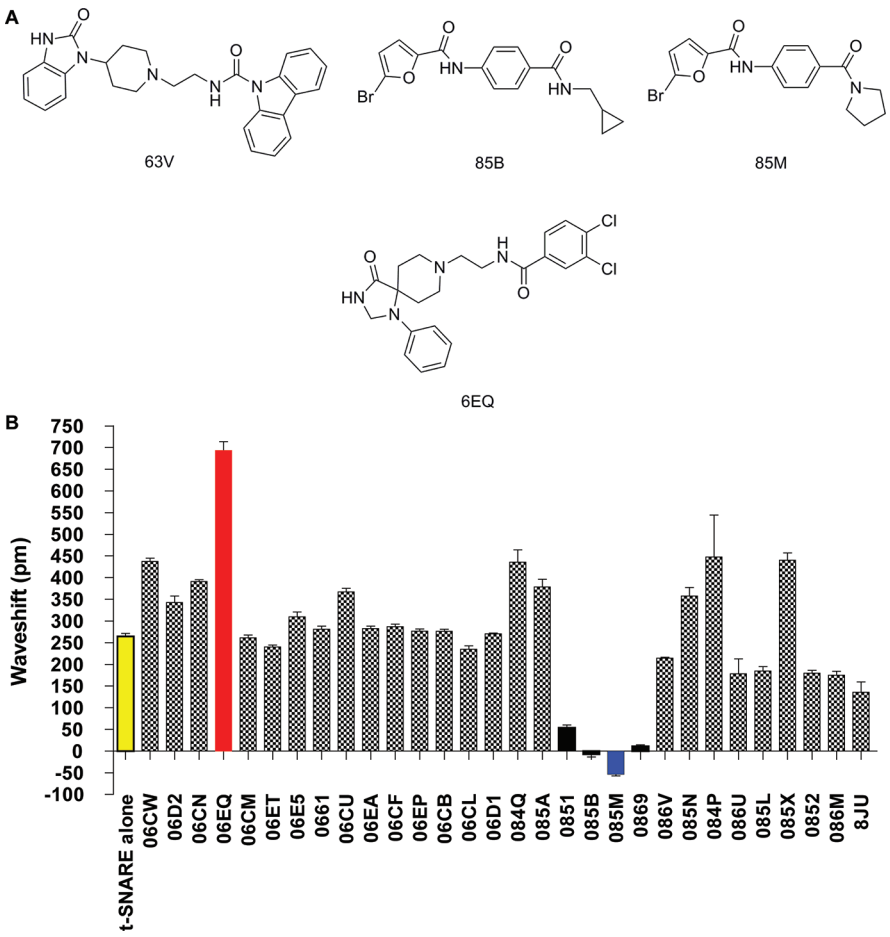

Figure 25. Screening of chemical compounds for modulation of $G\beta_1\gamma_1$ binding to t-SNARE. A) Shown are the chemical structures for four compounds from an initial screen of a library of compounds that had a waveshift detected that differed significantly from the waveshift for t-SNARE alone exposed to immobilized $G\beta_1\gamma_1$. B) $G\beta_1\gamma_1$ was immobilized overnight as described before. For each compound listed in the bar graph, a compound was mixed either with buffer alone in four wells, or buffer with 2μM t-SNARE in four wells, and allowed to thermally equilibrate before a binding read was taken. The waveshift of buffer alone with compound was subtracted from that of compound with t-SNARE, with the difference shown in the bar graph. For comparison, t-SNARE alone without compound in eight wells of this plate was seen to have an average waveshift of 265 pm shown in the first column (yellow). Red signifies an example of a compound that enhanced the waveshift, black signifies compounds that significantly reduced the waveshift, and blue is a compound that reduced the waveshift and showed a concentration dependent reduction in waveshift (Figure 26). Error bars shown are SEM.

To further examine lead compounds mentioned above as well as a number of other compounds in the initial screen, concentration response curves were obtained for those that showed a possible effect on the interaction of Gβγ with t-SNARE. The respective compounds were tested over the given range with at least replicates across 4 wells. These studies demonstrate that a signal of sufficient intensity using low volumes in a 384 well plate can be easily detected. The structures for representative lead compounds are shown in shown in Figure 26A with concentration response curves for each of those compounds in Figure 26B. Compound 85M (see screen in Figure 25A) appeared to be a weak inhibitor at higher (μM) concentrations with an estimated EC_{50} of 100 μM (Figure 26B). Compound 634 and 8HA were selected based on an initial screen of the remaining 39 compounds from the library (data not shown). Compound 634 appeared to be a weak enhancer of the interaction of t-SNARE with immobilized Gβγ with an estimated EC_{50} of 10 μM. Lastly, compound 8HA also appeared to be a weak enhancer with an estimated EC_{50} also of 10 μM. Current efforts are directed to making derivatives of these lead compounds to improve their potency.

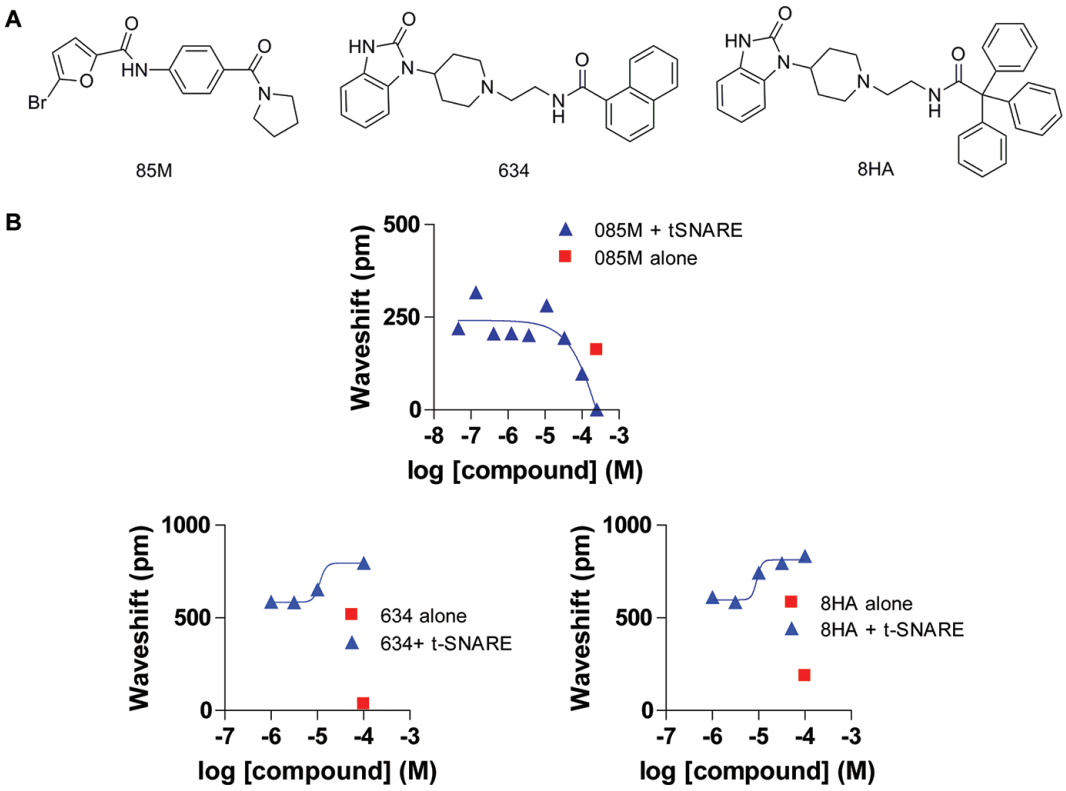

Figure 26. Concentration response curves for compounds that inhibit or enhance binding between Gβγ and t-SNARE. A) Shown are the chemical compounds (85M, 634, and 8HA) that had significantly affected the waveshift of the interaction between t-SNARE and immobilized $G\beta_1\gamma_1$. B) Compounds 85M, 634, and 8HA were tested in a concentration dependant manner on the detected waveshift of constant t-SNARE concentration exposed to immobilized $G\beta_1\gamma$. Shown are the concentration response curves from those compounds. Each point in the three concentration response curves represents the average of four wells on a plate.

Discussion

The label-free EPIC™ system provides a novel means to screen for modulators of protein-protein interactions in an *in vitro* setting with scalability to high-throughput screening of libraries of compounds. The ability of t-SNARE to bind immobilized Gβγ in this assay is reproducible and physiologically relevant as shown by the ability to correctly assess Gβγ's interaction with its cognate partner Gα in the presence of GDP but not in the presence of GTPγS. This system allows relevant testing of an interaction between two unlabeled proteins. As well, the immobilized Gβγ dimer was able to interact with other known ligands, $G\alpha_t$ and $G\alpha_i$. Although immobilized Gβγ had a higher affinity for t-SNARE than its cognate partner Gα, we expect this difference due to this system being a plate-based assay. In solution, we would expect Gα to have a higher affinity for Gβγ. The ability for either Gα or t-SNARE to bind Gβγ suggests not only the physiologic relevance of the detected interaction, but also further generalization of the EPIC™ for extending this initial work to examining other interactions with immobilized Gβγ dimers in the future, such as other Gα subunits or other effectors such as phospholipase B, phosphoinositide 3-kinase, or interaction of other Gβγ isoforms with other Gα subunits or effectors. Furthermore, initial screens have yielded compounds that either weakly inhibit or enhance the interaction of Gβγ with t-SNARE. The compounds are the subject of further refinement for potency, efficacy, and selectivity. As well, this system is readily adapted to structure-function studies of mutant Gβγ or SNARE proteins or screening of peptides from the interaction surface for their ability to modulate the interaction of Gβγ with t-SNARE (data not shown).

The direct interaction of Gβγ with the exocytotic machinery to regulate exocytosis has been shown in multiple areas of the brain[76,79,183,347] as well as in chromaffin cells[348] and β cells of

the endocrine pancreas[185]. There is a need to understand the physiological relevance of this interaction in further detail. Compounds specific for this interaction that either inhibit or potentiate the interaction would allow imaging and electrophysiological studies of synaptic exocytosis. The generality of this inhibitory mechanism on exocytosis, working both on small clear vesicles at synapses as well as large dense core vesicles, leads to the possibility that the effects of these small molecule inhibitors and enhancers of the Gβγ/SNARE interaction may affect the workings of many synapses. By their drug-like nature, the small molecule compounds that have emerged from this screen would likely pass through the cell membrane, and thus following testing of their specificity for the Gβγ/t-SNARE interaction, could be used in cellular and tissue settings such as slice preparations. Such studies have the potential to greatly enhance our understanding of the role of Gβγ regulation of exocytosis *in vitro.* Future studies will optimize these initial tool compounds into potent drug-like modulators with properties suitable for evaluation *in vivo*, including enhanced bioavailability and central penetration.

CHAPTER VI

SUMMARY AND FUTURE DIRECTIONS

Since the onset of the research project presented in this dissertation, much progress has been made in understanding the functional significance of unique G protein isoforms as well as the role Gβγ/SNARE interactions may play within the CNS and rest of the body. Heterotrimeric G proteins mediate the actions of many GPCRs to regulate a wide variety of signaling pathways. With such a large number of different β and γ isoforms, parsimony would dictate that that the compositions of the heterotrimer activated by a particular GCPR would play a role in defining effector-targeting. Despite this, identifying which isoforms exists *in vivo* and how they function physiologically has been challenging. High sequence identity between Gβγ subunits has hampered the development of subtype specific antibodies that would aid in localization studies, while *in vitro* promiscuity suggested isoforms were functionally interchangeable. Gene targeted deletion of specific isoforms has done much to counter this. In the past six years distinct phenotypes have been described for two of the beta and four of the gamma isoforms following genetic inactivaton, supporting the notion that functional specificity of the Gβγ dimers exists and plays an important role in physiological processes[102,264,280,281,312]. Similarly, the acceptance and understanding of G protein/SNARE interactions has grown substantially in the past six years. Early work using purified proteins and in lower organisms was viewed with skeptiscm as inhibition of evoked transmission was primarily attributed to channel modulation. In the intervening years, however, this modulatory effect has been shown to be physiologically important in animal models and humans, affecting processes such as diabetes, pain, and

learning and memory through a variety of GPCRs and raising the possibility that it may be a widespread regulatory mechanism[198, 315-317].

While the long-term research objectives of studying Gβγ/SNARE interactions are to determine the extent to which this modulatory effect operates within an organism and to decipher the roles that individual subunits may play, the goals of this current study were to examine the expression of different G protein isoforms throughout the CNS, study the functional specificity of α_{2A}AR receptor mediated Gβγ/SNARE interactions, and develop compounds which would allow its modulation. Development of a targeted mass spectrometry approach overcame the obstacles previously faced as it allowed differentiation of unique isoforms from complex mixtures. Application of this assay indicated a wide distribution of most G protein isoforms across brain regions and at synaptic terminals with distinct localization patterns observed for different Gβ and Gγ subunits. While some isoforms such as $G\beta_1$, $G\beta_2$, and $G\gamma_2$ exhibit broad distributions, others such as $G\beta_5$ and $G\gamma_7$ showed more resticted patterns. A greater understanding of G protein localization has important implications for mechanistic studies as it helps inform what is currently known while directing new hypotheses. In the case of $G\gamma_7$, previous studies indicated expression was highest within the striatum with this isoform acting through D_1 dopamine and A_{2A} adenosine receptors[98,102,280-282]. While this correlates well with our findings, definitive localization may inform researchers to focus on postsynaptic signaling as $G\gamma_7$ was significantly enriched within this region. Additionally, for isoforms such as $G\gamma_{12}$ and $G\gamma_{13}$ where little functional data is available, these localization results may provide a first step to assessing the function of these isoforms within the brain. Expression suggests a postsynaptic signaling role or a role in controlling motor control that researchers could pursue.

Efforts were also extended to investigate the functional specificity of SNARE modulation through the α_{2A}AR. These receptors operate as the main feedback regulator of noradrenaline

release from presynaptic terminals[304,313,314] and are important therapeutic targets[315,316,317]. α_{2A}AR-mediated inhibition of neurotransmitter release has been shown to occur through direct interactions with the SNARE proteins in both the amygdala[183] and pancreatic β cells[185] yet little is known about the factors controlling specificity. Using immunoprecipitation and targeted mass spectrometry, α_{2A}ARs were found to exhibit specificity in their interactions with Gβγ subunits upon receptor activation as only a subset of Gβ and Gγ isoforms were enriched in Tg samples. Taken together with previous studies that show preferences of the α_{2A}AR for unique Gβγ isoforms, this implies that specificity of signaling pathways could be in part, mediated through the receptor. While detailed proteomic analysis of Gβγ/SNARE interactions have yet to be finished, *in vitro* data and western blot analysis suggest this may add an additional layer of selectivity. Using immunoprecipitation and immunoblotting, Gβγ subunits were found associated with SNAP 25 regardless of receptor stimulation suggesting the possibility that G proteins may be precoupled to SNARE complexes. Although this remains to be elucidated, scaffolding could allow for fast, receptor-mediated activation, which would account for the rate at which SNARE inhibition occurs.

As many $G_{i/o}$-coupled GPCRs act as feedback regulators for transmitter release from presynaptic terminals, a greater understanding of the mechanisms by which they operate will be important for understanding normal neural processing as well as disease states. GPCRs such as the α_{2A}AR have been shown to act through different mechanisms in different regions of the brain, while presynaptic terminals have been shown to express multiple GPCRs that mediate inhibition through different mechanisms. At present little is known about how the type of inhibition is determined at a synapse, or whether the effects of Gβγ on calcium channels and on the exocytotic fusion machinery may be additive or synergistic. Using a label-free system to screen for modulators of protein-protein interaction, we identified three lead compounds that

had an effect on the interaction of Gβγ with SNARE proteins. Despite needing further refinement to enhance potency, efficacy, and selectivity, these initial efforts highlighted the possibility that small molecules can be developed to target a specific form of inhibition at synapses. This has important implications for understanding the role of Gβγ regulation of exocytosis such compounds could be used as a tool to tease apart the contribution this form of modulation makes at a given synapse. Additionally, compounds may have important therapeutic uses. Many $G_{i/o}$ coupled GPCRs are drug targets yet current therapies targeting the receptor often exhibit significant side effects that limit their efficacy. Compounds which selectively target Gβγ/SNARE interactions could alleviate some of these effects as synergistic actions could allow the same effect but at lower doses.

In summary, the results of the research aims discussed here contribute to a better understanding of G protein signaling within the CNS as well as the role of specificity in α_{2A}AR modulation of SNARE function. Further advancements such as those outlined below would provide additional information about this complex modulatory system.

Do α_{2A} heteroreceptors mediate feedback in the same manner as autoreceptors?

α_{2A}AR exist at both pre- and postsynaptic sites within the CNS. Presynaptically, they act as both auto- and heteroreceptors to limit exocytotic events. Autoreceptors are localized to adrenergic neurons and reduce the release of noradrenaline[303,324], whereas heteroreceptors modulate release of other neurotransmitters such as 5HT, GABA, and dopamine[326]. Using the FLAG-tagged α_{2A} mice described in the current study, Gilsbach et al.[304] recently dissected what functions of the α_{2A} receptor are mediated through autoreceptors or receptors located on nonadrenergic neurons (these included both heteroreceptors and postsynaptic receptors). Although they determined feedback regulation was limited to autoreceptors, both auto- and

heteroreceptors are thought to operate in this manner. What isn't known, however, is whether they mediate inhibition in the same manner. HA-tagged mice described in the current study express the tagged receptor on noradrenergic and non-adrenergic sites, offering a chance to compare how specificity may change depending on the type of neuron. Using immunoprecipitation and MRM, it would be possible to determine whether heteroreceptors also act through Gβγ/SNARE interactions. The G proteins identified from experiments using the HA mice could be compared to those from the current study (after proteomic analysis is finished) to assess a) whether activation of heteroreceptors mediates Gβγ/SNARE interactions and b) if so, whether it does so through a unique compliment of G proteins.

Is α_{2A} specificity affected by drug treatment?

α_{2A}ARs are thought to play a role in a number of disesases[315-319] and as such are important therapeutic targets with drugs such as the α_2 agonist, clonidine and the α_{2A} agonist, guanfacine, both being used for ADHD and anxiety and panic disorders. An interesting extension of the current study would be to assess the differences in specificity mediated through these drugs as compared to epinephrine. Although clonidine will affect all three α_2 subtypes, its effects through the α_{2A} receptor could be directed through the use of specific antagonists. Using synaptosomes from HA- and FLAG-tagged α_{2A} mice, immunoprecipitation, and mass spectrometry, it would be possible to determine whether specificity of receptor/G protein interactions following drug treatment is the same as seen with epinephrine. Similarly, as clonidine has inhibitory effects on catecholamine release, this agonist could also be used to examine G protein/SNARE associations. Although it might be expected that activation of the α_{2A} receptor would have the same effect with all treatments, it is possible that the drugs utilize unique compliments of G proteins to modulate their effect or, if they all utilize the same ones,

that the preference for one subunit over another may vary. This could have implications for potency and efficacy of one drug compared to another.

How do G protein modifications affect inhibition of evoked release?

$G\gamma_5$ and $G\gamma_{11}$ could not be detected in enriched fractions from any of the four brain regions examined, despite precursor and transition ions being determined from purified proteins. $G\gamma_2$, $G\gamma_5$, and $G\gamma_{11}$ are known to include multiple variants which undergo posttranslational modifications (PTM) and/or differential regulation[228,257] . We posited that this may explain why these isoforms weren't identified in brain samples despite transcript levels suggesting they should be. Using the published literature on these isoforms, it would be possible to identify modified peptides such as methylated forms of $G\gamma_{11}$ or unprocessed C termini of $G\gamma_5$ on a high-sensitivity mass spectrometer such as the LTQ-Orbitrap Velos, and use that information to modify the current MRM protocol. In doing so, it would be possible to more accurately determine whether the α_{2A}AR receptor and SNARE proteins also interacted with these isoforms within the CNS. Aside from just what is known from the published literature, however, further efforts could be undertaken to examine potential PTMs or variants of all of the G protein isoforms. This will be an important step for the future because it will be interesting to determine which forms of the G proteins have the greatest role in regulating interactions with specific receptors as well as $G\beta\gamma$/SNARE interactions. In the current studies, we found that the α_{2A} receptor exhibits specificity toward some G protein isoforms over others. In this case we were looking only at unmodified forms of the G proteins. Are we seeing all the regulation that is happening at a synapse or does that represent only a small subset of the regulation that is occurring since most utilizes modified forms of the G proteins? It is possible that some receptors utilize different forms of the G proteins, and similarly that specificity for $G\beta\gamma$/SNARE interactions

is achieved in this way as well. Only by systematically examining the different modifications of each of the G protein isoforms, however, will it be possible to determine whether this is an added layer of complexity in the CNS or not.

Does heterotrimer composition affect specificity of α_{2A}AR interactions?

Previous work has suggested that both Gα and Gβγ subunits may selectivity of G protein activation by α_{2A}ARs[333,335]. While Albarrán-Juárez et al.[334] demonstrated individual $G\alpha_i$ isoforms did not mediate inhibition of evoked release, trains of electrical stimulation were used to elicit neurotransmitter release from prefrontal cortex slices. Gβγ inhibition of SNARE occurs through competition with synaptotagmin for binding sites necessary to evoke fusion events. High levels of calcium have been shown to favor synaptotagmin actions over Gβγ inhibition[75,79]. Trains of stimuli such as those used by Albarrán-Juárez et al. may act to increase calcium levels enough that synaptotagmin would outcompete Gβγ for binding to SNARE leading to the assertion that Gα subunits do not play a role in conferring specificity. Using immunoprecipitation and immunoblotting, Gα subunits that are pulled down with the receptor/Gβγ complex could be assessed. If subunit specific antibodies were unavailable, a targeted approach such as that for Gβγ could be developed and used to identify which isoforms were present. This information could identify another possible way by which G protein specificity is achieved.

What role does Gβγ/SNARE play in disease?

$G_{i/o}$-coupled GPCRs are important drug targets as dysregulation of these receptors has serious health consequences[197,198,199,200]. A major goal for the development of compounds that modulate the Gβγ/SNARE interaction, is to determine if they could be used in combination with current therapies in a synergistic manner. While our initial efforts identified a few lead

compounds that could be developed, continued efforts will be needed. Although initial leads looked promising, later work was hampered by the inherent stickiness of Gβγ in a plate-based assay. Another graduate student in the lab, Zack Zurawski, has since developed a high-throughput, solution-based screening assay, which is conducive to high-throughput screening of small molecules (Figure 27A). The assay makes use of Amplified Luminescent Proximity Homogeneous Assay (AlphaScreen) technology whereby recombinant biotinylated SNAP 25 forms a complex with a His-tagged Gβγ subunit. These complexes are captured on Ni-NTA-conjugated acceptor beads before the protein-acceptor bead complexes further captured on streptavidin-coated donor beads and permitted to equilibrate in solution. Upon irradiation with 680nm light, dye molecules attached to the donor beads generate singlet oxygen, which is capable of traveling up to 200nm in solution and striking an acceptor bead. Acceptor beads are conjugated to molecules that will generate 520-620nm light. The 520-620nm light produced is then measured by the plate reader. If the biotinylated SNAP-25 is unable to form a complex with Gβγ few acceptor beads are within 200nm and minimal 620nm light is generated. Zack has made significant progress in screening compounds and developing Gβγ/SNARE inhibitors (Figure 27Bi) that are selective (Figure 27Bii, Biii). These compounds have further been applied in physiologically relevant settings (Figure 28). Using paired recordings in lamprey, application of the small molecule, VU0476078, has been shown to block 5HT and Gβγ mediated inhibition of exocytosis. Application of such compounds could be used in mouse models looking at depression, fear conditioning, or working memory to assess the role of α_{2A}AR mediated Gβγ/SNARE interaction. Although early compounds may not have favourable DMPK profiles, canulation of mice should allow direct application of the compounds to areas of the brain such as the cortex that are known to be important centers for α_{2A} activity. In doing so, it would be possible to use behavioural models to assess whether Gβγ/SNARE interactions play a role in

normal functioning such as specific types of learning and memory. Further, by doing the same experiments in disease models known to affect memory, it would be possible to determine how the process was dysregulated. For example, if the introduction of an inhibitor caused worsening of symptoms, it might indicate that the normal functioning of Gβγ/SNARE was downregulated in some way. Conversely, if the inhibitor alleviated the symptoms then it might suggest that Gβγ/SNARE interactions were upregulated for some reason in the disease state. Additionally transgenic mouse models such as the FLAG and HA-tagged α_{2A} models used in this dissertation could be used to tease apart whether the contributing receptors were hetero- or autoreceptors. One possibility such knowledge would yield is that it could allow for the development of more specific treatments. This could be through further development of small molecules that would target specific types of receptors or G protein isoforms, or simply allow drugs to be used synergistically, thereby maximizing efficacy while minimizing potential side effects.

In vivo behavioural models, as well as biochemical assays such as those used in the present study could provide important information about the role of Gβγ/SNARE in disease states as well as examine how specificity could be affected under different physiological conditions.

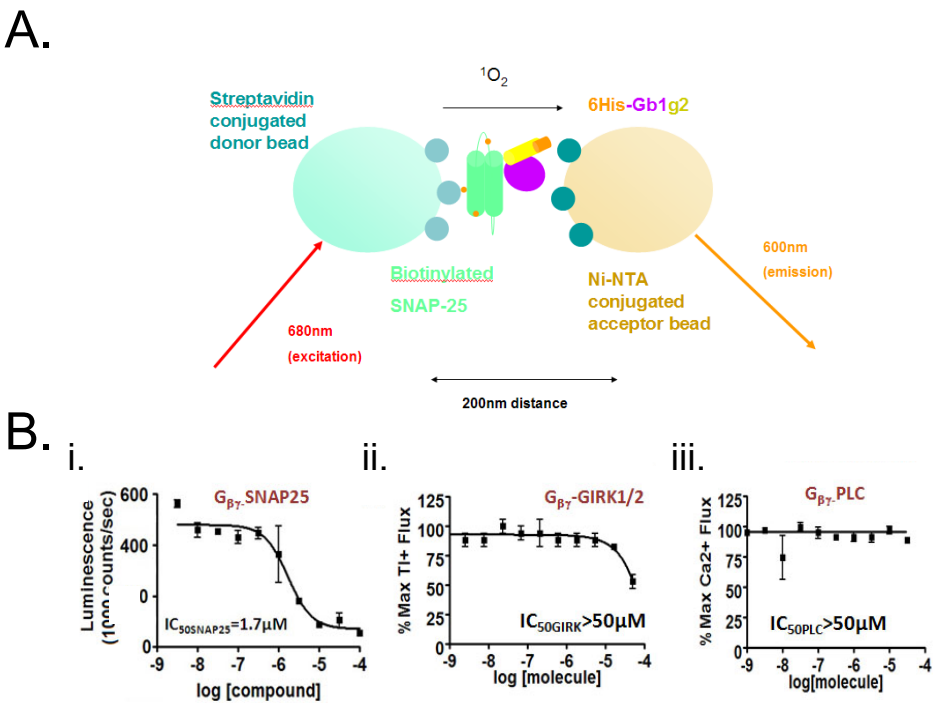

Figure 27. Continued development of compounds that modulate Gβγ/SNARE interactions. A) Alphascreen assay utilized to screen small molecule modulators of the Gβγ/SNARE interaction. B) Inhibitor 4 selectively inhibits Gβγ/SNARE interactions (see structures in panel C). Bi) 4 inhibits the Gβγ/SNARE interaction with micromolar potency as measured via Alphascreen. Bii) Inhibitor 4 does not inhibit Gβγ-GIRK channel interactions, as measured in cells expressing GIRK1/2 and the $G_{i/o}$-coupled GPCR mGluR8, along with an EC50 concentration of glutamate (8mM). Biii) Inhibitor 4 does not inhibit Gβγ-phospholipase C interactions, as measured by calcium flux assays in cell lines containing the $G_{i/o}$-coupled M2 muscarinic receptor at an EC_{50} concentration of acetylcholine of 800nM. Data provided by Zack Zurawski, Shaun Stauffer, Craig Lindsley, and Dave Weaver.

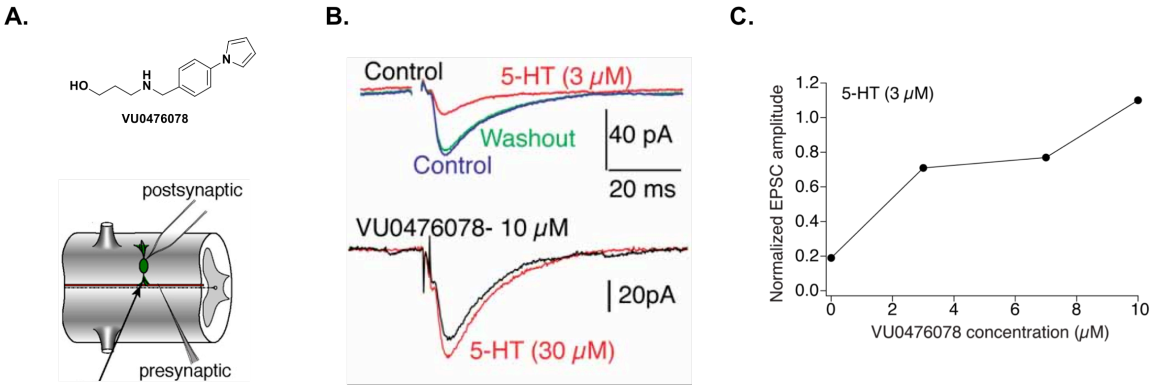

Figure 28. Small molecules block 5HT- and Gβγ mediated inhibition of exocytosis in neurons. A) Top: Chemical structure of VU0476078, a small molecule identified as inhibiting Gbg/SNARE interactions. Bottom: Schematic diagram showing paired recordings between reticulospinal axons and ventral horn neurons in the lamprey. B) Postsynaptic recordings from the lamprey. Application of 5HT causes a reduction in the excitatory post synaptic potentials. This inhibition is blocked with application of VU0476078. C) Concentration response curve of VU0476078 showing increased postsynaptic potential amplitude with increasing concentration of compound. Data provided by Zack Zurawski and Simon Alford.

LITERATURE CITED

1. Oldham, W.M., Hamm, H.E. 2008 Heterotrimeric G protein activation by G protein-coupled receptors. *Nat. Rev. Mol. Cell Biol. 9(1)*, 60-71.

2. Zhai, R.G., Bellen, H.J., 2004. The architecture of the active zone in the presynaptic nerve terminal. *Physiology. 19, 262-270.*

3. Schoch, S., Gundelfinger, E.D., 2006. Molecular organization of the presynaptic active zone. *Cell Tissue Res. 326(2),* 379-391.

4. Sudhof, T.C., 2004. The synaptic vesicle cycle. *Annu. Rev. Neurosci. 27,* 509-547.

5. Dresbach, T., Qualmann, B., Kessels, M.M., Garner, C.C., Gundelfinger, E.D. 2001. The presynaptic cytomatrix of brain synapses. *Cell. Mol. Life Sci. 58(1),* 94-116.

6. Phillips, G.R., Huang, J.K., Wang, Y., Tanaka, H., Shapiro, L., Zhang, W., Shan, W-S., Arndt, K., Frank., M., Gordon, R.E., Gawinowicz, MA., Zhao, Y., and Colman, D.R. 2001. *Neuron, 32:* 63-77.

7. Schweizer, F.E. and Ryan, T.A. 2006. *Current Opinion in Neurobiology, 16(3):* 298-304.

8. Park Y, Kim K-T. 2009. Short-term plasticity of small synaptic vesicle (SSV) and large dense-core vesicle (LDCV) exocytosis. *Cellular Signalling 21(10):*1465-1470.

9. Katz, B., 1969. The release of Neural Transmitter Substances (The Sherrington Lectures X). Charles C. Thomas, Springfield, IL.

10. Weimer, R.M., Gracheva, E.O., Meyrignac, O., Miller, K.G., Richmond, J.E., Bessereau, J.L. 2006. UNC-13 and UNC-10/rim localize synaptic vesicles to specific membrane domains. *J. Neurosci. 26(31),* 8040-8047.

11. Verhage, M., Sorensen, J.B. 2008. Vesicle docking in regulated exocytosis. *Traffic. 9(9),* 1414-1424.

12. Fernandez-Busnadiego, R., Zuber, B., Maurer, U.E., Cyrklaff, M., Baumeister, W., Lucic, V. 2010. Quantitative analysis of the native presynaptic cytomatrix by cryoelectron tomography. *J. Cell Biol. 188(1),* 145-156.

13. Toonen, R.F., Kochubey, O., de Wit, H., Gulyas-Kovacs, A., Konijnenburg, B., Sorensen, J.B., Klingauf, J., Verhage, M. 2006. Dissecting docking and tethering of secretory vesicles at the target membrane. *EMBO J. 25(16),* 3725-3737.

14. Becherer, U., Rettig, J. 2006. Vesicle pools, docking, priming, and release. *Cell Tissue Res. 326(2),* 393-407.

15. Malsam, J., Kreye, S., Sollner, T.H. 2008. Membrane fusion: SNAREs and regulation. *Cell. Mol. Life Sci. 65(18),* 2814-2832.

16. Parpura, V., Mohideen, U. 2008. Molecular form follows function: (un)snaring the SNAREs. *Trends Neurosci. 31(9),* 435-443.

17. de Wit, H. 2010. Molecular mechanism of secretory vesicle docking. *Biochem. Soc. Trans. 38,* 192-208.

18. Gerber, S.H., Rah, J.-C., Min, S.-W., Liu, X., de Wit, H., Dulubova, I., Meyer, A.C., Rizo, J., Arancillo, M., Hammer, R.E., Verhage, M., Rosenmund, C., Südhof, T.C. 2008. Conformational Switch of Syntaxin-1 Controls Synaptic Vesicle Fusion. *Science. 321(5895),* 1507-1510.

19. Misura, K.M., Scheller, R.H., Weis, W.I. 2000. Three-dimensional structure of the neuronal-Sec1-syntaxin 1a complex. *Nature. 404(6776),* 355-362.

20. Rizo, J., Chen, X., Arac, D. 2006. Unraveling the mechanisms of synaptotagmin and SNARE function in neurotransmitter release. *Trends Cell Biol. 16(7),* 339-350.

21. Rizo, J., Rosenmund, C. 2008. Synaptic vesicle fusion. *Nat. Struct. Mol. Biol. 15(7),* 665-674.

22. Sudhof, T.C., Rothman, J.E. 2009. Membrane fusion: grappling with SNARE and SM proteins. *Science. 323(5913),* 474-477.

23. Wojcik, S.M., Brose, N. 2007. Regulation of membrane fusion in synaptic excitation-secretion coupling: speed and accuracy matter. *Neuron. 55(1),* 11-24.

24. Weninger, K., Bowen, M.E., Choi, U.B., Chu, S., Brunger, A.T. 2008. Accessory proteins stabilize the acceptor complex for synaptobrevin, the 1:1 syntaxin/SNAP-25 complex. *Structure. 16(2),* 308-320.

25. Jahn, R., Scheller, R.H. 2006. SNAREs--engines for membrane fusion. *Nat. Rev. Mol. Cell Biol. 7(9),* 631-643.

26. Sollner, T., Bennett, M.K., Whiteheart, S.W., Scheller, R.H., Rothman, J.E. 1993a. A protein assembly-disassembly pathway in vitro that may correspond to sequential steps of synaptic vesicle docking, activation, and fusion. *Cell. 75(3),* 409-418.

27. Sollner, T., Whitehart, S.W., Brunner, M., Erdjumentbromage, H., Geromanos, S., Tempst, P., Rothman, J.E. 1993b. SNAP receptors implicated in vesicle targeting and fusion. *Nature. 362(6418),* 318-324.

28. Weber, T., Zemelman, B.V., McNew, J.A., Westermann, B., Gmachl, M., Parlati, F., Söllner, T.H., Rothman, J.E. 1998. SNAREpins: Minimal Machinery for Membrane Fusion. *Cell. 92(6),* 759-772.

29. Teng, F.Y., Wang, Y., Tang, B.L. 2001.. The syntaxins. *Genome Biol. 2(11),* reviews3012-reviews.

30. Sampo, B., Tricaud, N., Leveque, C., Seagar, M., Couraud, F., Dargent, B., 2000. Direct interaction between synaptotagmin and the intracellular loop I-II of neuronal voltage-sensitive sodium channels. *Proc. Natl. Acad. Sci. USA. 97(7),* 3666-3671.

31. Hong, W., 2005. SNAREs and traffic. *Biochim. Biophys. Acta. 1744(2),* 120-144.

32. Seagar, M., Leveque, C., Charvin, N., Marqueze, B., Martin-Moutot, N., Boudier, J.A., Boudier, J.L., Shoji-Kasai, Y., Sato, K., Takahashi, M., 1999. Interactions between proteins implicated in exocytosis and voltage-gated calcium channels. *Philos. Trans. R. Soc. Lond. B Biol. Sci. 354(1381),* 289-297.

33. Matteoli, M., Pozzi, D., Grumelli, C., Condliffe, S.B., Frassoni, C., Harkany, T., Verderio, C., 2009. The synaptic split of SNAP-25: Different roles in glutamatergic and GABAergic neurons? *Neuroscience. 158(1),* 223-230.

34. Dulubova, I., Sugita, S., Hill, S., Hosaka, M., Fernandez, I., Sudhof, T.C., Rizo, J., 1999. A conformational switch in syntaxin during exocytosis: role of munc18. *EMBO J. 18(16),* 4372-4382.

35. Voets, T., Toonen, R.F., Brian, E.C., de Wit, H., Moser, T., Rettig, J., Sudhof, T.C., Neher, E., Verhage, M., 2001. Munc18-1 promotes large dense-core vesicle docking. *Neuron. 31(4),* 581-591.

36. Yang, B., Steegmaier, M., Gonzalez, L.C., Scheller, R.H., 2000. nSec1 binds a closed conformation of syntaxin1A. *J. Cell Biol. 148(2),* 247-252.

37. Burgoyne, R.D., Morgan, A., 2011. Chaperoning the SNAREs: a role in preventing neurodegeneration? *Nat. Cell. Biol. 13(1),* 8-9.

38. Augustin, I., Rosenmund, C., Sudhof, T.C., Brose, N., 1999. Munc13-1 is essential for fusion competence of glutamatergic synaptic vesicles. *Nature. 400(6743),* 457-461.

39. Richmond, J.E., Davis, W.S., Jorgensen, E.M., 1999. UNC-13 is required for synaptic vesicle fusion in C-elegans. *Nat. Neurosci. 2(11),* 959-964.

40. Aravamudan, B., Fergestad, T., Davis, W.S., Rodesch, C.K., Broadie, K., 1999. Drosophila Unc-13 is essential for synaptic transmission. *Nat. Neurosci. 2(11),* 965-971.

41. Weimer, R.M., Gracheva, E.O., Meyrignac, O., Miller, K.G., Richmond, J.E., Bessereau, J.L., 2006. UNC-13 and UNC-10/rim localize synaptic vesicles to specific membrane domains. *J. Neurosci. 26(31),* 8040-8047.

42. Hammarlund, M., Palfreyman, M.T., Watanabe, S., Olsen, S., Jorgensen, E.M., 2007. Open syntaxin docks synaptic vesicles. *PLoS Biol. 5(8),* e198.

43. Stevens, D.R., Wu, Z.X., Matti, U., Junge, H.J., Schirra, C., Becherer, U., Wojcik, S.M., Brose, N., Rettig, J., 2005. Identification of the minimal protein domain required for priming activity of Munc13-1. *Curr. Biol. 15(24),* 2243-2248.

44. Fukuda, M., 2003a. Molecular Cloning, Expression, and Characterization of a Novel Class of Synaptotagmin (Syt XIV) Conserved from Drosophila to Humans. *J. Biochem. 133(5),* 641-649.v

45. Schiavo, G., Osborne, S.L., Sgouros, J.G., 1998. Synaptotagmins: More Isoforms Than Functions? Biochem. *Biophys. Res. Commun. 248(1),* 1-8.

46. Südhof, T.C., 2002. Synaptotagmins: Why So Many? *J. Biol. Chem. 277(10),* 7629-7632.

47. Geppert, M., Goda, Y., Hammer, R.E., Li, C., Rosahl, T.W., Stevens, C.F., Sudhof, T.C., 1994. Synaptotagmin I: a major Ca2+ sensor for transmitter release at a central synapse. *Cell. 79(4),* 717-727.

48. Maximov, A., Sudhof, T.C., 2005. Autonomous function of synaptotagmin 1 in triggering synchronous release independent of asynchronous release. *Neuron. 48(4),* 547-554.

49. Tang, J., Maximov, A., Shin, O.H., Dai, H., Rizo, J., Sudhof, T.C., 2006. A complexin/synaptotagmin 1 switch controls fast synaptic vesicle exocytosis. *Cell. 126(6),* 1175-1187.

50. Fernandez-Chacon, R., Konigstorfer, A., Gerber, S.H., Garcia, J., Matos, M.F., Stevens, C.F., Brose, N., Rizo, J., Rosenmund, C., Sudhof, T.C., 2001. Synaptotagmin I functions as a calcium regulator of release probability. *Nature. 410(6824),* 41-49.

51. Dai, H., Shen, N., Arac, D., Rizo, J., 2007. A quaternary SNARE-synaptotagmin-Ca2+-phospholipid complex in neurotransmitter release. *J. Mol. Biol. 367(3),* 848-863.

52. Gerona, R.R.L., Larsen, E.C., Kowalchyk, J.A., Martin, T.F.J., 2000. The C Terminus of SNAP25 Is Essential for Ca2+-dependent Binding of Synaptotagmin to SNARE Complexes. *J. Biol. Chem. 275(9),* 6328-6336.

53. Zhang, X., Kim-Miller, M.J., Fukuda, M., Kowalchyk, J.A., Martin, T.F.J., 2002. Ca2+-Dependent Synaptotagmin Binding to SNAP-25 Is Essential for Ca2+-Triggered Exocytosis. *Neuron. 34(4),* 599-611.

54. Lynch, K.L., Gerona, R.R., Larsen, E.C., Marcia, R.F., Mitchell, J.C., Martin, T.F., 2007. Synaptotagmin C2A loop 2 mediates Ca2+-dependent SNARE interactions essential for Ca2+-triggered vesicle exocytosis*. Mol. Biol. Cell. 18(12),* 4957-4968.

55. Chapman, E.R., Jahn, R., 1994. Calcium-dependent interaction of the cytoplasmic domain region of synaptotamin with membranes – autonomous function of a single C-2-homologou domain. *J. Biol. Chem. 269(8),* 5735-41.

56. Chapman, E.R., Davis, A.F. 1998. Direct interaction of a Ca2+-binding loop of synaptotagmin with lipid bilayers. *J. Biol. Chem. 273(22),* 13995-14001.

57. Fernandez, I., Arac, D., Ubach, J., Gerber, S.H., Shin, O.H., Gao, Y., Anderson, R.G.W., Sudhof, T.C., Rizo, J. 2001. Three-dimensional structure of the synaptotagmin 1 C2B-domain: Synaptotagmin 1 as a phospholipid binding machine. *Neuron. 32(6),* 1057-1069.

58. Choi, U.B., Strop, P., Vrljic, M., Chu, S., Brunger, A.T., Weninger, K.R. 2010. Single-molecule FRET-derived model of the synaptotagmin 1-SNARE fusion complex. *Nat. Struct. Mol. Biol. 17(3),* 318-324.

59. Lai, A.L., Huang, H., Herrick, D.Z., Epp, N., Cafiso, D.S. 2011. Synaptotagmin 1 and SNAREs Form a Complex That Is Structurally Heterogeneous. *J. Mol. Biol. 405(3),* 696-706.

60. Kochubey, O., Schneggenburger, R. 2011. Synaptotagmin Increases the Dynamic Range of Synapses by Driving Ca2+-Evoked Release and by Clamping a Near-Linear Remaining Ca2+ Sensor. *Neuron. 69(4),* 736-748.

61. Sun, J., Pang, Z.P., Qin, D., Fahim, A.T., Adachi, R., Sudhof, T.C. 2007. A dual-Ca2+-sensor model for neurotransmitter release in a central synapse. *Nature. 450(7170),* 676-682.

62. Groffen, A.J., Martens, S., Arazola, R.D., Cornelisse, L.N., Lozovaya, N., de Jong, A.P.H., Goriounova, N.A., Habets, R.L.P., Takai, Y., Borst, J.G., Brose, N., McMahon, H.T., Verhage, M. 2010. Doc2b Is a High-Affinity Ca2+ Sensor for Spontaneous Neurotransmitter Release. *Science. 327(5973),* 1614-1618.

63. Yao, J., Gaffaney, J., Kwon, S., Chapman, E. 2011. Doc2 is a Ca2+ sensor required for asynchronous neurotransmitter release. *Cell. 147(3),* 666-743.

64. Chicka, M.C., Chapman, E.R. 2009. Concurrent binding of complexin and synaptotagmin to liposome-embedded SNARE complexes. *Biochemistry. 48(4),* 657-659.

65. Hobson, R.J., Liu, Q., Watanabe, S. Jorgensen, E.M., 2011. Complexin Maintains Vesicles in the Primed State in C. elegans. *Current Biology. 21(2),* 106-113.

66. McMahon, H.T., Missler, M., Li, C., Südhof, T.C. 1995. Complexins: Cytosolic proteins that regulate SNAP receptor function. *Cell. 83(1),* 111-119.

67. Bracher, A., Kadlec, J., Betz, H., Weissenhorn, W. 2002. X-ray Structure of a Neuronal Complexin-SNARE Complex from Squid. *J. Biol. Chem. 277(29),* 26517-26523.

68. Chen, X., Tomchick, D.R., Kovrigin, E., Araç, D., Machius, M., Südhof, T.C., Rizo, J. 2002. Three-Dimensional Structure of the Complexin/SNARE Complex. *Neuron. 33(3),* 397-409.

69. Kümmel, D., Krishnakumar, S.S., Radoff, D.T., Li, F., Giraudo, C.G., Pincet, F., Rothman, J.E., Reinisch, K.M. 2011. Complexin cross-links prefusion SNAREs into a zigzag array. *Nat. Struct. Mol. Biol. 18(8),* 927-933.

70. Fujita, Y., Shirataki, H., Sakisaka, T., Asakura, T., Ohya, T., Kotani, H., Yokoyama, S., Nishioka, H., Matsuura, Y., Mizoguchi, A., Scheller, R.H., Takai, Y. 1998. Tomosyn: a syntaxin-1-binding protein that forms a novel complex in the neurotransmitter release process. *Neuron. 20(5),* 905-915.

71. Hatsuzawa, K., Lang, T., Fasshauer, D., Bruns, D., Jahn, R. 2003. The R-SNARE motif of tomosyn forms SNARE core complexes with syntaxin 1 and SNAP-25 and down-regulates exocytosis. *J. Biol. Chem. 278(33),* 31159-31166.

72. Burdina, A.O., Klosterman, S.M., Shtessel, L., Ahmed, S., Richmond, J.E. 2011. *In Vivo* Analysis of Conserved *C. elegans* Tomosyn Domains. *PLoS One. 6(10),* e26185.

73. Pobbati, A.V., Razeto, A., Böddener, M., Becker, S., Fasshauer, D. 2004. Structural Basis for the Inhibitory Role of Tomosyn in Exocytosis. *J. Biol. Chem. 279(45),* 47192-47200.

74. Blackmer, T., Larsen, E.C., Takahashi, M., Martin, T.F., Alford, S., Hamm, H.E., 2001. G protein betagamma subunit-mediated presynaptic inhibition: regulation of exocytotic fusion downstream of Ca2+ entry. *Science. 292(5515),* 293-7.

75. Blackmer, T., Larsen, E.C., Bartleson, C., Kowalchyk, J.A., Yoon, E.J., Preininger, A.M., Alford, S., Hamm, H.E., Martin, T.F. 2005. G protein betagamma directly regulates SNARE protein fusion machinery for secretory granule exocytosis. Nat. *Neurosci. 8(4),* 421-425.

76. Gerachshenko, T., Blackmer, T., Yoon, E.J., Bartleson, C., Hamm, H.E., Alford, S. 2005. Gbetagamma acts at the C terminus of SNAP-25 to mediate presynaptic inhibition. *Nat. Neurosci. 8(5),* 597-605.

77. Hamid, E., Church, E., Wells, C.A., Zurawski, Z., Hamm, H.E., and Alford, S. 2014. Modulation of neurotransmissio by GPCRs is dependent upon the microarchitecture of the primed vesicle complex. *The Journal of Neuroscience. 34(1):* 260-274

78. Photowala, H., Blackmer, T., Schwartz, E., Hamm, H.E., Alford, S. 2006. G protein betagamma-subunits activated by serotonin mediate presynaptic inhibition by regulating vesicle fusion properties. *Proc. Natl. Acad. Sci. U S A.* 103(11), 4281-4286.

79. Yoon, E.J., Gerachshenko, T., Spiegelberg, B.D., Alford, S., Hamm, H.E. 2007. Gbetagamma interferes with Ca2+-dependent binding of synaptotagmin to the soluble N-ethylmaleimide-sensitive factor attachment protein receptor (SNARE) complex. *Mol. Pharmacol. 72(5),* 1210-1219.

80. Yoon, E.J., Hamm, H.E., Currie, K.P. 2008. G protein betagamma subunits modulate the number and nature of exocytotic fusion events in adrenal chromaffin cells independent of calcium entry. *J Neurophysiol. 100(5),* 2929-2939.

81. Wells, C.A., Zuwarski, Z.Z., Betke, K.M., Yim, Y.Y., Rodriguez, S., Alford, S., and Hamm, H.E. 2012. G$\beta\gamma$ inhibits exocytosis via interaction with critical residues on soluble-N-ethylmaleimide-sensitive factor attachement protein-25. *Mol. Pharmacol. 82(6):* 1136-1139.

82. Eglen, R.M., Reisine, T. 2009. New insights into GPCR function: implications for HTS. *Methods Mol. Biol. 552,* 1-13.

83. Millar, R.P., Newton, C.L. 2010. The year in G protein-coupled receptor research. *Mol. Endocrinol. 24(1),* 261-274.

84. Millar, R.P., Newton, C.L., 2010. The year in G protein-coupled receptor research. *Mol. Endocrinol. 24(1),* 261-274.

85. Rosenbaum, D.M., Rasmussen, S.G., Kobilka, B.K. 2009. The structure and function of G-protein-coupled receptors. *Nature. 459(7245),* 356-363.

86. Schiöth HB, Fredriksson R. 2005. The GRAFS classification system of G-protein coupled receptors in comparative perspective. *General and Comparative Endocrinology. 142(1-2),* 94-101.

87. Bjarnadottir TK, Fredriksson R, Hoglund PJ, Gloriam DE, Lagerstrom MC, Schioth HB. 2004. The human and mouse repertoire of the adhesion family of G-protein-coupled receptors. *Genomics. 84(1),* 23-33.

88. Buranda, T., Waller, A., Wu, Y., Simons, P.C., Biggs, S., Prossnitz, E.R., Sklar, L.A. 2007. Some Mechanistic Insights into GPCR Activation from Detergent-Solubilized Ternary Complexes on Beads. In: Stephen, R.S., editor. Adv. Protein Chem. Academic Press, pp. 95-135.

89. Wilkie, T.M., Gilbert, D.J., Olsen, A.S., Chen, X.N., Amatruda, T.T., Korenberg, J.R., Trask, B.J., de Jong, P., Reed, R.R., Simon, M.I., et al. 1992. Evolution of the mammalian G protein alpha subunit multigene family. Nat. Genet. 1(2), 85-91.

90. Yokoyama, S., Starmer, W.T. 1992. Phylogeny and evolutionary rates of G protein alpha subunit genes. *J. Mol. Evol. 35(3),* 230-238.

91. Downes, G.B., Gautam, N. 1999. The G protein subunit gene families. *Genomics. 62(3),* 544-552.

92. Hildebrandt, J.D. 1997. Role of subunit diversity in signaling by heterotrimeric G proteins. *Biochem. Pharmacol. 54(3),* 325-339.

93. Simon MI, Strathmann MP, Gautam N. 1991. Diversity of G proteins in signal transduction. *Science. 252(5007),* 802–808.

94. Clapham, D.E., Neer, E.J. 1997. G protein beta gamma subunits*. Annu. Rev. Pharmacol. Toxicol. 37,* 167-203.

95. Gautam, N., Downes, G.B., Yan, K., Kisselev, O. 1998. The G-protein betagamma complex. *Cell. Signal. 10(7),* 447-455.

96. Smrcka, A.V. 2008. G protein betagamma subunits: central mediators of G protein-coupled receptor signaling. *Cell. Mol. Life Sci. 65(14),* 2191-2214.

97. Oldham, W.M., Hamm, H.E. 2007. How do receptors activate G proteins? *Adv. Protein Chem. 74,* 67-93.

98. Betty, M., Harnish, S.W., Rhodes, K.J., Cockett, M.I. 1998. Distribution of heterotrimeric G-protein beta and gamma subunits in the rat brain*. Neuroscience. 85(2)*, 475-486.

99. Albert, P.R., Robillard, L. 2002. G protein specificity: traffic direction required. *Cell. Signal. 14(5),* 407-418.

100. Lim, W.K., Myung, C.S., Garrison, J.C., Neubig, R.R. 2001. Receptor-G protein gamma specificity: gamma11 shows unique potency for A(1) adenosine and 5-HT(1A) receptors. *Biochemistry. 40(35),* 10532-10541.

101. Lindorfer, M.A., Myung, C.S., Savino, Y., Yasuda, H., Khazan, R., Garrison, J.C. 1998. Differential activity of the G protein beta5 gamma2 subunit at receptors and effectors. *J. Biol. Chem. 273(51),* 34429-3436.

102. Schwindinger, W.F., Betz, K.S., Giger, K.E., Sabol, A., Bronson, S.K., Robishaw, J.D. 2003. Loss of G protein gamma 7 alters behavior and reduces striatal alpha(olf) level and cAMP production. *J. Biol. Chem.* 278(8), 6575-6579.

103. Robishaw, J.D., Berlot, C.H. 2004. Translating G protein subunit diversity into functional specificity. *Curr. Opin. Cell Biol. 16(2),* 206-209.

104. Cabrera-Vera, T.M., Hernandez, S., Earls, L.R., Medkova, M., Sundgren-Andersson, A.K., Surmeier, D.J., Hamm, H.E. 2004. RGS9-2 modulates D2 dopamine receptor-mediated Ca2+ channel inhibition in rat striatal cholinergic interneurons. *Proc. Natl. Acad. Sci. USA. 101(46),* 16339-16344.

105. Logothetis, D.E., Kurachi, Y., Galper, J., Neer, E.J., Clapham, D.E. 1987. The beta gamma subunits of GTP-binding proteins activate the muscarinic K+ channel in heart. *Nature. 325(6102),* 321-326.

106. Myung, C.S., Lim, W.K., DeFilippo, J.M., Yasuda, H., Neubig, R.R., Garrison, J.C. 2006. Regions in the G protein gamma subunit important for interaction with receptors and effectors. *Mol. Pharmacol. 69(3),* 877-887.

107. Panchenko, M.P., Saxena, K., Li, Y., Charnecki, S., Sternweis, P.M., Smith, T.F., Gilman, A.G., Kozasa, T., Neer, E.J. 1998. Sites important for PLCbeta2 activation by the G protein betagamma subunit map to the sides of the beta propeller structure. *J. Biol. Chem. 273(43),* 28298-28304.

108. Peng, L., Mirshahi, T., Zhang, H., Hirsch, J.P., Logothetis, D.E. 2003. Critical determinants of the G protein gamma subunits in the Gbetagamma stimulation of G protein-activated inwardly rectifying potassium (GIRK) channel activity. *J. Biol. Chem. 278(50),* 50203-50211.

109. Zhao, Q., Kawano, T., Nakata, H., Nakajima, Y., Nakajima, S., Kozasa, T. 2003. Interaction of G protein beta subunit with inward rectifier K(+) channel Kir3. *Mol. Pharmacol. 64(5),* 1085-10891.

110. Stephens, G.J., Mochida, S. 2005. G protein bg subunits mediate presynaptic inhibition of transmitter release from rat superior cervical ganglion neurones in culture*. J. Physiol. 563(Pt 3),* 765-776.

111. Stephens, G.J. 2009. G-protein-coupled-receptor-mediated presynaptic inhibition in the cerebellum. *Trends Pharmacol. Sci. 30(8),* 421-430.

112. Brown, D.A., Sihra, T.S. 2008. Presynaptic signaling by heterotrimeric G-proteins. *Handb. Exp. Pharmacol. (184),* 207-260.

113. Delmas, P., Abogadie, F.C., Dayrell, M., Haley, J.E., Milligan, G., Caulfield, M.P., Brown, D.A., Buckley, N.J. 1998. G-proteins and G-protein subunits mediating cholinergic inhibition of N-type calcium currents in sympathetic neurons. *Eur. J. Neurosci. 10(5),* 1654-1666.

114. Haley, J.E., Delmas, P., Offermanns, S., Abogadie, F.C., Simon, M.I., Buckley, N.J., Brown, D.A. 2000. Muscarinic inhibition of calcium current and M current in Galpha q-deficient mice. *J. Neurosci. 20(11),* 3973-3979.

115. Gamper, N., Reznikov, V., Yamada, Y., Yang, J., Shapiro, M.S. 2004. Phosphatidylinositol [correction] 4,5-bisphosphate signals underlie receptor-specific Gq/11-mediated modulation of N-type Ca2+ channels. *J. Neurosci. 24(48),* 10980-10992.

116. DeFea, K.A. 2011. Beta-arrestins as regulators of signal termination and transduction: how do they determine what to scaffold? *Cell. Signal. 23(4),* 621-629.

117. Lynch, M.J., Baillie, G.S., Mohamed, A., Li, X., Maisonneuve, C., Klussmann, E., van Heeke, G., Houslay, M.D. 2005. RNA silencing identifies PDE4D5 as the functionally relevant cAMP phosphodiesterase interacting with beta arrestin to control the protein kinase A/AKAP79-mediated switching of the beta2-adrenergic receptor to activation of ERK in HEK293B2 cells. *J. Biol. Chem. 280(39),* 33178-33189.

118. Shigemoto, R., Kinoshita, A., Wada, E., Nomura, S., Ohishi, H., Takada, M., Flor, P.J., Neki, A., Abe, T., Nakanishi, S., Mizuno, N. 1997. Differential presynaptic localization of metabotropic glutamate receptor subtypes in the rat hippocampus. *J. Neurosci. 17(19),* 7503-7522.

119. Corti, C., Aldegheri, L., Somogyi, P., Ferraguti, F. 2002. Distribution and synaptic localisation of the metabotropic glutamate receptor 4 (mGluR4) in the rodent CNS. *Neuroscience. 110(3),* 403-420.

120. Miller, R.J. 1998. Presynaptic receptors. Annu. Rev. Pharmacol. *Toxicol. 38,* 201-227.

121. Fernandez-Alacid, L., Aguado, C., Ciruela, F., Martin, R., Colon, J., Cabanero, M.J., Gassmann, M., Watanabe, M., Shigemoto, R., Wickman, K., Bettler, B., Sanchez-Prieto, J., Lujan, R. 2009. Subcellular compartment-specific molecular diversity of pre- and post-synaptic GABA-activated GIRK channels in Purkinje cells. *J. Neurochem. 110(4),* 1363-1376.

122. Catterall, W.A., Perez-Reyes, E., Snutch, T.P., Striessnig, J. 2005. International Union of Pharmacology. XLVIII. Nomenclature and Structure-Function Relationships of Voltage-Gated Calcium Channels*. Pharmacol. Rev. 57(4),* 411-425.

123. Currie, K.P. 2010. Inhibition of Ca2+ channels and adrenal catecholamine release by G protein coupled receptors. *Cell. Mol. Neurobiol. 30(8),* 1201-1208.

124. Herlitze, S., Garcia, D.E., Mackie, K., Hille, B., Scheuer, T., Catterall, W.A. 1996. Modulation of Ca2+ channels by G-protein beta gamma subunits. *Nature. 380(6571),* 258-262.

125. Ikeda, S.R. 1996. Voltage-dependent modulation of N-type calcium channels by G-protein beta gamma subunits. *Nature. 380(6571),* 255-258.

126. Tedford, H.W., Kisilevsky, A.E., Peloquin, J.B., Zamponi, G.W. 2006. Scanning Mutagenesis Reveals a Role for Serine 189 of the Heterotrimeric G-Protein Beta 1 Subunit in the Inhibition of N-Type Calcium Channels. *J. Neurophysiol. 96(1),* 465-470.

127. Tedford, H.W., Zamponi, G.W. 2006. Direct G Protein Modulation of Cav2 Calcium Channels. *Pharmacol. Rev. 58(4),* 837-862.

128. Canti, C., Page, K.M., Stephens, G.J., Dolphin, A.C. 1999. Identification of Residues in the N Terminus of α1B Critical for Inhibition of the Voltage-Dependent Calcium Channel by Gβγ. *J. Neurosci. 19(16),* 6855-6864.

129. Zamponi, G.W., Bourinet, E., Nelson, D., Nargeot, J., Snutch, T.P. 1997. Crosstalk between G proteins and protein kinase C mediated by the calcium channel a1 subunit. *Nature. 385(6615),* 442-446.

130. Furukawa, T., Miura, R., Mori, Y., Strobeck, M., Suzuki, K., Ogihara, Y., Asano, T., Morishita, R., Hashii, M., Higashida, H., Yoshii, M., Nukada, T. 1998. Differential

Interactions of the C terminus and the Cytoplasmic I-II Loop of Neuronal Ca2+ Channels with G-protein α and βγ Subunits. *J. Biol. Chem. 273(28),* 17595-17603.

131. Li, B., Zhong, H., Scheuer, T., Catterall, W.A. 2004. Functional Role of a C-Terminal Gβγ-Binding Domain of Cav2.2 Channels. *Mol. Pharmacol. 66(3),* 761-769.

132. Qin, N., Platano, D., Olcese, R., Stefani, E., Birnbaumer, L. 1997. Direct interaction of Gβγ with a C-terminal Gβγ-binding domain of the Ca2+ channel α1 subunit is responsible for channel inhibition by G protein-coupled receptors. *Proc. Natl. Acad. Sci. USA. 94(16),* 8866-8871.

133. De Waard, M., Liu, H., Walker, D., Scott, V.E., Gurnett, C.A., Campbell, K.P. 1997. Direct binding of G-protein betagamma complex to voltage-dependent calcium channels [see comments]. *Nature. 385(6615),* 446-450.

134. Bean, B.P. 1989. Neurotransmitter inhibition of neuronal calcium currents by changes in channel voltage dependence. *Nature. 340(6229),* 153-156.

135. Boland, L., Bean, B. 1993. Modulation of N-type calcium channels in bullfrog sympathetic neurons by luteinizing hormone-releasing hormone: kinetics and voltage dependence. *J. Neurosci. 13(2),* 516-533.

136. Elmslie, K.S. 1992. Calcium current modulation in frog sympathetic neurones: multiple neurotransmitters and G proteins. *J. Physiol. 451(1),* 229-246.

137. Golard, A., Siegelbaum, S. 1993. Kinetic basis for the voltage-dependent inhibition of N-type calcium current by somatostatin and norepinephrine in chick sympathetic neurons. *J. Neurosci. 13(9),* 3884-3894.

138. Jarvis, S.E., Magga, J.M., Beedle, A.M., Braun, J.E.A., Zamponi, G.W. 2000. G Protein Modulation of N-type Calcium Channels Is Facilitated by Physical Interactions between Syntaxin 1A and Gβγ. *J. Biol. Chem. 275(9),* 6388-6394.

139. Kasai, H., Aosaki, T. 1989. Modulation of Ca-channel current by an adenosine analog mediated by a GTP-binding protein in chick sensory neurons. *Pflugers Arch. 414(2),* 145-149.

140. Dunlap, K., Fischbach, G.D. 1978. Neurotransmitters decrease the calcium component of sensory neurone action potentials. *Nature. 276(5690),* 837-839.

141. Zhu, Y., Ikeda, S.R., 1994. VIP inhibits N-type Ca2+ channels of sympathetic neurons via a pertussis toxin-insensitive but cholera toxin-sensitive pathway. *Neuron. 13(3),* 657-669.

142. Bennett, M.K., Calakos, N., Scheller, R.H. 1992. Syntaxin: a synaptic protein implicated in docking of synaptic vesicles at presynaptic active zones. Science. 257(5067), 255-259.

143. Leveque, C., el Far, O., Martin-Moutot, N., Sato, K., Kato, R., Takahashi, M., Seagar, M.J. 1994. Purification of the N-type calcium channel associated with syntaxin and

synaptotagmin. A complex implicated in synaptic vesicle exocytosis. *J. Biol. Chem. 269(9),* 6306-6312.

144. O'Connor, V.M., Shamotienko, O., Grishin, E., Betz, H. 1993. On the structure of the 'synaptosecretosome'. Evidence for a neurexin/synaptotagmin/syntaxin/Ca2+ channel complex. *FEBS Lett. 326(1-3),* 255-260.

145. Sheng, Z.-H., Rettig, J., Takahashi, M., Catterall, W.A. 1994. Identification of a syntaxin-binding site on N-Type calcium channels. *Neuron. 13(6),* 1303-1313.

146. Jarvis, S.E., Zamponi, G.W. 2001. Distinct molecular determinants govern syntaxin 1A-mediated inactivation and G-protein inhibition of N-type calcium channels*. J. Neurosci. 21(9),* 2939-2948.

147. Kulik, A., Vida, I., Fukazawa, Y., Guetg, N., Kasugai, Y., Marker, C.L., Rigato, F., Bettler, B., Wickman, K., Frotscher, M., Shigemoto, R. 2006. Compartment-dependent colocalization of Kir3.2-containing K+ channels and GABAB receptors in hippocampal pyramidal cells. *J. Neurosci. 26(16),* 4289-4297.

148. Luscher, C., Jan, L.Y., Stoffel, M., Malenka, R.C., Nicoll, R.A. 1997. G protein-coupled inwardly rectifying K+ channels (GIRKs) mediate postsynaptic but not presynaptic transmitter actions in hippocampal neurons. *Neuron. 19(3),* 687-695.

149. Luscher, C., Slesinger, P.A. 2010. Emerging roles for G protein-gated inwardly rectifying potassium (GIRK) channels in health and disease. *Nat. Rev. Neurosci. 11(5),* 301-315.

150. Ikeda, K., Yoshii, M., Sora, I., Kobayashi, T. 2003. Opioid receptor coupling to GIRK channels. In vitro studies using a Xenopus oocyte expression system and in vivo studies on weaver mutant mice. *Methods Mol. Med. 84,* 53-64.

151. Yokogawa, M., Osawa, M., Takeuchi, K., Mase, Y., Shimada, I. 2011. NMR analyses of the Gbetagamma binding and conformational rearrangements of the cytoplasmic pore of G protein-activated inwardly rectifying potassium channel 1 (GIRK1). *J. Biol. Chem. 286(3),* 2215-2223.

152. Dascal, N. 1997. Signalling via the G protein-activated K+ channels. *Cell. Signal. 9(8),* 551-573.

153. Finley, M., Arrabit, C., Fowler, C., Suen, K.F., Slesinger, P.A. 2004. betaL-betaM loop in the C-terminal domain of G protein-activated inwardly rectifying K(+) channels is important for G(betagamma) subunit activation. *J. Physiol. 555(Pt 3),* 643-657.

154. Sadja, R., Reuveny, E. 2009. Activation gating kinetics of GIRK channels are mediated by cytoplasmic residues adjacent to transmembrane domains. *Channels (Austin). 3(3),* 205-214.

155. Ponce, A., Bueno, E., Kentros, C., Vega-Saenz de Miera, E., Chow, A., Hillman, D., Chen, S., Zhu, L., Wu, M.B., Wu, X., Rudy, B., Thornhill, W.B. 1996. G-protein-gated inward

rectifier K+ channel proteins (GIRK1) are present in the soma and dendrites as well as in nerve terminals of specific neurons in the brain. *J. Neurosci. 16(6),* 1990-2001

156. Sadja, R., Alagem, N., Reuveny, E. 2003. Gating of GIRK channels: details of an intricate, membrane-delimited signaling complex. *Neuron. 39(1),* 9-12.

157. Huang, C.-L., Slesinger, P.A., Casey, P.J., Jan, Y.N., Jan, L.Y. 1995. Evidence that direct binding of Gβγ to the GIRK1 G protein-gated inwardly rectifying K+ channel is important for channel activation. *Neuron. 15(5),* 1133-1143.

158. Ford, C.E., Skiba, N.P., Bae, H., Daaka, Y., Reuveny, E., Shekter, L.R., Rosal, R., Weng, G., Yang, C.-S., Iyengar, R., Miller, R.J., Jan, L.Y., Lefkowitz, R.J., Hamm, H.E. 1998. Molecular Basis for Interactions of G Protein β Subunits with Effectors. *Science. 280(5367),* 1271-1274.

159. Albsoul-Younes, A.M., Sternweis, P.M., Zhao, P., Nakata, H., Nakajima, S., Nakajima, Y., Kozasa, T. 2001. Interaction sites of the G protein beta subunit with brain G protein-coupled inward rectifier K+ channel. *J. Biol. Chem. 276(16),* 12712-12717.

160. Mirshahi, T., Mittal, V., Zhang, H., Linder, M.E., Logothetis, D.E. 2002. Distinct sites on G protein beta gamma subunits regulate different effector functions. *J. Biol. Chem. 277(39),* 36345-36350.

161. Zhao, Y., Fang, Q., Straub, S.G., Lindau, M., Sharp, G.W. 2010. Noradrenaline inhibits exocytosis via the G protein betagamma subunit and refilling of the readily releasable granule pool via the alpha(i1/2) subunit. *J Physiol. 588(Pt 18),* 3485-3498.

162. Li, X., Hummer, A., Han, J., Xie, M., Melnik-Martinez, K., Moreno, R.L., Buck, M., Mark, M.D., Herlitze, S. 2005. G protein beta2 subunit-derived peptides for inhibition and induction of G protein pathways. Examination of voltage-gated Ca2+ and G protein inwardly rectifying K+ channels. *J. Biol. Chem. 280(25),* 23945-23959.

163. Lei, Q., Jones, M.B., Talley, E.M., Schrier, A.D., McIntire, W.E., Garrison, J.C., Bayliss, D.A. 2000. Activation and inhibition of G protein-coupled inwardly rectifying potassium (Kir3) channels by G protein beta gamma subunits. *Proc. Natl. Acad. Sci. USA. 97(17),* 9771-9776.

164. Lei, Q., Talley, E.M., Bayliss, D.A. 2001. Receptor-mediated inhibition of G protein-coupled inwardly rectifying potassium channels involves Gaq family subunits, phospholipase C, and a readily diffusible messenger. *J. Biol. Chem. 276(20),* 16720-16730.

165. Reuveny, E., Slesinger, P.A., Inglese, J., Morales, J.M., Iniguez-Lluhi, J.A., Lefkowitz, R.J., Bourne, H.R., Jan, Y.N., Jan, L.Y. 1994. Activation of the cloned muscarinic potassium channel by G protein beta gamma subunits. *Nature. 370(6485),* 143-146.

166. Takao, K., Yoshii, M., Kanda, A., Kokubun, S., Nukada, T. 1994. A region of the muscarinic-gated atrial K+ channel critical for activation by G protein beta gamma subunits. *Neuron. 13(3),* 747-755.

167. Wickman, K.D., Iniguez-Lluhl, J.A., Davenport, P.A., Taussig, R., Krapivinsky, G.B., Linder, M.E., Gilman, A.G., Clapham, D.E. 1994. Recombinant G-protein beta gamma-subunits activate the muscarinic-gated atrial potassium channel. *Nature. 368(6468),* 255-257.

168. Yamada, M., Ho, Y.K., Lee, R.H., Kontanill, K., Takahashill, K., Katadall, T., Kurachi, Y. 1994. Muscarinic K+ channels are activated by beta gamma subunits and inhibited by the GDP-bound form of alpha subunit of transducin. *Biochem. Biophys. Res. Commun. 200(3),* 1484-1490.

169. Lei, Q., Jones, M.B., Talley, E.M., Garrison, J.C., Bayliss, D.A. 2003. Molecular mechanisms mediating inhibition of G protein-coupled inwardly-rectifying K+ channels. *Mol. Cells. 15(1),* 1-9.

170. Xie, K., Allen, K.L., Kourrich, S., Colon-Saez, J., Thomas, M.J., Wickman, K., Martemyanov, K.A. 2010. Gbeta5 recruits R7 RGS proteins to GIRK channels to regulate the timing of neuronal inhibitory signaling. *Nat. Neurosci. 13(6),* 661-663.

171. Ladera, C., del Carmen Godino, M., Jose Cabanero, M., Torres, M., Watanabe, M., Lujan, R., Sanchez-Prieto, J. 2008. Pre-synaptic GABA receptors inhibit glutamate release through GIRK channels in rat cerebral cortex. *J. Neurochem. 107(6),* 1506-1517.

172. Lujan, R., Maylie, J., Adelman, J.P. 2009. New sites of action for GIRK and SK channels. *Nat. Rev. Neurosci. 10(7),* 475-480.

173. Michaeli, A., Yaka, R. 2010. Dopamine inhibits GABA(A) currents in ventral tegmental area dopamine neurons via activation of presynaptic G-protein coupled inwardly-rectifying potassium channels. *Neuroscience. 165(4),* 1159-1169.

174. Silinsky, E.M. 1984. On the mechanism by which adenosine receptor activation inhibits the release of acetylcholine from motor nerve endings. *J. Physiol. 346(1),* 243-256.

175. Miller, L.C., Swayne, L.A., Kay, J.G., Feng, Z.-P., Jarvis, S.E., Zamponi, G.W., Braun, J.E.A. 2003. Molecular determinants of cysteine string protein modulation of N-type calcium channels. *Journal of Cell Science. 116(14),* 2967-7294.

176. Meldolesi, J., Huttner, W.B., Tsien, R.Y., Pozzan, T. 1984. Free cytoplasmic Ca2+ and neurotransmitter release: studies on PC12 cells and synaptosomes exposed to alpha-latrotoxin. *Proc. Natl. Acad. Sci. USA. 81(2),* 620-624.

177. Ahnert-Hilger, G., Brautigam, M., Gratzl, M. 1987. Ca2+-stimulated catecholamine release from alpha-toxin-permeabilized PC12 cells: biochemical evidence for exocytosis and its modulation by protein kinase C and G proteins. *Biochemistry. 26(24),* 7842-7848.

178. Knight, D.E., Baker, P.F. 1985. Guanine nucleotides and Ca-dependent exocytosis. Studies on two adrenal cell preparations. *FEBS Lett. 189(2),* 345-349.

179. Luini, A., De Matteis, M.A. 1990. Evidence that the receptor-linked G protein inhibits exocytosis by a post-second messenger mechanism in AtT-20 cells. *J. Neurochem. 54,* 30-38.

180. Kajikawa, Y., Saitoh, N., Takahashi, T. 2001. GTP-binding protein beta gamma subunits mediate presynaptic calcium current inhibition by GABA(B) receptor. *Proc. Natl. Acad. Sci. U S A. 98(14),* 8054-8058.

181. Binz, T., Blasi, J., Yamasaki, S., Baumeister, A., Link, E., Sudhof, T.C., Jahn, R., Niemann, H. 1994. Proteolysis of SNAP-25 by types E and A botulinal neurotoxins. *J. Biol. Chem. 269(3),* 1617-1620.

182. Schiavo, G., Santucci, A., Dasgupta, B.R., Mehta, P.P., Jontes, J., Benfenati, F., Wilson, M.C., Montecucco, C. 1993. Botulinum neurotoxins serotypes A and E cleave SNAP-25 at distinct COOH-terminal peptide bonds. *FEBS Lett. 335(1),* 99-103.

183. Delaney, A.J., Crane, J.W., Sah, P. 2007. Noradrenaline Modulates Transmission at a Central Synapse by a Presynaptic Mechanism. *Neuron. 56(5),* 880-892.

184. Zhang, X.-l., Upreti, C., Stanton, P.K. 2011. Gβγ and the C Terminus of SNAP-25 Are Necessary for Long-Term Depression of Transmitter Release*. PLoS One. 6(5),* e20500.

185. Zhao, Y., Fang, Q., Straub, S.G., Lindau, M., Sharp, G.W. 2010. Noradrenaline inhibits exocytosis via the G protein betagamma subunit and refilling of the readily releasable granule pool via the alpha(i1/2) subunit. *J Physiol. 588(Pt 18),* 3485-3498.

186. Herring, B.E., McMillan, K., Pike, C.M., Marks, J., Fox, A.P., Xie, Z. 2011. Etomidate and propofol inhibit the neurotransmitter release machinery at different sites. *J. Physiol. 589(5),* 1103-1115.

187. Need FORD 1998 here

188. Searl, T.J., Silinsky, E.M. 2005. Modulation of Ca(2+)-dependent and Ca(2+)-independent miniature endplate potentials by phorbol ester and adenosine in frog. British journal of pharmacology. *145(7),* 954-962.

189. Silinsky, E.M. 2008. Selective disruption of the mammalian secretory apparatus enhances or eliminates calcium current modulation in nerve endings. *Proc. Natl. Acad. Sci. USA. 105(17),* 6427-6432.

190. Stanley, E.F., Mirotznik, R.R. 1997. Cleavage of syntaxin prevents G-protein regulation of presynaptic calcium channels. *Nature. 385(6614),* 340-433.

191. Schwartz, E.J., Gerachshenko, T., Alford, S. 2005. 5-HT prolongs ventral root bursting via presynaptic inhibition of synaptic activity during fictive locomotion in lamprey. *J. Neurophysiol. 93(2),* 980-988.

192. Gabriel, J.P., Mahmood, R., Kyriakatos, A., Soll, I., Hauptmann, G., Calabrese, R.L., El Manira, A. 2009. Serotonergic modulation of locomotion in zebrafish: endogenous release and synaptic mechanisms. *J. Neurosci. 29(33),* 10387-10395.

193. Sillar, K.T., Wedderburn, J.F., Simmers, A.J. 1992. Modulation of swimming rhythmicity by 5-hydroxytryptamine during post-embryonic development in Xenopus laevis. *Proc. Biol. Sci. 250(1328),* 107-114.

194. Liu, J., Jordan, L.M. 2005. Stimulation of the Parapyramidal Region of the Neonatal Rat Brain Stem Produces Locomotor-Like Activity Involving Spinal 5-HT7 and 5-HT2A Receptors. *J. Neurophysiol. 94(2),* 1392-1404.

195. Komatsu, M., Schermerhorn, T., Aizawa, T., Sharp, G.W. 1995. Glucose stimulation of insulin release in the absence of extracellular Ca2+ and in the absence of any increase in intracellular Ca2+ in rat pancreatic islets. *Proc. Natl. Acad. Sci. USA. 92(23),* 10728-10732.

196. Iremonger, K.J., Bains, J.S. 2009. Retrograde opioid signaling regulates glutamatergic transmission in the hypothalamus. *J. Neurosci. 29(22),* 7349-7358.

197. Le François, B., Czesak, M., Steubl, D., Albert, P.R. 2008. Transcriptional regulation at a HTR1A polymorphism associated with mental illness. *Neuropharmacology. 55(6),* 977-985.

198. Rosengren, A.H., Jokubka, R., Tojjar, D., Granhall, C., Hansson, O., Li, D.Q., Nagaraj, V., Reinbothe, T.M., Tuncel, J., Eliasson, L., Groop, L., Rorsman, P., Salehi, A., Lyssenko, V., Luthman, H., Renstrom, E. 2010. Overexpression of alpha2A-adrenergic receptors contributes to type 2 diabetes. *Science. 327(5962),* 217-220.

199. Devedjian, J.C., Pujol, A., Cayla, C., George, M., Casellas, A., Paris, H., Bosch, F. 2000. Transgenic mice overexpressing alpha2A-adrenoceptors in pancreatic beta-cells show altered regulation of glucose homeostasis. *Diabetologia. 43(7),* 899-906.

200. Albrecht, C., Bloss, H.G., Jackisch, R., Feuerstein, T.J. 1999. Evaluation of autoreceptor-mediated control of [3H]acetylcholine release in rat and human neocortex. *Exp. Brain Res. 128(3),* 383-389.

201. Arnsten, A., Cai, J., Murphy, B., Goldman-Rakic, P. 1994. Dopamine D1 receptor mechanisms in the cognitive performance of young adult and aged monkeys. Psychopharmacology. *116(2),* 143-151.

202. Breitenstein, C., Korsukewitz, C., Floel, A., Kretzschmar, T., Diederich, K., Knecht, S. 2006. Tonic Dopaminergic Stimulation Impairs Associative Learning in Healthy Subjects. *Neuropsychopharmacology. 31(11),* 2552-2564.

203. Janssen, P.A., Niemegeers, C.J., Awouters, F., Schellekens, K.H., Megens, A.A., Meert, T.F, 1988. Pharmacology of risperidone (R 64 766), a new antipsychotic with serotonin-S2 and dopamine-D2 antagonistic properties. *J. Pharmacol. Exp. Ther. 244(2),* 685-693.

204. Taylor, D.P., Eison, M.S., Riblet, L.A., Vandermaelen, C.P. 1985. Pharmacological and clinical effects of buspirone. *Pharmacol. Biochem. Behav. 23(4),* 687-694.

205. Hunt, R.D., Arnsten, A.F.T., Asbell, M.D. 1995. An Open Trial of Guanfacine in the Treatment of Attention-Deficit Hyperactivity Disorder. *J. Am. Acad. Child Adolesc. Psychiatry. 34(1)*, 50-54.

206. Hamm, H.E. 1998 The many faces of G protein signaling. *J. Biol. Chem. 273(2),*669-672.

207. Tang, W.J. and Gilman, A.G. 1991 Type-specific regulation of adenylyl cylcase by G proten beta gamma subunits. *Science 254,* 1500-1503.

208. Myung, C.S., Yasuda, H., Liu, W.W., Harden, T.K., and Garrison, J.C. 1999 Role of isoprenoid lipids on the heterotrimeric G protein g subunit in determining effector activation*. J. Biol. Chem. 274,* 16595-16603.

209. Vanderbeld, B. and Kelly, G.M. 2000 New thoughts on the role of the beta-gamma subunit in G-protein signal transduction. *Biochem. Cell Biol. 78,* 537-550.

210. Goldsmith, Z.G. and Dhanasekaran, D.N. 2007 G protein regulation of MAPK networks. *Oncogene, 26(22),* 3122-3142.

211. McIntire, W.E., MacCleery, G., and Garrison, J.C. 2001 The G protein beta subunit is a determinant in the coupling of Gs to the beta 1-adrenergic and A2a adenosine receptors. *J. Biol. Chem., 276(19),* 15801-15809.

212. Kerchner, K.R., Clay, R.L., McCleery, G., Watson, N., McIntire, W.E., Myung, C.S., and Garrison, J.C. 2004 Differential sensitivity of phosphatidylinositol 3-kinase p110gamma to isoforms of G protein betagamma dimers. *J. Biol. Chem.,279(43),* 44554-44562.

213. Kleuss, C., Hescheler, J., Ewel, C., Rosenthal, W., Schultz, G., and Wittig, B. 1991 Assignment of G-protein subtypes to specific receptors inducing inhibition of calcium currents. *Nature, 353,* 43-48.

214. Kleuss, C., Scherübl, H., Hescheler, J., Schultz, G., and Wittig, B. 1992 Different β subunits determine G-protein interaction with transmembrane receptors. *Nature, 358,*424-426.

215. Wang Q., Mullah, B.K., and Robishaw, J.D. 1999 Ribozyme approach identifies a functional association between the G protein $\beta_1\gamma_7$ subunits in the b-adrenergic receptor signaling pathway. *The Journal of Biological Chemistry 274(24),* 17365-17371.

216. Schwindinger, W.F., Mirshahi, U.L., Baylor, K.A., Sheridan, K.M., Stauffer, A.M., Usefof, S., Stecker, M.M., Mirshahi, T., and Robishaw, J.D. 2012 Synergistic roles for G-protein

γ_3 and γ_7 in seizure susceptibility as revealed in double knockout mice. *J. Biol. Chem. 287(10),* 7121-7133.

217. Fisher, K.J. and Aronson Jr., N.N. 1992 Characterization of the cDNA and genomic sequence of a G protein gamma subunit (gamma 5). *Molecular and Celullar Biology.12(4),* 1585-1591.

218. Gautam, N., Northup, J., Tamir, H., and Simon, M.I. 1990 G protein diversity is increased by associations with a variety of γ subunits. *Proc Natl. Acad. Sci. USA.87*, 7973-7977.

219. Kalyanaraman, S., Kalyanaraman, V., and Gautam, N. 1995 A brain-specific G protein gamma subunit. *Biochemical and Biophysical Research Communications. 216(1),* 126-132.

220. Morishita, R., Fukada, Y., Kokame, K., Yoshizawa, T., Masuda, K., Niwa, M., Kato,K., and Asano, T. 1992 Identification and isolation of common and tissue specific geranylgeranylated γ subunits of guanine-nucleotide binding regulatory proteins in various tissues. *Eur. J. Biochem. 210*, 1061-1069.

221. Watson, A.J., Katz, A., and Simon, M.I. 1994 A fifth member of the mammalian G protein β-subunit family. Expression in brain and activation of the β_2 isotype of Phospholipase C. *The Journal of Biological Chemistry, 269(35),* 22150-22156.

222. Weizsäcker E.V., Strathmann, M.P., and Simon, M.I. 1992 Diversity among the beta subunits of heterotrimeric GTP-binding proteins: characterization of a novel beta subunit cDNA. *Biochemical and Biophysical Research Communications, 183(1),* 350-356.

223. Cali, J.J., Baleueva, E.A., Rybalkin, I., and Robishaw, J.D. 1992 Selective tissuedistribution of G protein γ subunits, including a new form of the γ subunits identified by cDNA cloning. *The Journal of Biological Chemistry 267(33),* 24023-24027.

224. Jones, P.G., Lombardi, S.J., and Cockett, M.I. 1998 Cloning and tissue distribution of the human G protein β_5 cDNA. *Biochimica et Biophsica Acta. 1402,* 288-291.

225. Largent, B.L., Jones, D.T., Reed, R.R., Pearson, C.A., and Snyder, S.H. 1988 G protein mRNA mapped in rat brain by in situ hybridization. *Proc. Natl. Acad. Sci. USA. 85,* 2864-2868.

226. Liang, J-J., Cockett, M., and Khawaja, X.Z. 1998 Immunohistochemical localization of G protein β_1, β_2, β_3, β_4, β_5, and γ_3 subunits in the adult rat brain. *Journal of Neurochemistry 71,* 345-355.

227. Zhang, J-H., Lai, Z., and Simonds, W. 2000 Differential expression of the G protein β_5 gene: analysis of mouse brain, peripheral tissues, and cultured cell lines. *Journal of Neurochemistry 75,* 393-403.

228. Morishita, R., Ueda, H., Kato, K., and Asano, T. 1998 Identification of two forms of the γ subunit of G protein, γ_{10} and γ_{11}, in bovine lung and their tissue distribution in the rat. *FEBS Letters 428,* 85-88.

229. Robishaw, J.D., Kalman, V.K., Moomaw, C.R., and Slaughter, C.A. 1989 Existence of two γ subunits of the G proteins in brain. *The Journal of Biological Chemistry 264(27),* 15758-15761.

230. Bigler Wang, D., Shermann, N.E., Shannon, J.D., Leonhardt, S.A., Mayeenuddin, L.H., Yeager, M., and McIntire, W.E. 2011 Binding of b_4g_5 by Adenosine A_1 and A_{2A} receptors determined by stable isotope labeling with amino acids in cell culture and mass spectrometry. *Biochemistry 50,* 207-220.

231. Bai, F. and Witzmann, F. A. 2007 Synaptosome Proteomics. *Subcell Biochem. 43,* 77-98.

232. Boyd-Kimball, D., Castegna, A., Sultana, R., Poon, H.F., Petroze, R., Lynn, B.C., Klein, J.B.,and Butterfield, D.A. 2005 Proteomic identification of proteins oxidized by Ab(1-42) in synaptosomes: Implications for Alzheimer's Disease. *Brain Research 1044,* 206-215.

233. Burré, J. and Volknandt, W. 2007 The synaptic vesicle proteome. *Journal of Neurochemistry 101,* 1448-1462.

235. Fountoulaki, M. 2004 Application of proteomics technologies in the investigation of the brain. *Mass Spectrometry Reviews 23,* 231-258.

236. Li, K.W., Hornshaw, M.P., Van der Schors, R.C., Watson, R., Tate, S., Casetta, B., Jimenez, C.R., Gouwenberg, Y., Gundelfinger, E.D., Smalla, K-H., and Smit,A.B. 2004 Proteomics analysis of rat brain postsynaptic density. *The Journal of Biological Chemistry 279(2),* 987-1002.

237. Liberatori, S., Canas, B., Tani, C., Bini, L., Buonocore, G., Godovac-Zimmermann, J., Mishra, O.P., Delivoria-Papadopoulos, M., Bracci, R., and Pallini, V. 2004 Proteomic approach to the identification of voltage-dependent anion channel protein isoforms in guinea pig brain synaptosomes. *Proteomics 4,* 1335-1340.

238. Mallei, A., Giambelli, R., Gass, P., Racagni, G., Mathé, A.A., Vollmayr, B., and Popoli, M. 2011 Synaptoproteomics of learned helpless rats involve energymetabolism and cellular remodeling pathways in depressive-like behavior and antidepressant response. *Neuropharmacology 60,* 1243-1253.

239. Stasyk, T. and Huber, L.A. 2004 Zooming in: fractionation strategies in proteomics. *Proteomics 4,* 3704-3716.

240. Witzmann, F.A., Arnold, R.J., Bai, F., Hrncirova, P., Kimpei, M.W., Mechref, Y.S., McBride, W.J., Novotny, M.V., Pedrick, N.M., Ringham, H.N., and Simon, J.R. 2005 A proteomic survey of rat cerebral cortical synaptosomes. *Proteomics 5,* 2177-2201.

241. Gylys, K.H., Fein, J.A., Yang, F., Wiley, D. J., Miller, C.A., and Cole, G.M. 2004 Synaptic changes in Alzheimer's Disease – increased amyloid-β and gliosis in surviving terminal is accompanied by decreased PSD-95 fluorescence. *Neurobiology 165(5),* 1809-1817.

242. Morciano, M., Burré, J., Corvey, C., Karas, M., Zimmermann, H., and Volknandt, W. 2005 Immunoisolation of two synaptic vesicle pools from synaptosomes: a proteomic analysis. *Journal of Neurochemistry 95,* 1732-1745.

243. Morciano, M., Beckhaus, T., Karas, M., Zimmermann, H., and Volknandt, W. 2009 The proteome of the presynaptic active zone: from docked synaptic vesicles to adhesion molecules and maxi-channels. *Journal of Neurochemistry 108,* 662-667.

244. Satoh, K., Takeuchi, M., Oda, Y., Deguchi-Tawarada, M., Sakamato, Y., Matsubara, K., Nagasu, Y., and Takai, Y. 2002 Identification of activity-regulated proteins in the postsynaptic density fraction. *Genes to Cells 7,* 187-197.

245. Volknandt, W. and Karas, M. 2012 Proteomic analysis of the presynaptic active zone. *Exp. Brain Res. 217,* 449-461.

246. Boja, E.S. and Rodriguez, H. 2012 Mass spectrometry-based targeted quantitative proteomics: achieving sensitive and reproducible detection of proteins. *Proteomics 12(8),* 1093-1100.

247. Shi, T., Su, D., Liu, T., Tang, K., Camp, D.G. 2nd, Qian, W.J., and Smith, R.D. 2012 Advancing the sensitivity of selected reaction monitoring-based targeted quantitative proeomics. *Proteomics 12(8),* 1074-1092.

248. Mazzoni MR, Malinski JA and Hamm HE (1991) Structural analysis of rod GTP binding protein, Gt. Limited proteolytic digestion pattern of Gt with four proteases defines monoclonal antibody epitope. *J Biol Chem 266(21),* 14072-14081.

249. Phillips, G.R., Huang, J.K., Wang, Y., Tanaka, H., Shapiro, L., Zhang, Q., Shan, W., Arndt, K., Frank, M., Gordon, R.E., Gawinowicz, A., Zhao, Y., and Colman, D.R. 2001 The presynaptic particle web: ultrastructure, composition, dissolution, and reconstitution, *Neuron 32,* 63-77.

250. Eng, J.K., McCormack, A.L., Yates, I. and John, R. 1994 An approach to correlate tandem mass spectral data of peptides with amino acid sequenes in a protein database. *J. Am. Soc. Mass Spectrom. 5*, 976-989.

251. MacLean, B., Tomazela, D.M., Shulman, N., Chambers, M., Finney, G.L., Frewan, B., Kern, R., Tabb, D.L., Liebler, D.C., MacCoss, M.J. (2010) Skyline: an open source document editor for creating and analyzing targeted proteomics experiments. *Bioinformatics 26(7):* 966-968.

252. Zhang, H., Lio, Q., Zimmerman, L.J., Ham, A-J, L., Slebos, R.J.C., Rahman, J., Kikuchi, T., Massion, P.P., Carbone, D.P., Billheimer, D., and Liebler, D.C. 2011 Methods for peptide

and protein quantitation by liquid chromatography multiple reaction monitoring mass spectrometry. *Molecular and Cellular Proteomics 10(6),* M110.006593.

253. Tobin, V., Schwab, Y., Lelos, N., Onaka, T., Pittman, Q.J., and Ludwig, M. 2012 Expression of exocytosis proteins in rat supraoptic nucleus neurones. *J.Neuroendrocinol. 24(4),* 629-641.

254. Daimon, M., Sato, H., Kain, W., Tada, K., Takase, K., Karasawa, S., Wada, K., Kameda, W., Susa, S., Oizumi, T., Kayama, T., Muramatsu, M., and Kato, T. 2013 Association of the G-protein β_3 subunit gene polymorphism with the incidence of cardiovascular disease independent of hypertension: the Funagata study. *Journal of Human Hypertension 27,* 612-616.

255. Ryba, N.J.P. and Tirindelli, R. (1995) A novel GTP-binding protein g-subunit, $G\gamma_8$, is expressed during neurogenesis in the olfactory and vomeronasal neuroepithelia. *Journal of Biological Chemistry 270(12),* 6757-6767.

256. Hurley, J.B., Fong, H.K.W., Teplow, D.B., Dreyer, W.J., and Simon, M.I. 1984 Isolation and characterization of a cDNA clone for the gamma subunit of bovine retinal transducin. *Proc. Natl. Acad. Sci. USA 81,* 6948-6952.

257. Kilpatrick, E.L. and Hildebrandt, J.D. 2007 Sequence dependence and differential expression of $G\gamma_5$ subunit isoforms of the heterotrimeric G proteins variably processed after prenylation in mammalian cells. *Journal of Biological Chemistry 282(19),* 14038-14047.

258. Kirkpatrick, D.S., Gerber, S.A., and Gygi, S.P. 2005 The absolute quantification strategy: a general procedure for the quantification of proteins and post translational modificiations. *Methods 35,* 265-273.

259. Stehno-Bittel, L., Krapivinsky, G., Krapivinsky, L., Perez-Terzic, C., and Clapham, D.E. (1995) The G protein $\beta\gamma$ subunit transduces the muscarinic receptor signal for Ca^{2+} release in xenopus oocytes. *The Journal of Biological Chemistry 270(50),* 30068-30074.

260. Lindorfer, M.A., Myung, C.S., Savino, Y., Yasuda, H., Khazan, R., Garrison, J.C. 1998 Differential activity of the G protein beta5 gamma2 subunit at receptors and effectors. *J. Biol. Chem. 273(51),* 34429-34436.

261. Lim, W.K., Myung, C.S., Garrison, J.C., Neubig, R.R. 2001 Receptor-G protein gamma specificity: gamma11 shows unique potency for A(1) adenosine and 5HT(1A) receptors. *Biochemistry 40(35),* 10532-10541.

262. Albert, P.R. and Robillard, L. 2002 G protein specificity: traffic direction required. *Cellular Signalling 14,* 407-418.

263. Okae. I, and Iwakura, Y. 2010 Neural tube defects and impaired neural progenitor cell proliferation in Gbeta1-deficient mice. *Developmental Dynamics 239,* 1089-1101.

264. Schwindinger,W.F., Borrell, B.M., Waldman, L.C., and Robishaw, J.D. 2009 Mice lacking the G protein γ_3-subunit show resistance to opioids and diet induced obesity. *American Journal of Physiology – Regulatory, Integrative, and Comparative Physiology 297,* R1494-R1502.

265. Dippel, E., Kalkbrenner, F., Wittig, B., and Schultz, G. 1996 A heterotrimeric G protein complex couples the muscarinic m1 receptor to phospholipase C-β. *PNAS 93,* 1391-1396.

266. Mahmoud, S., Yun, J.K. and Ruiz-Velasco, V. 2012 Gβ_2 and Gβ_4 participate in the opioid and adrenergic receptor-mediated Ca^{2+} channel modulation in rat sympathetic neurons. *The Journal of Physiology 590.19,* 4673-4689.

267. Zachariou, V., Georgescu, D., Sanchez, N., Rahman, Z., DeLeone, R., Berton, O., Neve, R.L., Sim-Selley, L.J., Selley, D.E., Gold, S.J., and Nestler, E.J. 2003 Essential role for RGS9 in opiate action. *J. Neurosci. 29:* 13656-13661.

268. López-Fando, A., Rodríguez-Muñoz, M., Sánchez-Blázquez, P., and Garzón, J. 2005 Expression of neural RGS-R7 and Gβ_5 proteins in response to acute and chronic morphine. *Neuropsychopharmacology 30*, 99-110.

269. Anderson, G.R., Cao, Y., Davidson, S., Truong, H.V., Pravetoni, M., Thomas, M.J., Wickman, K., Giesler, G.J., and Martemyanov, K.A. 2010 R7BP complexes with RGS9-2 and RGS7 in the striatum differentially control motor learning and locomotor responses to cocaine. *Neuropsychopharmacology 35*, 1040-1050.

270. Psifogeorgou, K., Terzi, D., Papachatzaki, M.M., Varidaki, A., Ferguson, D., Gold, S.J., and Zhachariou, V. 2011 A unique role of RGS9-2 in the striatum as a positive or negative regulator of opiate analgesia. *The Journal of Neuroscience 31(15),* 5617-5624.

271. Mashuho I., Xie, K., and Martemyanov, K.A. 2013 Macromolecular composition dictates receptor and G protein selectivity of regulator of G protein signaling (RGS) 7 and 9-2 protein complexes in living cells. *The Journal of Biological Chemistry 288,* 25129-25142.

272. Gold, S.J., Ni, Y.G., Dohlman, H.G., and Nestler, E.J. 1997 Regulators of G protein signaling (RGS) proteins: region specific expression of nine subtypes in rat brain. *J. Neurosci 17,* 8024-8037.

273. Anderson, G.R., Lujan, R., Semenov, A., Pravetoni, M., Posokhova, E.N., Song, J.H., Uversky, V., Chen, C-K., Wickman, K., and Martemyanov, K.R. 2007 Expression and localization of RGS9-2/Gβ_5/R7BP complex *in vivo* is set by dynamic control of its constitutive degradation by cellular cysteine proteases. *The Journal of Neuroscience 27(51),* 14117-14127.

274. Anderson, G.R., Lujan, R., and Martemyanov, K.R. (2009) Changes in striatal signaling induce remodeling of RGS complexes containing Gβ_5 and R7BP subunits. *Molecular and Cellular Biology 29(11),* 3033-3044.

275. Song, J.H., Waataja, J.J., and Martemyanov, K.A. 2006 Subcellular targeting of RGS9-2 is controlled by multiple molecular determinants on its membrane anchor, R7BP. *The Journal of Biological Chemistry 281,* 15361-15369.

276. Cook, L.A., Schey, K.L., Wilcox, M.D., Dingus, J., Ettling, R., Nelson, T., Knapp, D.R., and Hildebrandt, J.D. 2006 Proteomic analysis of bovine G protein gamma sub*unit processing heterogeneity. Mol. Cell. Proteomics 5(4),* 671-685.

277. Kelley, A.E., Bakshi, *V.P.,* Haber, S.N., Steininger, T.L., Will, M.J., and Zhang, M. 2002 Opioid modulation of taste hedonics within the ventral striatum. *Physiology and Behavior 76(3),* 365-377.

278. Ward, H.G., Nicklous, D.M., Aloyo, V.J., and Simansky, K.J. 2006 Mu-opioid receptor cellular function in the nucleus accumbens is essential for hedonically driven eating. *European Journal of Neuroscience 23,* 1605-1613.

279. Brudege, J.M. and Williams, J.T. 2002 Differential modulation of nucleus accumbens synapses. *Journal of Neurophysiology 88(1),* 142-151.

280. Schwindinger, W.F., Betz, K.S., Giger, K.E., Sabol, A., Bronson, S.K., and Robishaw, J.D. 2003 Loss of G protein γ_7 alters behavior and reduces striatal α_{olf} level and cAMP production. *The Journal of Biological Chemistry 278(8),* 6575-6579.

281. Schwindinger, W.F., Mihalcik, L.J.M., Giger, K.E., Betz, K.S., Stauffer, A.M. Linden, J., Herve, D., and Robishaw, J.D. 2010 Adenosine A_{2A} receptor signaling and G_{olf} assembly show a specific requirement for the g_7 subtype in the striatum. *The Journal of Biological Chemistry 285(39),* 29787-29796.

282. Watson, J.B., Coulter, P.M. 2nd., Marguiles, J.E., de Lecea, L., Danielson, P.E., Erlander, M.G., and Sutcliffe, J.G. 1994 G-protein gamma 7 subunit is selectively expressed in medium-sized neurons and dendrites of the rat neostriatum. *Journal of Neuroscience Research 39(1),* 108-116.

283. Caillé, I., Dumartin, B., and Bloch, B. 1996 Ultrastructural localization of D1 dopamine reactivity in rat striatonigral neurons and its relation with dopamine innervation. *Brain Research 730,* 17-31.

284. Hettinger, B.D., Lee, A., Linden, J., and Rosin, D.L. (2001) Ultrastructural localization of Adenosine A_{2A} receptors suggests multiple cellular sites for modulation of GABAergic neurons in rat striatum. *The Journal of Comparative Neurology 431,* 331-346.

285. Kalkbrenner, F., Degtiar, V.E., Schenker, M., Brendal, S., Zobel, A., Heschler, J.,Wittig, B., and Schultz, G. 1995 Subunit composition of G_o proteins functionally coupling galanin receptors to voltage-gated calcium channels. *The EMBO Journal 14(19),* 4728-4737.

286. Hosohata, K., Logan, J.K., Varga, E., Burkey, T.H., Vanderah, T.W., Porreca, F. Hruby, V.J., Roeske, W.R., and Yamamura, H.I. 2000) The role of the G protein γ_2 subunit in opioid antinociception in mice. *European Journal of Pharmacology 392,* R9-R11.

287. Varga, E.V., Hosohata, K., Borys, D., Navratilova, E., Nylen, A., Vanderah, T.W., Porreca, F., Roeske, W.R., Yamamura, H.I. 2005 Antinociception depends on the presence of G protein γ_2-subunits in brain. *European Journal of Pharmacology 508,* 93-98.

288. Mitsukawa, K., Lu, X., and Bartfai, T. 2010 Galanin, galanin receptors, and drug targets. *Experientia Supplementum 102,* 7-23.

289. Kitchen, I., Slowe, S.J., Matthes, H., and Kieffer, B. 1997 Quantitative autoradiographic mapping of mu-, delta-, and kappa-opioid receptors in knockout mice lacking the mu-opioid receptor gene. *Brain Research 778,* 73-88.

290. Slowe, S.J., Simonin, F., Kieffer, B., and Kitchen, I. 1999 Quantitative autoradiography of mu-, delta-, and kappa-opioid receptors in kappa-opioid receptor knockout mice. *Brain Research 818,* 335-345.

291. Goody, R.J., Oakley, S.M., Filliol, D., Kieffer, B., and Kitchen, I. 2002 Quantitative autoradiographic mapping of opioid receptors in the brain of delta opioid receptor gene knockout mice. *Brain Research 945,* 9-19.

292. Huang, L., Shanker, Y.G., Dubauskaite, J., Zheng, J.Z., Yan, W., Rosenzweig, S., Spielman A.I., Max, M., and Margolskee, R.F. 1999 Ggamma13 colocalizes with gustducin in taste receptor cells and mediates IP3 responses to bitter denatonium. *Nature Neuroscience 2,* 1055-1062.

293. Blake, B.L., Wing, M.R., Zhou, J.Y., Lei, Q., Hillmann, J.R., Behe, C.I., Morris, R.A., Harden, T.K., Bayliss, D.A., Miller, R.J., and Siderovski, D.P. (2001) Gβ association and effector interaction selectivities of the divergent Gγ subunit Gγ_{13}. *The Journal of Biological Chemistry 276(52),* 49267-49274.

294. Fujino, A., Pieretti-Vanmarcke, R., Wong, A., Donahoe, P.K., and Arango, N.A. 2007 Sexual dimorphism of G-protein subunit *Gng13* expression in the cortical region of the developing mouse ovary. *Developmental Dynamics 236,* 1991-1996.

295. Li, Z., Benard, O., and Margolskee, R.F. 2006 Gγ_{13} interacts with PDZ domain containing proteins. *The Journal of Biological Chemistry 81(16),* 11066-11073.

296. Huang, Q., Zhou, D., Chase, K., Gusella, J.F., Aronin, N., and DiFiglia, M. 1992 Immunohistochemical localization of the D1 dopamine receptor in rat brain reveals its axonal transport, pre- and postsynaptic localization, and prevalence in the basal ganglia, limbic system, and thalamic reticular neurons. *Proc. Natl., Acad. Sci. USA. 89,* 11988-11992.

297. Kreitzer, A.C. and Malenka, R.C. 2008 Striatal plasticity and basal ganglia circuit function. *Neuron 60(4)*, 543-554.

298. Prange-Kiel, J. and Rune, G.M. 2006 Direct and indirect effects of estrogen on rat hippocampus. *Neuroscience 138(3),* 765-772.

299. Leranth, C. and Hajszan, T. 2007 Extrinsic afferent systems to the dentate gyrus. *Prog. Brain Res.* 163, 63-84.

300. Harley, C. 2007 Norepinephrine and the dentate gyrus. *Progress in Brain Research 163,* 299-318.

301. Schliebs, R. and Arendt, T. 2011 The cholinergic system in aging and neurona degeneration. *Behavioural Brain Research 221(2),* 555-563.

302. Cesa, R. and Strata, P. 2009 Axonal competition in the synaptic wiring of the cerebellar cortex during development and in the mature cerebellum. *Neuroscience Research 163,*299-318.

303. Hein, L., Altman, J.D., and Kobilka, B.K. 1999 Two functionally disctinct a_2-adrenergic receptors regulate sympathetic neurotransmission. *Nature 402, 181-184.*

304. Gilsbach, R., Roser, C., Beetz, N., Brede, M., Hadamek, K., Haubold, M., Leemhuis, J., Philipp, M., Schneider, J., Urbanski, M. et al. 2009 Genetic dissection of a_2 adrenoceptor functions in adrenergic vs non-adrenergic cells. *Molecular Pharmacology 75, 160-170.*

305. Michaeli, A., Yaka, R. 2010. Dopamine inhibits GABA(A) currents in ventral tegmental area dopamine neurons via activation of presynaptic G-protein coupled inwardly-rectifying potassium channels. *Neuroscience, 1159-1169.*

306. Scholz, K.P. and R.J. Miller. 1992. Inhibition of quantal transmitter release in the absence of calcium influx by a G protein linked adenosine receptor at hippocampal synapses, *Neuron 8,* 1139-1150.

307. Scanziani, M., B.H. Gahwiler, and S.M. Thompsom 1995. Presynaptic inhibition of excitatory synaptic transmission by muscarinic and metabotropic glutamate receptor activation in the hippcampus: are Ca2+ channels involved? *Neuropharmacology**, 34,***

308. Gereau, R.W.T. and P.J. Conn. 1995. Multiple presynatic metabotropic glutamate recptors modulate excitatory and inhibitory synaptic transmission in hippocampal area C1. *Journal of Neuroscience 15,*6879-6889.

309. Fasshauer, D. 2003. Structural insights into the SNARE mechanism. *Biochim Biophys Acta 1641(2-3),* 87-97.

310. Lim, W.K., Myung, C.S., Garrison, J.C., and Neubig, R.R. 2001. Receptor-G protein gamma specificity: gamma11 shows uniqute potency for A(1) adenosine and 5-HT(1A) receptors. *Biochemistry, 40(35),* 10532-10541.

311. Moon, A.M., Stauffer, A.M., Schwindinger, W.F., Sheridan, K., Firment, A., and Robishaw, J.D. 2014. Disruption of **G-protein γ**5 subtype causes embryonic lethality in mice. *PLoS*

One. 9(3), e90970

312. Zhang, J.H., Pandey, M., Seigneur, E.M., Panicker, L.M., Koo, L., Schwartz, O.M., Chen, W., Chen, C-K., and Simonds, W.F. 2011. Knockout of G protein β5 impairs brain development and causes multiple neurologic abnormalities in mice. *Journal of Neurochemistry 119,* 544-554

313. Philipp, M., Brede, M. and Hein, L. 2002 Physiological significance of alpha(2)-adrenergic receptor subtype diversity: one receptor is not enough. *Am J Physiol Regul Integr Comp Physiol. 283*, R287-295.

314. Philipp, M. and Hein, L. 2004 Adrenergic receptor knockout mice: distinct functions of 9 receptor subtypes. *Pharmacol Ther*. *101*, 65-74

315. Gribble, F.M. 2010 Alpha2A-adrenergic receptors and type 2 diabetes. *New Engl. J. Med. 362,* 361-362.

316. Comings, D.E., Johnson, J.P., Gonzalez, N.S., Huss, M., Saucier, G., McGue, M., MacMurray, J. (2000) Association between the adrenergic alpha 2A receptor gene (ADRA2A) and measures of irritability, hostility, impulsivity, and memory in normal subjects. *Psychiatr. Genet. 10, 39-42.*

317. Wakeno, M., Kato., M., Okugawa, G., Fukuda, T., Hosoi, B., Takekita, Y., Yamashita, M., Nonen, S., Azuma, J., and Kinoshita, T. 2008 The alpha 2A-adrenergic receptor gene polymorphism modifies antidepressant responses to milnacopran. *Journal of Clinical Psychopharmacology 28(5), 518-524.*

318. Davies, M.F., Tsui, J.Y., Flannery, J.D., Li, X., DeLorey, T.M., and Hoffman, B.B. 2003 Augmentation of the noradrenergic system in alpha-2 adrenergic receptor deficient mice: anatomical changes associated wtih enhanced fear memory. *Brain Research, 986, 157-165.*

319. Marrs, W., Kuperman, J., Avedian, T., Roth, R.H., and Jentsch, J.D. 2005 Alpha-2 adrenoceptor activation inhibits phencyclidine-induced deficits of spatial working memory in rats. *Neuropsychopharmacology 30, 1500-1510.*

320. Robishaw, J.D., and Berlot, C.H. 2004 Translating G protein subunit diversity into functional specificity. *Current Opinions in Cell Biology, 16, 204-209.*

321. Berridgea, C.W. and Waterhouse, B.D. 2003 The locus coeruleus-noradrenergic system: modulation of behavioral state and state-dependent cognitive processes, *Brain Research Reviews 42,* 33-84.

322. Itoi, K. and Sugimoto, N. 2010. The brainstem noradrenergic systems in stress, anxiety, and depression. *Journal of Neuroendocrinology 22,* 355-361.

323. Chamberlain, S.R. and Robbins, T.W. 2013. Noradrengeric modulatoin of cognition: therapeutic implications. *Journal of Psychopharmacology 27(8),* 695-718.

324. Szabadi, E. 2013. Functional neuroanatomry of the central noradrenergic system. *Journal of Psychopharmacology 27(8),* 659-693.

325. Gobert, A., Billiras, R., Cistarelli, L., and Millan, M.J. 2004 Quantification and pharmacological characterization of dialysate levels of noradrenaline in the striatum of freely-moving rats: release from adrenergic terminals and modulation by α2 autoreceptors. *Journal of Neuroscience Methods 140,* 140-152.

326. Richter, H., Teixeira, F.M., Ferreira, S.G., Kittel, A., Kofalvi, A., Sperlagh, B. 2012. Presynaptic α2-adrenoceptors control the inhibitory action of presynaptic CB1 cannabinoid receptors on prefrontal norepinephrine release in the rat. *Neuropharmacology 63(5),* 784-797.

327. Norenberg, A.P., Schoffel, E., Szabo, B., and Starke, K. 1997. Subtype determination of soma-dendritic α2-adrenoceptors in slices of rat locus coeruleus. *Naunyn-Schmiedeberg's Arch. Pharmacol. 356,* 159-165.

328. Mateo, Y. and Meana, J.J. 1999. Determination of the somatodendritic a2-adrenoceptor subtype located in rat locus coeruleus that modulates cortical noradrenaline release in vivo. *Eur. J. Pharmacol 379,* 53-57.

329. Cotecchia, S., Kobilka, B.K., Daniel. K.W., Nolan, R.D., Lapetina, E.Y., Caron, M.G., Lefkowitz, R.J., and Regan, J.W. 1990. *J. Biol. Chem 256,* 63-69.

330. Fraser, C.N., Arakawa, S., McCombie, W.R., and Venter, J.C. 1989. *J. Biol. Chem. 264,* 11754-11761.

331. Eason, M.G., Kurose, H., Holt, B.D., Raymond, J.R., and Liggett, S.B. 1992. *J. Biol. Chem. 267,* 15795-15801.

332. Chabre, O., Conklin, B.R., Brandon, S., Bourne, H.R., and Limbid, L.E. 1994. Coupling of the α_{2A}-adrenergic receptor to multiple G proteins. *The Journal of Biological Chemistry 269(8),* 5730-5734.

333. Gibson, S.K., and Gilman, A.G. 2006. Gαi and Gβ subunits both define selectivity of G protein activation by α2-adrenergic receptors. *PNAS 103(1),* 212-217.

334. Albarran-Juarez, J., Gilsbach, R., Piekorz, R.P., Pexa, K., Beetz, N., Schneider, J., Nurnberg, B., Birnbaumer, L., and Hein, L. 2009. Modulation of α2-adrenceptor functions by heterotrimerica Gαi protein isoforms. *The Journal of Pharamcolgoy and Experimental Therapeutics 331(1),* 35-44.

335. Richardon, M. and Robishaw, J.D. 1999. The α_{2A}-adreneric receptor discriminates between Gi heterotrimers of different $\beta\gamma$ subunit composition in Sf9 insect cell membranes. *The Journal of Biological Chemistry 274(19),* 13525-13533.

336. Nobles, M., Benians, A., and Tinker, A. 2005. Heterotrimeric G proteins precouple with G protein-coupled receptors in living cells. *Proc, Natl. Acad. Sci. USA 102(51),* 18706-18711.

337. Straiker, A. J., Borden, C. R., and Sullivan, J. M. 2002 G-Protein α Subunit Isoforms Couple Differentially to Receptors that Mediate Presynaptic Inhibition at Rat Hippocampal Synapses *J. Neurosci.* 22, 2460–2468.

338. Cooper, M. 2003 Label-free screening of bio-molecular interactions *Anal. Bioanal. Chem. 377,* 834– 842

339. Shiau, A. K., Massari, M. E., and Ozbal, C. C. 2008 Back to basics: label-free technologies for small molecule screening *Combinatorial Chem. High Throughput Screening 11*, 231–237.

340. Cooper, M. A. 2006 Optical biosensors: where next and how soon? *Drug Discovery Today 11*, 1061–1067.

341. Fang, Y. 2011 Label-Free Biosensors for Cell Biology *Int. J. Electrochem.*10.4061/2011/460850

342. Lavieri, R., Scott, S. A., Lewis, J. A., Selvy, P. E., Armstrong, M. D., Alex Brown, H., and Lindsley, C. W. 2009 Design and synthesis of isoform-selective phospholipase D (PLD) inhibitors. Part II. Identification of the 1,3,8-triazaspiro[4,5]decan-4-one privileged structure that engenders PLD2 selectivity *Bioorg. Med. Chem. Lett. 19,* 2240–2243

343. Lavieri, R. R., Scott, S. A., Selvy, P. E., Kim, K., Jadhav, S., Morrison, R. D., Daniels, J. S., Brown, H. A., and Lindsley, C. W. 2010 Design, synthesis, and biological evaluation of halogenated N-(2-(4-oxo-1-phenyl-1,3,8-triazaspiro[4.5]decan-8-yl)ethyl)benzamides: discovery of an isoform-selective small molecule phospholipase D2 inhibitor *J. Med. Chem. 53,* 6706– 6719

344. Lewis, J. A., Scott, S. A., Lavieri, R., Buck, J. R., Selvy, P. E., Stoops, S. L., Armstrong, M. D., Brown, H. A., and Lindsley, C. W. 2009 Design and synthesis of isoform-selective phospholipase D (PLD) inhibitors. Part I: Impact of alternative halogenated privileged structures for PLD1 specificity *Bioorg. Med. Chem. Lett. 19*, 1916– 1920

345. Lindsley, C. W., Zhao, Z., Leister, W. H., Robinson, R. G., Barnett, S. F., Defeo-Jones, D., Jones, R. E., Hartman, G. D., Huff, J. R., Huber, H. E., and Duggan, M. E. 2005 Allosteric Akt (PKB) inhibitors: discovery and SAR of isozyme selective inhibitors *Bioorg. Med. Chem. Lett. 15*, 761– 764

346. Scott, S. A., Selvy, P. E., Buck, J. R., Cho, H. P., Criswell, T. L., Thomas, A. L., Armstrong, M. D., Arteaga, C. L., Lindsley, C. W., and Brown, H. A. 2009 Design of isoform-selective

phospholipase D inhibitors that modulate cancer cell invasiveness *Nat. Chem. Biol*. 5, 108– 117

347. Zhao, Z., Leister, W. H., Robinson, R. G., Barnett, S. F., Defeo-Jones, D., Jones, R. E., Hartman, G. D., Huff, J. R., Huber, H. E., Duggan, M. E., and Lindsley, C. W. 2005 Discovery of 2,3,5-trisubstituted pyridine derivatives as potent Akt1 and Akt2 dual inhibitors *Bioorg. Med. Chem. Lett. 15*, 905– 909

348. Arkin, M. R. and Wells, J. A. 2004 Small-molecule inhibitors of protein-protein interactions: progressing towards the dream *Nat. Rev. Drug Discovery* 3, 301– 317

349. Blazer, L. L. and Neubig, R. R. 2009 Small molecule protein-protein interaction inhibitors as CNS therapeutic agents: current progress and future hurdles *Neuropsychopharmacology* 34, 126– 141.

350. Fang, Y., Ferrie, A. M., Fontaine, N. H., Mauro, J., and Balakrishnan, J. 2006Resonant Waveguide Grating Biosensor for Living Cell Sensing *Biophys. J. 91*, 1925– 1940

351. Fang, Y., Ferrie, A. M., Fontaine, N. H., and Yuen, P. K. 2005 Characteristics of dynamic mass redistribution of epidermal growth factor receptor signaling in living cells measured with label-free optical biosensors *Anal. Chem* *77,* 5720-5725.